UNIVERSITY OF SOUTHAMPTON

FACULTY OF ENGINEERING AND THE ENVIRONMENT

An investigation of thick-film electrodes for environmental monitoring

by

Monika Glanc-Gostkiewicz

Submitted for the degree of Doctor of Philosophy

December 2016

Supervised by Prof. J. K. Atkinson and Prof. M. Hill

Every discovery opens a new field for investigation of facts, shows us the imperfection of our theories. It has justly been said, that the greater the circle of light, the greater the boundary of darkness by which it is surrounded.

- Sir Humphry Davy

UNIVERSITY OF SOUTHAMPTON

ABSTRACT

FACULTY OF ENGINEERING AND THE ENVIRONMENT

Doctor of Philosophy

AN INVESTIGATION OF THICK-FILM ELECTRODES FOR ENVIRONMENTAL MONITORING

By Monika Glanc-Gostkiewicz

Rivers and streams are one of the most fragile elements of the whole environmental structure that provides fresh water-useful to humans. Therefore, it is necessary to detect the contamination of watercourses rapidly. To monitor the pollution at various watercourses points, a network of upstream early warning systems consisting of in-situ miniaturized electrochemical sensors is required. The electrochemical sensors are a fast responding, sensitive, and low-maintained alternative to the current methods of downstream detection of pollution in watercourses.

Thick-film (TF) technologies together with electrochemical methods adopt those requirements and offer new types of portable devices that are particularly well suited to on-line monitoring and analysis outside laboratories. Additionally, thick-film technology offers a competitive solution to the current expensive environmental monitoring devices by manufacturing multi-parameter sensors in the thick-film process and employs electrochemical technology in the sensor design. Ideally, those sensing devices will consist of multi-sensing elements and will be used for measurements of pH, ions, gases and organics in solution.

Thus, this project work, collectively sponsored by the Environmental Agency and Faculty of Engineering and the Environment of the University of Southampton, describes the development of low-cost, robust, and miniaturised environmental and chemical sensor arrays that can be used for pH water quality monitoring. Different sensory materials of commercial and in-house origin have been employed to produce various potentiometric solid-state thick-film (TF) reference electrodes and

TF working ion-selective electrodes. The novel thick-film devices described herein are an advantageous alternative to most widely used commercial liquid electrolyte Ag/AgCl reference electrodes and glass bulb pH electrode. These small (50.8 mm x 8.5 mm) devices are mimicking the structure of the conventional available electrodes that are bulky, fragile and expensive. The responses of these novel sensors - such as the hydration time, the potential drift trend and the potential stability to chloride ion concentration - have been experimentally evaluated in the laboratory setup, compared and discussed. The performance of the TF screen-printed silver-silver chloride (Ag/AgCl) reference electrodes were examined with variations of the potassium chloride (KCl) concentration in the final (top) polymer (ESL 242 SB) salt matrix layer of the electrode. Additionally, different types of binder (glass and polymer) were tested for the underlying Ag/AgCl layer. The choice of binders and the amount of the potassium chloride in the salt matrix layer were crucial in manufacturing the Ag/AgCl reference electrode. The results showed a trade-off effect between the potential drift and sensitivity of the electrodes to chloride ions activity related to the porosity of the salt matrix layer. The reference electrodes with different layer compositions converge to a roughly equivalent common potential. It was due to the chloridisation of Ag and dissolution of AgCl in the Ag/AgCl layer to reach equilibrium layer. The addition of another layer on top of the KCl-containing salt matrix layer provided a better stability in varying concentrations of KCl test solutions. The chloride susceptibilities of the electrodes decreased to +2 mV/decade$[Cl^-]$that made the electrodes stable enough to be used at any chloride ion concentration. The screen-printed Ag/AgCl reference electrodes were also used in combination with a screen-printed metal oxide (RuO_2) ion-selective electrode. The pH sensor exhibited a sensitivity of approximately 50 mV/pH at ambient temperature. The reported results help to explain better the behaviour of thick-film electrodes and contribute towards the optimisation of their design and fabrication for use in solid-state chemical sensors.

To my daughters - Iga and Lenka,
my husband Przemek,
my parents Anna and Boleslaw
and my grandmother Maria.

Table of Contents

List of Tables

List of Figures

DECLARATION OF AUTHORSHIP

I, **Monika Glanc-Gostkiewicz**

Declare that the thesis and the work presented in it are my own and has been generated by me as the result of my own original research.

'*An investigation of thick-film electrodes for environmental monitoring*'

I confirm that:

1. This work was done wholly or mainly while in candidature for a research degree at this University;
2. Where any part of this thesis has previously been submitted for a degree or any other qualification at this University or any other institution, this has been clearly stated;
3. Where I have consulted the published work of others, this is always clearly attributed;
4. Where I have quoted from the work of others, the source is always given. With the exception of such quotations, this thesis is entirely my own work;
5. I have acknowledged all main sources of help;
6. Where the thesis is based on work done by myself jointly with others, I have made clear exactly what was done by others and what I have contributed myself;
7. Parts of this work have been published and these publications are listed in the following pages.

Signed:……

Date:……

List of Publications

Journal papers:

1. **Glanc-Gostkiewicz M.**, Sophocleous M., Atkinson J. K., Garcia-Breijo E., 2013. *Performance of miniaturised Thick film solid state pH sensors*, Sensors and Actuators A: Physical, 202, pp. 2-7.

2. Atkinson J.K., **Glanc M.**, Prakorbjanya M., Sophocleous M., Sion R.P., Garcia-Breijo E., 2013. *Thick film screen printed environmental and chemical sensor array reference electrodes suitable for subterranean and subaqueous deployments*, Microelectronics International, 30, 2, pp. 92-98.

3. Soleimani M., Sophocleous M., **Glanc M.**, Atkinson J.K., Wang L., Wood R. J. K., Taylor R. I., 2013. *Engine oil acidity detection using solid state ion selective electrodes*, The Journal of Tribology International, 65, pp. 48-56.

4. Garcia-Breijo E., Atkinson J. K., Gil-Sanchez L., Masot R., Ibañez J., Garrigues J., **Glanc M.**, Laguarda-Miro N., Olguin C., 2011. *A comparison study of pattern recognition algorithms implemented on a microcontroller for use in an electronic tongue for monitoring drinking waters*, Sensors and Actuators A: Physical, 172, 2, pp. 570-582.

5. Atkinson J. K., **Glanc M.**, Boltryk P., Sophocleous M., Garcia-Breijo E., 2011. *An investigation into the effect of fabrication parameter variation on the characteristics of screen-printed thick-film silver/silver chloride reference electrode*, Microelectronics International, 28, 2, pp. 49-52(4).

6. **Glanc M.**, Sophocleous M., Atkinson J. K., Garcia-Breijo E., 2013. *The Effect on Performance of Fabrication Parameter Variations of Thick-Film Screen Printed Silver/Silver Chloride Potentiometric Reference Electrodes*, Sensors and Actuators A: Physical, 197, pp. 1-8.

7. Conference papers:

1. Garcia-Breijo E., Atkinson J. K., Garrigues J., Gil L., Ibanez J., **Glanc M.**, Olguin C. 2011. An electronic tongue for monitoring drinking waters using a fuzzy ARTMAP neural network implemented on a microcontroller, IEEE International Symposium on Industrial Electronics (ISIE), Gdansk, Poland.

2. Gil-Sanchez L., Garcia-Breijo E., Garrigues J., Laguarda N., Masot R., Ibanez J, Atkinson J. K., **Glanc M.**, 2011. *Embedded pattern recognition systems for liquids classification: A comparison study*, IEEE Sensors, pp. 1720-1723.

3. Atkinson J. K., **Glanc M.**, Prakorbjanya M., Sion R. P., Garcia-Breijo E., 2011. *Screen printed thick film subterranean and subaqueous environmental chemical sensor arrays*, IEEE 13th Electronics Packaging Technology Conference (EPTC), pp. 245-250, Singapore.

4. Sophocleous M., **Glanc-Gostkiewicz M.,** Atkinson J. K., Garcia-Breijo E., 2012. *An Experimental Analysis of Thick film Solid-State Reference Electrodes*, IEEE Sensors, pp. 1-4, Taipei.

Abbreviations

Ag	-	Silver
Ag/AgCl	-	Silver-Silver Chloride
AgCl	-	Silver Chloride
Al_2O_3	-	Aluminium Oxide
CaO	-	Calcium Oxide
CSE	-	Copper/Copper Sulfate Electrode
DC	-	Direct Current
EMF	-	Electromotive Force
ESL	-	Electro-Science Lab
GEM	-	Gwent Electronic Materials
IUPAC	-	International Union of Pure and Applied Chemistry
IrO_2	-	Iridium Oxide
ISE	-	Ion-Selective Electrode
KCl	-	Potassium Chloride
KNO_3	-	Potassium Nitrate
Li_2O	-	Lithium Oxide
MacroReflex	-	Macro Solid State Reference Electrode
MOEs	-	Metal Oxide Electrodes
Na_2O	-	Sodium Oxide
OsO_2	-	Osmium Oxide
PC	-	Personal Computer
PtO_2	-	Platinum Oxide
PVC	-	Polyvinyl Chloride
RE	-	Reference Electrode
RuO_2	-	Ruthenium Oxide
SCE	-	Saturated Calomel Electrode
SHE	-	Standard Hydrogen Electrode
SEM	-	Scanning Electron Microscopy
SiO_2	-	Silicon Dioxide
Ta_2O_5	-	Tantalum Oxide
TF	-	Thick-film
TiO_2	-	Titanium Oxide
V	-	Electrical Voltage
WE	-	Working Electrode

Acknowledgements

Undertaking this PhD has been a truly life-changing experience for me. It would not have been possible without those who have contributed to this research and supported me during this amazing journey.

First and foremost, I want to thank my academic supervisor, Prof. John Atkinson, for giving me the opportunity of doing a PhD at the University of Southampton. I am forever indebted for his guidance, motivation, independence and continuous support during my PhD study and related research.

A very special thank I owe to Dr Eduardo Garcia-Brejio for enlightening me the first glance of research and for fruitful collaboration.

I would like to address a very special thanks to Marios Sophocleous for all his help, Mehdi Hendijanizadeh for giving me the time whenever needed, Toninno Raffa for listening and offering me advice and to all my university friends for their unremitting encouragement.

I gratefully acknowledge the funding received towards my PhD from the Environmental Agency and Faculty of Engineering and the Environment of the University of Southampton.

I specifically want to thank my parents, Anna and Boleslaw Glanc, who have always supported my scientific interest, for never questioning my career choices and the freedom they gave me throughout my life. Kocham Was bardzo!

Thanks to Lukasz and Aga and all my friends in Poland and in the United Kingdom for your friendship and your help when I need it. Very special thanks go to Elizabeth for her being there to listen when I needed an ear and true faith in me.

Finally, I would like to thank my husband Przemek and our lovely daughters Iga and Lenka for their love that had an immense impact on this work.

Chapter 1 **Introduction**

1.1 Background

Water is the key to life and its condition needs to be sufficiently assessed and evaluated. To maintain the environmental levels of chemical, biological and physical variables within accepted norms the regulatory agencies employ water quality monitoring programs, where the state of water resources can be determined and effective preservation programs can be applied. Agricultural industry is a major user of water resources. It also contributes intensively to water pollution through processes such as the use of pesticides and fertilisers, and the spreading of slurries or manure. To detect the contamination of watercourses, a network of upstream early warning systems consisting of in-situ miniaturised electrochemical sensors are required as a simple alternative to the current methods of downstream detection of pollution in rivers [1]. This approach enables the localization of pollution sources and better control of the environment but requires large numbers of rugged devices suitable for wide scale field deployment.

Traditionally, the water system was monitoring the condition of the water via discrete water sampling from the site, preserve, transport, and analysis in the laboratory. This traditional more complex measurements method offers some advantages as well as limitations. The laboratory techniques are more accurate but the data obtained are not continuous with respect to time. There is a long period between sampling and laboratory investigation. In addition, the laboratory techniques report incorrect results due to water sample handling errors. There is, therefore, a great need for new, intensive, and long-term data acquisition that can replace traditional costly, time-and labour-intensive on-site sampling and data collection water quality evaluation methods [2]. Nowadays the rapid progress in information technology and the advent of microelectronics opens the advances in development of new and low-cost chemical and environmental sensors for continuous environmental monitoring measurement. In-situ, real-time data collection method provides a constant surveillance where all changes can be rapidly detected and as a result, an early warning monitoring can take place. Sensor data-logging system stores experimental data (it can be retrieved anytime for processing and analysis) and enables experiments to be repeated several times.

In recent years, there has been a growing interest in the development of new, miniaturised, and low-cost electrochemical sensors suitable for data acquisition for environmental applications. Thick-film (TF) technologies together with electrochemical methods embrace the requirements for these devices by giving cost competitive solutions for the fabrication of compact, rugged and robust systems [3]. Thick-film chemical and environmental sensors offer alternative solutions and allow flexible design with a wide range of materials, low-cost infrastructure and mass production capability [4-6]. The Environmental Agency and Faculty of Engineering and the Environment of the University of Southampton jointly sponsor the research presented in this thesis. It revisits previous work on multi-parameter TF sensors and brings into focus two types of solid-stated TF devices: Ag/AgCl reference electrode and pH electrode.

The traditional way of monitoring and measuring of water quality parameters has changed with the development of lab-on a-chip thick-film sensors. Thick-film water quality environmental sensors typically consist of a variety arrays of sensors integrated onto a single piece of substrate (Figure 1-1) [3].

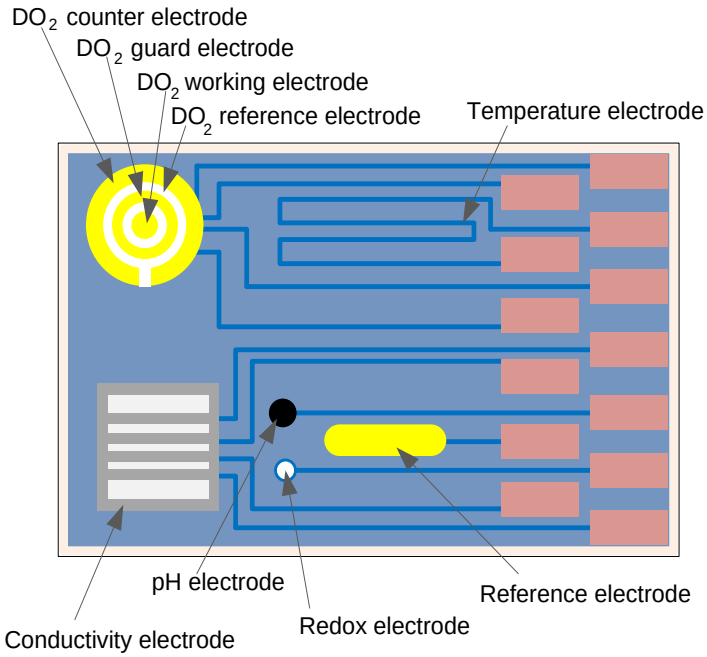

Figure 1-1: A thick-film water quality environmental sensor for the measurement of conductivity, redox, pH, dissolved-oxygen concentration (DO_2) and temperature [3, 5]

They have the advantage of being able to obtain the simultaneous measurements of pH level, temperature, dissolved oxygen concentration, redox potential and conductivity [7]. The electrochemical measuring principles of the different sensor arrays are based on amperometric, potentiometric or impedimetric measurements. The sensitivity, stability and selectivity of these sensors are influenced mainly by temperature, pressure and chemical environment. Thick-film water quality environmental sensors can be used for real-time, continuous survey by in-situ measurement without the need of sampling. They are connected to an electronic acquisition system and computer for data acquisition as a consequence all data can be remotely accessed [8].

The response of any electrochemical potentiometric electrode is meaningless without a reference electrode against which comparisons can be made. Therefore, each single sensor from the sensor arrays presented in Figure 1-1 requires a common stable reference electrode in order to quantify measurements [9]. The commercially available fragile and expensive Ag/AgCl reference electrode is a classic type of conventional electrolyte-filled reference electrode that is often chosen as the traditional electrode to mimic. This thesis presents screen printed thick-film reference electrodes and pH sensors implemented on the same principle as the conventional electrolyte-filled reference electrode and conventional glass bulb pH electrode [10, 11].

1.2 Aim and Objectives

The overall aim of the thesis is to develop a stable, low-cost, disposable, miniature and rugged thick-film reference electrode employed together with thick-film pH sensor. The thick-film reference electrode can be used for longer deployment duration in both subterranean and submerged unknown analyte matrices. It can be employed for in-situ water quality sample collection alongside passive samplers and provide better estimations of environmental concentrations and uptake rates of pollutants in watercourses. This requires a thick-film reference electrode of better stability and lifetime. The novel thick-film silver-silver chloride (Ag/AgCl) reference electrodes developed in this thesis are an alternative to the otherwise well-

established, fragile, costly, high maintained, and difficult to calibrate commercial electrodes.

The objectives of this research are:

- To develop a low-cost, disposable, miniature and robust thick-film screen-printed silver-silver chloride (Ag/AgCl) reference electrode and pH sensor for in-situ environmental measurements.
- To investigate the characteristics of thick-film screen-printed silver-silver chloride (Ag/AgCl) reference electrode and pH sensor with respect to variations in the fabrication parameters and electrode designs.
- To investigate the behaviour of thick-film devices in various chloride ion concentrated solutions.
- To evaluate the performance of thick-film devices such as sensitivity, potential drift (stability and lifetime) and hydration time.

The main challenges of the research are to investigate the electrode lifetime and its ability to provide a constant and stable potential in various test solution against which the potential of other sensing electrode can be measured. The manufacturing process will involve designing and fabricating Ag/AgCl reference electrode and pH sensor with various materials and compositions.

1.2.1 Thesis Structure

The quest for better selective and miniaturised chemical sensors has been subject to intense research for the past 50 years [12, 13]. Indeed, over those years more than 2000 sensor-related papers have been published per year that it is no longer possible to commit the time required to read at length about every contribution to the field [12]. The literature review presented in the thesis is not an attempt to do this but it has been made broad enough to understand all included topics that are relevant.

This thesis is divided into five chapters. In Chapter 1 the basic background information to this research project has been presented and aim and objectives have been specified.

The literature review presented in Chapter 2 is divided into five successive subchapters where each one gives information on the review topic. The first subchapter (2.1) provides an introduction to sensors with a focus on chemical and electrochemical sensors. In the second subchapter (2.2), the conventions for describing potentiometric electrochemical cells and the relationship between the measured potential and the analyte's activity are introduced. In the consecutive two subchapters (2.3 and 2.4), the conventional Ag/AgCl reference electrode and the glass pH ion-selective electrode are described together with the available miniaturized planar TF electrodes as their desirable counterparts. The final fifth subchapter (2.5) reviews the thick-film technology that was used in the development of miniaturised TF reference and ion-selective electrodes.

Chapter 3 is partitioned into two subsections that provide summary of the research experimental approach. In the first subsection, a description of the electrode fabrication process, including TF screen design, development and fabrication of reference electrode and pH sensor with diverse material types, is presented. The second subsection describes the details of the electrode testing process in various test solutions to evaluate their performance such as sensitivity, potential drift (stability and lifetime), and hydration time.

Finally, in Chapter 4 and Chapter 5 the experimental results and a general discussion summarising the results of these two related individual studies have been included. In addition, limitations and improvements for the actual devices are discussed as well as opportunities for future works are included in Chapter 5.

Chapter 2 **Literature Review**

2.1 Sensors

2.1.1 Sensor Definition

Today, there are many different types of sensors that are commonly used in everyday objects. Despite this, it is still difficult to find a general and agreed definition of ‘sensor’. The word ‘sensor’ has derived from Latin word sēnsus/sentīre, which means perceived/to observe.

Sensors (also called detectors) are widely used in technical literature when describing measurement systems. They are converting devices that detect or measure a physical or chemical property of a system. It records, indicates, and responds to singular or multiple input signals and transforms it into an output signal which can be read by an instrument at the sensor location or transmitted electronically over a network for reading or further processing Figure 2-1. Gábor Harsányi defines a sensor as a transducer that converts the measurand (a quantity or a parameter) into an electrical, optical or mechanical signal carrying information [14].

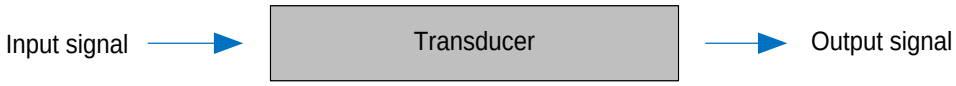

Figure 2-1: The sensing process

According to the International Union of Pure and Applied Chemistry (IUPAC) (1991), *a chemical sensor is a device that transforms chemical information, ranging from the concentration of a specific sample component to the total composition analysis, into an analytically used signal* [15].

There is a broad agreement about attributes of sensors. The sensor’s sensitivity to the measurand is defined as the magnitude of the variation of the sensor output in response to a unit change in the parameter being measured. Ideally, a sensor’s output should be linearly proportional to the value of the measured property. A perfect sensor has to be highly sensitive to detect very small changes of a measured property; it does not influence it and is insensitive to any other property.

It should respond rapidly and maintain its activity over a long period. Desirably it needs to be entirely reproducible and therefore for a constant measurand the output signal will be the same on every repeat of the experiment [16, 17]. It requires relatively simple instrumentation. A sensor-based system needs little (if any) treatment of the sample. Lastly it should be small and cheap [18].

2.1.2 Sensor Classification

Sensors described in the literature were used in many different sensing situations. The sensor's classification is accomplished in different ways and it can range from very simple to complex. Sensors are commonly divided, according to the principles of signal transduction, into groups: optical sensors, chemical sensors, electrochemical sensors, electrical sensors, mass sensitive sensors, magnetic sensors, thermometric sensors and other sensors (based on emission or absorption of radiation) [15]. Today, sensors are most often categories by type of measurand into chemical sensors, physical sensors and biological sensors; afterwards they are subdivided into groups within each category [19, 20].

2.1.2.1 Chemical Sensors

Chemical sensors appeared on the commercial market 50 years ago. In recent years, an increased concern with the natural environment protection matters has broadened and expanded an interest in chemical sensors. The literature offers many pragmatic descriptions of chemical sensors.

Commonly they are characterized as miniaturized analytical devises, which can deliver real-time information on the presence of specific compounds or ions in complex samples. The device core is made up of two main components connected in order: a recognition system, the receptor, and a physiochemical transducer (Figure 2-2).

Generally, the receptor (sensor) is in direct contact with the target analyte of the sample to be monitored. During the selective sensor interactions, a primary signal (electric, mass, thermal, optical) is produced.

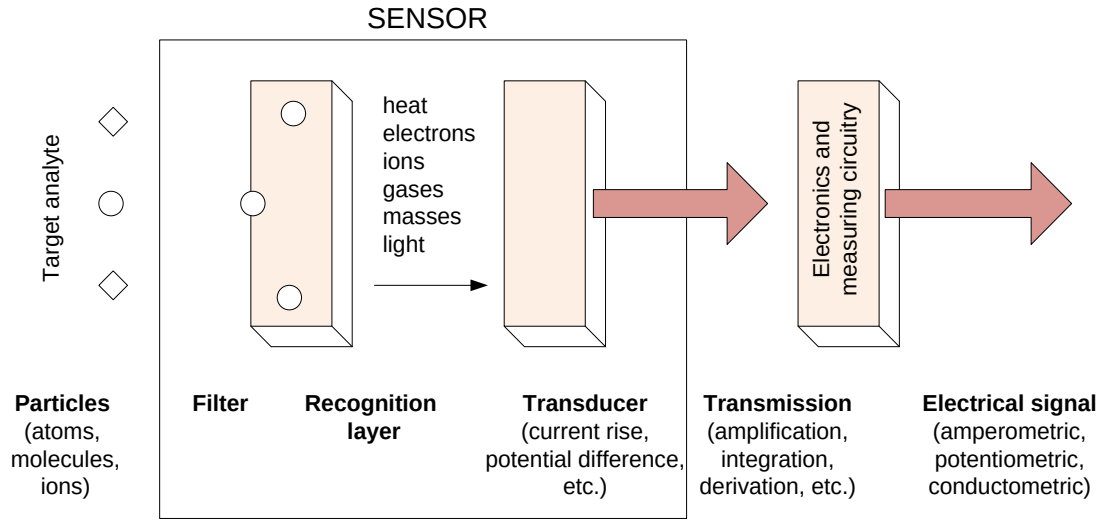

Figure 2-2: Schematic of typical chemical or biochemical sensor to detect atoms, molecules, or ions in the gas or liquid phase (adapted from Göpel [21], Gründler [16], and Wang [22])

The analytical information in form of chemical changes of the potentiometric electrochemical sensor is converted subsequently by the transduction element into a secondary electrical output signal. The electrical signal is proportional to the concentration (activity) of species produced or used up in the recognition event (Figure 2-2) [18, 22]. The potential signal of the potentiometric devices is obtained at zero current conditions from the ion selective electrodes through a perm-selective ion-conductive membrane.

2.1.2.2 Electrochemical Sensors

Electrochemical sensors are the oldest and by far the most rapidly growing class of chemical devices. They are very attractive for environmental monitoring because they are simple and portable, fast and accurate, inexpensive, sensitive, and selective towards electro-active species and compatible with on-line analysis. Electrochemical sensors, apart from satisfying many requirements for on-site environmental analysis, can be used for monitoring of a wide range of inorganic and organic nutrient pollutants. The main sources of inorganic nutrient pollutants are nitrates (very soluble) and phosphates (not very soluble). Whatever amount of inorganic nutrient pollutant is not taken up by plants in a field is washed away from farmland as fertiliser, manure or as silage fluid and get into rivers, streams, ponds,

and lakes where it become sources of food for algae, resulting in the formation in the eutrophication of ponds and lakes. Organic pollutants originate from domestic sewage, urban run-off, industrial effluents and farm wastes (e.g. solvents, fragrances, pesticides and herbicides).

Most of electrochemical devices used for the task of environmental monitoring fall into categories: amperometric and voltammetric, potentiometric and conductimetric [17]. The measurements of the potentiometric sensors are based on a local equilibrium established at the sensor interface where the information about the sample composition is obtained from the potential difference between two electrodes. Thick-film environmental and electrochemical sensor arrays reported in this thesis belong to the potentiometric category. They simply mimic their macro scale electrochemical equivalents, such as commercially available pH sensor and Ag/AgCl reference electrode, and are designed for deployment in both subterranean and submerged aqueous applications.

2.2 Methods for Study of Electrode Reactions

Electrochemistry is a branch of chemistry concerned with a charge-transfer phenomenon that occurs when two dissimilar conducting phases - a piece of metal and an electrolyte solution - are brought into contact and an inter phase electric potential difference is developed between the metal and the solution interface [23]. Electrochemical methods used in electrochemistry are associated with the interplay boundary between chemistry and electricity. They are a class of techniques in electro-analytical chemistry which study an analyte solution of electrochemical cell by measuring three principal sources for the electrical signal (potential, current, and charge) and their relationship to the chemical parameters.

All basic experimental designs are based on Ohm's law:

$$E = iR \qquad \text{Eq. 1}$$

Where current (i) passing through an electric circuit of resistance (R) generates a potential (E).

The simplest classification of electrochemical methods, presented in Figure 2-3, is between bulk methods and interfacial methods.

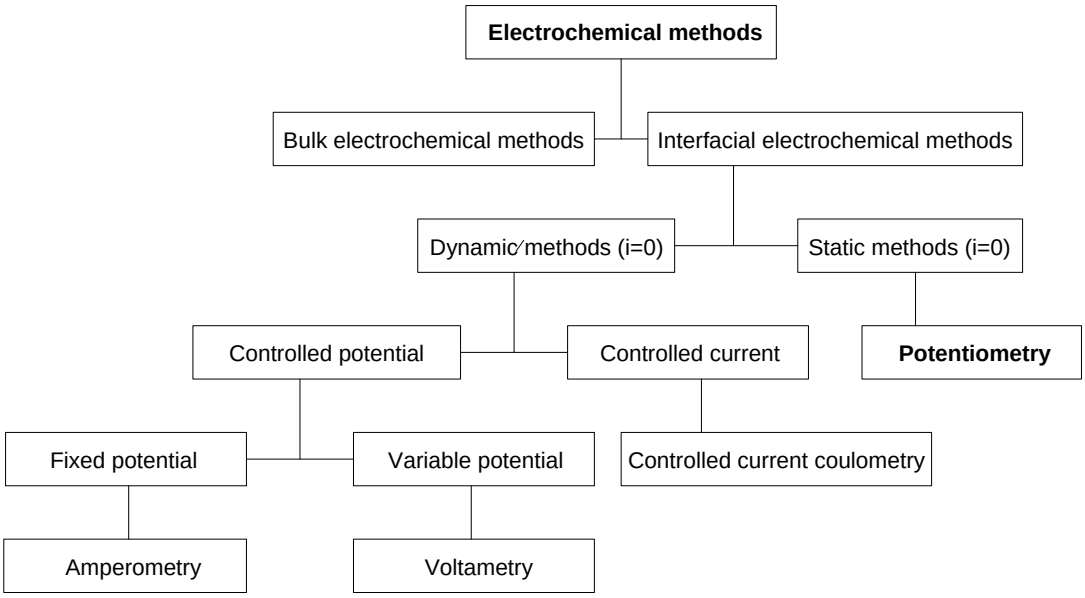

Figure 2-3: Electrochemical methods of analysis [24]

The electrochemical bulk methods measure properties of the whole solution whereas the interfacial electrochemical methods determine the signal which is a function of phenomena happening at the interface between an electrode and the solution in contact with the electrode [17]. The interfacial electrochemical methods of analysis can be divided into steady state (passive or static) techniques and non-steady state (dynamic or active) techniques. A steady state technique, in contrary to a non-steady state technique, does not allow current to pass through the analyte's solution. Thus, technique such as potentiometry is an example of passive category, whereas e.g. voltammetry and amperometry belong to the dynamic techniques. Potentiometry and amperometry are the most basic and most commonly chosen electrochemical methods used for analytical purposes. They are easier to perform because they require a simple instrumentation. Generally, potentiometric measurements determinate the potential difference between two electrodes, the reference electrode and the working electrode, where there is no current flowing between them. The amperometric technique measures a direct current at a constant applied potential between two electrodes (working or counter electrodes) or a three-

electrode arrangement (working, counter, and reference electrodes). The measured current changes as an electroactive analyte is oxidized at the anode or reduced at the cathode. [18, 25]. All the experimental work presented in this thesis was obtained by potentiometric method.

2.2.1 Electrochemical Cells

Simplest potentiometric electrochemical cells are used in analytical chemistry for titration or direct determination of ion activities. An electrochemical potentiometric pH sensor made up of a reference electrode and a pH ISE can determine the pH of a solution. The most commonly used Ag/AgCl reference electrode provides a stable constant potential regardless of the solution in which is immersed while the ion-selective electrode responds to the change of the hydrogen ion activity in the solution [11]. The quantitative analysis is used to measure the equilibrium potential of an electrochemical cell using a high-impedance voltmeter under static conditions where no current passes through the cell and it is proportional to the pH of the solution [26]. The composition of the electrochemical cell remains unchanged at zero current flows and therefore, it is a useful quantitative method.

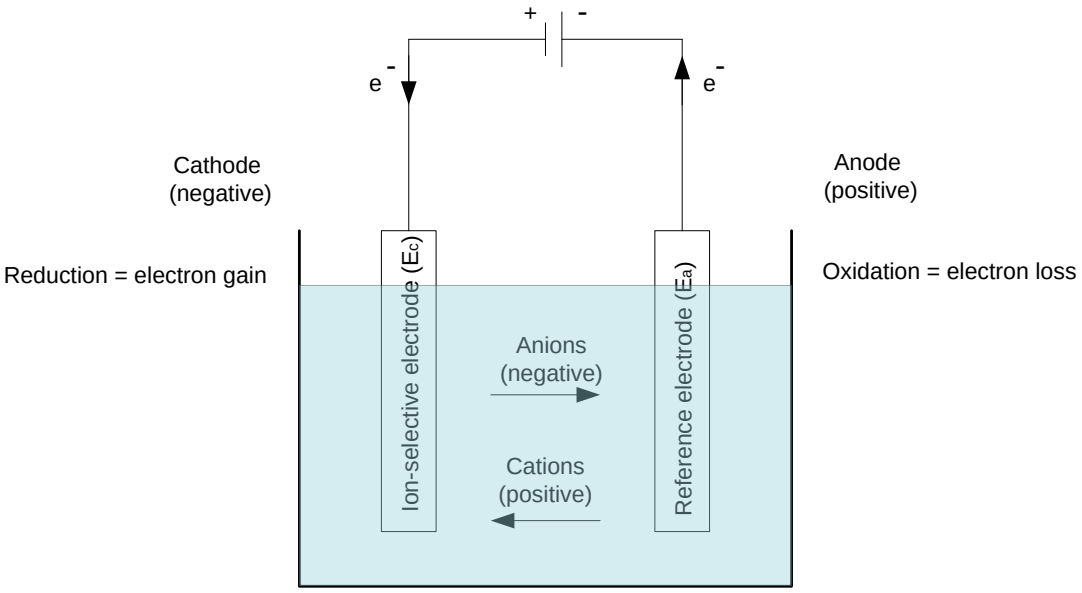

Figure 2-4: An electrolytic electrochemical cell

Figure 2-4 shows a schematic diagram of the potentiometric measurement system consisting of an electrolytic cell divided into two half-cells where one is a reduction cell ($\mathrm{E_c}$), and the other is an oxidation cell ($\mathrm{E_a}$).

By convention, the reference electrode is the anode $(\mathrm{E_a})$ and the ion-selective electrode is the cathode $(\mathrm{E_c})$. The reduction cell is also called a working electrode (WE) and will respond to the measurand. The oxidation cell, a reference electrode (RE) stays unaffected by solution changes. Many considerations (such as the type of solution under examination or the conditions and place of use) must be taken into account when choosing a suitable RE for electrochemical investigations. Commercial reference electrodes are calibrated with respect to the fundamental reference electrode, which is a standard hydrogen electrode (SHE). The SHE is the usually chosen reference point for standard electrochemical reduction potential $\mathrm{E^0}$, assigned as 0.0000 volts V) at all temperatures by convention [27]. It is made up of a platinum electrode immersed in a solution in which the activity of hydronium ions $(\mathrm{H_3O^+})$ is equal to 1 and the hydrogen must be at 25°C and 1 atmospheric pressure. Despite its importance, this electrode is not practical and rarely used for routine analytical work. Therefore, other reference electrodes, such as saturated calomel electrode (SCE), copper/copper sulfate electrode (CSE) and silver-silver chloride electrode, are employed (Chapter 2, section 2.3.1).

The potential of the reference electrode is fixed in every solution therefore in practice any changes in the potential difference of the measured cell is due to changes in the half-cell potential of the ion-selective electrode (ISE). An ion-selective membrane is the key component of a chemical ion-selective electrode that establishes the sensor response preferences to the analyte [28]. It means that the construction of ISE determines its own response. The sensor can only react with specific species and it should not affect any other interfering ions present in the solution. The reaction reaches a state of equilibrium between two phases when there is no further transfer of ions between the boundaries. The transfer of ions is equal from the membrane into solution and back. The potential difference formed between the two phases can be governed by the activity of only one target ion exchanged between those two phases. The potential difference across the ion-selective membrane, separating two solutions of different ionic activities and only

permeable to a single type of ion, can be measured by the Nernst equation (refer to Chapter 2, section 2.2.6).

2.2.2 Reversible Reactions

The electrode oxidation-reduction reactions, also called the redox reactions, can be written into separate half-reactions that show the oxidation process and reduction process. They occur when electrons move between the oxidised and reduced species, Ox or (O) and Red or (R) in a dilute solution [29].

$$\mathrm{O}_{(\mathrm{aq})} + \mathrm{ne}^{-} \leftrightarrow \mathrm{R}_{(\mathrm{aq})} \qquad \text{Eq. 2}$$

Where n is the number of moles of electrons (e^{-}) transferred between the oxidant (O) and the reductant (R) species.

In the redox reactions the electrons (ne^{-}) are transferred between converted species, from the reducing agent to an oxidizing agent, therefore it is convenient to view the reaction's thermodynamics in term of the electron. This process occurs at an inert electrode surface in the electrochemical cell where current flows and the electrons move from areas of higher potential energy to areas of lower potential energy.

The direction of electron flow in electrolytic cells is reversed from the direction of spontaneous electron flow in galvanic cells as shown in Figure 2-5.

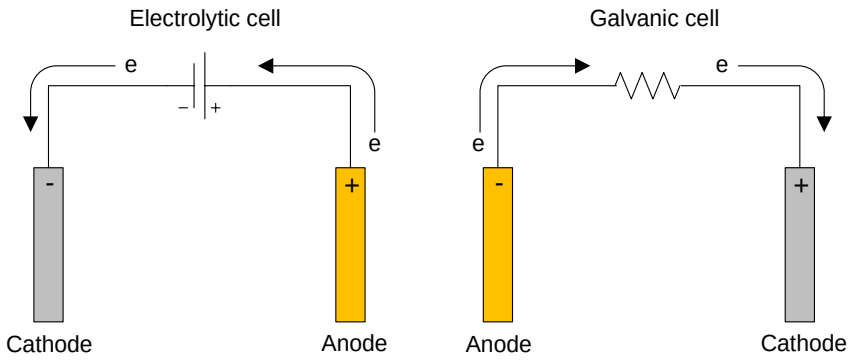

Figure 2-5: Comparison of electrolytic cell (left) and galvanic cell (right) (after Bard [30])

The reverse reaction is non-spontaneous and requires electrical energy (a power supply) to occur. The sign of the electrolytic cell potential, but not its magnitude, as well as the direction of the cell oxidation-reduction reaction have been reversed in comparison to the galvanic counterpart.

At the electrode-electrolyte interface, the exchange or movement of charges across the electrode-electrolyte interface causes a separation of charges and the electrode may get positive or negative charge with respect to the solution (Figure 2-6).

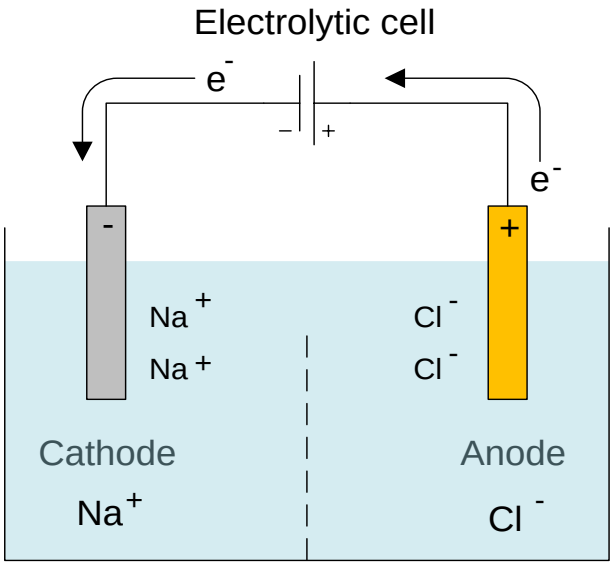

Figure 2-6: Movement of electrons in electrolytic cell

In the solution, made of dissolved sodium ions and chloride ions, the negatively charged chloride ions are attracted by the positively charged anode and move towards it. The anode receives current or electrons from the electrolyte mixture and it becomes oxidized. The atoms or molecules evolve into positive ions, as seen in Eq. 3 and Eq. 4.

$$2\mathrm{Cl}^- \rightarrow \mathrm{Cl}_2 + 2\mathrm{e}^- \qquad \text{Eq. 3}$$

$$2\mathrm{H}_2\mathrm{O} \rightarrow 4\mathrm{H}^+ + \mathrm{O}_2 + 4\mathrm{e}^- \qquad \text{Eq. 4}$$

The antonymous process occurs with the cathode where the positively charged sodium ions are collected next to the negatively charged electrode. The cathode becomes reduced while the electrons are released from the electrode and the solution around (Eq. 5 and Eq. 6).

$$2Na^{+} + 2e^{-} \rightarrow 2Na \quad \text{Eq. 5}$$

$$2H_2O + 2e^{-} \rightarrow H_2 + 2OH \quad \text{Eq. 6}$$

The amount of reduction at the cathode and oxidation at the anode must be equal to maintain an overall balance, the equilibrium. This can be presented in a simple overall electro-transfer net reaction:

$$2NaCl_{(aq)} + 2H_2O_{(l)} \rightarrow Cl_{2(g)} + H_{2(g)} + 2OH_{(aq)} + 2Na_{(aq)} \quad \text{Eq. 7}$$

If the electron transfer is fast and the concentrations of the oxidant O and the reductant R species at the electrode surface reaches a state of chemical equilibrium (dynamic equilibrium) then the system follows the Nernst equation and the electrode reaction is electrochemically reversible (or Nernstian) [30], refer to Chapter 2, section 2.2.6.

2.2.3 Chemical Equilibrium and Equilibrium Constant

The net reaction shown in Eq. 7 follows the concept of the chemical equilibrium that was developed after Berthollet (1809) found that some chemical reactions are reversible [24, 31]. The chemical equilibrium reaction (dynamic equilibrium reaction) shown in 8 involves the A and B species (the reactant or oxidised species) and C and D species (the product or the reduced species) with their stoichiometric coefficients (a, b, c, and d) that represent moles of the respective reactants and products. The arrows pointing both ways indicate equilibrium.

$$aA + bB \underset{k_2}{\overset{k_1}{\leftrightarrow}} cC + dD \quad \text{Eq. 8}$$

In which a moles of a reactant A and b moles of a reactant B react to give moles c of a product C and moles d of a product D.

The relative amounts of reactants and products determine the direction in which the reaction occurs and the final composition of the reaction mixture. Guldberg and Waage (1864-1879) formulated the Law of Mass Action in which they showed that

for the reaction in Eq. 8 the rate (speed) of the reaction in either direction is proportional to the concentrations of the reactants and products [32]:

$$\text{forward reaction rate} = k_1[A]^a[B]^b \quad \text{Eq. 9}$$

$$\text{backward reaction rate} = k_2[C]^c[D]^d \quad \text{Eq. 10}$$

Where A, B, C and D represents active masses, the proportionality constants k_1 and k_2 are called rate constants and the quantities in square brackets represent concentrations. Depending on initial conditions such as concentration, temperature, or pressure, the reaction is able to move to the left, to the right, or be in a state of equilibrium according to Le Châtelier's principle. Le Châtelier's principle states whether more reactants or more products will be made. A reaction at equilibrium exists in a steady-state, in which the rates of the forward and backward reactions are equal [24]:

$$k_1[A]^a[B]^b = k_2[C]^c[D]^d \quad \text{Eq. 11}$$

2.2.4 Gibbs Free Energy, Equilibrium constant and Reaction Quotient

Dynamic equilibrium is a useful measure to predict whether the forward or reverse reaction is spontaneous or non-spontaneous. To explain how this works, three quantities must be introduced: the free energy of reaction (ΔG), the reaction quotient (Q) and the equilibrium constant (K).

2.2.4.1 Gibbs Free Energy and Equilibrium Constants

Gibbs' free energy of a system (G) is related to the chemical species concentration change during the reaction and it is a function of the concentrations of reactants and products. As the reaction proceeds, the concentration of reactants begins to decrease while the concentration of products begins to increase. Eventually a chemical equilibrium is reached in which the concentration of reactants and products does not change. This is the point of greatest entropy. The change in Gibbs free energy (ΔG) under non-standard-state conditions is defined as:

$$\Delta G = \Delta G^0 + RT\ln Q \quad \text{Eq. 12}$$

Where ΔG^0 is the standard-state free energy reaction, R is the gas constant, T is the temperature, and Q is the reaction quotient. ΔG^0 has only one value for a reaction at a given temperature in contrary to ΔG where an infinite number of values is possible. The reaction quotient (Q) is written by multiplying the activities (which are approximated by concentrations) for the species of the products and dividing by the activities of the reactants:

$$Q = \frac{[C]^c[D]^d}{[A]^a[B]^b} \qquad \text{Eq. 13}$$

Where the products are in the numerator of the reaction quotient and the reactants are in the denominator of it.

When the reaction quotient for the system is equal to 1 and the value of ΔG is equal to the standard-state free energy reaction, ΔG^0 then the system is at the standard-state conditions. It means that the driving force behind a chemical reaction is zero $(\Delta G = 0)$ and therefore the reaction is at equilibrium $(Q = K)$. Thus, the equation can be arranged into:

$$\Delta G^0 = -RT\ln K \qquad \text{Eq. 14}$$

Where K is an equilibrium constant that characterise the reaction's equilibrium position.

The value of K is determined by equilibrium concentrations and is defined as:

$$K = \frac{[C]_{eq}^c[D]_{eq}^d}{[A]_{eq}^a[B]_{eq}^b} \qquad \text{Eq. 15}$$

The subscript 'eq' indicates a concentration at equilibrium. The reaction quotient (Q) and the equilibrium constant (K) indicate the reaction direction shifts and in which side of the reaction is favoured. At equilibrium, no shift occurs and neither reaction side (the reactants or the products) are in favour. If $Q > K$ then the reaction produces more reactants and the system shifts to the left to reach equilibrium. If $Q < K$

then the reaction favours the products. The system needs to produce more products and therefore it shifts to the right to reach the equilibrium.

2.2.4.2 Driving Forces and Gibbs Free Energy

Gibbs' free energy of a system (G) at any moment in time builds a relationship between the enthalpy (H), the product of the temperature (T) and the entropy (S) of the system:

$$\mathrm{G} = \mathrm{H} - \mathrm{TS} \qquad \text{Eq. 16}$$

It also dictates whether a reaction is product-favored or reactant-favored and can predict direction of chemical reaction. If the reaction is run at non-standard-state conditions, the equation of free energy of reaction $(\Delta\mathrm{G})$ is defined as follows:

$$\Delta\mathrm{G} = \Delta\mathrm{H} - \Delta\mathrm{TS} \qquad \text{Eq. 17}$$

Where T is the temperature, and $\Delta\mathrm{G}$, $\Delta\mathrm{H}$, and ΔS are the differences in the Gibb's free energy, the enthalpy, and the entropy between the products and the reactants.

The free energy of reaction $(\Delta\mathrm{G})$ at standard-state conditions, such as gases' pressure of 1 atm, solutes' concentrations of 1 mol dm^{-3} and a temperature of 25°C (298K), is called standard-state free energy of reaction $(\Delta\mathrm{G}^0)$. It can be present as followed:

$$\Delta\mathrm{G}^0 = \Delta\mathrm{H}^0 - \mathrm{T}\Delta\mathrm{S}^0 \qquad \text{Eq. 18}$$

The change in enthalpy $(\Delta\mathrm{H}^0)$ classified the reaction. Exothermic reactions transfer energy to the surroundings and release heat $(\Delta\mathrm{H}^0 < 0)$. Endothermic reactions take in energy from the surroundings and absorb heat $(\Delta\mathrm{H}^0 > 0)$.

The reaction can also be classified according to the change in the free energy during a reaction. It measures the balance between the two driving forces that determine whether a reaction is spontaneous or non-spontaneous [24]. The spontaneous or favourable (exergonic) chemical reaction happens when $\Delta\mathrm{G}^0$ is negative $(\Delta\mathrm{G}^0 < 0)$ while the non-spontaneous or unfavourable (endergonic) reaction occurs when

ΔG^0 is positive $(\Delta G^0 > 0)$. The sign of (ΔG^0) indicates the direction in which a chemical reaction (at any temperature) moves from its initial, non-equilibrium conditions to its equilibrium position where the value of (ΔG^0) approaches 0.

2.2.5 Cell Potentials and Gibbs Free Energy

Electrochemical cells convert chemical energy to electrical potential energy that can be used to do an electrical work. The cell potential and the total number of electrons transferred during redox reaction govern the electrochemical cell energy production. Electrical work is done when the free energy (ΔG) moves an electric charge (q) over a change in cell potential (E) therefore the reaction takes place:

$$\Delta G = Eq \qquad \text{Eq. 19}$$

The total transfer of charge (q) from the reductant to the oxidant is:

$$q = nF \qquad \text{Eq. 20}$$

Where n is the number of moles of electrons transferred and F is Faraday's constant, which is the total charge (in coulombs) of mole of electrons (96,485 C mol^{-1}).

The standard-state free energy change (ΔG^0) expresses the tendency for any process to occur under the standard-state conditions (a constant temperature and pressure).

Thus, the standard-state potential (E^0) and the standard-state free energy of reaction (ΔG^0) measure the same thing, and are related in the following way:

$$\Delta G^\circ = -nFE^\circ_{cell} \qquad \text{Eq. 21}$$

ΔG can be expressed as:

$$\Delta G = -nFE_{cell} \qquad \text{Eq. 22}$$

The reduction potentials may be related to the free energies of reaction:

$$E^{\circ}_{cell} = -\frac{\Delta G^{\circ}}{nF} \quad \text{Eq. 23}$$

$$E_{cell} = -\frac{\Delta G}{nF} \quad \text{Eq. 24}$$

The sign of change in free energy (ΔG), for a redox reaction at any moment in time, indicate in which direction the reaction has to shift to reach equilibrium whereas the cell potential is a measure of how far the reaction is from equilibrium. In thermodynamics, as Le Châtelier's principle predicts a reaction is favoured (spontaneous or "driving to the right") when free energy change ΔG is more negative then ΔG°, but a redox reaction is favoured when E is more positive than E°. Substituting Eq. 21 and Eq. 22 into Eq. 12:

$$-nFE = -nFE^{\circ}_{cell} + RT\ln Q \quad \text{Eq. 25}$$

Equation Eq. 25 can be rearranged to the well-known Nernst equation.

2.2.6 Nernst Equation

The voltage is also called as the electromotive force (EMF or E_{cell}) or simply the electrochemical cell potential between the electrodes in the absence of any cell current, is the most fundamental kind of measurement. The electrochemical potential of the working electrode can be measured versus a reference electrode and is given by the Nernst equation. It relates the non-equilibrium properties of a reaction to those at equilibrium and therefore includes two terms that are used to describe the cell potential. The first one reflects the potential difference between products and reactants under standard-state conditions (E°) and the second one is for non-standard conditions $(RT / nF \times \ln Q)$.

$$E_{cell} = E^{\circ}_{cell} - \frac{RT}{nF}\ln Q \quad \text{Eq. 26}$$

where E is the cell potential (V), E^{0} is the standard electric potential at the temperature of interest of the reference electrode, R is the universal gas constant $(8.314\ JK^{-1}mol^{-1})$, T is the temperature $(298K)$, n is the number of moles of

electrons (e^-) transferred in the balanced redox (oxidation/reduction) reaction, F is the Faraday's constant $(96{,}485\ C\ mol^{-1})$.

If the reactions are carried out at room temperature $(25℃)$, the Nernst equation is more commonly expressed in terms of base 10 logarithms, and using a conversion between natural and common logarithm $\ln(x) = 2.303\log(x)$ it becomes:

$$E_{cell} = E^{\circ}_{cell} - 2.303\frac{RT}{nF}\log_{10}Q \qquad \text{Eq. 27}$$

At standard temperature $T = 25\ ℃\ (298\ K)$, the value of $\frac{2.303RT}{F}$ term equals to $0.05916\ V$ and the above equation turns into:

$$E_{cell} = E^{\circ}_{cell} - \frac{0.05916}{n}\log_{10}Q \qquad \text{Eq. 28}$$

All the redox reactions drive toward equilibrium. When this happens, the reaction quotient $Q = K_{eq}$, $\Delta G = 0$ and $\Delta G = -nFE$, so $E = 0$. Therefore, the Nernst equation is defined as:

$$0 = E^{\circ}_{cell} - \frac{RT}{nF}\ln K_{eq} \qquad \text{Eq. 29}$$

At room temperature:

$$0 = E^{\circ}_{cell} - \frac{0.05916}{n}\log_{10}K_{eq} \qquad \text{Eq. 30}$$

$$E^{\circ}_{cell} = \frac{0.05916}{n}\log_{10}K_{eq} \qquad \text{Eq. 31}$$

Therefore, the equilibrium constant for the reaction under standard-state condition is:

$$\log_{10}K_{eq} = \frac{nE^{\circ}}{0.05916} \qquad \text{Eq. 32}$$

The Nernst equation tells us that a half-cell potential will change by 59 millivolts per 10-fold change in the concentration of a substance involved in a one-electron oxidation or reduction $(n = 1)$.

2.2.7 pH Measurements

Water plays many essential roles for life. Therefore, it is important to describe concentrations of chemical species of water quantitatively. This can be done in a number of ways, such as measuring the temperature or density of water, measuring the concentration of solutes, such as salt etc., but the most common ways to quantify a water solution is to measure its pH.

The conventional definition of pH is defined as the negative logarithm of the hydrogen ion concentration and is expressed mathematically as:

$$\mathrm{pH} = -\log_{10}[\mathrm{H}^+] \qquad \text{Eq. 33}$$

Where $[\mathrm{H}^+]$ is hydrogen ion concentration in mol/L. Most of the time, concentration is used to measure the number of ions in a specific volume. However, activity is also a measure of composition similar to concentration. Ions attract and repel each other with coulomb forces. These interactions influence ions behaviour, which is different both in higher concentrated solution and in the lower concentrated solutions. The number of effective ions is called the activity and can be presented as:

$$\mathrm{a_{ion}} = f \times [\mathrm{ion}] \qquad \text{Eq. 34}$$

where f is the activity coefficient [33].

Hence, the pH of aqueous solution can be described in terms of a hydrogen ion activity $(\mathrm{a_{H^+}})$ or a hydronium ion activity $(\mathrm{a_{H_3O^+}})$:

$$\mathrm{pH} = -\log_{10}(\mathrm{a_{H^+}}) \qquad \text{Eq. 35}$$

$$\mathrm{pH} = -\log_{10}(\mathrm{a_{H_2O^+}}) \qquad \text{Eq. 36}$$

The concept of pH, a quantity that is a measure of acidity and basicity, was introduced in 1887 by the Danish biochemist Søren Peder Lauritz Sørensen in the course of his pioneering research into proteins, amino acids and enzymes in the laboratories of Carlsberg Breweries in Copenhagen in 1909 [34-36].

He stated that those two compounds dissolve in aqueous solutions and release certain ions into the solution. Acids were substances that produce hydrogen ions (H^+) in solution:

$$\text{Acids:} \quad HA \rightarrow H^+ + A^- \qquad \text{Eq. 37}$$

Bases were substances that produce hydroxide ions (OH^-) in solution:

$$\text{Bases:} \quad MOH \rightarrow OH^- + M^+ \qquad \text{Eq. 38}$$

Water contains hydronium ions (H_3O^+) and some hydroxide (hydroxyl) (OH^-) ions. It is called an amphiprotic solvent and is capable of reacting with itself in an acid-base reaction that is commonly called the self-ionization of water [24]. During this reaction, water molecules collide and a hydrogen ion is transformed between them, a negatively charged hydroxide ion (hydroxyl) (OH^-), and a positively charged hydronium ion (H_3O^+) are created.

$$H_2O_{(l)} + H_2O_{(l)} \leftrightarrow H_3O^+_{(aq)} + OH^-_{(aq)} \qquad \text{Eq. 39}$$

In case of pure water the concentrations of H_3O^+ ions and OH^- ions is in balance

$$[H_3O^+] = [OH^-] \qquad \text{Eq. 40}$$

In all other aqueous solutions the concentrations of H_3O^+ and OH^- is unequal. It can increase or decrease with ion addition or subtraction to the solution. The product of these ions is always equal to:

$$[H_3O^+][OH^-] = 1.00x10^{-14} = K_w \qquad \text{Eq. 41}$$

The equilibrium constant in water solutions at 25°C is defined as water dissociation constant K_w:

$$K_w = (a_{H_3O^+})(a_{OH^-}) \qquad \text{Eq. 42}$$

Where $a_{H_3O^+}$ and a_{OH^-} represent the activities of the ions. The value of K_w for water depends on temperature. At 25°C, water dissociation constant K_w is 1.008 x 10^{-14}, which is sufficiently close to 1.00 x 10^{-14}.

Pure water is known to be neutral solution because it has a hydronium ion concentration of 1.00 x 10^{-7} M and a pH of 7.00.

$$[\mathrm{H_3O^+}]^2 = \sqrt{1.00 \times 10^{-14}} = 1.00 \times 10^{-7} \qquad \text{Eq. 43}$$

Today, the determination of pH has grown to be one of the most frequent quantitative analytical measurements. However, its potentiometric determination is not deprived of complications such as the meaning of pH.

Sørensen developed a simple way of expressing hydrogen ion concentrations in form of numerical pH scale [34]. The pH unit measures the degree of acidity or basicity of a solution. Most water solutions have a pH in the range from 0 to 14, corresponding to - $\log(1)$ to - $\log(10^{-14})$. Water solution always contains $\mathrm{H^+}$ and $\mathrm{OH^-}$ ions. Neutral solution, such as water, contains same amounts of both ions $[\mathrm{H^+}] = [\mathrm{OH^-}] = 10^{-7}$ and its pH is 7. Acidic solutions have a higher relative number of hydrogen ions $(\mathrm{H^+})$ than hydroxide ions $(\mathrm{OH^-})$ and have pH values of less than 7, while alkaline solutions have pH values greater than 7 and there is more $\mathrm{OH^-}$ than $\mathrm{H^+}$ as shown is Figure 2-7.

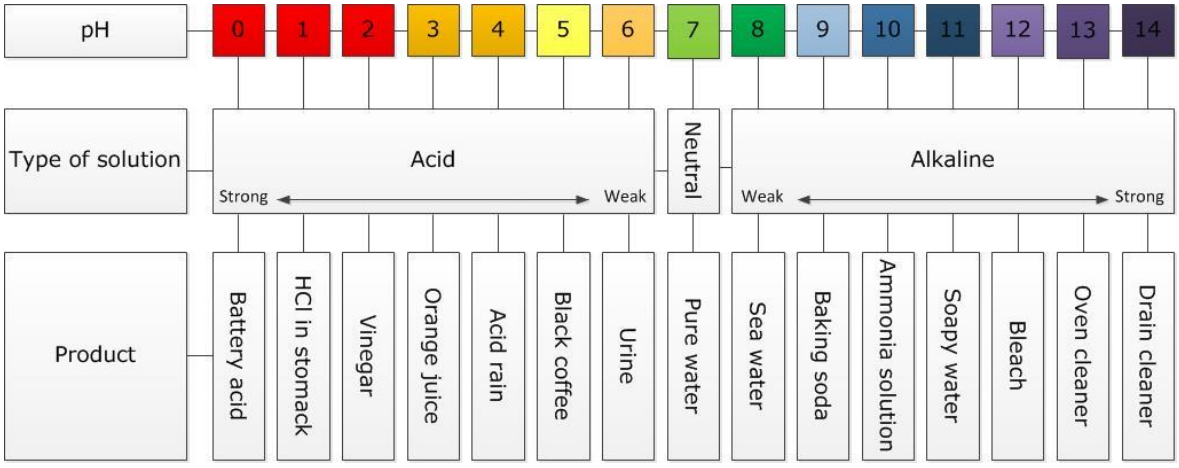

Figure 2-7: pH values in some common products (after Plambeck [33]**)**

The solution's pH can be measured in two ways: using indicators or by existing electrochemical cell. The indicators are cheaper and easier option but are not the best solution. Instead of them, in the situation when digital data and continuous monitoring is required, electrochemical cells are in operation.

2.2.8 Nernst Equation and pH

The pH of a solution can be determined by a potentiometric pH sensor where the potential difference between two electrodes, i.e. an indicating electrode and a reference electrode, is measured. The glass electrode is an ideal indicator electrode used for pH measurements [37, 38]. It allows a direct measure of a_{H^+} and thus of $-\log_{a_{H^+}}$, which is the pH. The potential of the external surface (membrane) of the glass electrode corresponds to the potential of the hydrogen gas electrode (E_H), the primary reference for hydrogen ion measurements.
The electron transfer half-reaction of the hydrogen electrode is [38]:

$$H_{2\,(g)} \leftrightarrow 2H^+ + 2e^- \qquad \text{Eq. 44}$$

The pH cell consists of a reference electrode of constant potential, a liquid junction, and an indicator electrode. Its potential changes with hydrogen ion activity (a_{H^+}) in accordance with Nernst equation in the same manner as hydrogen gas electrode potential (E_H) [37]:

$$E_H = E^\circ - \frac{RT}{F} \ln \frac{1}{a_{H^+}} \qquad \text{Eq. 45}$$

By convention, $E^\circ = 0$ for the hydrogen electrode at $25℃$. It will not usually be so for a glass electrode. The changes in the electrode potential (E_e) and the activity of hydrogen ions (a_{H^+}) can be presented by Nernst equation:

$$E_{\text{glass wall/solution}} = \frac{2.303\ RT}{F} \log_{(a_{H^+})} \qquad \text{Eq. 46}$$

The glass membrane has two wall/solution interfaces. The potential builds up on each of them potential of a glass electrode is a logarithmic function of hydronium activity Eq. 45 and it can be presented as a linear function of pH:

$$E_{Gl} = E^\circ_{Gl} - \frac{2.303\ RT}{F} pH \qquad \text{Eq. 47}$$

The reduction potential thus decreases by 2.3RT/F = 0.059 V per pH unit. At standard temperature $\mathrm{T} = 298\ \mathrm{K}$, the value of $\frac{2.303\mathrm{RT}}{\mathrm{F}}$ term equals to $0.05916\ \mathrm{V}$ and the above equation turns into:

$$\mathrm{E}_{\text{glass electrode}} = \mathrm{E}^{\circ} - 59.15\ \mathrm{pH} \qquad \text{Eq. 48}$$

2.3 Reference Electrodes

2.3.1 Commercial Reference Electrodes

In an electrochemical cell linked by the voltmeter, one half-cell (a reference electrode) provides a known potential and the other half-cell (a working electrode) indicates the analyte's concentration. The reference electrode is used as a reference point because ideally it should provide a stable/constant electrochemical potential over time that is well defined and reproducible as well as independent from changing temperature or analyte ions in solution. There is no a single reference electrode that will satisfy all the requirements of an ideal reference electrode. As a result, there are few different electrode types on a market that appear more often than others as reference electrodes appear and are suitable in many specific applications. The following three sections present a brief description of three common commercially available reference electrodes (the hydrogen electrode, the saturated calomel electrode and the silver chloride electrode) and miniaturised thick-film Ag/AgCl reference electrodes as an alternative to the conventional Ag/AgCl reference electrode.

2.3.1.1 Standard Hydrogen Electrode

The commercial references electrodes are calibrated with respect to the fundamental reference electrode, which is a standard hydrogen electrode (SHE).

The SHE, shown in Figure 2-8, is the usually chosen standard reference point for standard electrochemical reduction potential $\mathrm{E}^0$with a half-cell potential arbitrary assigned a value of zero ($\mathrm{E}^0 = 0.000\ \mathrm{V}$) at all temperatures by convention [39].

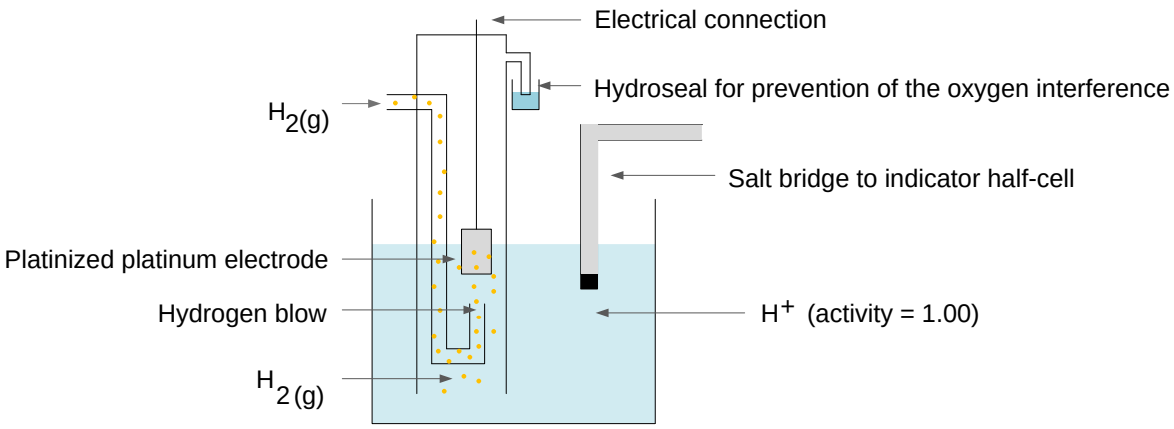

Figure 2-8: Schematic diagram showing the Saturated Hydrogen electrode (SHE)

It is made up of a platinum electrode immersed in a solution in which the activity of hydronium ions (H_3O^+) is equal and the hydrogen must be at 25°C and 1atmospheric pressure. The half-cell reaction for the SHE is as follows [38]:

$$H_{2\,(aq)} \leftrightarrow 2H^+_{(aq)} + 2e^- \qquad \text{Eq. 49}$$

while the Nernst equation is [38]:

$$E = \frac{RT}{F} \ln \frac{a_{H^+}}{(p_{H^+}/p^0)^{1/2}} \qquad \text{Eq. 50}$$

where R is the universal gas constant $(JK^{-1}mol^{-1})$, T is the temperature (K), F is the Faraday's constant $(C\,mol^{-1})$, a_{H^+} is the activity of hydrogen ions in the electrolyte, p_{H_2} is the partial pressure of hydrogen gas (Pa) and p^0 is the standard pressure $(10^5 Pa)$. The hydrogen ion activity, implied by the Nernst equation, is primarily responsible for the observed potential [40]. The SHE theoretical potential is estimated about 4.44 $\pm$ 0.02 V at standard conditions of 25°C.

Despite its importance, this electrode is not practical and rarely used for routine analytical work. Most experiments carried out in aqueous solutions utilize one or two other common reference electrodes, such as the saturated calomel electrode (SCE) or the silver/silver chloride electrode.

2.3.1.2 Saturated Calomel Electrode

The calomel electrode is one of the most common reference electrodes used for measurements in aqueous solutions. The electrode design consists of mercury element (Hg) covered by a solid mercury chloride paste (Hg_2Cl_2), also known as calomel, attached to a rod that is immersed in a saturated KCl solution encapsulated inside a glass tube that has a porous salt bridge to allow the electrons to flow back through (Figure 2-9). When potassium chloride solution is saturated, the electrode is known as saturated calomel electrode (SCE).

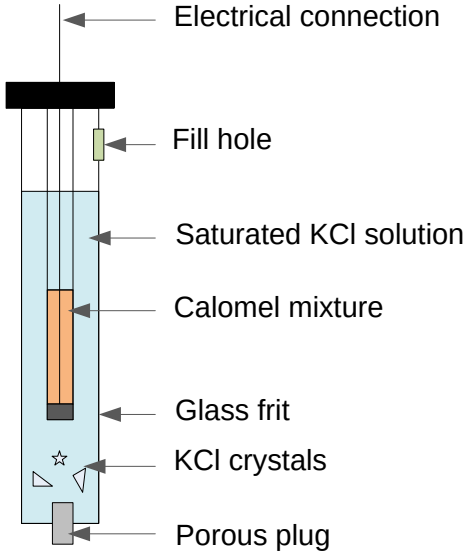

Figure 2-9: Schematic diagram showing the Saturated Calomel electrode (SCE)

The calomel electrode is based on the following redox reaction [38]:

$$Hg_2Cl_{2(s)} + 2e^- \leftrightarrow 2Hg_2^{2+} + 2Cl^-_{(aq)} \qquad \text{Eq. 51}$$

for which the Nernst equation is [24, 38, 40, 41]:

$$E = \underbrace{E^0_{Hg/Hg_2^{2+}} + \frac{RT}{2F}\ln K_s}_{E^0_{Hg_2Cl_2}} - \frac{RT}{F}\ln a_{Cl^-} \qquad \text{Eq. 52}$$

where the activity solubility product of mercurous salt chloride K_s is [38]:

$$K_s = a_{Hg_2^{2+}} \cdot a_{Cl^-}^2 \qquad \text{Eq. 53}$$

The saturated calomel reference electrode has a big disadvantage such as being toxic at vapour phase and liquid at room temperature.

2.3.1.3 Silver-Silver Chloride Electrode

The conventional commercial silver-silver chloride electrode, shown in Figure 2-10, is arguably the most practical and far more frequently used by practitioners reference electrode in industry and research [42].

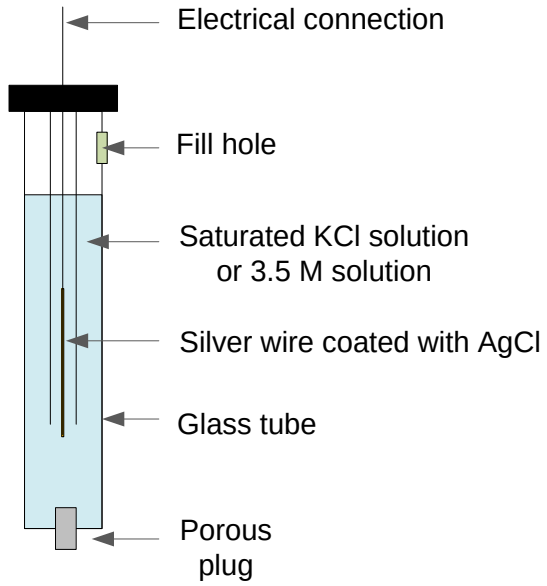

Figure 2-10: Schematic diagram showing the Ag/AgCl reference electrode

It consists of a Ag metal wire partially electroplated/chloridised with AgCl which is immersed in a saturated filling solution of AgCl (approximately 3.5 M). The electrode performance is affected by the thickness of silver chloride coating. To achieve an invariant electrode potential about 20% of the wire must be transformed to silver chloride [38]. The silver-silver chloride electrode internal element is enclosed in a glass or plastic cylindrical tube separated from the test solution via a microporous plug, made of ceramic or frit, which forms the liquid junction with the external test solution [43]. The

silver-silver chloride layer forms the interaction between the ion movement in the KCl solution and the electron movement in the silver wire. In the idealised system, the internal element is at equilibrium.

The overall electron-transfer reaction of the classic Ag/AgCl reference electrode can be given by the expression:

$$\mathrm{AgCl_{(s)} + e^- \leftrightarrow Ag_{(s)} + Cl^-_{(aq)}} \qquad \text{Eq. 54}$$

The electrode response is made of two simultaneous reactions on the surface in contact with the solution. The first one is the oxidized reaction where the electrode silver metal forms an equilibrium reaction:

$$\mathrm{Ag_{(s)} \rightarrow Ag^+_{(aq)} + e^-} \qquad \text{Eq. 55}$$

The second one is the reversible reduction reaction that depends on the solubility of silver chloride in water:

$$\mathrm{AgCl_{(s)} \rightarrow Ag^+_{(aq)} + Cl^-_{(aq)}} \qquad \text{Eq. 56}$$

The symbols (aq) indicate that the $\mathrm{Ag^+}$ ions and the $\mathrm{Cl^-}$ ions are surrounded by the water molecules that are in the solution.

The potential (E) of the electrode is defined by the Nernst equation [38]:

$$\mathrm{E = E^\theta - \left(\frac{RT}{F}\right) \ln\left(a_{Ag^+}\right)} \qquad \text{Eq. 57}$$

The silver-silver chloride halide reference electrode belongs to the second kind of reversible electrodes where a solid phase in the form of sparingly soluble $\mathrm{AgCl_{(S)}}$ salt is in equilibrium with a saturated solution of the same salt participating in the electrode reaction like the one demonstrated in Eq. 56. The equilibrium constant expression (K) is:

$$\mathrm{K = \frac{a_{Ag^+} \cdot a_{Cl^-}}{a_{AgCl}}} \qquad \text{Eq. 58}$$

The activity of solid AgCl in the solution is equal to 1, i.e. $\mathrm{a_{AgCl} = 1}$; therefore the electrode activity depends only on the oxidized reaction Eq. 55 where the $\mathrm{Ag^+}$ ion

activity controlled by the activity solubility product (K_{sp}) is constant at a given temperature [38]:

$$K = K_{sp} = a_{Ag^+} \cdot a_{Cl^-} = \gamma_+ c_{Ag^+} \gamma_- c_{Cl^-} \quad \text{Eq. 59}$$

Where a_{Ag^+}, a_{Cl^-} are activities of cation and anion, c_{Ag^+}, c_{Cl^-} are concentrations of cation and anion, γ_{Ag^+}, γ_{Cl^-} are ionic activity coefficients.

2.3.2 Thick-Film Ag/AgCl Reference Electrode Structures

For a long time, a substantial effort has been put in the development of miniaturised all-solid-state environmental sensors often integrated onto a single piece of substrate. To characterise those potentiometric electrochemical devices a conventional electrolyte filled reference electrode is employed. Those reference electrodes are made from glass causing them to be fragile and therefore not practical for in-situ environmental monitoring measurements. In addition, miniaturised applications are nowadays highly desirable. To overcome this problem many attempts have been made to design a solid-state reference electrodes with properties completely identical to the commercially-available reference electrodes but this dilemma is still not achieved [43].

The major challenges with reference electrode are their long-term stability (they tend to drift after a certain amount of time depending on their construction), accuracy and reliability. Those three major problems have been investigated by many researches. In 1890, Ostwald introduced the calomel electrode used as a reference electrode for glass pH electrode measurements. The mercury used in this type of electrode is highly toxic and, from environmental concern, deemed unsafe to use [44]. The Ag/AgCl reference electrode is the most attractive reference electrode employed in the environmental measurements. Satochi Ito et al. [44] stated that the continuous exudation of KCl in the reference electrodes is said to be the most important parameters for the electrode reliable performance. They also brought to light a problem of metallic silver (Ag) and silver chloride possibly effusion into sample solution via a liquid junction frit. To overcome this dilemma, a double junction electrode was developed by putting chelating resins in 3M KCl solution in the outer chamber. The inner chamber of a conventional Ag/AgCl reference electrode in 3M

KCl solution was placed. Ceramic junction connected the two chambers. The outcome of the reference electrode operation shows that chelating resins can eliminate Ag ions in the KCl inner solution and therefore the reference electrode operated for a long period.

Most laboratory equipments used for chemical analysis are based on the classic silver-silver chloride (Ag/AgCl) reference electrodes which are made up of a liquid filled tube making the electrode fragile and inappropriate for in situ measurements outside of the laboratory environment, and therefore miniaturized versions are desired [10]. Atkinson et al. combined several chemical sensors in a compact device made with a thick-film technique [45]. They presented benefits of using the thick-film technique by developing small, robust, cost competitive, disposable batches of an integrated sensor arrays containing elements capable of sensing simultaneously a variety of different measurands such as temperature, conductivity, pH, dissolved oxygen and redox potential. The authors tested two different types of reference electrodes, the polymer Ag/AgCl electrodes and the glass silver chloride electrodes (Figure 2-11).

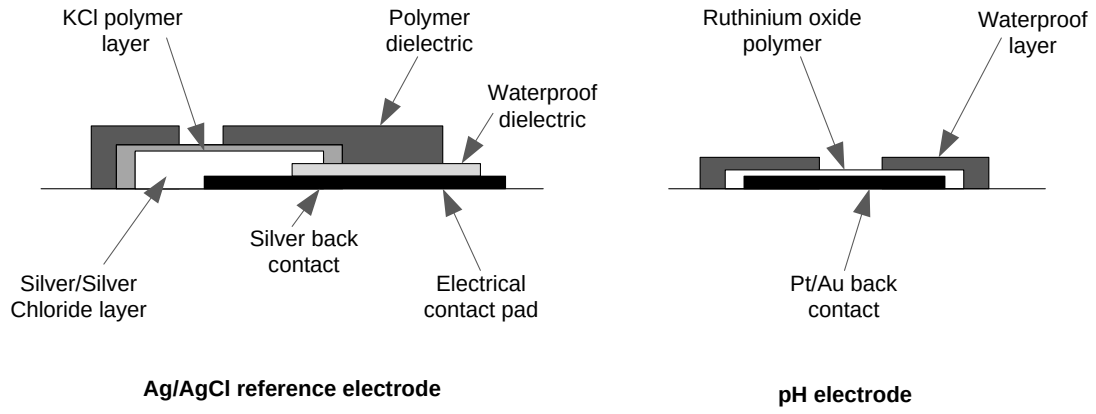

Figure 2-11: Cross-sections of reference electrode and pH electrode showing individual layers [45]

Cranny and Atkinson in 1998 called the scientific community attention to a miniaturized, low cost Ag/AgCl chloride reference electrode produced using thick-film printing techniques [9]. Their thick-film reference electrode version was mimicking the traditional, bulky and expensive single junction Ag/AgCl reference electrode. Several variations in the basic electrode design were fabricated using three different types of pastes for the Ag/AgCl layer: a commercially available

polymeric Ag/AgCl paste (GEM, C50672R1) and two in-house formulated glassy AgCl and glassy Ag/AgCl pastes with distinct silver-to-silver chloride ratio. In addition, the salt matrix layer (the potassium chloride layer) that overprinted the Ag/AgCl layer was formed from glass or polymer based inks depending on the underlying Ag/AgCl layer ink type. The Figure 2-12 shows the electrode structure.

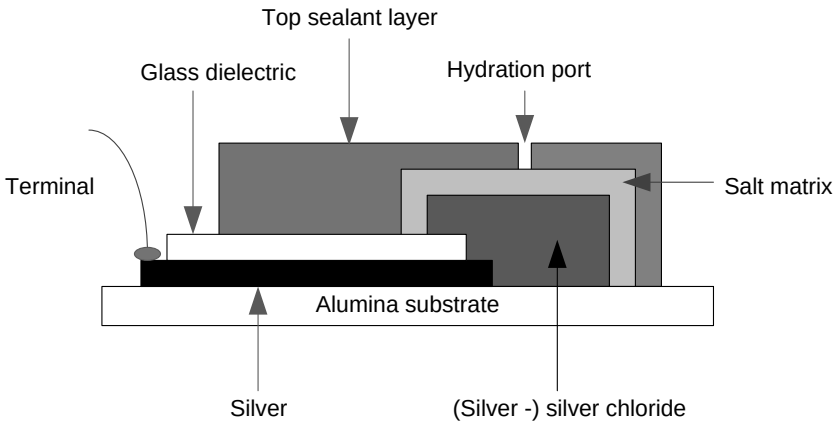

Figure 2-12: Thick-film Ag/AgCl reference electrode cross section [9]

The paper has introduced the new salt matrix electrolyte layer and attempted to explain the losses, which may depend on the choice of the top sealant and size of the hydration port. By correct choice of these two, it should be feasible to design a reference electrode that loses salt in controlled manner. This paper gave foundation to the further research work described thoroughly in Chapter 3Chapter 4 and Chapter 5 in this thesis, which brings some new ideas to initial work on Ag/AgCl reference electrode by Cranny and Atkinson. Attempts at solid-state Ag/AgCl reference electrodes have been reported employing various techniques appropriate for the specific application of the electrode [10, 40, 43, 46, 47].

In 1977, Desmond et al. studied two types of Ag/AgCl micro reference electrodes fabricated by combining silicon fabrication and screen printing technologies [4]. They analysed the performance of a commercially available macro solid-state reference electrode, called MacroReflex. Both reference electrodes, Type 1 and Type 2, were made of a silver/silver chloride ink screen printed onto platinum on silicon (Figure 2-13). Type 2 Ag/AgCl was also covered with a chloride doped vinyl ester resin to make a miniaturised version of the MacroReflex reference electrode

and to mimic its behaviour. The MacroReflex reference electrode has a silver/silver chloride wire inside covered with a chloride doped vinyl ester resin.

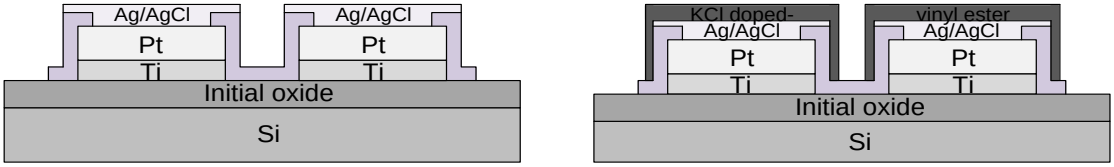

Type 1 Ag/AgCl

Type 2 Ag/AgCl

Figure 2-13: Type 1 Ag/AgCl (a) and type 2 Ag/AgCl (b) reference electrode cross section [4]

The potential difference, between the electrodes and a saturated calomel electrode, was evaluated and measured in various KCl solutions over different time scales at 25°C. The results showed that the Type 1 Ag/AgCl reference electrode acted as a chloride selective electrode with a slope of 55.83 mV per decade for chloride activity, which gave near-Nernstian response of 59.2 mV per decade at 25°C. There has been a drawback of the solid-state electrode, with no internal electrolyte solutions, that required a constant chloride concentration in the solution at all times during an analysis to maintain a fixed potential. Type 2 Ag/AgCl reference electrode together with MacroReflex reference electrode have shown some promising results. The MacroReflex reference electrode has demonstrated greater insensitivity to chlorides (of a mean potential -32.6 mV with associated standard deviation of 0.1 mV) than Type 2 Ag/AgCl reference electrode (a mean potential of -11.7 mV and standard deviation of 0.7 mV). These distinctions between the last two types of electrodes could emerge from the KCl distribution in the vinyl ester resin. The Type 2 Ag/AgCl reference electrode has combined two methods: a screen printing technique for inside electrode layers and a manual method using a micropipette tip to dispense the homogenous mixture of KCl doped-vinyl ester for the cover layer. This paper has presented an interesting manufacturing technique. However, the fabrication process needs some improvement in the way the KCl is distributed in the vinyl ester mixture material.

The main advantage of thick-film electrodes is their low cost in mass production. They require minimal in-situ treatment and this is becoming increasingly important

in analytical chemistry. Mroz et al. concentrated on the above attributes [48]. They developed a disposable reference electrode, which can be used for environmental analysis. The Ag/AgCl reference electrodes possessed an integrated junction made of a glass-fibre filter with the internal electrolyte and screen-printed heat-sealing film encapsulated by lamination (Figure 2-14).

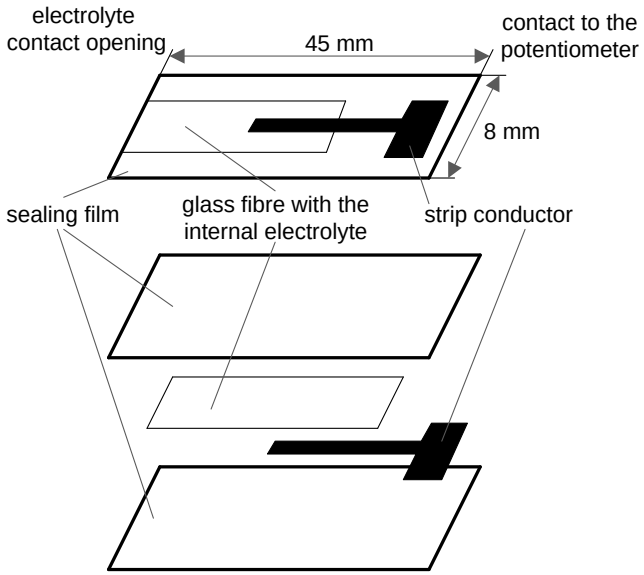

Figure 2-14: Schematic view of the disposable reference electrode [48]

The aim of the experiment was to specify if the disposable Ag/AgCl reference electrode would have a stable potential, which is not influenced by the composition of the analyte solution, and to test its shelf life. The findings showed that the thick-film Ag/AgCl reference electrode has a repeatable response (54.9 mV per decade) in solutions of different compositions and has a long shelf-life plus sufficient operational lifetime. The role of the reference electrode in the electrochemical system is to provide a stable potential with respect to the potential of another electrode. The thick-film Ag/AgCl reference electrode developed by Mroz et al. meets this requirement. This paper has proved that the method described is suitable for the mass production of disposable and low cost thick-film reference electrode.

L. Tymecki et al. [6] used thick-film technology to develop a planar Ag/AgCl/KCl reference electrode. All elements of the electrode such as a layer of Ag/AgCl (inner electrode), an immobilized electrolyte (junction) and an encapsulation were fabricated by means of screen printing technology. In the fabrication process simple,

inexpensive and commercially available materials, such as flexible, plastic substrate and easily cured low temperature polymer-based pastes were used. Potentiometry allowed various in-situ medical and environmental tests to be carried out using Ag/AgCl/KCl reference half-cell.

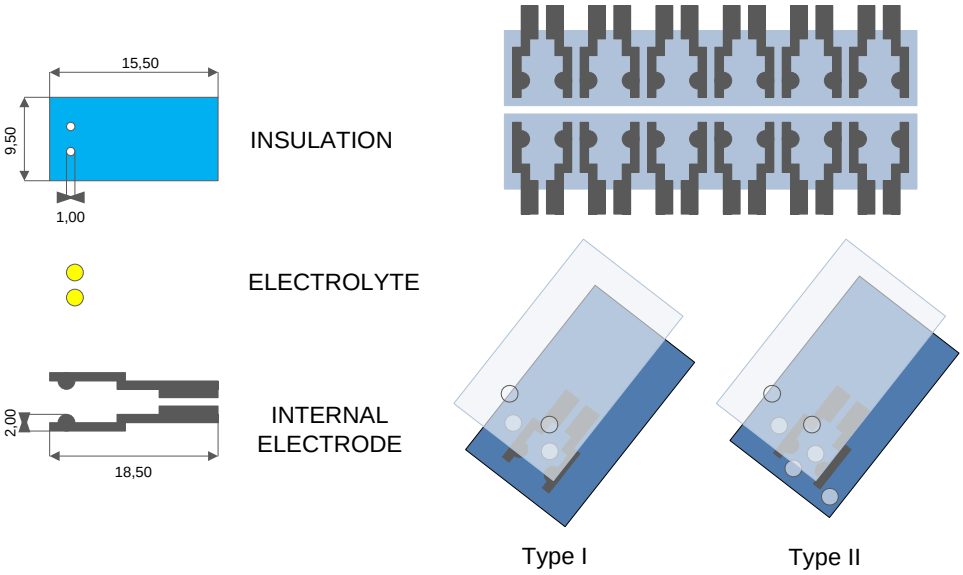

Figure 2-15: Thick-film reference electrode design [6]

Two different types of the thick-film reference electrodes were tested (Figure 2-15). In both of them, the same highly hydrophobic Ag/AgCl paste, being simultaneously conductor and sensing layer, was used. Electrode Type I consisted of three layers printed on polyester flexible foil: Ag/AgCl paste (inner electrode and an electric contact), protective paste filled with KCl powder (electrolyte layer) and non-modified protective paste (insulation). Electrode Type II had four printed layers on polyester flexible foil: a protective paste doped with KCl, Ag/AgCl paste, protective paste doped with KCl and non-modified protective paste. The developed reference electrodes exhibited good long-term (at least 9 months) storage stability evaluated under ambient conditions, such as dry storage without humidity and temperature control. Their operational lifetimes were limited due to electrolyte leakage. Electrode Type II with double thick-film of electrolyte exhibited slightly longer operation stability (over one week) than the electrode with single thick-film electrolyte (less than one week). The potential has been monitored after addition of various chemicals to the solutions and it had been invariant to it. This paper has shown an interesting

approach of a ‘sandwich’ layered reference electrode with use of a conductor-sensing Ag/AgCl paste and not penetrable by water KCl-free films. However the particles of KCl protective paste were forming micro channels and slightly unsealed the film.

Cranny et al. [49] at the University of Southampton in 2011, has produced a thick-film silver-silver chloride electrode, based on commercial thick-film dielectric paste and non-commercial pastes formulated with a glass binder, for detection of chloride ions concentration in soil over time. The chloride responses observed over the first 162 days for all formulations were almost identical and gave near Nernstian responses of -51.12 ± 0.45 mV/decade(Cl^-). The devices with pastes formulated with glass binder began to exhibit a loss in sensitivity after 6 months in contrary to the electrodes formulated from a commercial dielectric paste. The investigation demonstrated conclusively that the Ag/AgCl electrodes lifetime performance difference was due to the inclusion of proprietary additives in the commercial paste aiding adhesion and minimising AgCl leaching. This chloride sensor was tested in 2016 at different depths in a soil column in controlled laboratory-based experiments but also the initial experiments were conducted outside of the laboratory at multiple points in situ such as a fluvarium and in a greenhouse [50]. The sensor allowed real-time measurements of chloride concentration in soil and in water and had a lifetime comparable with typical crop-growing seasons. The experimental data was collected with simple logging electronics that allowed to measure and track the movement of chloride over small distances in the real environment.

2.3.3 Novel Planar Thick-Film Ag/AgCl Reference Electrodes Structure

TF screen-printed silver-silver chloride (Ag/AgCl) reference electrodes have been fabricated and investigated as an alternative to liquid electrolyte Ag/AgCl reference electrodes. TF reference electrodes reported here are fabricated as screen-printed planar electrodes with a halide salt containing polymer layer deposited on top of the electrode to give some measure of electro-potential stability in a similar manner to that of a conventional electrolyte filled silver-silver chloride reference electrode (Figure 2-16).

Figure 2-16: Comparison of the conventional silver-silver chloride reference electrode (right) and the thick-film screen printed (left) ones, shown on same scale

Table 1: Conventional Ag/AgCl reference electrode versus thick-film Ag/AgCl reference electrode

Conventional Ag/AgCl reference electrode	**Thick-film Ag/AgCl reference electrode**
Fragile	Robust
Expensive to fabricate	Low production cot, simple fabrication technique, mass production, disposable
Bulky	Miniaturised, a variety of sensors integrated on a single substrate
Liquid filled saturated KCl electrolyte	Solid state

The constructions of the TF Ag/AgCl reference electrodes and the conventional Ag/AgCl reference electrodes are shown in Figure 2-17.

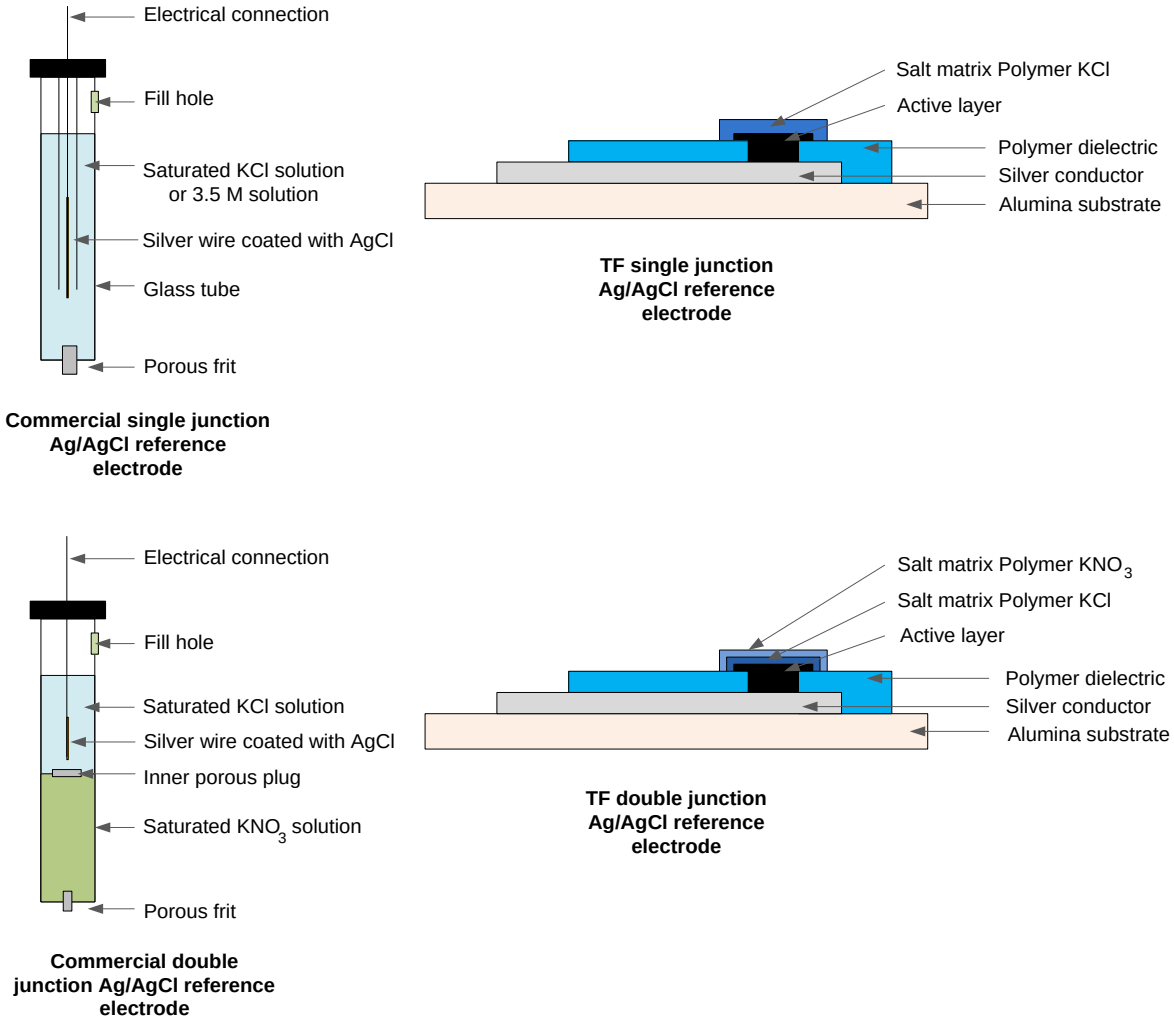

Figure 2-17: Constructions of the conventional reference electrodes vs. the TF Ag/AgCl reference electrodes

Details of the component materials and fabrication procedure employed for the suggested TF Ag/AgCl device were documented in Chapter 3. The typical planar structure of the thick-film equivalent consists of a silver back contact, a waterproofing layer, a silver-silver chloride interfacial layer and one or more overlapping salt matrix layers containing typically potassium chloride (KCl) powder in a lower layer and potassium nitrate (KNO_3) powder in an upper layer. This double layer approach mimics the double junction type of liquid electrolyte reference electrode that typically contains two liquid electrolytes separated by an inner porous plug.

An array of such sensors can be designed economically such that many of the individual layers of the sensors are fabricated simultaneously with those of their neighbours. For example, many of the underlying conductor materials and overlying waterproofing materials are common to more than one of the sensing elements in the array.

The TF Ag/AgCl electrode attempts to mimic the operation of commercial silver-silver chloride reference electrode (Beckman Coulter 57193). It does this through the immobilizing of halide salt reservoirs in the form of a solid salt matrix layer fabricated as an upper layer of a planar design that is in contact with the analyte [7, 42]. This idea was previously documented by Mroz, Tymecki, Simmonis and Maminska [6, 48, 51, 52].

The following semi reaction occurs on the TF Ag/AgCl reference electrode:

$$AgCl_{(s)} + e^- <=> Ag_{(s)} + Cl^-_{(aq)} \quad \text{Eq. 60}$$

It is made of two following equilibrium reactions [38]:

$$Ag^+ + Cl^- \leftrightarrow AgCl_{(s)} \quad \text{Eq. 61}$$

$$Ag^+ + 1e^- \leftrightarrow Ag^0 \quad \text{Eq. 62}$$

The potential of the electrode can be determined by two different Nernst equations [42]:

$$E = E^\theta + \frac{RT}{nF} \ln\left(\frac{a_{Ag^+_{(aq)}}}{a_{Ag_{(s)}}}\right) \quad \text{Eq. 63}$$

$$E = E^\theta + \frac{RT}{nF} \ln\left(\frac{\left(a_{Ag^+_{(aq)}}\right)(a_{Cl^-})}{\left(a_{AgCl_{(s)}}\right)}\right) \quad \text{Eq. 64}$$

The activity of species, a, is defined as the product of the activity coefficient of specific substance and its concentration. When the species is at its standard state the activity coefficient can be approximated to 1. In the case of AgCl and Ag, since they are in the solid state, their activity can be equated to their concentrations. Therefore, the electrode potential can be expressed as:

$$E = E^{\theta} - \left(\frac{RT}{nF}\right)\ln[a_{Cl^-}] + \left(\frac{RT}{nF}\right)\ln\left(\frac{[AgCl]}{[Ag]}\right) \quad \text{Eq. 65}$$

For low chloride ion concentration, the activity coefficient of chloride ions can also be taken as unity [53-55]. The number of electrons involved in the reaction is 1.

The Eq. 65 can be written in simplified form:

$$E = E^{\theta} + 0.0592\log(K_{sp}) - 0.0592[Cl^-_{(aq)}] \quad \text{Eq. 66}$$

The potential of a Ag/AgCl is dependent upon variation in concentration of chloride ions in the electrolyte. The electrode is said to have a Nernstian response with respect to the chloride ion concentration. The potential will decrease by 59.2 mV for every decade (10 fold) increase in chloride ion concentration. In the situation when the concentration of chloride ions is constant then the potential of the Ag/AgCl electrode is also constant at fixed temperature.

2.4 pH Ion-Selective Electrodes

The pH of a solution can be determined by a potentiometric pH sensor where the potential difference between two electrodes, i.e. a pH sensitive electrode and a reference electrode, is measured. The reference electrode provides a stable constant reference potential regardless of the solution in which is immersed while the ion-selective electrode (ISE) responds to the change of the hydrogen ion (H^+) concentration in the solution. The theory of potential difference calculation according to the Nernst equation was discussed in Chapter 2, section 2.2.6.

A schematic of a potentiometric electrochemical cell is illustrated in Figure 2-18. It consists of two electrodes called the indicator electrode (also called the ISE) and reference electrode. They are used under no current flow in conjunction with a high impedance voltmeter to complete the measuring circuit.

The glass electrode is the most reliable and well-characterised electrochemical sensor commonly used for pH measurement in aqueous solutions (Chapter 2, section 2.4.1). However, it is made of fragile glass membrane and not stable in

aggressive electrolytes. Traditional glass membrane pH electrode employs potentiometric method to continuously measure the pH of a solution.

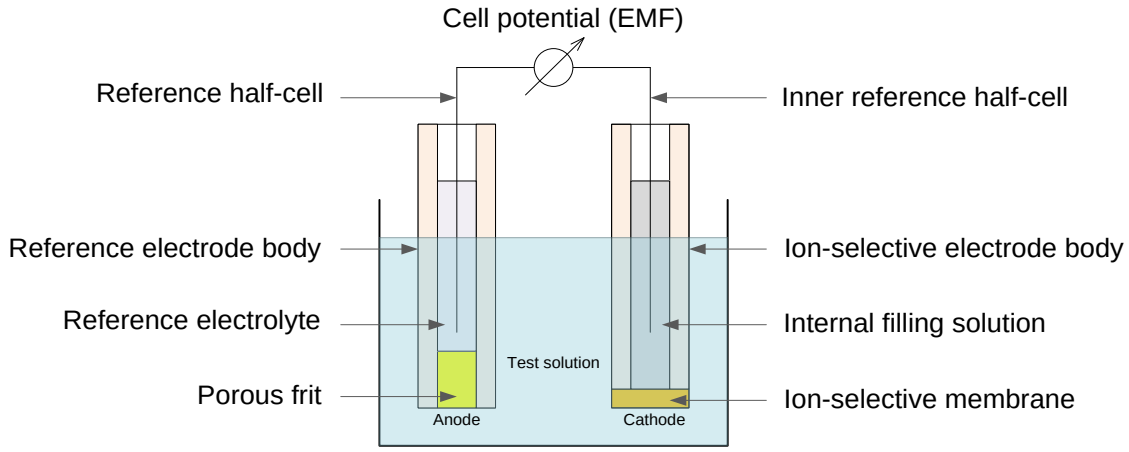

Figure 2-18: A typical electrochemical cell configuration with two electrodes

Recently, a high demand for non-expensive, non-fragile and on-line chemical sensors brought metal oxides such as platinum oxide (PtO_2), iridium oxide (IrO_2), ruthenium oxide (RuO_2), osmium oxide (OsO_2), tantalum oxide (Ta_2O_5) and titanium oxide (TiO_2) to light to be used along with the glass pH electrode for pH sensing [56-59]. In the next chapters the structure of thick-film screen-printed ion-selective electrodes based on solid-state materials are presented.

2.4.1 Thick-Film pH Ion-selective Electrode Structures

In 1984, Fog and Buck reported the fundamentals of ion-exchange electrodes. They demonstrated the properties of the response of electronically-conducting oxides, such as PtO_2, IrO_2, RuO_2, OsO_2, Ta_2O_5 and TiO_2, as pH sensors [56]. Those metal oxides showed near-Nernstian behaviour in the pH range 2-12. They are insoluble and stable in aqueous environments and were considered as alternative pH-sensor materials. Fog and Buck's work was innovative at that time and their findings have led to further research in electrochemical field.

In 1998, J.A. Mihell and J.K. Atkinson reported planar electrodes for the potentiometric measurements of pH [58]. The manufacturing process involved thick-

film screen printing techniques. The active layer of the electrodes was based on two components: a ruthenium oxide hydrate and a polymer matrix (Figure 2-19).

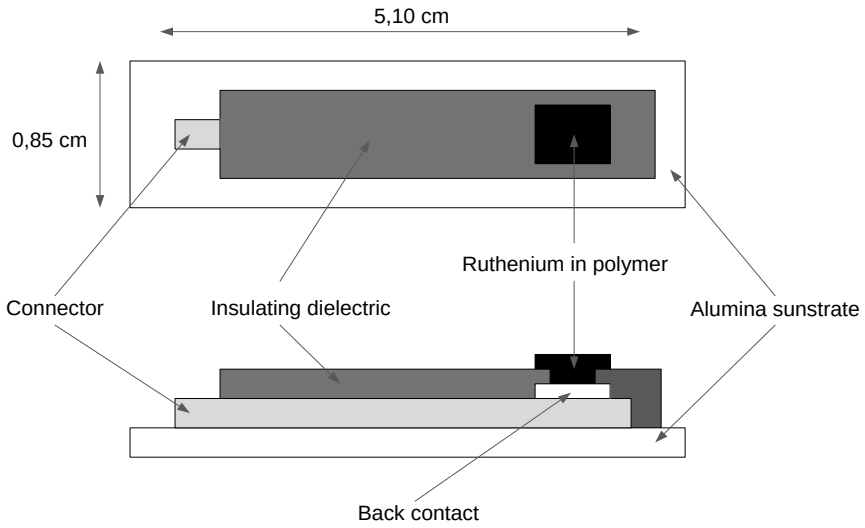

Figure 2-19: Thick-film pH electrode cross section [58]

Mihell and Atkinson have substantiated Fog and Buck's findings. They have demonstrated the general mechanism, which describes the response of metal oxides to pH, and have suggested that pH response could be due to ion exchange in a surface layer containing OH^- groups. The electrodes have been demonstrated to act as Nernstian pH sensors with quite fast response to changes in pH. They have shown near-Nernstian behaviour (-59.15 mV/pH) in the pH range 2-10 similar to theoretical mechanisms for metal oxides pH response. This paper has laid foundations for the further research work described thoroughly in Chapter 4 and Chapter 5.

Liu et al. [60] developed a new kind of thick-film pH sensor with thick-film heater. This solid-state pH sensor can be a substitute for the traditional sterilizable pH glass electrode for which fabrication is complicated and the bubble of the glass electrode can be easily broken. The experimental process contained several steps. Firstly, pastes were prepared by mixing sensitive powders such as Li_2O, CaO, Na_2O, SiO_2 and an organic vehicle. They were printed on Al_2O_3 substrate with Pt-based thick-film conductors and then they were fired.

After that, the thick-film heater for sterilization was made on the back of the pH sensor. The sensor structure was sturdy and durable. The presence of the thick-film heater has shown good stability and allowed the sensor to be sterilized at 140˚C. Lastly, the thick-film pH sensors can be fabricated easily, have high sensitivity and good repeatability, but their response time, less than 2 min on average, is long. This paper has presented an easy approach to utilise thick-film technology in the design of the heater for sterilization. The thick-film technique allowed the ink, used in the manufacturing process, to be arranged in the preferred pattern, density and to concentrate the power exactly where it is needed.

R. Koncki and M. Mascini in 1997 presented plastic, screen printed and disposable ruthenium dioxide electrodes for pH measurements as the alternatives for glass electrodes which are expensive and easy breakable [57]. In this work low-firing temperature inks have been used on the polyester foil. The electrodes had low resistance therefore, there is no need for special, high input impedance equipment. They have enabled fast measurements, with good sensitivity (51 mV/pH). They are cheaper, robust and can tolerate operation in aggressive environments, with linear range of response up to pH=8, at high temperatures. This paper has demonstrated conclusively that thick-film technology is a cheap, simple and mass production process, which predominantly was used for fabrication of amperometric devices and now can be potentially useful for the fabrication of some potentiometric sensors.

In 1995, McMurray, Douglas and Abbot described novel thick-film metal oxide electrodes (MOEs) based on ruthenium dioxide-glass composites sintered onto Pyrex glass substrate [61]. The screen-printed inks (ink I and ink II) of the composites consisted of submicron particles of RuO_2 and high order lead silicate, or borosilicate, glass dispersed in a viscous organic liquid (terpineol). Three MOEs were fabricated.

The first electrode, electrode A (Figure 2-20), was made manually by painting the pattern onto an 8 mm diameter Pyrex glass rod using ink I (0.5 g $RuO_2 \cdot xH_2O$ powder, 0.5 g of lead borosilicate glass powder with 0.5 g of a 2 % solution of ethyl cellulose in terpineol; a viscous black suspension).

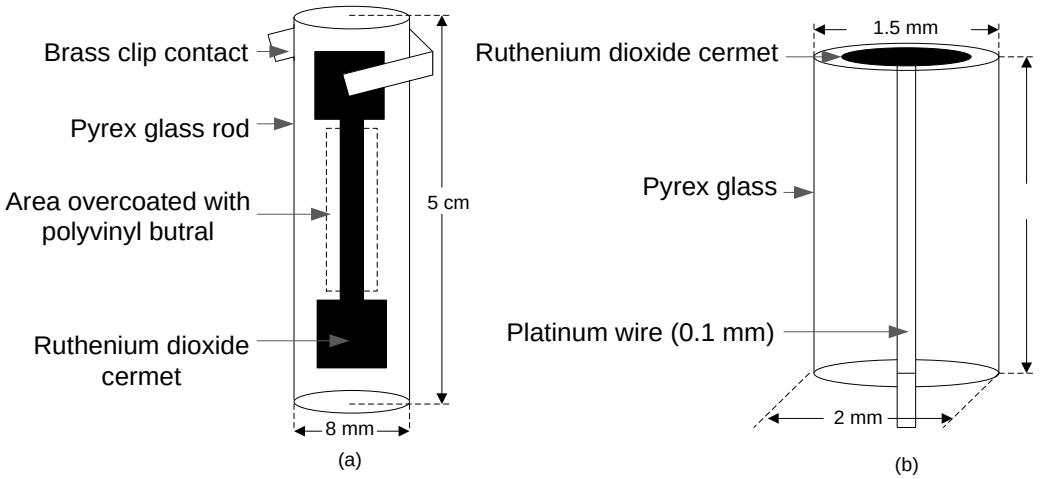

Figure 2-20: (a) Electrode A: physically large electrically free-standing RuO_2-glass composite electrode. (b) Electrode C: physically small RuO_2-glass composite electrode with Pt wire contact underlying the active portion of the electrode [61]

The second electrode B was made in the same manner but with ink II (0.35 g of $RuO_2 \cdot xH_2O$ powder, 0.65 g of lead borosilicate glass powder and 0.5 g of 2% ethyl cellulose in terpineol). The third electrode C (Figure 2-20) had a 1.5 mm diameter disk painted onto the flat ground end of a 2 mm diameter Pyrex glass capillary and inside it a 0.1 mm long platinum was sealed. After that, the ink pattern was converted to RuO_2- glass composite by drying and firing. Potentiometric measurements were obtained versus a saturated calomel reference electrode. The metal oxides electrodes showed a near-Nernstian dependence of potential upon pH in aqueous buffer between pH 2 and 12.

2.4.2 Novel Planar Thick-Film pH Ion-Selective Electrode Structure

The pH sensors consist of two electrodes, an ion-selective electrode and a silver-silver chloride (Ag/AgCl) reference electrode. The metal oxide pH sensors presented in this thesis were based on a polymer bound ruthenium oxide top layer (GEM C50502D7) and a platinum gold conductor (ESL 5837), as shown in Figure 3-16. They were constructed in a similar manner to the TF Ag/AgCl reference electrodes shown in Figure 3-14. TF pH ISEs were tested against a commercial gel-filled single junction Ag/AgCl reference electrode (Beckman Coulter A57193). Ruthenium dioxide (RuO_2) is the most widely promising material used in the working electrode structure

because it have the highest sensitivity to pH changes compared to any other metal oxides tested [58]. The TF ISE were cycled through various pH test solutions in order to ascertain their electrode potential. Fog and Buck suggested the most probable pH response mechanism of ruthenium oxide electrodes that can be represented by the following equilibrium reaction [56]:

$$MO_x + 2\delta H^+ + 2\delta e^- \leftrightarrow MO_{x-\delta} + \delta H_2O \qquad \text{Eq. 67}$$

Where, MO_x is a higher oxidation state metal oxide and $MO_{x-\delta}$ is the lower oxidation state metal oxide. The electrode's potential for this reaction is given by:

$$E = \frac{RT}{F} \ln a^l_{H^+} + \frac{RT}{2F} \ln a^s_O + constant \qquad \text{Eq. 68}$$

Where, $a^l_{H^+}$ is the proton activity in the liquid phrase and a^s_O the activity of oxygen in the solid phase. Activities of solids are defined as unity and the second part of the equation is equal to zero.

In aqueous media ruthenium oxide pH sensors work on another mechanism of only one redox equilibrium between two insoluble ruthenium oxides presented by McMurray et al. [61]:

$$RuO_2 + 2H_2O + H^+ + e^- \leftrightarrow H_2O + Ru(OH)_3 \qquad \text{Eq. 69}$$

The reaction potential being expressed by [61]:

$$E = E_0 - 0.0591\ pH \qquad \text{Eq. 70}$$

Where, E_0 is the standard potential of the cell.

Assuming a near constant activity of the metal oxide, both of these mechanisms predict a Nernstian response of approximately -59 mV/pH, at ambient temperature in aqueous solutions.

2.5 Thick-Film Technology

In the second half of the twentieth century, industry has witnessed a revolution due to the advent of microelectronics. The most significant step in modern electronics was development of the transistor by Bell Laboratories in 1948. The creation of new types of transistor and solid-state diodes opened the door to the new advances in the microelectronic. It helped to drive the development of new and low cost chemical and environmental sensors, which are crucial in measurement and control systems. Microelectronics comprises of important technologies, among which thick-film technology has been reported in the design and construction of new, miniaturised and cost competitive chemical and environmental sensors. The miniaturization trend of chemical sensors started with the introduction of sensing arrays in the early 1970's [12]. Thick-film technology together with electrochemical methods embraces the requirements by giving cost competitive solutions for fabrication of compact, rugged and robust electrochemical devices [45].

2.5.1 History of the Screen-Printing Process

Screen-printing technique is also known as serigraphy and serigraphy printing. The term serigraph derivers from the Latin word *seri,* which means *silk,* and from Greek word *graphos*, meaning to draw and write. The origin of screen-printing evolved from advanced forms of stenciling. The earliest documented examples of it, represent negative prints of the human hand, were found in Paleolithic cave paintings dating from 30,000 B.C [62]. The stencils of primitive cultures were made from perishable materials such as leaves or animal skins. Stenciling methods developed together with the civilization progress: the ancient Egyptians employed stencils to decorate tombs while the Greeks and the Romans used stencils to paint murals or outline mosaics.

The earliest applications of stenciling, which utilize the craft for production purposes, can be found in China during the Song Dynasty (960-1279 AD) [63, 64] and in medieval Japan. At that time some of the most intricate and detailed images were created firstly in China and afterward in Japan. They were made with carved wooden blocks stenciled on paper (China) and on cotton and silk (Japan). The Japanese

used simple stencils glued onto a screen made of human hair that was stretched over a wooden frame.

This more advanced technique spread from Asia to the West of Europe in the 18th century through trade routes and immediately after was used in the rapidly advancing European textile industry. In England, screen-printing was used for wall designs, such as wallpaper in upper-class homes. To allow more intricate and uniform prints Englanders replaced human hair with silk. This is also where the name silk screen printing derived, although silk is rarely used anymore; man-made plastics or metal are the preferred materials for modern screen printers.

The evolution from stenciling to screen-printing happened in 1907 in England, when a young sign painter named Samuel Simpson from Manchester patented the first industrial screen-printing process. His process paved the way for modern screen printers, which used woven silk to hold the stencil in place and allowed detailed designs [65]. In 1914, San Franciscan John Pilsworth patented a multicolor screen printing process. Six years later, Albert Kosloff demonstrated a screen-printing process in Berlin for the first time. He stretched a cloth over a wooden frame and used a rubber-bladed squeegee to print the ink through the stencil which is still in used today (Figure 2-21).

Figure 2-21: Ways of screen printing: (left) hand printing (photo: M. Karvos) and (right) mechanical printing

The foundation of the thick-film electronic industry lies in the 1940's and it has originated from the 'missile program' developed during the World War II [66]. The manufacturing process of electronic proximity fuses for bombs involved using silver-based inks (pastes) and primitive silk-screening methods. Despite the initial interest of the thick-film technology, it did not progress smoothly until the 1960's. IBM, together with Du Point, developed a series of palladium based pastes called the 7800 series and used them in its 360 computer series [14]. In contemporary times, the technology is used mainly for gas and chemical sensors as well as biosensors and graphics.

2.5.2 State-of-the-art

Thick-film (TF) technology (more precisely 'printed-and-fired') enables simple and flexible manufacturing of multilayered devices, such as surface mount devices, hybrid integrated circuits and sensors, in an additive screen printing process where several successive layers of conductive, insulating or resistive pastes are deposited onto an electrically insulating substrate (Figure 2-22).

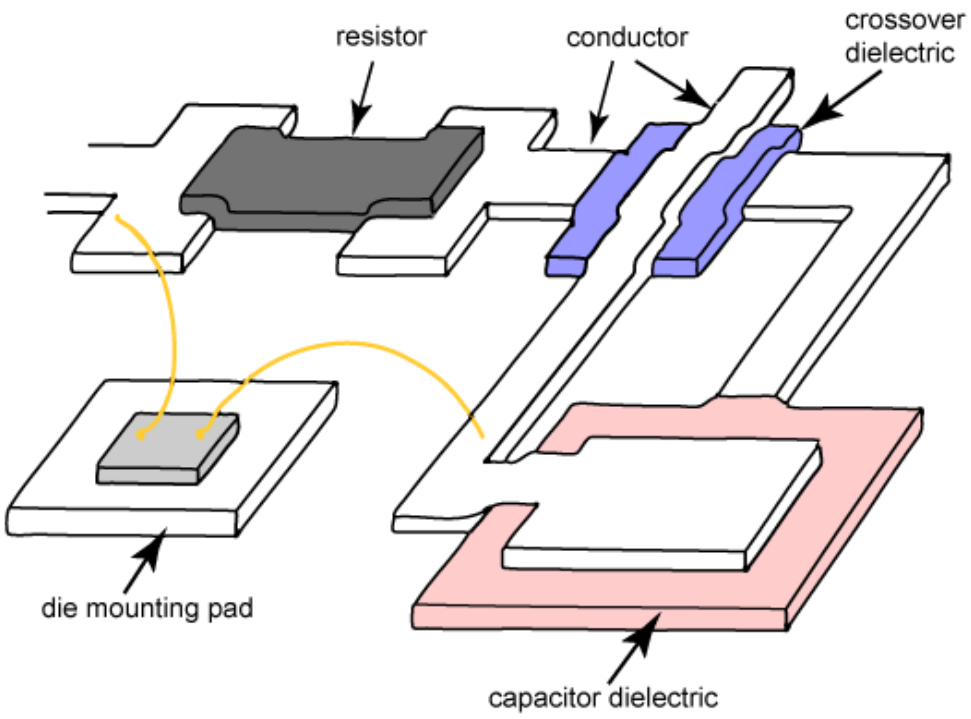

Figure 2-22: Thick-film printing components [67]

The distinctive feature of TF fabrication is the deposition of pastes in the screen printing process and their transformation to functional layers at high temperatures. A typical TF process consists of the following stages: lasering of substrates, ink preparation, screen printing, drying/curing and firing. In the final firing process, the pastes - which contain glass frit - are exposed to a high temperature (850°C-1000°C) so that the glass melts and bonds metal particles on the substrate. At this stage the final film properties such as electrical values and adhesive strength are established and a fired composite is produced that will control the electrical conduction process [68]. The films thickness range from 5-20 μm and there is the ability for building multi-layer configuration were minimum structure resolutions of 80-100 μm can be achieved.

The passive part of the chemical sensor is a substrate. This material forms the body of the sensor and is generally chemically and physically inert. The substrate needs to have strong and stable support, good electrical insulation properties as well as maintain dimensional stability on firing [69]. The commonly used substrates are ceramics (alumina and beryllium) [11], but the substrates can also be made from PVC [70], cardboard covered by acrylic paint [71] and polycarbonate [65]. Classical TF technology mostly uses pre-fired and unglazed alumina substrate that is stable and inert in severe environments and exhibits excellent mechanical properties (e.g. flexural strength) and thermal properties (e.g. maximum operating temperature) [72]. These properties play a vital role in the application of multisensors and contribute to the widespread use of thick-film sensors in automotive and industrial applications [73].

The inks used in the printing process form the printed layer. The function of the layer depends on the paste components. Each paste is formed of four basic constituents such as the functional phase, the binder phase, the carrier phase and the modifiers [74]. The relative proportions of these four components define the electrical characteristics of the ink [69]. The formulation of paste is a process during which components are mixed to yield a homogeneous ink that is ready for printing. In a TF printed material, the functional elements are typically pure metals, alloys, and metal oxides; these determine electrical resistivity [75]. The binding agent (e.g. glasses in powder form or resins) is other and solid acting as a sintering aid and it helps to

determinate the adhesion of functional phase to substrate. The solvent acts as a vehicle (e.g. pine oil or methyl) and controls paste viscosity that needs to be printed uniformly on substrate and will undergo combustion during firing stage. There is always a trade-off on the viscosity. A low viscosity ink can spread after printing and decrease the resolution of the process. In contrast to this, a very thick ink can block the screen mesh and to form a uniform layer. The modifiers are added in small quantities to the ink to alter the ink's rheological properties. They are also removed from the ink during the drying and firing stages [76].

The thick-film inks are divided into three main categories: conductors, resistors and dielectrics. The conductor ink/paste contains precious powdered metals such as gold, silver, platinum and palladium of particle size less than 5 μm. Gold is a good conductor material but it is expensive, has poor solderability, and is not leach-resistant with tin/lead solders. Silver can overcome the drawbacks of gold because it is cheaper and has good solderability. However, silver atoms migrate under the influence of DC electric field and can cause short-circuits and can react with many other inks changing their properties. The properties of gold and silver conductor inks can be modified by adding palladium and platinum to the paste thereby improving adhesion to the substrate, solderability and wire bonding characteristics. Nobel metals can be also replaced by copper and nickel but they express some problems in processing therefore real cost savings have been difficult to achieve. The thick-film conductor ink should have high conductivity, exhibit good adhesion and show a high resistance to leaching as well as be 'solderable' - all of which are important during the firing process. As a result of the increase in temperature, the individual particles sinter to each state alloying occurs and this gives rise to decrease in resistivity of the composite. Figure 2-23 shows a non-homogeneous fired surface and metal particles arrangement of the deposited layer after firing process [67].

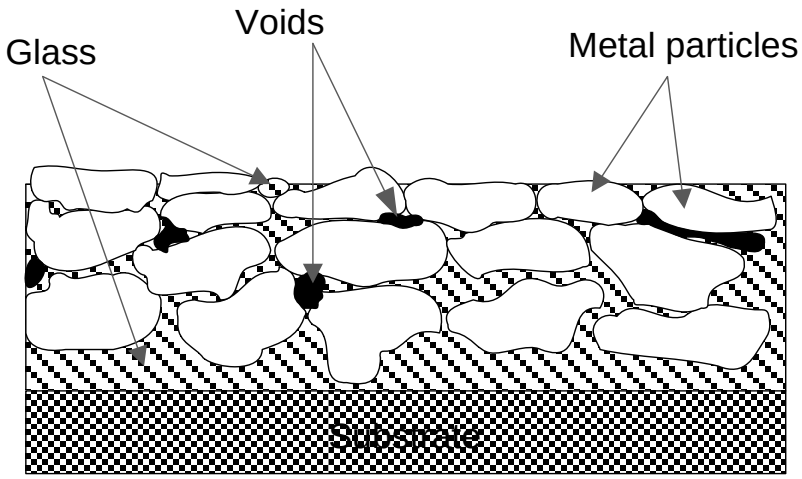

Figure 2-23: A printed TF paste illustrating particle arrangement [67]

The modern resistor pastes are made of ruthenium, iridium and rhenium oxides. Those pastes require a good stability of resistance values even at high temperatures (the firing temperature for thick-film materials can be 600-1000°C), low and reproducible temperature coefficient of resistance, low voltage coefficient of resistance, a wide range of sheet resistivity, low noise and they need to be compatible with conductor paste systems [67].

2.5.3 Principles of Screen Printing

Screen-printing is the most widely used thick-film deposition technique. The fundamental principles for screen-printing are similar to that used in the traditional silk screen-printing where a quantity of ink is deposited in a film of controlled pattern and thickness. The major differences are related to the degree of sophistication of the printer and the nature of the screen materials used in screen printing process. The essential components, used for making a screen print, are showed and labelled in Figure 2-24.

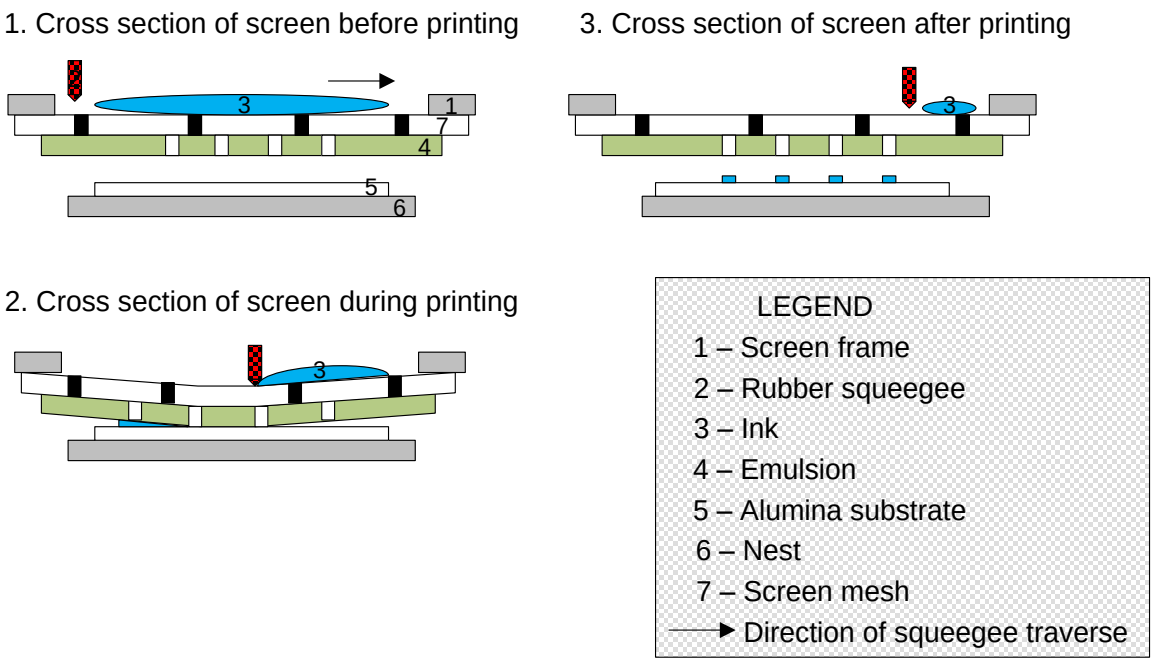

Figure 2-24: The schematic of thick-film screen printing and the screen printer operation (adapted from both Hobby [65] and Holmes et al. [66])

Screen-printing is an important process because it adds rheological constraints to pastes resulting from the relation of the paste flow and its internal structure, and excludes some complicated processes (e.g. etching) that might change the electrochemical characteristics of the sensing layer [77, 78]. The screen-printing process requires different materials and procedures each time, and therefore it is hard to describe the general approach. However, several main phases can be outlined. The first phase is the printing process. The technology utilizes conductive, dielectric and resistive pastes. The paste is placed on the opposite side of the screen. The deposition is attained by pressing the paste through a finely woven and directly pattern screen mesh with the use of a rubber squeegee. The possibility to directly pattern the film through the selectively masked mesh eliminates the need of future film etching and is one of the advantages associated with the screen printing technique [17]. The paste traverses the screen under pressure onto the surface of a ceramic substrate. The thick-film screens are made from monofilament nylon, a stainless steel or monofilament polyester finely woven mesh mounted under tension on a metal frame.

There is no single type of mesh that will satisfy the requirements of all types of work and the proper screen type needs to be carefully selected before printing commences [65]:

Table 2: Ranking for selecting the mesh type (with 1 being the highest).

	Nylon	Polyester	Stainless Steel
Flexibility	3	1	2
Resilience	3	1	2
% open area	2	2	1
Stability of print size	3	2	1
Squeegee wear	1	2	3
Accidental damage	1	2	3
Cost	1	1	3

Screen stencils are made by coating screen fabric with light-sensitive filling material that is exposed to ultra-violet light through a mask depicting the required pattern and after that, the unexposed regions are washed away forming the stencil. After drying the screen stencil is ready for printing. This process is called photolithography. The ink goes easier through the stainless steel mesh compared to polyester because it has better dimensional stability and a greater percentage open area. The ink is also less likely to be damaged and is more easily deflected (Table 2).

The gap between the screen and substrate is called the ‘snap’ and should be set using the adjustable rear hinge pivots and the front adjustable stops. It is very important that the screen is held at a distance of approximately 6 mm (1/4 in) from the surface of the substrate. During printing process the mesh must lift clear of the substrate immediately after the squeegee has passed, otherwise any slight movement of screen register will cause a smudge or imperfect printed image. After printing, the substrates are left to stand in the air at room temperature so the ink can settle and level off.

The second phase of the screen-printing process is to dry/cure the printed film in an infrared belt drier at a temperature between 100°C and 150°C. During this process,

the organic solvents, needed in order to produce the correct viscosity for the printing process, are removed from the paste. The film sticks to the substrate making it resistant to smudging.

The third phase of screen-printing is a firing (annealing) process in a multi-zone belt furnace at temperatures of up to 1000°C. The parameters of the belt furnace, including throughput speed, peak temperature, and dwell time, can be adjusted and controlled. The belt furnace is divided into three zones: a preheat time zone, a hot zone and a cooling zone (Figure 2-25).

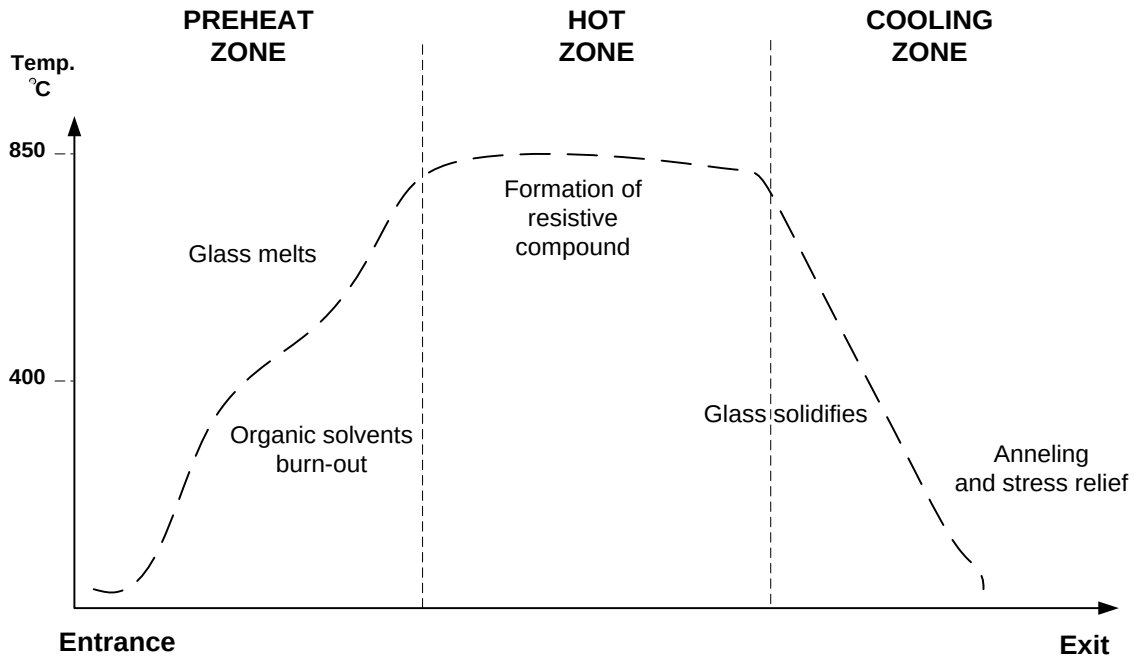

Figure 2-25: Proper curing profile (adapted from Tarr [67] and Holmes [66])

The total firing cycle typically last 60 min. In the first zone the temperature rises slowly and the remaining organic solvents are removed from the ink. The second zone is a high temperature region where the various chemical reactions take places and electrical characteristics of the sensor are developed.

In the third zone, the film is cooled slowly in order to avoid cracking and allow good adherence to the substrate during solidification. After firing additional screen-printed layers can be added as required.

2.6 Summary

Initially, the essential requirements for the engineering of the electrochemical potentiometric pH sensors were described, starting with sensor classification, methods for study of electrode reactions and the review of laboratory-based electroanalytical equipment. Next, the examples of existing and novel miniaturized planar thick-film Ag/AgCl reference electrodes and thick-film pH ion-selective electrodes were inspected. Furthermore, the well-established thick-film technology for the mass production of miniaturized electrochemical and environmental sensors was discussed.

Both novel thick-film Ag/AgCl reference electrodes and pH ion-selective electrodes reported here derive and largely build on work previously reported by Cranny and Atkinson [9], and Mihell and Atkinson [58]. The approach adopted here for improvement of the ruggedness of the pH electrode through its implementation as a screen-printed ion-selective electrode based on ruthenium dioxide (RuO_2) used in combination with A/AgCl reference electrode. The presented results demonstrate the development of low-cost, rugged thick-film alternatives to the commercially available liquid electrolyte filled Ag/AgCl reference electrode and glass pH electrode [11]. As will be discussed later, the thick-film Ag/AgCl reference electrodes are not generally well suited for unlimited operation because they suffer from electrode drift due to salt loss from electrodes.

Chapter 3 **Experimental Approach**

3.1 Electrode Fabrication

3.1.1 Screen Design

Screen-printing design is the heart of the thick-film (TF) technology matter and one of the most important steps in electrode manufacturing process. It is crucial because during its operation several sensors might be incorporated in one device, which requires a complex circuit. The screen is the most important part of the screen printing equipment because it is responsible for the printed pattern and controls of the ink thickness deposited on the substrate surface [77].

The screen-printing fabrication process of all TF electrodes analysed in this thesis has begun with the design of four layer screens in a programme known as the AUTOCAD, which gives precise dimensions' mesh openings. The same types of screens were used alternately for certain layers of Ag/AgCl reference electrodes and pH ion-selective devices. MCI Cambridge manufactured (Figure 3-1) the screens (A, B and C) for the first three layers.

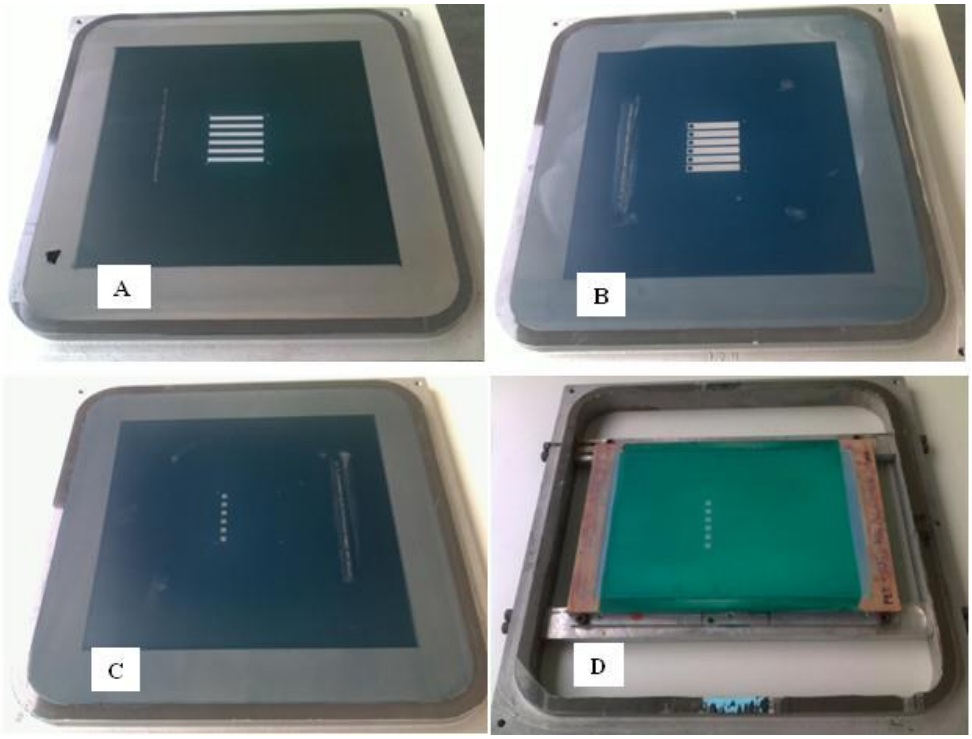

Figure 3-1: Thick-film screens used in electrodes manufacturing process: A - conductive layer, B -dielectric layer, C – active layer, D – salt matrix layer

They were stainless steel with 250 lines per inch, 15-micron emulsion thickness and 45° mesh. The last screen (D) was supplied by the Instituto de Reconocimiento Molecular y Desarrollo Tecnológico in Valencia in Spain. It was composed of polymer 70W PW 123-70W:133-µm mesh opening with photopolymer emulsion POLYCOL UNO: 113-µm thickness. All the screens were manufactured for the Aurel Mod C880 Printer, as shown in Figure 3-2.

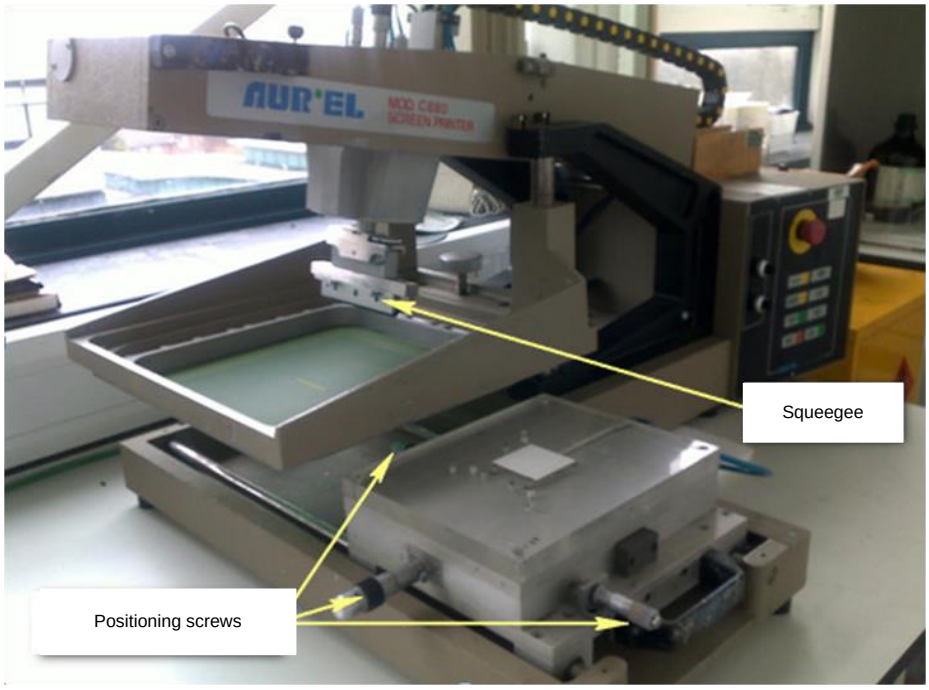

Figure 3-2: Aurel Mod C880 thick-film screen printer

An array of TF sensors was economically designed and screen-printed onto 96% alumina substrates (Coorstek) measuring 50 mm x 50 mm in dimension and 0.626 mm thickness. An economical design of each sensor type permitted the simultaneous fabrication of six identical individual electrodes on a single, laser prescribed substrate, as shown in Figure 3-3, which could be snapped easily off. This reduces fabrication cost and time.

The screen printing process required different types of pastes therefore both commercial and modified commercial ones as well as homemade pastes were deposited on a substrate (Figure 3-3 and Figure 3-4).

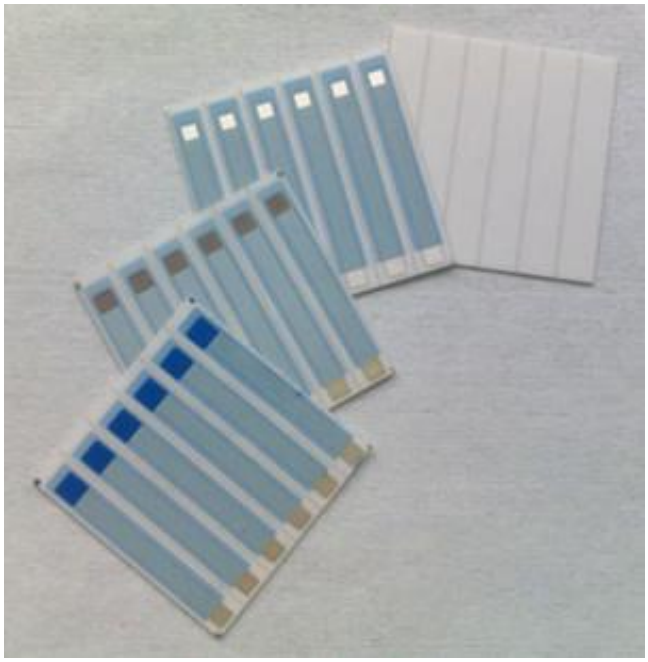

Figure 3-3: Stages of the screen printing process of the TF reference electrodes

Figure 3-4: Different types of pastes used in the manufacturing process

The TF Ag/AgCl reference electrodes and pH ion-selective sensors were constructed by successive screen-printing of each individual layer onto the alumina substrate, which was put on the substrate holder of the Aurel MOD C880 and locked by a vacuum to ensure it would not move during screen printing process (Figure 3-2).

The first layer (Layer 1), for both types of electrodes, was the conductor strip (a silver paste - for Ag/AgCl reference electrode and a platinum/gold paste - for pH ion-selective sensors) as shown in Figure 3-5.

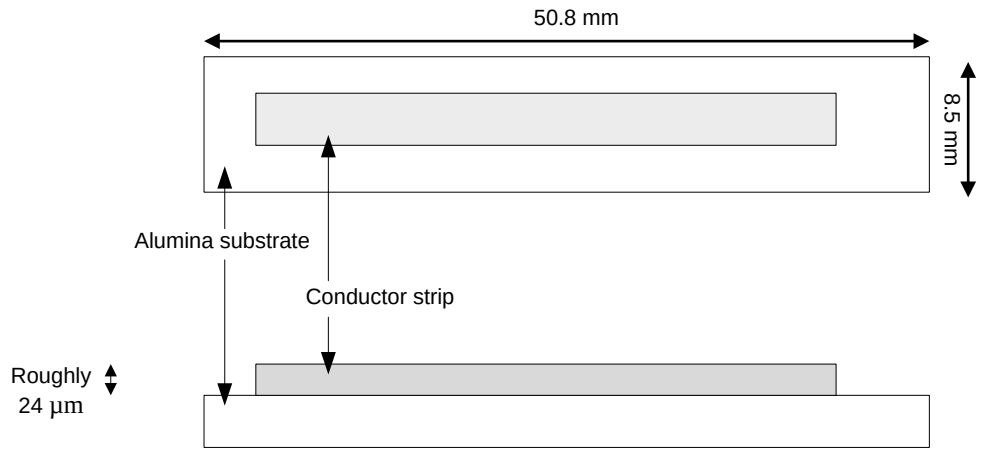

Figure 3-5: Top view and cross sections of the first layer- a conductor strip - for Ag/AgCl reference electrode and pH ion-selective sensor (not to scale)

For Layer 1 screen A was used (Figure 3-6A). The screen mesh opening of a conductor layer was a rectangle with dimensions of 4.6 mm x 44.6 mm (Figure 3-6a).

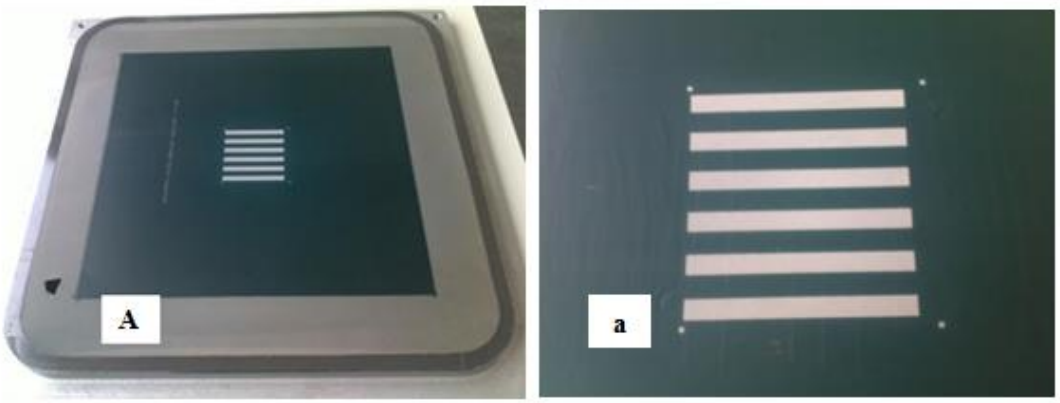

Figure 3-6: Thick-film screen (A) and mesh opening (a) for the first layer

On top of the conductor strips, a dielectric sealant layer (Layer 2) with a rectangular shape of 6.5 mm x 43.8 mm was deposited, leaving a small square window size of 3.4 mm x 3.4 mm exposing the underlying paste. The openings of the dielectric layer were smaller than the following active layer. This was done on purpose to avoid any

possibility of the conductor strip being exposed to anything other than the active layer. On the other end, a soldering pad approximately 4.2 mm x 4.6 mm was exposed, as can be seen in Figure 3-7.

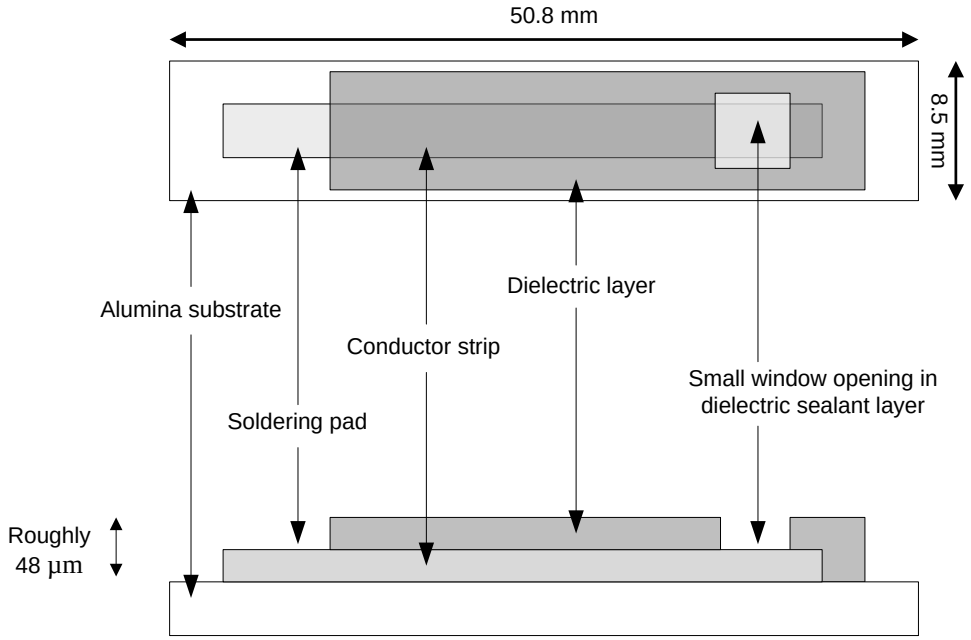

Figure 3-7: Top view and cross sections of the second layer – a dielectric layer - for Ag/AgCl reference electrode and pH ion-selective sensor (not to scale)

For the second layer screen B was used (Figure 3-8).

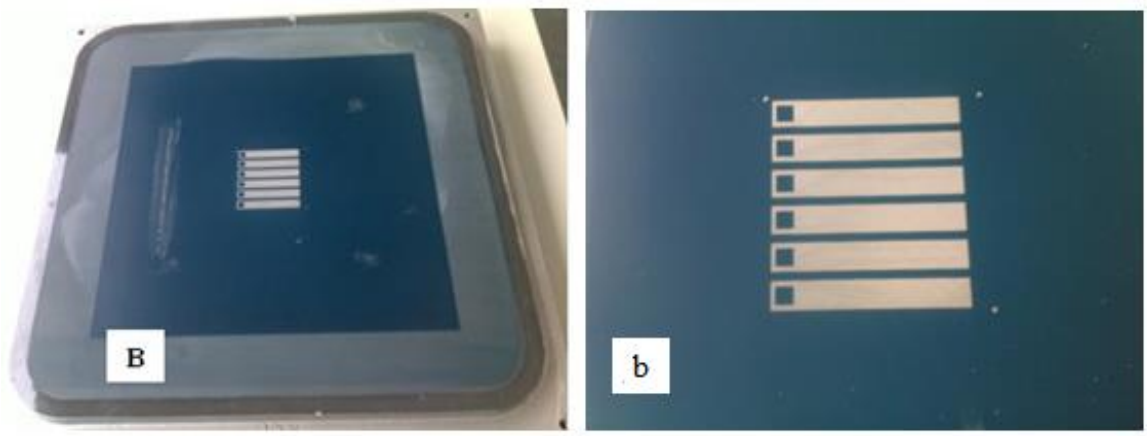

Figure 3-8: Thick-film screen (B) and mesh opening (b) for the second layer

The screen for the Ag/AgCl layer and ruthenium oxide layer (Layer 3) was a square window of 4 mm x 4 mm, slightly bigger than the exposed conductor paste to ensure

all the paste covered the window beneath (Figure 3-9). For the third layer screen C was used (Figure 3-10).

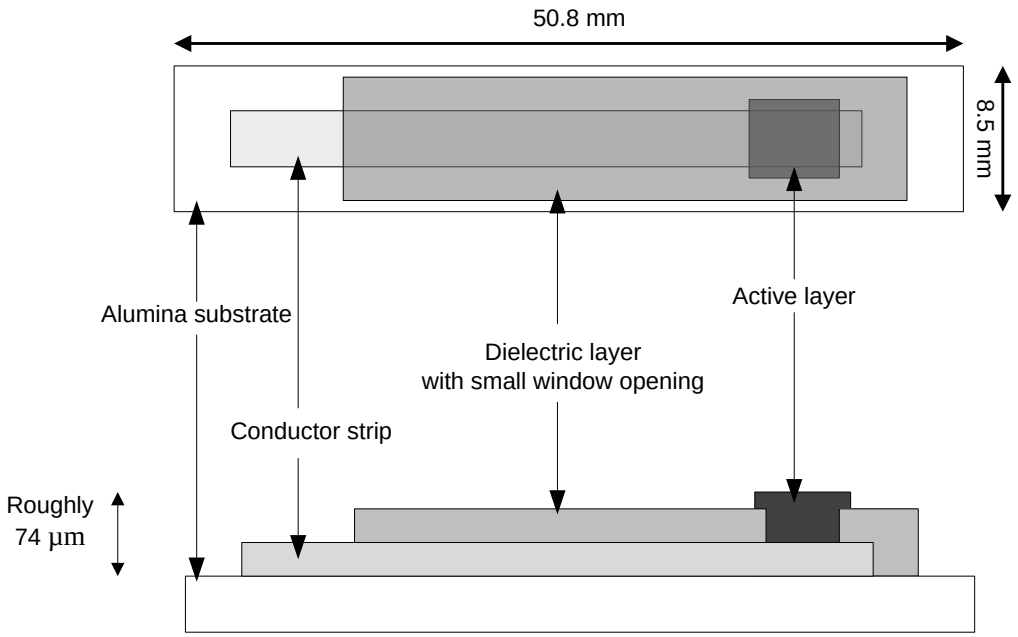

Figure 3-9: Top view and cross sections of the third layer- an active layer - for Ag/AgCl reference electrode and pH ion-selective sensor (not to scale)

Figure 3-10: Thick-film screen (C) and mesh opening (c) for the third layer

The fourth screen (D) for reference electrodes (for KCl and for KNO_3; both Layer 4) had simple square mesh openings, like the Ag/AgCl window, but with increasing

dimensions of 4.5 mm x 4.5 mm and 5 mm x 5 mm respectively, to ensure complete coverage of the previous layer (Figure 3-11 and Figure 3-12).

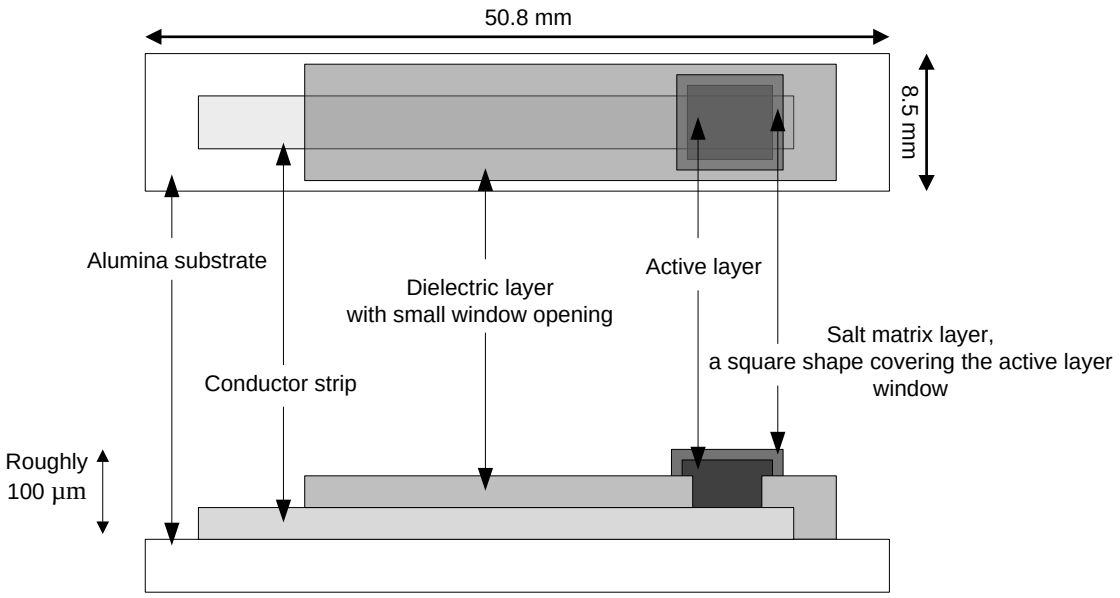

Figure 3-11: Top view and cross-sections of the fourth layer – a salt matrix layer - for Ag/AgCl reference electrode (not to scale)

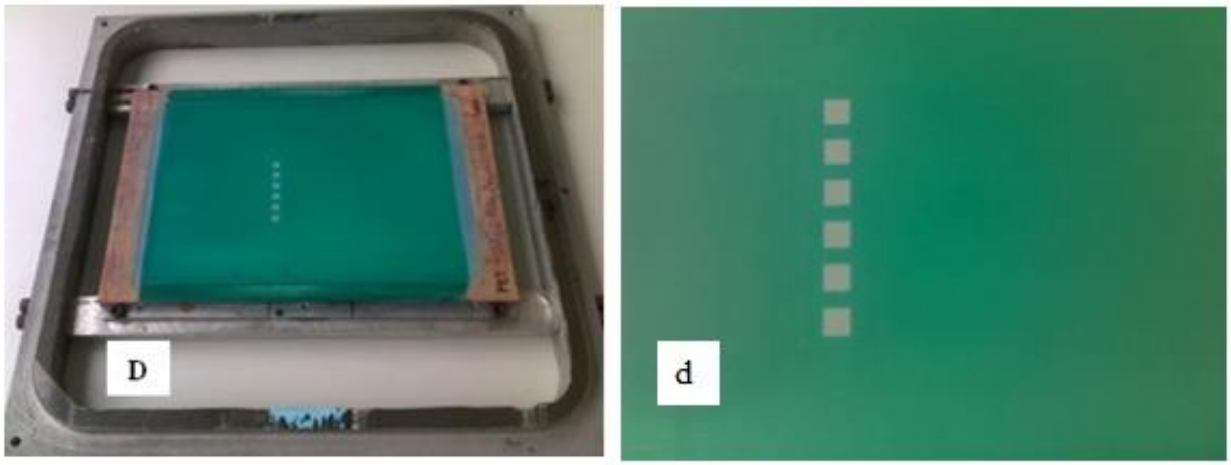

Figure 3-12: Thick-film screen (D) and mesh opening (d) for the fourth layer

3.1.2 Electrode Fabrication Process

Laboratory tests comprised the following steps:

I. Research into materials which could be used in fabrication including:
   1. Choice and use of suitable ink thinners
   2. Choice if sensor body suitable for TF screen-printing
   3. Choice of inks

II. Manufacturing in the TF screen printing process using the following machinery (Figure 3-13):
   1. Aurel Mod C880 TF screen printer
   2. DEK 1209 mini dryer
   3. 6 Zone belt furnace (BTU VQ41)
   4. Gallenkamp fan oven

Figure 3-13: The machinery used in the electrode manufacturing process

After printing, the substrates with the printed pastes were held at room temperature for a suitable length of time to allow relaxation of surface stress. After that, the inks were dried in a DEK 1209 infrared mini dryer at suitable temperature. Then, they were cured in the Gallenkamp fan oven or they were fired in a 6 zone belt furnace (BTU VQ41). Figure 2-25 shows the curing profile for the belt furnace. Drying and curing temperatures for each of the pastes comprising the subsequent layers are as detailed in Table 3 below.

Table 3: Properties of pastes used in fabrication process

Layer	**Paste**	**Processing**				
		Settling time at 25°C (min)	**Drying**		**Curing**	
			Temp (°C)	Time (min)	Temp (°C)	Time (min)
Ag/AgCl reference electrode						
Silver Conductor	ESL 9912-A	5-10	125	10-15	850	~45
Dielectric Insulator	ESL 4905-CH	5-10	125	10-15	850	~45
Polymer Ag/AgCl	GEM C61003P7	5-10	60	30	-	-
Glass 1	Ag/AgCl PPCFB_2	5-10	150	10	390	~30
Glass 2	Ag/AgCl PPCFC_3	5-10	150	10	420	~30
Polymer KCl & KNO_3	ESL 242-SB	5-10	125	10-15	150	30
pH ion-selective electrode						
Platinum Gold Conductor	ESL 5837	5-10	125	10-15	850	10-12
Polymer Dielectric	GEM 2020823D2	5-10	80	30	150*	5-10
Ruthenium Polymer	Paste C50502D7	5-10	60-80*	10-15	-	-

III. TF electrodes for water monitoring were fabricated using screen printing technology:
   1. Reference electrode
   2. pH ion-selective electrode.

3.1.2.1 Reference Electrode

TF screen-printed silver-silver chloride (Ag/AgCl) reference electrodes were designed to mimic the construction of a single junction liquid electrolyte commercial Ag/AgCl reference electrode. The total structure of the TF Ag/AgCl reference electrode consists of 5 layers (Figure 3-14).

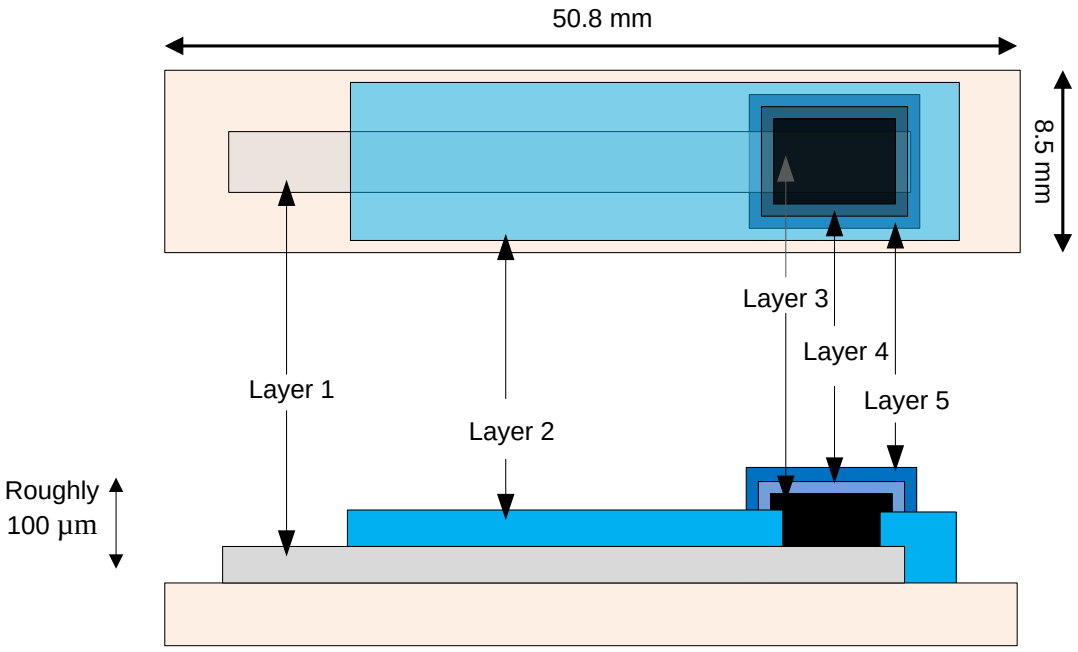

Figure 3-14: TF Ag/AgCl reference electrode top view and cross section (not to scale)

To conduct the TF Ag/AgCl reference electrode study several types of distinct electrodes were fabricated. The electrode structure remained the same for all of the compositions, only the composition variations of an active Ag/AgCl layer and a salt matrix layer were modified. The first two layers - a silver conductor and a polymer dielectric - were in common to all types of reference electrodes.

Table 4 provides the names of each layer type together with a list of pastes and suppliers.

Table 4: Types of TF Ag/AgCl reference electrode layers

No.	Layer type		Paste type	Product supplier
1	Silver Conductor		ESL 9912-A	Electro-Science Laboratories
2	Polymer Dielectric		ESL 4905-CH	Electro-Science Laboratories
3	Active Ag/AgCl	Polymer Ag/AgCl	GEM C61003P7	Gwent Electronic Materials
		Glass 1	Valencia $PPCFB_2$	Universidad de Politécnica de Valencia, Spain
		Glass 2	Valencia $PPCFC_3$	Universidad de Politécnica de Valencia, Spain
4	Salt matrix	Polymer KCl	ESL 242-SB	Electro-Science Laboratories
5		Polymer KNO_3	ESL 242-SB	Electro-Science Laboratories

The silver conductor was printed using 9912 ink (Electro-Science Laboratories), on top of which the dielectric insulator 4905-C (Electro-Science Laboratories) was deposited as shown in Figure 3-15. The purpose of dielectric layer was to isolate (waterproof) the conductor from the electrolyte.

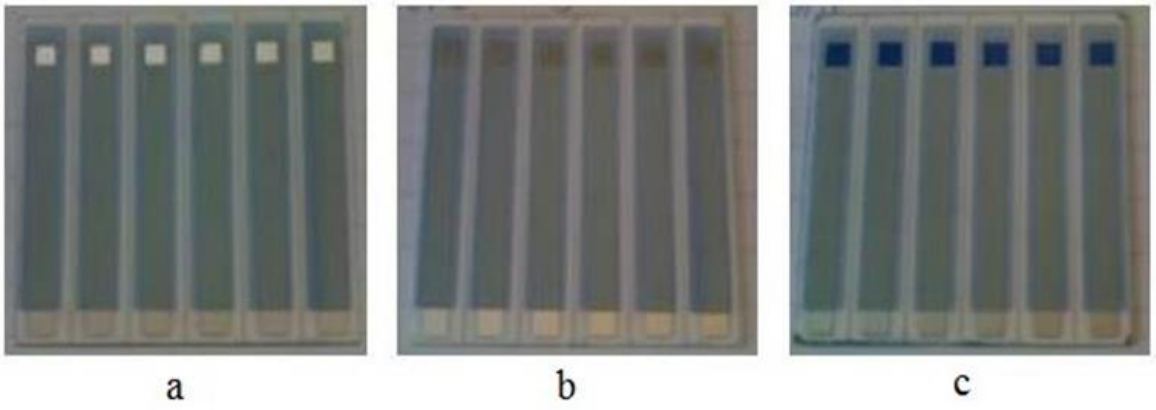

Figure 3-15: TF Ag/AgCl reference electrode with: a - conductive and dielectric layers, b - conductive, dielectric and active layers, c - conductive, dielectric, active and salt matrix KCl layer

In the first investigation three different types of binders, both polymer and glass binders, were tested for the third active Ag/AgCl layer (Table 4). The first type used in the experimental investigations was a polymer-based paste provided by Gwent Electronic Materials (GEM C61003P7). The other two types of binders, where non-

commercial glass based inks, supplied by Universidad de Politécnica de Valencia, Spain ($PPCFB_2$ and $PPCFC_3$).

The top layer for a single junction Ag/AgCl reference electrode was the salt matrix polymer KCl layer (Figure 3-15c). This layer was printed using a silicone based polymer paste 242-SB (Electro-Science Laboratories). Potassium chloride (KCl) (Analytical Reagent, Fisher Scientific UK Ltd) was milled into powder of grains smaller than 100μm and was directly added to the ESL 242-SB paste, adding 402 solvent (Electro-Science Laboratories) when required to keep the paste in printable condition [42]. The performance of the TF reference electrodes was examined with different weight ratios of the potassium chloride (KCl) in the electrode top layer. The glass bound Ag/AgCl layers were fabricated from two screen printable pastes that were prepared (in Valencia by Dr Eduardo Garcia-Breijo) as follows. Glass 1 - $PPCFC_3$: AgCl (Aldrich) milled (Pulverisette Fritsch) to 400 rpm/ 30 minutes with ethanol, sieve/100μm, Ag (Aldrich) sieve/100μm, low temperature cure powder frit CF7567FC (Ferro) sieve/100μm, vehicle V-006 (Heraeus), mixed in the ratios 3 grams Ag + 3 grams AgCl + 2 grams frit + 3.84 grams vehicle and triple roll milled (Exakt) for 5 minutes. Glass 2 - $PPCFB_2$ - is exactly the same as Glass 1 with the exception of a different powder frit EG2020VEG (Ferro). Double junction electrolyte-filled electrodes are generally found to be more stable and more reliable in time. To provide a better stability of the TF reference electrodes in varying concentrations of KCl test solutions some double junction electrodes were also fabricated with additional salt matrix polymer KNO_3 layer (Layer 5). They were containing KNO_3 (Analytical Reagent, Fisher Scientific UK Ltd) with 1:4 weight ratio in polymer 242-SB and printed on top of the salt matrix polymer KCl layer. Table 5 shows the collation of all TF Ag/AgCl reference electrodes types described above [42].

Table 5: All investigated TF Ag/AgCl reference electrode types – Bare Ag

No.	**Bare Ag (ESL 9912-A)**
	Materials used
1	Bare
2	ESL 242-SB
3	ESL 242-SB 20% KCl
4	ESL 242-SB 20% KNO_3
5	ESL 242-SB 66% KCl
6	ESL 242-SB 71% KCl
7	ESL 242-SB 20% KCl + ESL 242-SB
8	ESL 242-SB 20% KCl + ESL 242-SB 20% KCl
9	ESL 242-SB 50% KCl + ESL 242-SB
10	ESL 242-SB 50% KCl + ESL 242-SB 20% KCl
11	ESL 242-SB 66% KCl + ESL 242-SB
12	ESL 242-SB 66% KCl + ESL 242-SB 20% KCl

Table 6: All investigated TF Ag/AgCl reference electrode types – Polymer Ag/AgCl

No.	**Polymer Ag/AgCl (GEM C61003P7)**
	Materials used
1	Bare
2	Bare Fired
3	ESL 242-SB
4	ESL 242-SB Fired
5	ESL 242-SB 6% KCl
6	ESL 242-SB 20% KCl
7	ESL 242-SB 20% KCl Fired
8	ESL 242-SB 33% KCl
9	ESL 242-SB 50% KCl
10	ESL 242-SB 66% KCl
11	ESL 242-SB 71% KCl

Table 7: All investigated TF Ag/AgCl reference electrode types – Glass 1 Ag/AgCl

No.	**Glass 1 Ag/AgCl ($PPCFB_2$)**
	Materials used
1	Bare
2	Bare Fired
3	ESL 242-SB 6% KCl
4	ESL 242-SB 20% KCl
5	ESL 242-SB 20% KCl Fired
6	ESL 242-SB 66% KCl
7	ESL 242-SB 71% KCl
8	ESL 242-SB20% KCl + ESL 242-SB 20% KNO_3

Table 8: All investigated TF Ag/AgCl reference electrode types – Glass 2 Ag/AgCl

No.	**Glass 2 Ag/AgCl ($PPCFC_3$)**
	Materials used
1	Bare
2	Bare Fired
3	ESL 242-SB 6% KCl
4	ESL 242-SB 10% KCl
5	ESL 242-SB 15% KCl

3.1.2.2 pH Ion-Selective Electrode

Thick-film screen printed pH ion-selective electrodes (TF ISEs) are an alternative to the glass bulb type pH electrode, that exhibits several drawbacks such us large size, high cost and mechanical fragility [10]. The manufacturing process, screens and the electrode structure of the TF ISEs are in common with TF Ag/AgCl reference electrode. Assorted conductor pastes were considered for the first layer and a platinum gold ink (ESL 5837) turned out to be the one among them. For the third layer of the electrode structure an active polymer ruthenium oxide (RuO_2) material was used (Figure 3-16).

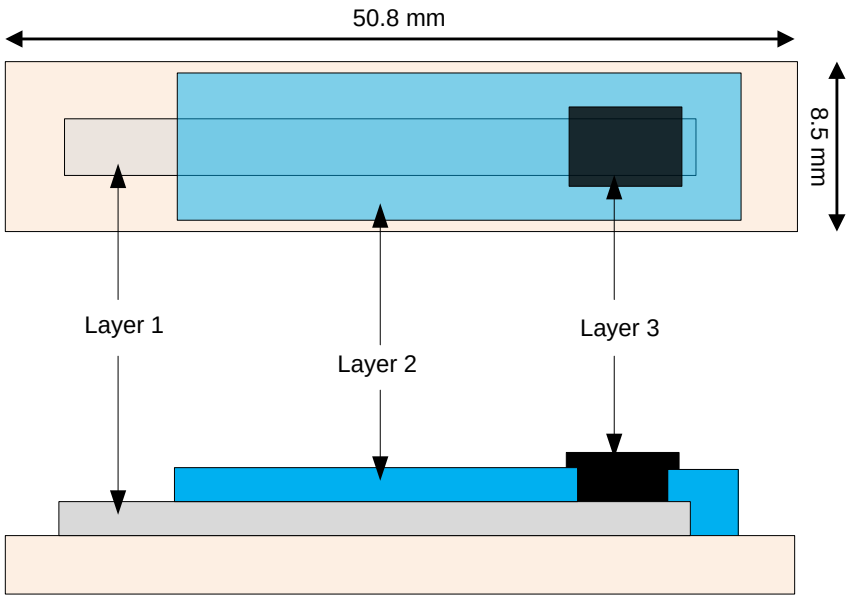

Figure 3-16: TF ion-selective electrode top view and cross section (not to scale)

Table 9: TF pH ion-selective electrode layer types.

Layer no.	Layer type	Paste type	Product supplier
1	Platinum Gold Conductor	ESL 5837	Electro-Science Laboratories
2	Polymer Dielectric	GEM 2020823D2	Gwent Electronic Materials
3	Ruthenium Polymer Paste	C50502D7	Gwent Electronic Materials

3.2 Electrode Testing

3.2.1 Testing Setup

3.2.1.1 Equipment

The entire experimental work was divided in two individual laboratory investigations under which the performance and stability of TF Ag/AgCl reference electrodes and pH sensors were analysed. The electrodes electro-potentials were measured with respect to a commercial gel-filled single junction reference electrode (Beckman Coulter A57193) located centrally within a beaker containing the test solution and surrounded by the TF electrodes under test as shown in Figure 3-17. Three

electrodes of each type were tested by soldering wires onto their exposed silver conductor layers and connecting them to the voltmeter.

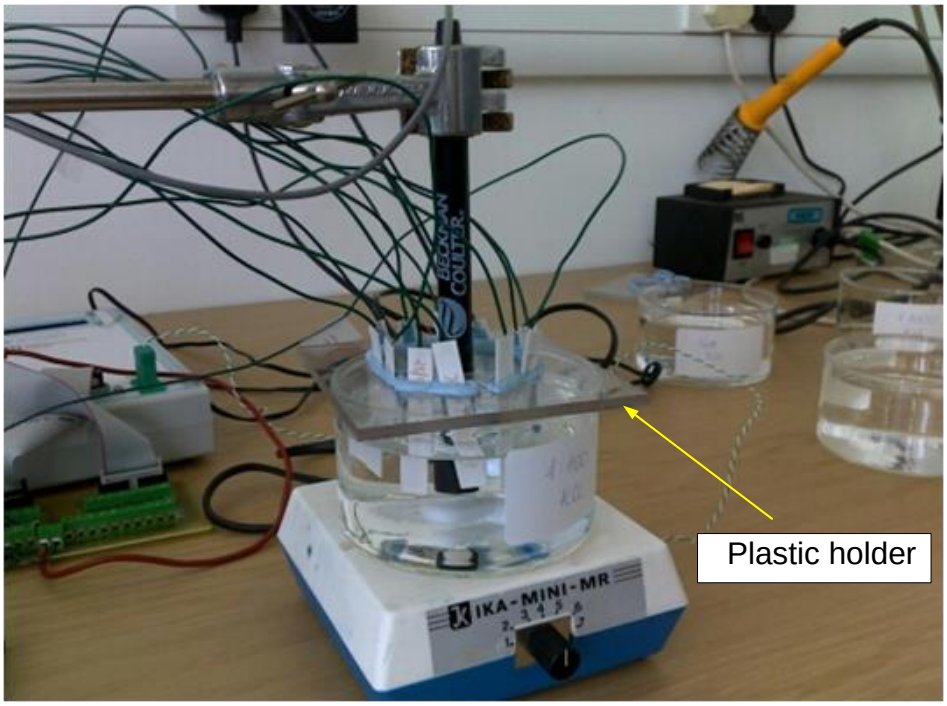

Figure 3-17: Electrodes set up ready to record their potential with the magnetic stirrer

Initial experimental data (Experiment # 1 and Experiment # 2 in Chapter 4) was recorded using Keithley 2000 multimeter. It has very high input impedance for measuring potential difference and therefore gives accurate voltage readings. The obtained data was manually logged into computer data file (Figure 3-18) so the recorded data could include the human error.

Figure 3-18: Keithley 2000 multimeter

Each individual electrode was soldered separately to the copper wire, which later was connected to the ten channels card of the multimeter (Figure 3-19 and Figure 3-20).

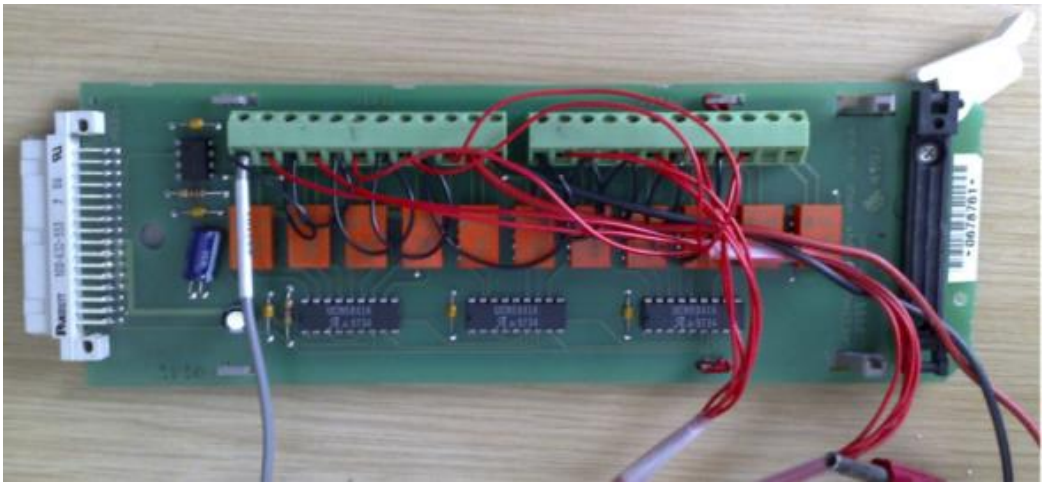

Figure 3-19: Keithley 2000's connection card with copper wires

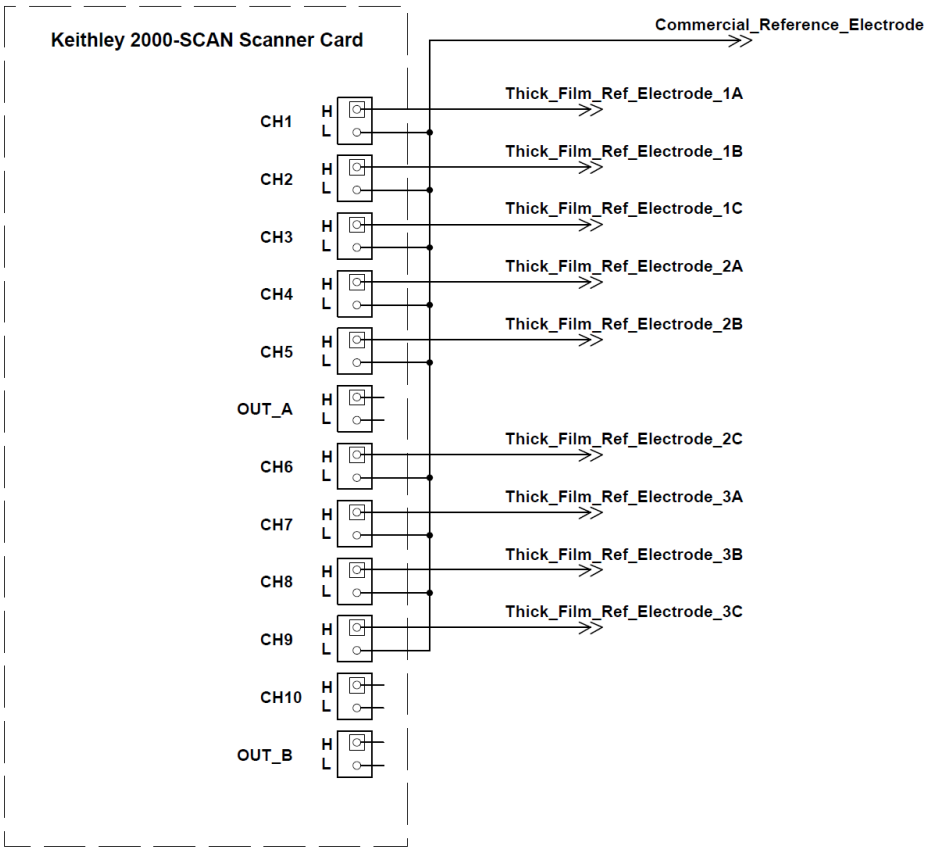

Figure 3-20: The electronic configuration of Keithley 2000's card

Every channel has two input channels, one high and one low. The Beckman Coulter reference electrode was attached to the low input channel of the connection card while the TF electrodes were connected to the high input voltage channel. When the potential of the TF electrodes was higher, a positive potential difference was obtained and alternatively a negative potential difference was created for a lover potential of the TF electrodes. The potential changes, in the range of a couple of tenths of millivolts, were very small. Any kind of noise could disturb them and in the result, unstable readings could be recorded.

To implement the data collection from the latest experiments (Experiment # 3, Experiment # 4, Experiment # 5 in Chapter 4), a portable data logger used provided by the Universidad Politécnica de Valencia in Spain. This microelectronic device could control various numbers of electrodes (up to 36 electrodes) in each experimental setting and included a port for the commercial reference electrode (Figure 3-21). The electronic device was attached to the PC and all the experimental data were automatically recorded in an Excel spreadsheet.

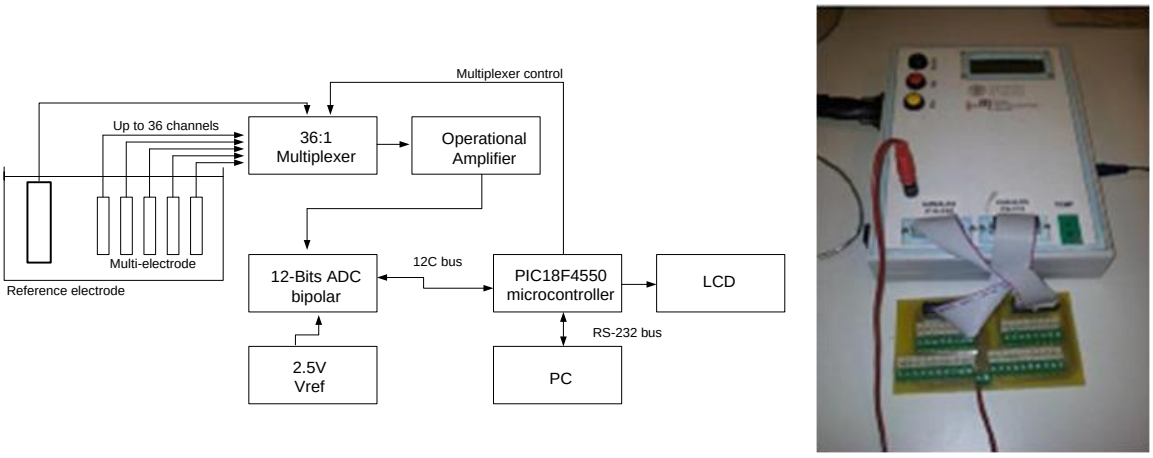

Figure 3-21: The block diagram and photograph of the measurement system for the data logger [11]

The potentials of the multi-electrodes were acquired using a 36:1 multiplexer architecture, which was formed from two 18:1 channel MOS analogue multiplexers (MAX306, Maxim) and one 2:1 channel analogue multiplexer (MAX308, Maxim) in this way 36 channels could be measured simultaneously (Figure 3-21). The microcontroller (PIC18F4550, Microchip Technology) controlled the selection of each channel, in the multiplexer. The sampling raw data was logged every 100 ms

at 10 s periods. A precision CMOS quad micro power operational amplifier (LMC646, National SMC), was connected to the output multiplexer as a buffer stage. This operational amplifier, working in buffer configuration, has very high input impedance and an ultra-low input bias current of less than 16 fA and hence is suited to the signal impedance generated by the potentiometric multi-electrodes. An analogue to digital converter (MAX128, Maxim) with a resolution of 12-bits was used, with selectable variable external or internal reference voltage in order to obtain different full scale ranges (a 2.5 V external reference and a bipolar input signal were used). The resolution (equivalent to 1 Least Significant Bit) was 1.22 mV.

The PIC18F4550 had low power consumption (sleep mode currents down to 0.1 A typical), 32 K of memory program and 2 K of RAM and USB port. The software for the PIC18F4550 microcontroller has been designed to scan the voltage for each channel and send the data to a PC via an RS232 serial communications channel. The PC acquisition software was developed using Visual Basic® 6.0 and Microsoft Excel® 2003 software [42].

3.2.1.2 Experiments Setup

The initial step of the experimental setup was to prepare the TF electrodes for testing. To obtain better results from the raw data three electrodes of the same type were tested in each experiment. At first, the exposed conductor layers of TF electrodes were polished with a steel brush. This process removed the oxides layer formed during the fabrication process due to oxidation.

After that, the copper wires were mounted to the electrode soldering pad. Then, they were connected to a microelectronic device and subsequently to a computer. All the recorded measurements were saved autonomously at every 5 seconds, 10 seconds, 30 seconds, and 1 minute or 5 minute intervals depends on the experiment. The use of the microelectronics and computer set up resolved the problem of human error related to manually recorded data in initial experiments.

The electrodes were attached to a transparent plastic mounting holder, which allows them to be easily moved between various test solutions during the experiment, and

after that the electrodes active windows were submerged into testing solutions (Figure 3-17).

3.2.2 Solution Setup

TF electrodes were immersed sequentially into different strength KCl solutions where their performance and stability were tested by measuring their electro potential difference with respect to a commercial gel-filled single junction reference electrode (Beckman Coulter A57193). Entire experimental work was conducted at room temperature of 20 ±3 °C and it was believed that these small variations in temperature can be considered insignificant since the electrode potential sensitivity to temperature is known to be very low.

Each chloride ion solution was prepared on the same day when the experiment was commenced. Potassium chloride test solutions were prepared by dissolving potassium chloride powder (analytical Reagent, Fisher Scientific UK Ltd) in deionised water until the solution reached saturation (Sat KCl solution). All the other solutions were made by diluting saturated solution in the ratios of one tenth (1:10 Sat KCl solution), one hundredth (1:100 Sat KCl solution) and one thousandth (1:1000 Sat KCl solution).

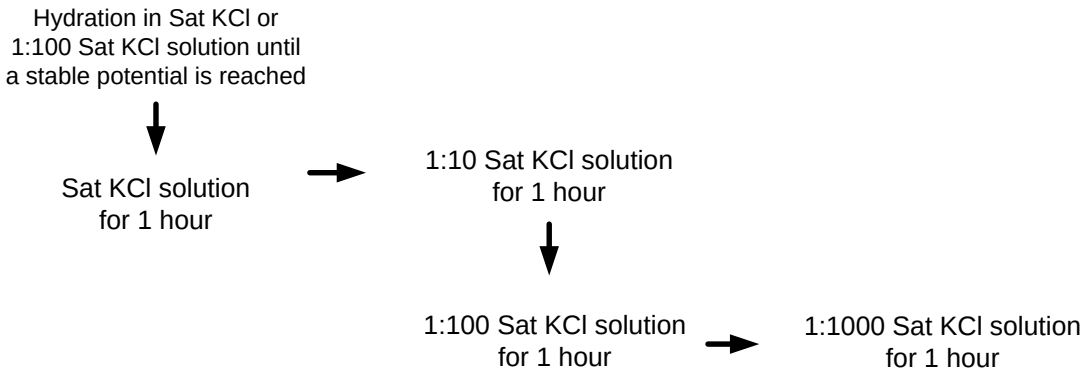

Figure 3-22: Test sequence for TF Ag/AgCl reference electrode

3.2.3 Hydration and Calibration

All electrodes were hydrated initially in either Sat KCl solution or 1:100 Sat KCl solutions overnight to determine the baseline response of the TF electrodes and confirm their functionality. For calibration purposes, the Beckman Coulter commercial reference electrode was used as a comparison. After that, they were cycled subsequently through KCl test solutions (Figure 3-22). After that, a group of the same type of reference electrodes was examined simultaneously with TF pH electrode in three pH buffers in a solution sequence of pH 7, 10, 7, 4, 7, 4, 7, 10 and 7.

To minimise the effect of mass transport from the solution to the electrodes during testing, (which is more crucial at lower concentrations) a magnetic stirrer was placed underneath the experimental setup and constantly rotated the solution in crystallizing dish (Figure 3-17).

Chapter 4 **Results and Conclusion**

4.1 Experimental Background

The response of any electrochemical potentiometric electrode is meaningless without a reference electrode against which comparisons can be made [9]. A potentiometric pH sensor can determine the pH of a solution where the potential difference between two electrodes, i.e. a pH ion-sensitive and a reference electrode, is measured. The reference electrode provides a stable reference potential regardless of the solution in which is immersed, while the pH ion-selective electrode responds to the change of the H^+ concentration in the solution.

The most practical and the simplest type of reference electrode used in industry and research is the conventional silver-silver chloride (Ag/AgCl) reference electrode where the potassium chloride is used as the electrolyte. This electrode does cause the least concern for the environment in comparison with other commercially available reference electrodes e.g. calomel reference electrode. The traditional Ag/AgCl reference electrode is bulky and fragile. Thick-film technique can overcome these drawbacks by fabricating miniaturised, rugged and robust electrochemical sensors.

The experimental work presented in this thesis stems from the two separate investigations on two types of screen printed planar thick-film electrodes. The principal research focused on the investigation of the TF Ag/AgCl reference electrode, which mimic the single junction electrolyte-filled Ag/AgCl reference electrode structure, with respect to variations in the paste choice for Ag/AgCl active layer and amount of KCl powder in the matrix layer. At the same time, the alternative investigation is concentrated on ruthenium oxide (RuO_2) working electrode that was implemented on the same principle as the conventional glass pH electrode by attempting to mimic their operation. In the experimental investigation, many material formulas were tested in varying concentrations of KCl solution and pH buffers. The experimental setup for both types of TF devices was exactly the same and has been explained in more detail elsewhere [11, 42].

The research derives from the conclusions gathered from the previous experimental work where the characteristics and responses of thick-film planar Ag/AgCl reference electrode and ruthenium oxide (RuO_2) pH electrode were investigated [9, 58]. The

past investigations on thick-film Ag/AgCl reference electrodes focused on different electrode parameters such as various window sizes of the waterproofing layer, the thickness of the salt matrix layer and the electrode structure dependability.

In addition, the hydration time and lifetime of the reference electrode-waterproofing layer with different window sizes was tested. The results demonstrated that the reference electrode lifetime and hydration time increases while the window dimensions' decreases. The next set of tests concentrated on the electrode fabrication structure reliability. The results have shown that the total potential of the same structured reference electrodes tested for few days in pH=7 buffer solution is repeatable. At the same time, the electrode potential drift was inspected. The results revealed that the potential drift was essentially the same to all electrodes from the same batch. The last investigation focused on the thickness of the salt matrix layer versus the electrode hydration time. In the laboratory environment three kinds of reference electrodes with different thickness of potassium chloride (KCl) layer we tested. The results have shown that the hydration time is influenced by the thickness of the KCl layer; the thicker the KCl layer is it becomes more difficult for the water to penetrate the KCl salt matrix and therefore the hydration time becomes longer.

The main objectives of this thesis are summarised as followed: i) investigation of different materials used in the electrode fabrication process, ii) to test the electrodes in different concentrations of chloride ion solution and pH buffers, iii) to investigate the reference electrodes behaviour in chloride ion solution over a long time.

4.2 Thick-Film Electrode Results

Several different types of miniaturised TF screen-printed Ag/AgCl reference electrodes and ruthenium oxide pH ion-sensitive electrodes were tested by following the same procedure described in Chapter 3, section 3.2. The results of the first group of electrodes, the TF Ag/AgCl reference electrodes, are tabulated below. They are shown in terms of the electrode sensitivity to chloride ions (mV/decade change in chloride concentration). Figure 3-14 shows the TF Ag/AgCl reference electrode structure.

The electrodes were listed in separated tables depending on their Ag/AgCl layer type [42]. Table 10 shows the results for the electrodes employing only a bare silver layer. The materials used, as listed in the table, are for the layer deposited on top of the bare Ag layer in the electrode fabrication process are in Table 4.

Table 10: Bare Ag electrodes

No.	Materials used	Sensitivity (mV/dec)	Sensitivity difference between electrodes (mV)	R^2
1	Bare	-129	±2	0.998
2	ESL 242-SB	-	-	-
3	ESL 242-SB 20% KCl	+11	±7	0.9652
4	ESL 242-SB 20% KNO_3	-	-	-
5	ESL 242-SB 66% KCl	-84	+8/-4	0.9454
6	ESL 242-SB 71% KCl	-90	±6	0.9611
7	ESL 242-SB 20% KCl + ESL 242-SB	+2	±1	0.8762
8	ESL 242-SB 20% KCl + ESL 242-SB 20% KCl	+2	+4/-5	0.6214
9	ESL 242-SB 50% KCl + ESL 242-SB	+2	+2/-1	0.9276
10	ESL 242-SB 50% KCl + ESL 242-SB 20% KCl	+4	-	0.8701
11	ESL 242-SB 66% KCl + ESL 242-SB	-0.3	±1	0.32
12	ESL 242-SB 66% KCl + ESL 242-SB 20% KCl	-3	±3	0.0876

Three different types of Ag/AgCl layer were tested. One of them was the polymer bound paste (GEM C61003P7) provided by Gwent Electronics Materials. The electrodes listed in Table 11 were with the additional Ag/AgCl layer deposited above the Ag layer.

Table 11: Polymer Ag/AgCl (GEM C61003P7)

No.	Materials used	Sensitivity (mV/dec)	Sensitivity difference between electrodes (mV)	R^2
1	Bare	-82	-	0.9586
2	Bare Fired	-122	+20/-13	0.9985
3	ESL 242-SB	-82	±1	0.9625
4	ESL 242-SB Fired	-26	±1	0.9405
5	ESL 242-SB 6% KCl	-54	-	1
6	ESL 242-SB 20% KCl	-81	-/-1	0.966
7	ESL 242-SB 20% KCl Fired	-1	+3/-2	0.9469
8	ESL 242-SB 33% KCl	-48	±1	0.9976
9	ESL 242-SB 50% KCl	-51	±1	0.9986
10	ESL 242-SB 66% KCl	-58	-	0.995
11	ESL 242-SB 71% KCl	-58	-	0.9951

The other two types were glass-based inks provided by Universidad de Politécnica de Valencia, Spain (Table 12 and Table 13). More details about both Glassy Ag/AgCl layers could be found in Chapter 3, Section 3.1.2.1.

Table 12: Glass 1 Ag/AgCl ($PPCFB_2$)

No.	Materials used	Sensitivity (mV/dec)	Sensitivity difference between electrodes (mV)	R^2
1	Bare	-50	±4	0.999
2	Bare Fired	-35	+7/-8	0.583
3	ESL 242-SB 6% KCl	-45	±1	0.998
4	ESL 242-SB 20% KCl	-43	±1	0.994
5	ESL 242-SB 20% KCl Fired	-8	±4	0.174
6	ESL 242-SB 66% KCl	-62	-/-1	0.98
7	ESL 242-SB 71% KCl	-66	±1	0.99
8	ESL 242-SB20% KCl + ESL 242-SB 20% KNO_3	-15	-	0.907

Table 13: Glass 2 Ag/AgCl ($PPCFC_3$)

No.	Materials used	Sensitivity (mV/dec)	Sensitivity difference between electrodes (mV)	R^2
1	Bare	-44	±17	0.9996
2	Bare Fired	-80	+21/-35	0.9331
3	ESL 242-SB 6% KCl	-33	±5	0.9984
4	ESL 242-SB 20% KCl	-29	+10/-4	0.9927
5	ESL 242-SB 20% KCl Fired	-5	±1	0.4754
6	ESL 242-SB 66% KCl	-59	±1	0.9837
7	ESL 242-SB 71% KCl	-61	-	0.9903
8	ESL 242-SB20% KCl + ESL 242-SB 20% KNO_3	+4	±1	0.8819

pH ISEs based on ruthenium oxide (RuO_2) as the active layer form the second group of researched electrodes. Figure 3-16 shows the pH electrode cross section that was the same as the Ag/AgCl reference electrodes. Drying and curing temperatures for each of the pastes comprising the subsequent layers are as detailed in Table 3. The same screens were used in the manufacturing process. All finding are presented in Appendix 2. The most interesting results are described below are in Chapter 4, sections 4.2.1, 4.2.2, 4.2.3, 4.2.4 and 4.2.5.

4.2.1 Experiment # 1

4.2.1.1 Materials

In the initial tests, four types of TF reference electrodes were tested (Table 14). The electrode salt matrix layer consisted of a silicone-based polymer paste (ESL242-SB) containing different concentrations of potassium chloride (Table 15-Table 17).

Table 14: TF Polymer Ag/AgCl (GEM C61003P7) reference electrode types

No.	Reference electrode types
1	Bare Ag ESL 9912-A
2	Polymer ESL 242-SB/Ratio 1:10 KCl
3	Polymer ESL 242-SB/Ratio 1:2 KCl
4	Polymer ESL 242-SB/Saturated KCl

Table 15: Reference electrode materials – Polymer ESL 242-SB/Ratio 1:10 KCl

Polymer ESL 242-SB/Ratio 1:10 KCl			
Layer no.	**Layer type**		**Paste type**
1	Silver Conductor		ESL 9912-A
2	Glass Dielectric		ESL 4905-CH
3	Active Ag/AgCl	Polymer Ag/AgCl	GEM C61003P7
4	Salt matrix	Polymer Ratio 1:10 KCl	ESL 242-SB 1:10 KCl

Table 16: Reference electrode materials – Polymer ESL 242-SB/Ratio 1:2 KCl

Polymer ESL 242-SB/Ratio 1:2 KCl			
Layer no.	**Layer type**		**Paste type**
1	Silver Conductor		ESL 9912-A
2	Glass Dielectric		ESL 4905-CH
3	Active Ag/AgCl	Polymer Ag/AgCl	GEM C61003P7
4	Salt matrix	Polymer Ratio 1:2 KCl	ESL 242-SB 1:2 KCl

Table 17: Reference electrode materials – Polymer ESL 242-SB/Saturated KCl

Polymer ESL 242-SB/ Saturated KCl			
Layer no.	**Layer type**		**Paste Type**
1	Silver Conductor		ESL 9912-A
2	Glass Dielectric		ESL 4905-CH
3	Active Ag/AgCl	Polymer Ag/AgCl	GEM C61003P7
4	Salt matrix	Polymer Sat KCl	ESL 242-SB Sat KCl

The main purpose of using the polymer was to retain the KCl on the electrode as long as possible. KCl (Analytical Reagent, Fisher Scientific UK Ltd) was milled into powder of grains smaller than 100 µm and was directly added to the ESL 242-SB paste. At this stage, no ESL 402 solvent was added to the ESL 242-SB paste. The salt matrix pastes were prepared in the laboratory. The KCl powder was mixed with the polymer paste in following quantities: the maximum KCl amount (Saturated) and two ratios: 1:2 (Ratio 1:2) and 1:10 (Ratio 1:10).

4.2.1.2 Results

The electrode potentials were obtained using a Keithley 2000 Digital Multimeter. The ten electrodes were connected to the multimeter via a K2000 scan card. They were held in solution using a mounting plate as shown in Figure 3-17 and Figure 3-18. In all experimental tests, TF electrodes were measured with respect to a commercial Beckman Coulter (A57193) reference electrode as shown in Figure 3-17. The electrodes were initially hydrated in a dibasic sodium phosphate/monobasic potassium phosphate pH7 buffer solution (Oakton) and after that they were immersed to chloride ion solution in different molarities: Sat KCl, 1:10 Sat KCl, 1:100 Sat KCl and 1:1000 Sat KCl, respectively. The complete experimental results are also presented in Appendix 4.

Figure 4-1 shows the response of three types of Polymer Ag/AgCl reference electrodes with various KCl concentrations in the KCl salt matrix layer with respect to time.

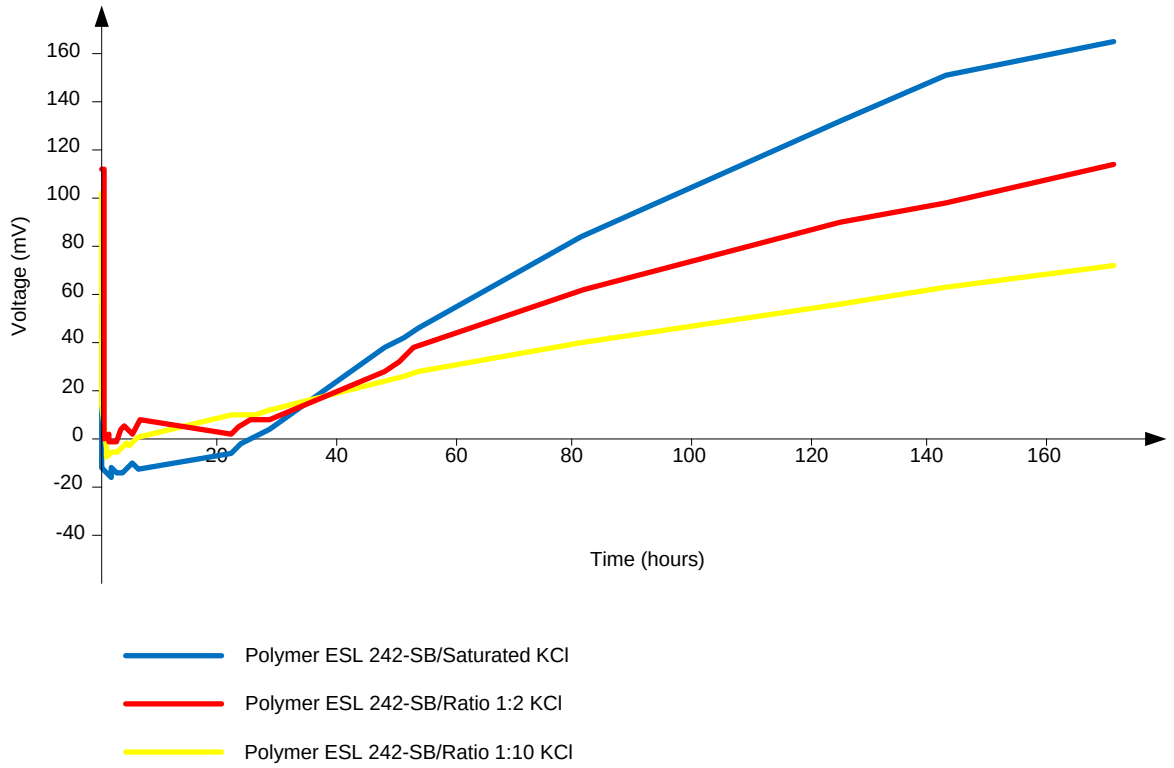

Figure 4-1: The ensemble average potential vs. time of the TF Polymer Ag/AgCl reference electrodes initially hydrating and then drifting in pH7 buffer [10]

All the slopes have similar shape and they can be divided into three distinct phases in terms of potential. At the beginning, as shown in Figure 4-1, the electrodes experienced an abrupt and rapid period of electro-potential instability indicated by the significant potential drop for all polymer Ag/AgCl reference electrodes that lasted about 1 hour. Then they became hydrated and remained relatively stable for a period of nearly 24 hours.

During the short period of stability, the reference electrodes with the KCl reservoir in the polymer KCl layer were drifting in a positive direction, consistent with chloride salt loss. It can be seen from Figure 4-1 that the higher the initial concentration of KCl contained in the electrode KCl salt matrix layer the faster they drift.
Furthermore, the average electro-potential responses of the electrodes to consecutive immersions in four different test solutions are shown in Figure 4-2.

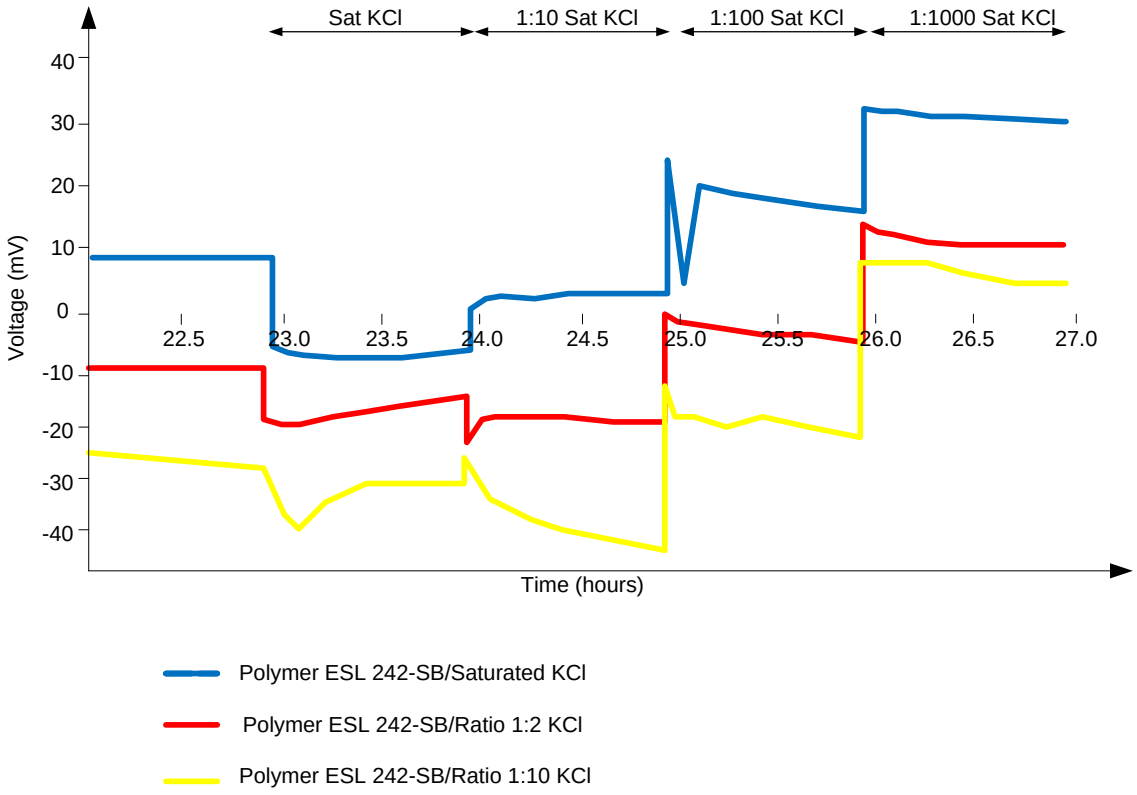

Figure 4-2: The ensemble average potential vs. time of the TF Polymer Ag/AgCl reference electrodes immersed in different concentration KCl solutions [10]

The electrodes exhibited smaller potential steps (approx. 10 mV per decade of potassium chloride concentration) while cycling between test solutions with the smaller step sizes for the electrodes containing higher initial concentrations of KCl in the salt matrix layer. The electrode potentials become more negative with decreasing potassium chloride of the testing solutions.

4.2.1.3 Conclusions

The experiments showed an interesting result which gave the beginning for further investigations and their findings are presented in this thesis. The first set of results (Figure 4-1) showed that the TF polymer Ag/AgCl reference electrodes were stable for a limited length of time and after that, they stared to drift. This was thought to be due to a mixed response of the silicone polymer itself and the KCl salt concentration in the polymer KCl layer. The electrodes with higher KCl salt concentration possessed more paths that enabled water to penetrate the KCl salt matrix layer

therefore the salt held in the paste could easily leave the electrode and dissolve in the testing solution. This tends to suggest that higher initial KCl levels would result in shorter useful lifetimes as a result of higher drift.

In the second part of the experiment, the electrodes' sensitivity to chloride was investigated. This time, the electrode potential decreased while the electrodes circled from the higher concentrated KCl solution to the lower concentrated ones. The higher concentrations of KCl gave lower step sizes. This could suggest that increasing the KCl salt concentration in the salt matrix layer to an optimum level might improve electrode responses by providing a reference electrode with stable potential response to changing potassium chloride concentration.

4.2.2 Experiment # 2

4.2.2.1 Materials

In this experiment, four types of TF reference electrodes with gelatine KCl Hydrogel (top layer) were tested (Table 18).

Table 18: TF Polymer Ag/AgCl (GEM C61003P7) electrode types

No.	Reference electrode types
1	Bare Ag ESL 9912-A
2	Hydrogel/Ratio 1:10 KCl
3	Hydrogel/Ratio 1:2 KCl
4	Hydrogel/Saturated KCl

The four tables below introduce the TF reference electrode materials.

Table 19: Reference electrode materials – Bare Ag ESL 9912-A

Bare Ag ESL 9912-A			
Layer no.	**Layer type**		**Paste type**
1	Silver Conductor		ESL 9912-A
2	Glass Dielectric		ESL 4905-CH
3	Active Ag/AgCl	Polymer Ag/AgCl	GEM C61003P7

Table 20: Reference electrode materials – Hydrogel/Ratio 1:10 KCl

Hydrogel/Ratio 1:10 KCl			
Layer no.	**Layer type**		**Paste type**
1	Silver Conductor		ESL 9912-A
2	Glass Dielectric		ESL 4905-CH
3	Active Ag/AgCl	Polymer Ag/AgCl	GEM C61003P7
4	Salt matrix	Hydrogel	Gelatine gel 1:10 KCl

Table 21: Reference electrode materials – Hydrogel/Ratio 1:2 KCl

Hydrogel/Ratio 1:2 KCl			
Layer no.	**Layer type**		**Paste type**
1	Silver Conductor		ESL 9912-A
2	Glass Dielectric		ESL 4905-CH
3	Active Ag/AgCl	Polymer Ag/AgCl	GEM C61003P7
4	Salt matrix	Hydrogel	Gelatine gel 1:2 KCl

Table 22: Reference electrode materials – Saturated KCl

Hydrogel/ Saturated KCl			
Layer no.	**Layer type**		**Paste type**
1	Silver Conductor		ESL 9912-A
2	Glass Dielectric		ESL 4905-CH
3	Active Ag/AgCl	Polymer Ag/AgCl	GEM C61003P7
4	Salt matrix	Hydrogel	Gelatine gel Sat KCl

The gelatine KCl Hydrogel layer (salt matrix layer) was made from commercially obtained gelatine dissolved in different concentrations of potassium chloride solution in deionised water and deposited on top of Ag/AgCl layer in three different

concentrations, using saturated KCl, and dilutions of this at 10:1 and 100:1 to make the gel.

4.2.2.2 Results

The electrode potentials were measured versus the commercial reference electrode (Beckman Coulter A57193). It was obtained using a Keithley 2000 Digital Multimeter. The gelatine KCl Hydrogel electrodes can be used immediately and do not need to be hydrated, therefore they were directly tested in solution of Sat KCl (1.5 hours), 1:10 Sat KCl (1 hour), 1:100 Sat KCl (1hour) and buffer pH7 (48 hours). It is believed that gelatine KCl Hydrogel layer stabilized the electrodes and they became less sensitive to the chloride concentration.

Figure 4-3 has shown the potential responses of the gelatine Hydrogel KCl electrodes after immersion in different molarities solutions.

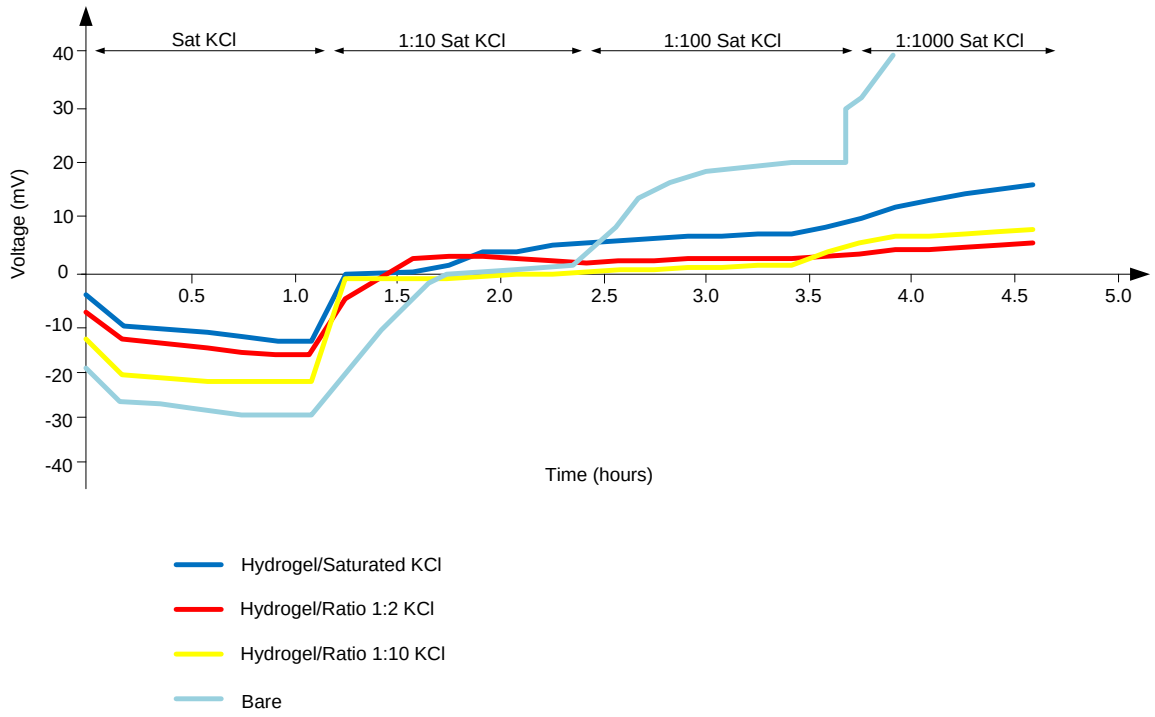

Figure 4-3: The ensemble average potential vs. time of the Hydrogel/KCl reference electrodes in different concentration KCl solutions [10]

The reference electrodes had relatively stable potentials and followed the same pattern with four distinct albeit small potential steps. The bare Ag/AgCl electrode

plots resemble the same pattern as the other reference electrodes but with larger potential steps between 50 and 100 mV per decade $[Cl^-]$.

The gelatine KCl Hydrogel electrodes, alike their polymer counterparts were drifting and leaking salt from the solgel membrane. They were drifting towards the same potential level as the bare Ag/AgCl electrode. According to the Nernst equation, the bare electrode potential should change by 59 mV per decade $[Cl^-]$ after each solution alteration. This particular experiment showed that the potential of the bare electrodes changed by about 120 mV (Sat KCl), then by about 100 mV (1:10 KCl solution) and finally about 60 mV (1:100 KCl solution). It is possible that the ion exchange reaction is slower in the lower molarities solutions and leads to a lower change of electrode potential.

4.2.2.3 Conclusions

The experimental results brought some positive findings. The gelatine KCl Hydrogel electrodes hydrated far more rapidly (within minutes) and gave a useful lifetime sooner than their polymer counterparts. They behaved similarly in lower concentrated solutions (1:10 Sat KCl, 1:100 Sat KCl (1hr) and 1:1000 Sat KCl) in comparison to the Sat KCl solution where the potential decreased. This result might be the outcome of slower ion exchange reaction in the lower molarities solutions, which led to a lower change of electrode potential. The negative side of the KCl Hydrogel membrane was that it did not retain long on the electrode and eventially dissolved into the solution.

4.2.3 Experiment # 3

4.2.3.1 Materials

Four TF reference electrodes with the KCl reservoir in the polymer containing 6% and 20% by weight of potassium chloride (KCl) were fabricated, as shown in Table 23.

The upper layer of polymer bound KCl was in contact with an underlying Ag/AgCl layer that was fabricated on top of a silver back contact. In this experiment, only one commercially obtained polymer bound Ag/AgCl (GEM C610003P7) paste was employed Table 24.

Table 23: TF Polymer Ag/AgCl (GEM C61003P7) electrode types

No.	Reference electrode types
1	Bare Ag ESL 9912-A
2	Polymer ESL 242-SB
3	Polymer ESL 242-SB 6% KCl
4	Fired Polymer ESL 242-SB 20% KCl

It was found later that the polymer Ag/AgCl ink was accidentally fired during the manufacturing process at 850°C. This was done accidentally at first, but later it was repeated on purpose. Throughout the incorrect fabrication, procedure chlorine escaped from the melted AgCl leaving behind Ag metal and some unknown layer was formed on the silver back contact or AgCl was changed to Ag. This was investigated further in Chapter 4, Experiment # 4 and Experiment # 5.

Table 24: Reference electrode materials – Bare Ag ESL 9912-A

Layer no.			
Layer no.	**Layer type**		**Paste type**
1	Silver Conductor		ESL 9912-A
2	Glass Dielectric		ESL 4905-CH
3	Active Ag/AgCl	Polymer Ag/AgCl	GEM C61003P7

Table 25: Reference electrode materials – Polymer ESL 242-SB

Polymer ESL 242-SB			
Layer no.	**Layer type**		**Paste type**
1	Silver Conductor		ESL 9912-A
2	Glass Dielectric		ESL 4905-CH
3	Active Ag/AgCl	Polymer Ag/AgCl	GEM C61003P7
4	Salt matrix	Polymer no KCl	ESL 242-SB

Table 26: Reference electrode materials – Polymer ESL 242-SB 6% KCl

Cured Polymer ESL 242-SB 6% KCl			
Layer no.	**Layer type**		**Paste type**
1	Silver Conductor		ESL 9912-A
2	Glass Dielectric		ESL 4905-CH
3	Active Ag/AgCl	Cured Polymer Ag/AgCl	GEM C61003P7
4	Salt matrix	Polymer 6% KCl	ESL 242-SB 6% KCl

Table 27: Reference electrode materials – Fired Polymer ESL 242-SB 20% KCl

Fired Polymer ESL 242-SB 20% KCl			
Layer no.	**Layer type**		**Paste type**
1	Silver Conductor		ESL 9912-A
2	Glass Dielectric		ESL 4905-CH
3	Active Ag/AgCl	Fired Polymer Ag/AgCl	GEM C61003P7
4	Salt matrix	Polymer 20% KCl	ESL 242-SB 20% KCl

It could be said that the electrode was not Ag/AgCl reference electrode because the Ag/AgCl layer was destroyed. Nevertheless, this device gave the most stable

potential in all KCl solutions. The different concentrations of KCl in the reference TF electrodes KCl salt matrix layer were shown in four tables above.

4.2.3.2 Results

The performance and stability of the electrodes were measured versus a commercial gel-filled single junction reference electrode (Beckman Coulter A57193). Three electrodes of each type were tested by soldering wires onto their exposed silver conductor layers and connecting them to different channels of the data logger (Figure 3-17 and Figure 3-21). The recorded raw measurements from individual electrode's channel were very noisy with significant random noisy peaks. In addition, each individual electrode of the same type gave slightly different measurements due to different paste homogeneity that could not be guaranteed and fully controlled. The electrodes fabricated within the same batch had some difference in their nominal salt concentration.

The electrodes were firstly hydrated into a 1:100 Sat KCl solution overnight to establish equilibrium of the reversible reaction occurring at the electrode. Subsequently, the electrodes were tested for susceptibility in chloride by successive immersion in different concentrations of KCl solutions (Figure 4-4).

It appeared that polymer ESL 242-SB, polymer ESL 242-SB 6% KCl and fired polymer ESL 242-SB 20% KCl electrodes were connected incorrectly to the Keithley meter as the step responses for these electrodes were opposite to the expected values (both Figure 4-4 and Figure 4-5).

Multiple electrodes of the same type were tested to obtain a more statistically reliable and less noisy results from more electrodes. Hence, raw measurements from three electrodes of the same type, were summed together and averaged to form a single ensemble averaged reading. The recorded measurements of all types of TF electrodes shown in Figure 4-4 demonstrated some level of noise. This could be due to electronic circuit noises, electrochemical noises of ionic movement in the test solutions and ionic diffusion across interfaces of the electrodes. The polymer ESL 242-SB (no KCl) electrodes were those with the higher degree of noise in

comparison to the least noisy polymer ESL 242-SB 6% KCl and fired polymer ESL 242-SB 20% KCl.

The bare electrodes shown in Figure 4-4 clearly indicated the electrodes potential change between the testing solutions and the time length of the electrodes immersion in each solution. The bare electrode potential step sizes varied between different testing solutions. The electrode potential obtained during the electrode examination in each set of solutions is more or less stable.

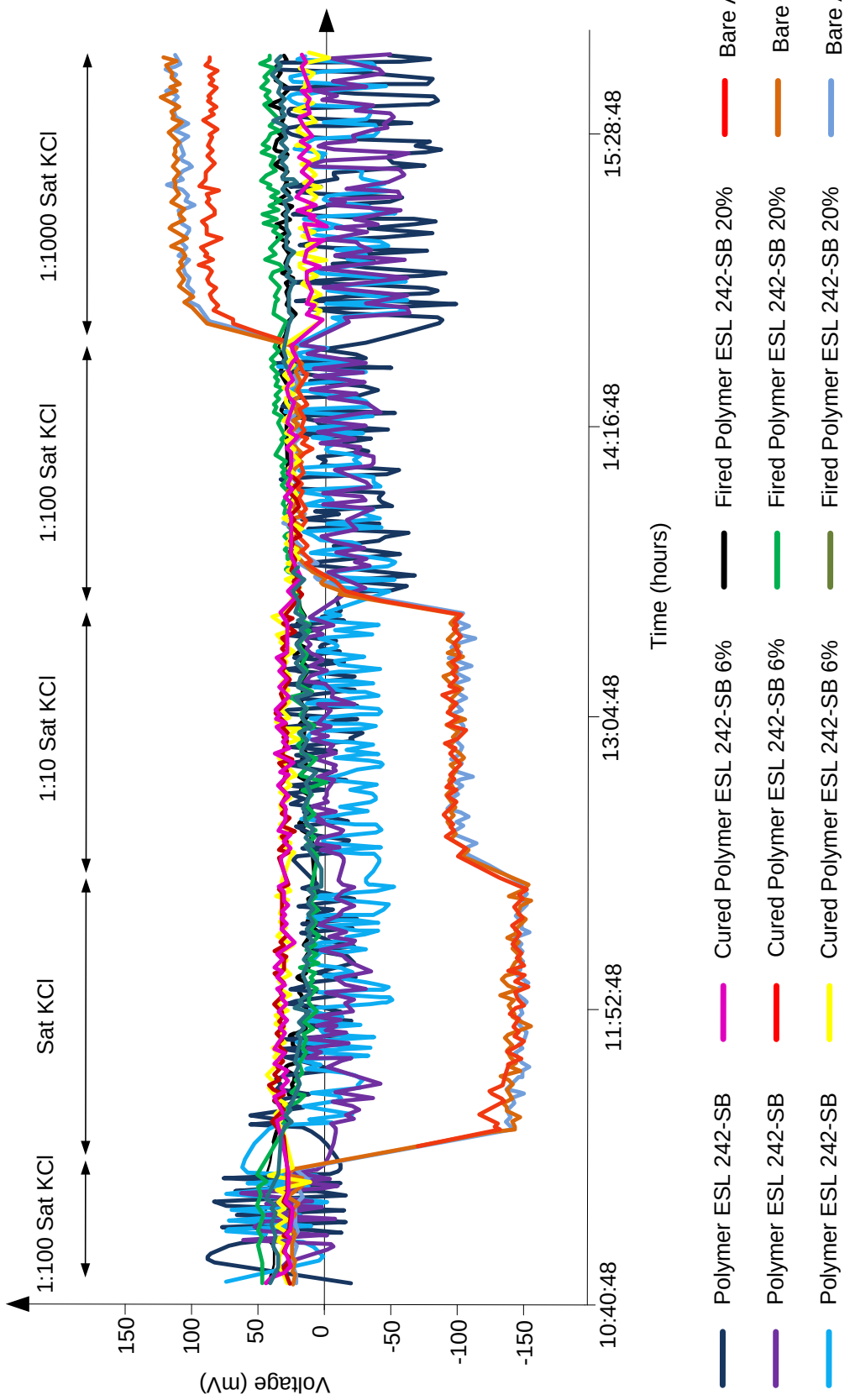

Figure 4-4: The non-ensemble average potential vs. time of TF polymer Ag/AgCl reference electrodes with various amount of KCl powder by weight in salt matrix layer

The polymer ESL 242-SB 6% KCl and fired polymer ESL 242-SB 20% KCl were more stable than those without any KCl reservoir. However, the small differences between the potential of the polymer ESL 242-SB 6% KCl in different solutions can be seen more clearly in Figure 4-5.

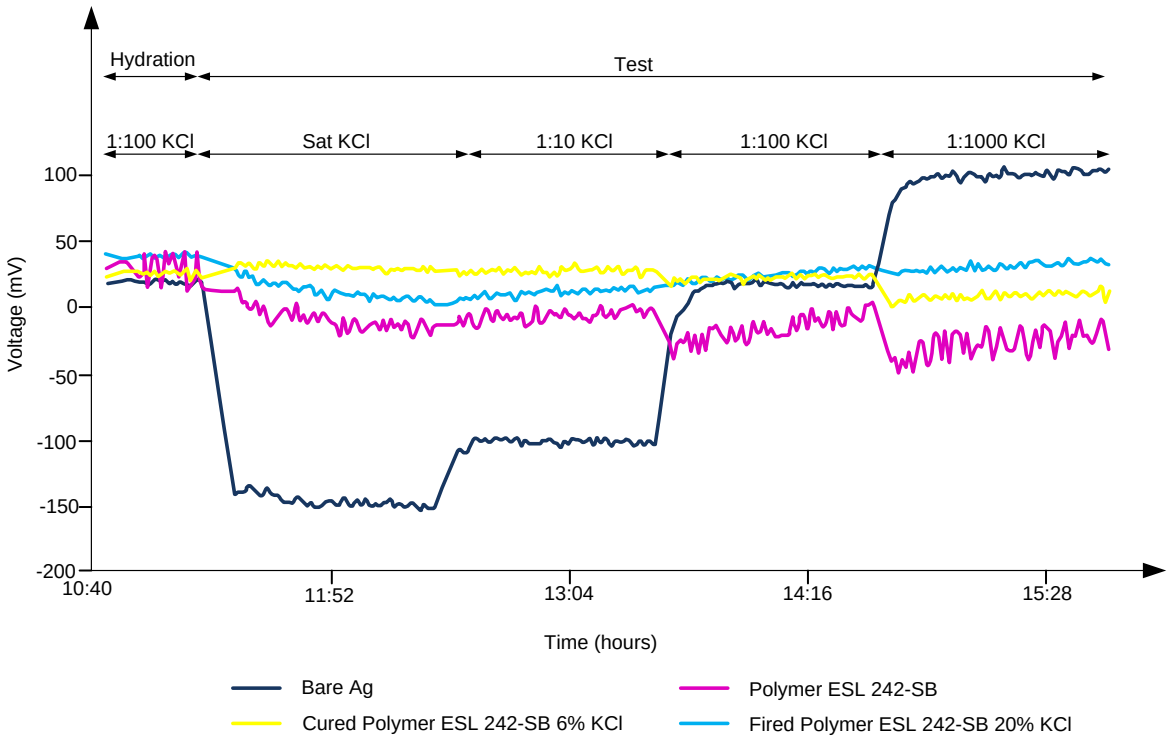

Figure 4-5: The ensemble average potential vs. time of TF Ag/AgCl reference electrodes with various amount of KCl powder by weight in salt matrix layer

4.2.3.3 Conclusions

The reference electrodes with pure ESL 242-SB layer gave very noisy and random responds, which is believed to be because the solution could not easily penetrate the ESL 242-SB layer. Hence, the recorded potential was mainly due to noise from the surrounding. Experiment # 3 in Chapter 4 did not specified the optimum salt intake for the salt matrix layer but showed that the reference response can be improved by adding KCl powder into the polymer KCl salt matrix layer and significantly decrease the sensitivity of the electrodes therefore, further investigations were undertaken.

The most stable potential results with the incorrectly fired Ag/AgCl polymer ink suggested that the Ag/AgCl layer needed to be studied to the greater extend. Therefore, another TF reference electrodes with non-commercial glass bound Ag/AgCl pastes (Experiment # 4) as well as electrodes with a thin layer of AgCl that was chemically grown on the Ag conductor (Experiment # 5) were developed and tested [7, 11].

4.2.4 Experiment # 4

4.2.4.1 Materials

In this experiment, five different reference electrode types were tested (Table 28). The TF electrode potentials were measured with respect to a commercial gel-filled reference electrode (Beckman Coulter A57193).

Table 28: TF polymer and glass bound Ag/AgCl active layer reference electrodes

No.	Reference electrode types
1	Glass Type 1 ESL 242-SB 20% KCl
2	Glass Type 2 ESL 242-SB 20% KCl
3	Polymer ESL 242-SB
4	Polymer ESL 242-SB (no Ag/AgCl layer)
5	Fired Polymer ESL 242-SB 20% KCl

Table 3 shows the properties of all pastes used in the electrode manufacturing process.

Two types of material for Ag/AgCl layer were used, as shown in Table 29-Table 35. Both types were glass based inks provided by Universidad de Politécnica de Valencia, Spain. The paste recipes are written in Chapter 3, section 3.1.2.1. The reference electrodes types 1, 2 and 5 (Table 28) salt reservoir contained 6% and 20% by weight of potassium chloride. Two kinds of binders for Ag/AgCl later were investigated. The first types, employed for the active Ag/AgCl layer, were two non-

commercial glass bound pastes: Valencia PPCFC$_3$ and Valencia PPCFB$_2$ (Table 29,Table 30Table 31 Table 32).

Table 29: Reference electrode materials – Glass bound Ag/AgCl pastes

Glass 1 ESL 242-SB 6% KCl			
Layer no.	**Layer type**		**Paste type**
1	Silver Conductor		ESL 9912-A
2	Glass Dielectric		ESL 4905-CH
3	Active Ag/AgCl	Glass 1 Ag/AgCl	Valencia PPCF$_2$
4	Salt matrix	Polymer 6% KCl	ESL 242-SB 6% KCl

Table 30: Reference electrode materials – Glass 2 ESL 242-SB 6% KCl

Glass 2 ESL 242-SB 6% KCl			
Layer no.	**Layer type**		**Paste type**
1	Silver Conductor		ESL 9912-A
2	Polymer Dielectric		ESL 4905-CH
3	Active Ag/AgCl	Glass 2 Ag/AgCl	Valencia PPCFC$_3$
4	Salt matrix	Polymer 6% KCl	ESL 242-SB 6% KCl

Table 31: Reference electrode materials – Glass 1 ESL 242-SB 20% KCl

Glass 1 ESL 242-SB 20% KCl			
Layer no.	**Layer type**		**Paste type**
1	Silver Conductor		ESL 9912-A
2	Glass Dielectric		ESL 4905-CH
3	Active Ag/AgCl	Glass 1 Ag/AgCl	Valencia PPCF$_2$
4	Salt matrix	Polymer 20% KCl	ESL 242-SB20% KCl

Table 32: Reference electrode materials – Glass 2 ESL 242-SB 20% KCl

Glass 2 ESL 242-SB 20% KCl			
Layer no.	**Layer type**		**Paste type**
1	Silver Conductor		ESL 9912-A
2	Glass Dielectric		ESL 4905-CH
3	Active Ag/AgCl	Glass 2 Ag/AgCl	Valencia PPCFC$_3$
4	Salt matrix	Polymer 20% KCl	ESL 242-SB 20% KCl

Table 33, Table 34 and Table 35 show the second type of paste used for the electrode active Ag/AgCl layer, that was the commercially obtained polymer bound paste, provided by Gwent Electronic Materials (GEM C61003P7).

Table 33: Reference electrode materials – Polymer ESL 242-SB 6% KCl

Polymer ESL 242-SB 6% KCl			
Layer no.	**Layer type**		**Paste type**
1	Silver Conductor		ESL 9912-A
2	Glass Dielectric		ESL 4905-CH
3	Active Ag/AgCl	Cured Polymer Ag/AgCl	GEM C61003P7
4	Salt matrix	Polymer 6% KCl	ESL 242-SB 6% KCl

Table 34: Reference electrode materials – Polymer ESL 242-SB 20% KCl

Polymer ESL 242-SB 20% KCl			
Layer no.	**Layer type**		**Paste type**
1	Silver Conductor		ESL 9912-A
2	Glass Dielectric		ESL 4905-CH
3	Active Ag/AgCl	Cured Polymer Ag/AgCl	GEM C61003P7
4	Salt matrix	Polymer 20% KCl	ESL 242-SB 20% KCl

Table 35: Reference electrode materials – Polymer ESL 242-SB 20% KCl (no Ag/AgCl layer)

Polymer ESL 242-SB 20% KCl (no Ag/AgCl layer)			
Layer no.	**Layer type**		**Paste type**
1	Silver Conductor		ESL 9912-A
2	Glass Dielectric		ESL 4905-CH
3	Salt matrix	Polymer 20% KCl	ESL 242-SB 20% KCl

The last type of reference electrodes examined in the Experiment # 4 was the Fired Polymer ESL 242-SB 20% KCl (Table 36).

Table 36: Reference electrode materials – Fired Polymer ESL 242-SB 20% KCl

Fired Polymer ESL 242-SB 20% KCl			
Layer no.	**Layer type**		**Paste type**
1	Silver Conductor		ESL 9912-A
2	Glass Dielectric		ESL 4905-CH
3	Active Ag/AgCl	Fired Polymer Ag/AgCl	GEM C61003P7
4	Salt matrix	Polymer 20% KCl	ESL 242-SB 20% KCl

As mentioned previously in Experiment # 3, the Polymer Ag/AgCl electrodes went twice through the annealing process. Firstly, the polymer Ag/AgCl paste (GEM C61003P7) was cured at 60°C (Figure 4-6B). This was the curing temperature recommended by the manufacturer's data sheet. Then, to maintain the same window size, as the one on the dielectric layer below, additional insulating layer of ESL 4905-CH paste was added on top of Ag/AgCl layer and the electrode structure was fired at 850°C (Figure 4-6D). Lastly, the final KCl Salt matrix layer was printed (Figure 4-6E).

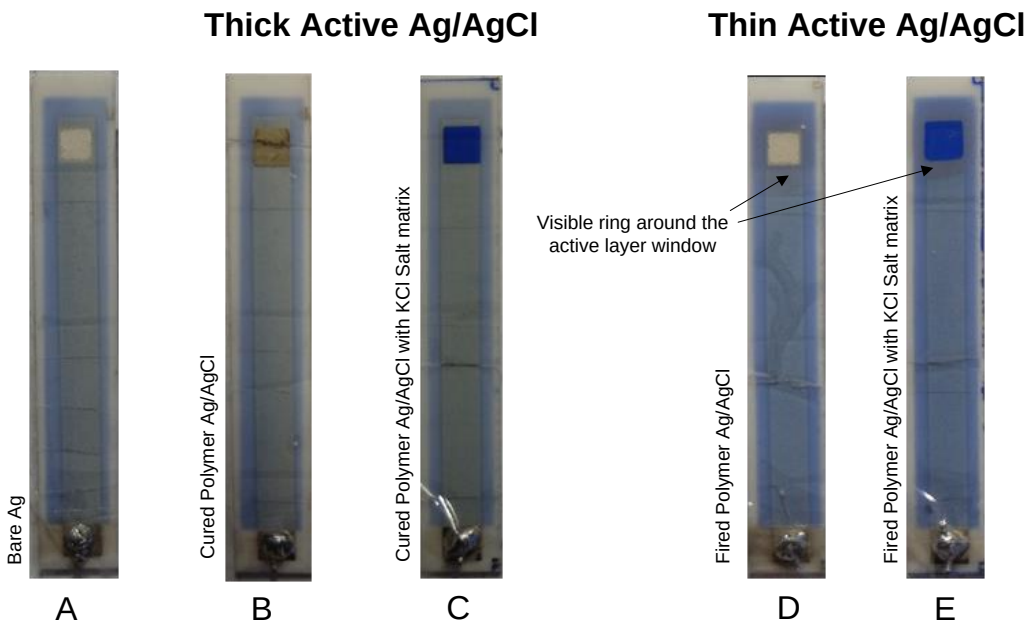

Figure 4-6: Examples of cured (b and c) and fired (d and e) reference electrodes

It was hypothesized that during the firing process the Ag/AgCl layer underwent decomposition and probably AgCl was removed from the reference electrode making it into effectively a bare Ag electrode. To prove this, a SEM scanning analysis was performed for two types of electrodes, a Bare Ag electrode and a Bare Ag electrode with KCl salt matrix layer deposited on top (Figure 4-7).

a)

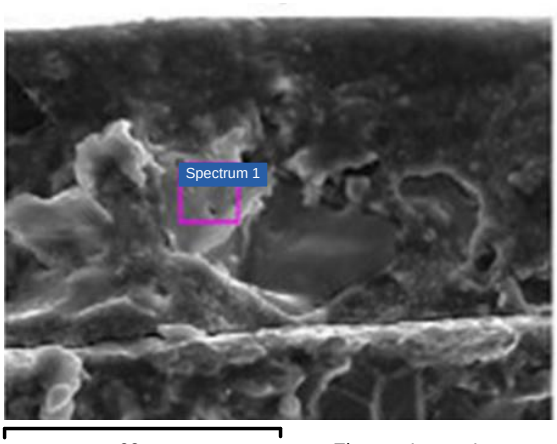

Element	Weight %	Atomic %
Cl	46.23	48.49
K	52.89	50.30
Others	0.88	
Totals	100.00	

b)

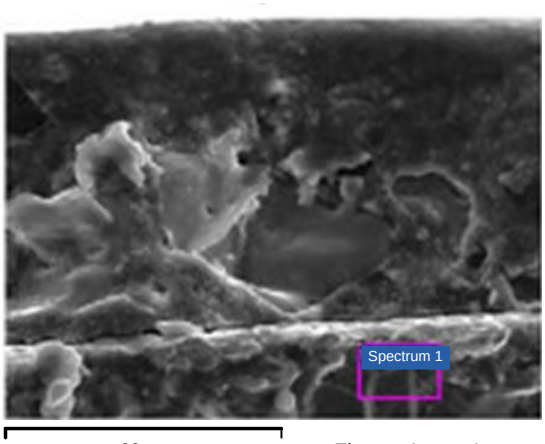

Element	Weight %	Atomic %
Cl	2.06	4.92
Ag	90.71	71.32
Others	7.23	
Totals	100.00	

Figure 4-7: SEM analysis of a Bare Ag electrode with KCl polymer salt matrix layer.

The SEM analysis proved that a thin AgCl layer was still present on the Fired Bare Ag electrode with KCl Salt layer on top. Most probably, some of the surface of the underlying Ag reacted with the KCl forming a small amount of AgCl when the ESL 242-SB layer containing KCl was cured.

Figure 4-8 shows cross section of a TF reference electrode with thick active layer (A) and with thin active layer (B). The Polymer ESL 242-SB with KCl salt matrix layer, now referred to as a thick Ag/AgCl active layer electrode, was cured accordingly to the data sheet recommendations. The Fired Polymer ESL 242-SB with KCl salt matrix layer is, by comparison, referred to as a thin AgCl active layer electrode Figure 4-8B.

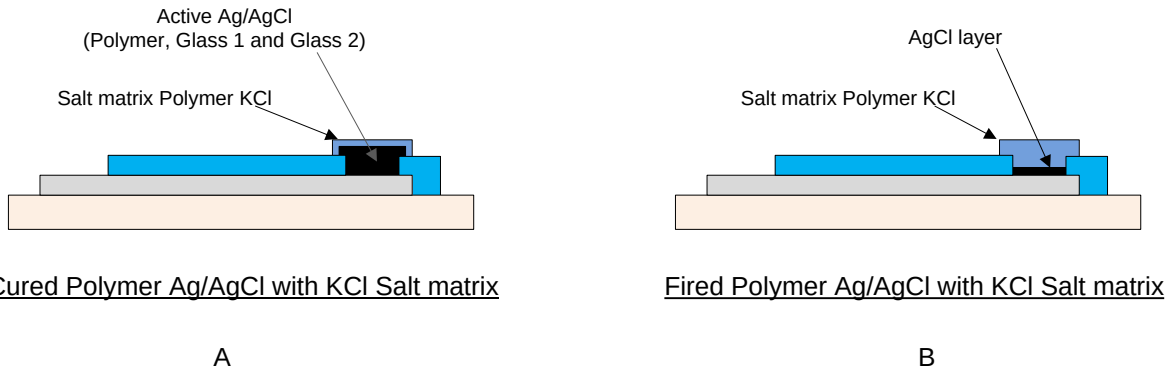

Figure 4-8: TF Ag/AgCl reference electrodes with thick active layer (A) and with thin active layer (B)

4.2.4.2 Results

Batches of TF reference electrodes were left to hydrate in 1:100 Sat KCl solution for approximately 12 hours. After the hydration period, they went through two cycles of testing in varying chloride ion concentrations (Sat KCl solution, 1:10 Sat KCl solution, 1:100 Sat KCl solution and 1:1000 KCl solution) as shown in Figure 4-9.

After immersing in all four concentrations, they were left to soak in a solution of 1:100 Sat KCl for three days during which their drift was observed. Lastly, they were cycled again through the same kind of varying chloride concentrated test solutions.

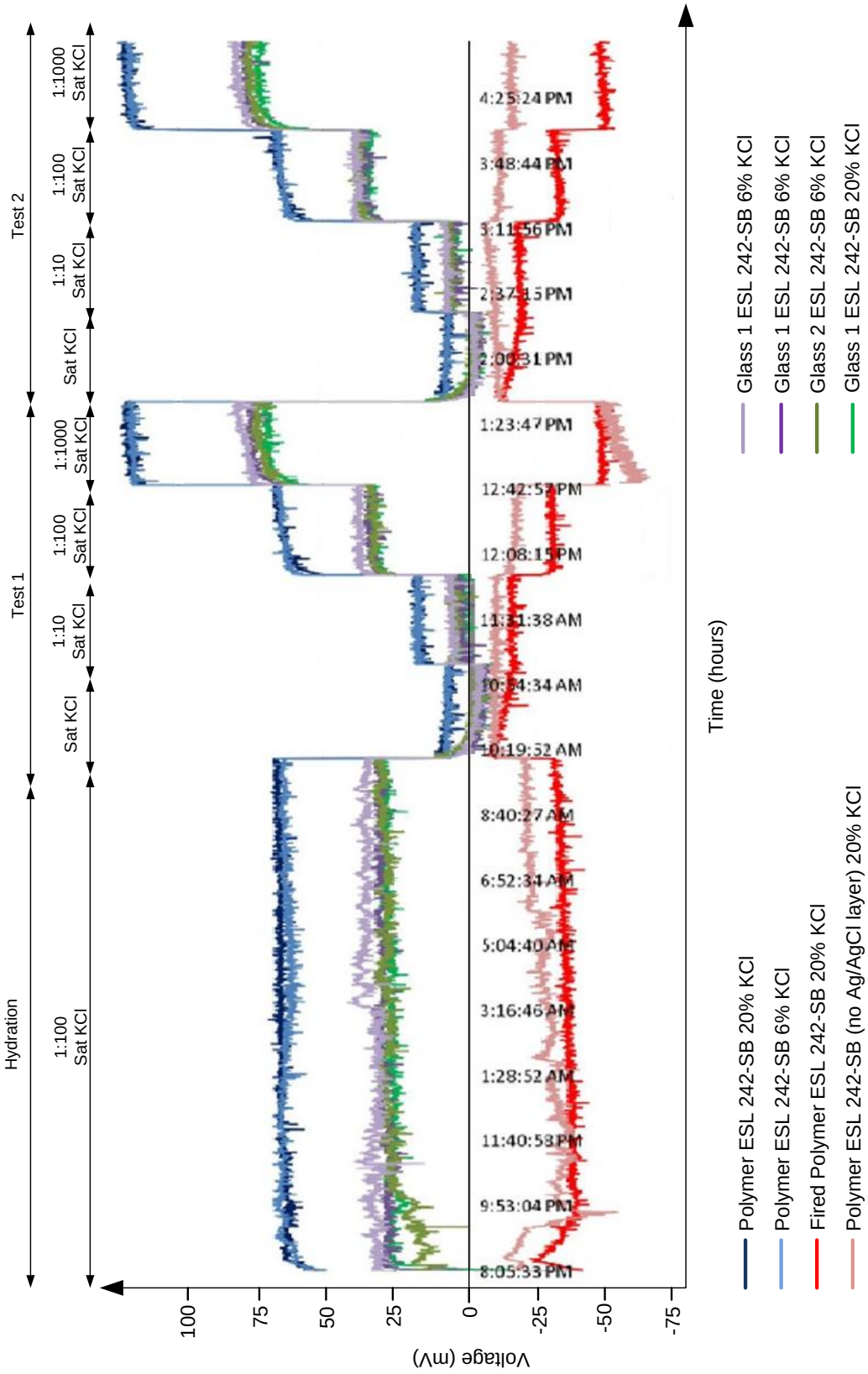

Figure 4-9: Responses of TF reference electrodes to different concentrated chloride ion solutions

In this experiment, the behaviour of two groups of TF Ag/AgCl reference electrodes with thin and thick active layer were observed. All electrodes had different initial potentials that were reasonably stable during the hydration time. It was anticipated that the electrodes behaviour would change in a manner that was observed previously. However, the experimental results were unexpected. The two groups of devices exhibited opposite responses as shown in Figure 4-9.

The reference electrodes with thick Ag/AgCl layers followed the Nernstian response. The Polymer bound Ag/AgCl electrodes exhibited the greatest sensitivity of approx. -50 mV/decade $[Cl^-]$. The sensitivity of the Glass bound (Glass 1 and Glass 2) Ag/AgCl reference electrodes was slightly lower between -30 and -33 mV/decade $[Cl^-]$ and between -33 and -38 mV/decade $[Cl^-]$ respectively as shown in Table 37, Appendix 3.

Table 37: Sensitivity of all reference electrode types before and after 3-day drift test

No.	Reference electrode types	Ag/AgCl layer binder type	mV/decade $[Cl^-]$ before drift test	mV/decade $[Cl^-]$ after drift test
1	Glass 1 ESL 242-SB 20% KCl	Glass	-30	-33
2	Glass 2 ESL 242-SB 20% KCl		-33	-38
3	Polymer ESL 242-SB 20% KCl	Polymer	-47	-49
4	Fired Polymer ESL 242-SB 20%KCl		+12.6	-7.6
5	Polymer ESL 242-SB 20% KCl (no Ag/AgCl layer)	No Ag/AgCl	+2.5	-9.6

Previous investigations assumed that the higher concentration of KCl in the salt matrix layer would give smaller potential change during electrodes cycling through different testing solutions. Both Polymer based electrodes with 6% and 20% of KCl in salt matrix layer as well as the Glass based electrodes with the same amount of salt in the top layer salt reservoir shown similar trends (Figure 4-9). The electrode potential increased while the electrodes moving from the higher to lower saturated test solutions.

The Polymer ESL 242-SB (no Ag/AgCl layer) 20% KCl and the Fired Polymer ESL 242-SB 20% KCl reference electrode showed surprisingly different response over

time to the first group of electrodes with thick active Ag/AgCl layer. Arguably, these electrodes were not Ag/AgCl reference electrodes. The SEM investigations evidenced this as shown in Chapter 4, section 4.2.4.1 via Figure 4-7. Presumably, the surface of the TF reference electrodes with a thin AgCl active layer underwent some changes during immersion in test solution of different salt concentrations, refer to Figure 4-10.

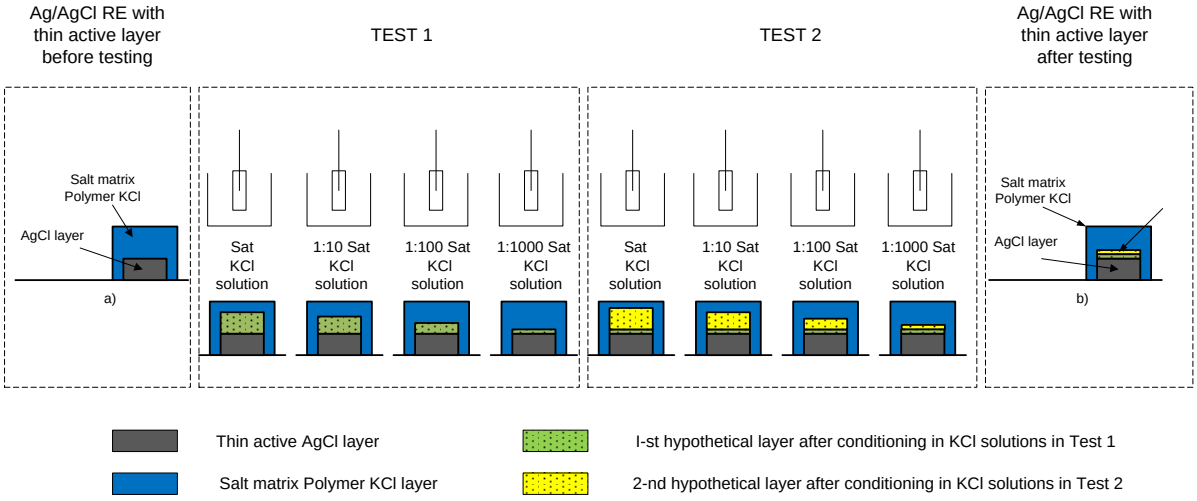

Figure 4-10: Hypothetical changes in the surface of the thin AgCl active layer.

To understand the operation of both groups of TF reference electrodes, the TF reference electrodes with a thick Ag/AgCl layer and TF reference electrodes with a thin AgCl layer, it is important to comprehend the theory behind the operation of the conventional Ag/AgCl reference electrode (Chapter 2, section 2.3.1.3).

The general potential of TF reference electrodes with a thick active Ag/AgCl layer and for TF reference electrode with a thin AgCl layer involved in Experiment # 4 can be described by the Nernst equation:

$$E = E^0 + \frac{0.059}{n}\log_{10}\frac{[AgCl_{(s)}]}{[Ag_{(s)}]} - \frac{0.059}{n}\log_{10}[Cl^-] \qquad \text{Eq. 71}$$

The value of the first term that is the standard potential in the Nernst equation (E^0) was assumed to be constant throughout the experiments.

The potential of the TF reference electrodes with a thick active Ag/AgCl layer could be explained by the Nernst equation where $\log_{10} \frac{[AgCl_{(s)}]}{[Ag_{(s)}]}$ corresponded to the number of ion activity $\frac{a_{AgCl}}{a_{Ag}} = 1$ where $\log_{10} 1 = 0$. Consequently, the potential of the TF reference electrode with a thick Ag/AgCl layer can be described by the following question:

$$E = E^0 - \frac{0.059}{n} \log_{10}[Cl^-] \quad \text{Eq. 72}$$

The potential of the TF reference electrode with a thin AgCl layer could however be expressed by the second term in the Nernst equation:

$$E = E^0 + \frac{0.059}{n} \log_{10} \frac{[AgCl_{(s)}]}{[Ag_{(s)}]} \quad \text{Eq. 73}$$

When the TF reference electrode with a thin active layer was immersed in the test KCl solutions, the chloride ions present in the test solution could have conditioned the surface Fired Polymer Ag/AgCl layer electrode (Figure 4-10). Therefore, the exposed Ag could be chloridised to AgCl, which is a partially soluble salt that could dissolve into the test solution. The process of changing surface morphology of the TF reference electrode with a thin AgCl layer has changed the ratio of $\frac{[AgCl_{(s)}]}{[Ag_{(s)}]}$ and therefore influenced the electrode potential.

Figure 4-11 and Figure 4-12 show the average of the voltages of each electrode type in every solution that was calculated and plotted to show the general relationship between chloride concentration and electrode potential.

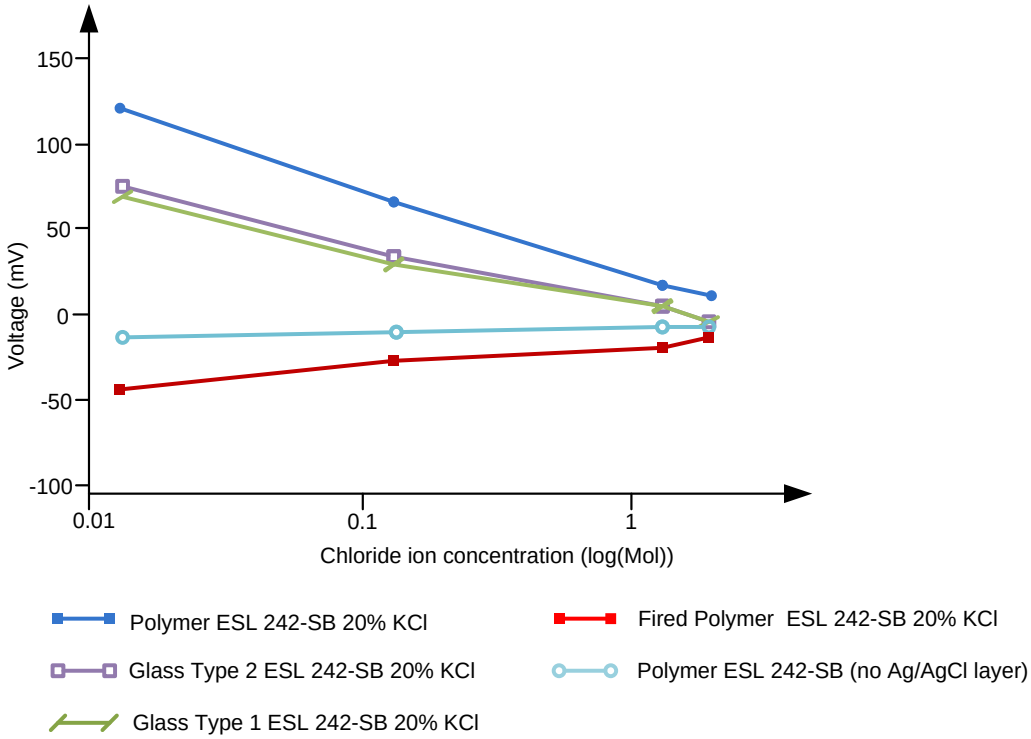

Figure 4-11: Voltage versus chloride ion concentration on logarithmic scale before 3-day drift test.

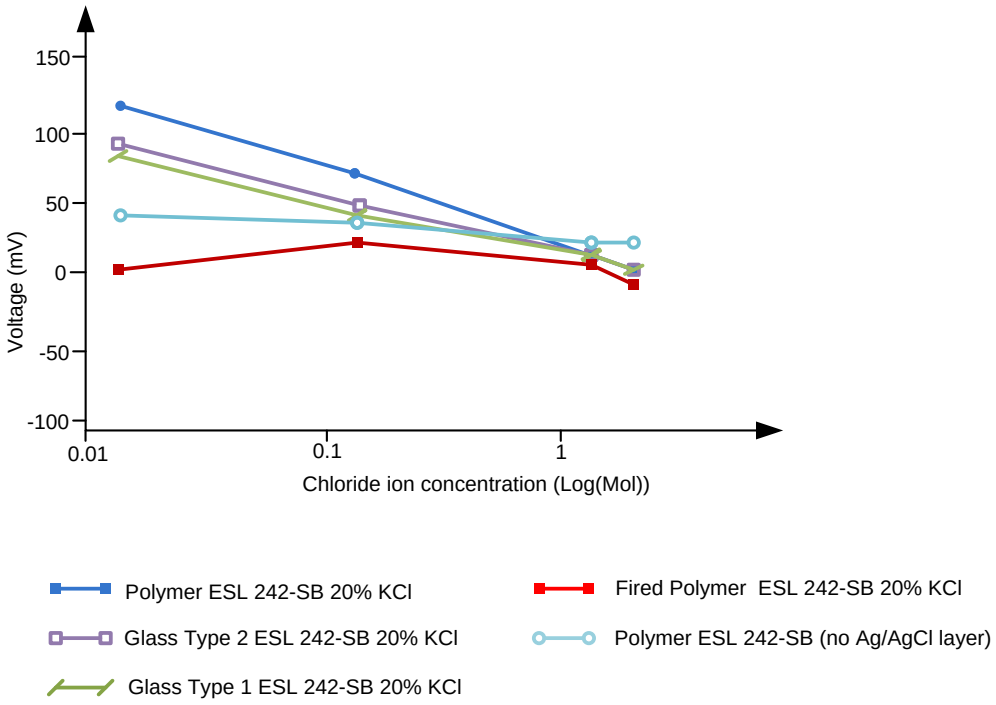

Figure 4-12: Voltage versus chloride ion concentration on logarithmic scale after 3-day drift test.

The TF reference electrodes with a thick active Ag/AgCl layer were more susceptible to chloride ions compared with the TF reference electrodes with a thin AgCl layer.

The second group of electrodes displayed the best chloride ion stabilities but also they were the most susceptible to longer-term drift.

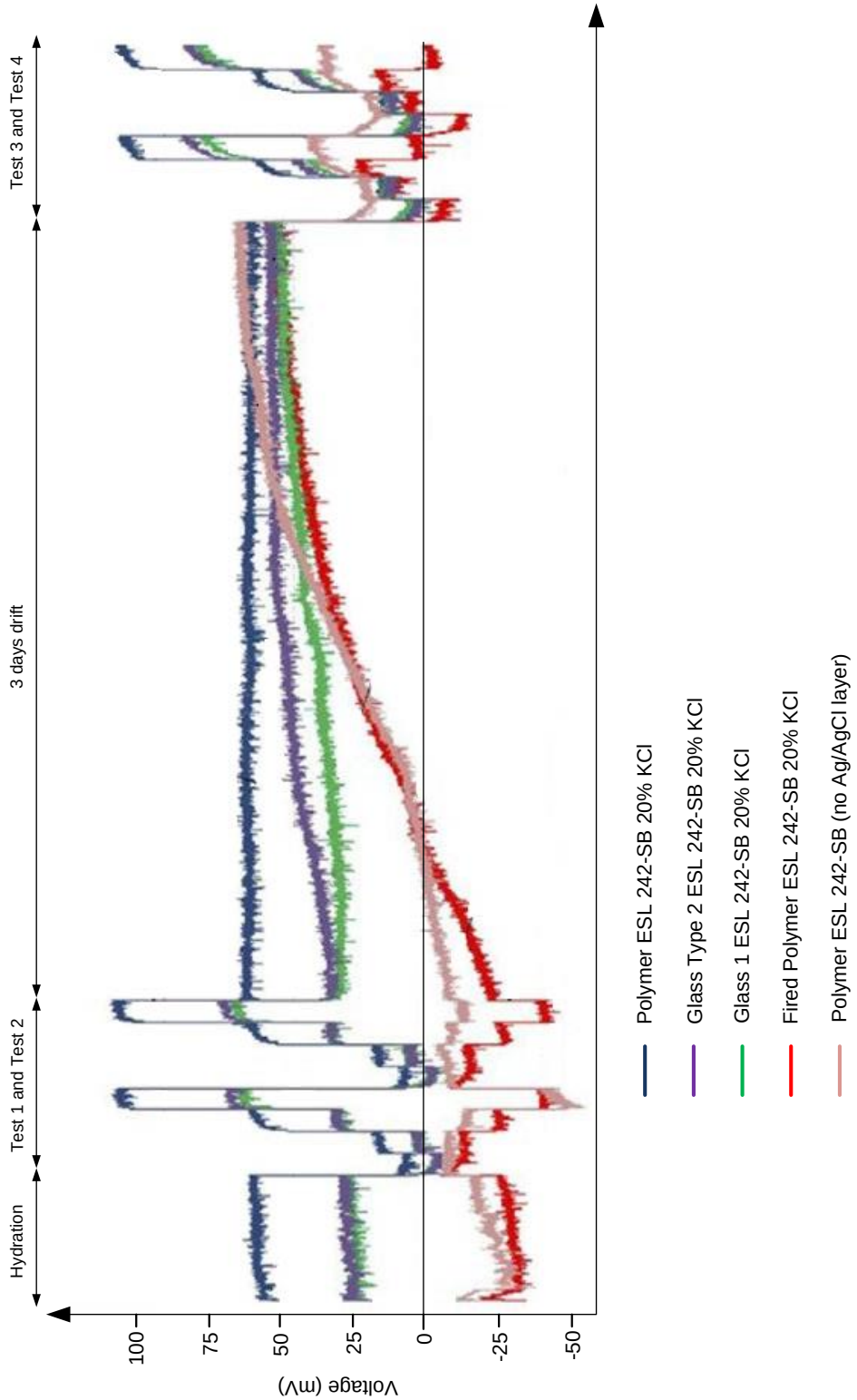

Figure 4-13: Various types of thick-film reference electrodes immerse in KCl solution for over 3-day [7]

Figure 4-13 has shown their drift trend from an initial potential of approximately -25 mV. Fired Polymer ESL 242-SB 20% KCl and Polymer 242-SB 20% KCl (no Ag/AgCl layer) 20% KCl had almost identical behaviour Figure 4-13.

4.2.4.3 Conclusions

The conclusions listed below summarise the test results of TF reference electrodes in varying chloride ion concentrations. The response of Polymer ESL 242-SB 20% KCl with no Ag/AgCl layer, as indicated by the change in slope shown in Figure 4-11 and Figure 4-12, has changed from positive to negative with respect to increasing chloride ion concentration before and after the 3-day drift period. This would suggest that the initial bare silver back contact of these electrodes chloridised during the intermediate 3-day period. In addition, the initial bare Ag electrode covered by salt matrix layer with 20% KCl has a different mechanism compared to the Ag/AgCl chloride layer.

The response of the Fired Polymer ESL 242-SB 20% KCl reference electrode was different although very repeatable over a series of experiments after the 3-days drift period (Figure 4-13). The behaviour of the Fired Polymer electrodes needs to be investigated further.

It was indicated by the earlier work described in Experiment # 1 [10] that the Polymer salt matrix layer rapidly loses its salt on immersion in solution through dissolution of the KCl, leaving behind a porous layer. The exposed Ag at the electrode surface is likely chloridised in increasing chloride ion concentrated solutions to give an increasingly positive potential. It can also dissolve into lower concentrated chloride ion solutions and give a subsequently negative change in electrode potential.

The results of TF reference electrodes with a thin Ag/AgCl active layer, the Fired Polymer ESL 242-SB electrode and Polymer ESL 242-SB (no Ag/AgCl layer), both with 20% KCl in the salt matrix layer has shown that the Polymer bound KCl salt matrix layer was a source of chloride ions. As a result of their presence, a thin layer of silver chloride was able to grow on the electrode surface. The porous KCl salt matrix layer on both electrodes did not behave as a buffer layer and did not maintain a relatively stable chloride ion concentration. The increased dissolution of silver

chloride is increasingly lower chloride ion concentration solutions influenced the potential that become more negative.

The polymer bound Ag/AgCl devices exhibited a near Nernstian slope of 50 mV per decade of chloride ion concentration in comparison to the glass bound Ag/AgCl devices (approx. 30 mV/decade $[C^-]$). The Polymer bound and the Glass bound Ag/AgCl layers morphologies need to be further investigated.

4.2.5 Experiment # 5

4.2.5.1 Materials

In this experiment, five types of TF reference electrodes and one types of pH electrodes were tested (Table 38).

Table 38: Thick-film Ag/AgCl reference electrode types

No.	Reference electrode types
1	Bare Ag ESL 9912-A
2	Polymer ESL 242-SB 20% KCl
3	Fired Polymer ESL 242-SB 20% KCl
4	Chemically grown chloride 2m + 20% KCl
5	Chemically grown chloride 1h + 20% KCl

The metal oxide pH sensor was constructed in a very similar manner to the reference electrodes (Figure 3-14). They were fabricated with a top layer of Polymer bound Ruthenium oxide (GEM C50502D7) as shown in Table 39.

The tested reference electrodes varied in terms of their electrode active layer construction (23). Type of TF reference electrodes and their materials used during the manufacturing process are demonstrated in Table 40-Table 43. The same Polymer bound Ag/AgCl layer (GEM C61003P7) was used for the Polymer ESL 242-SB 20% KCl and the Fired Polymer ESL 242-SB 20% KCl electrodes (Table 40 and Table 41). Two further types of TF reference electrodes were tested that do not

possess a printed Ag/AgCl layer but instead they have a thin layer of AgCl that was chemically grown on the Ag conductor (Table 42 and Table 43).

Table 39: TF pH electrode materials

pH electrode		
Layer no.	**Layer type**	**Paste type**
1	Platinum Gold Conductor	ESL 5837
2	Polymer Dielectric	GEM 2020823D2
3	Ruthenium Polymer	GEM C50502D7

Table 40: Reference electrode materials – Polymer ESL 242-SB 20% KCl

Polymer ESL 242-SB 20% KCl			
Layer no.	**Layer type**		**Paste type**
1	Silver Conductor		ESL 9912-A
2	Glass Dielectric		ESL 4905-CH
3	Active Ag/AgCl	Cured Polymer Ag/AgCl	GEM C61003P7
4	Salt matrix	Polymer 20% KCl	ESL 242-SB 20% KCl

Table 41: Reference electrode materials – Fired Polymer ESL 242-SB 20% KCl

Fired Polymer ESL 242-SB 20% KCl			
Layer no.	**Layer type**		**Paste type**
1	Silver Conductor		ESL 9912-A
2	Glass Dielectric		ESL 4905-CH
3	Active Ag/AgCl	Fired Polymer Ag/AgCl	GEM C61003P7
4	Salt matrix	Polymer 20% KCl	ESL 242-SB 20% KCl

Table 42: Reference electrode materials – Chemically grown chloride 2m + 20% KCl

Chemically grown chloride 2m + 20% KCl			
Layer no.	**Layer type**		**Paste type**
1	Silver Conductor		ESL 9912-A
2	Glass Dielectric		ESL 4905-CH
3	Active Ag/AgCl	*	
4	Salt matrix	Polymer 20% KCl	ESL 242-SB 20% KCl

Table 43: Reference electrode materials – Chemically grown chloride 1h + 20% KCl

Chemically grown chloride 1h + 20% KCl			
Layer no.	**Layer type**		**Paste type**
1	Silver Conductor		ESL 9912-A
2	Glass Dielectric		ESL 4905-CH
3	Active Ag/AgCl	*	
4	Salt matrix	Polymer 20% KCl	ESL 242-SB 20% KCl

*An exposed silver window was chemically coated with a thin layer of silver chloride by electroplating in 1M HCl.

4.2.5.2 Results

The complete data analyses are presented in Appendix 2. Firstly, the performance of the TF reference electrodes in sequential testing solutions in different strength KCl solutions was measured. After that batches of the same TF electrodes were subjected to cycling through varied number of buffer solutions (pH 7, 10, 7, 4, 7, 4, 7, 10, and 7). At each change of buffer, the electrodes were rinsed in deionised water. The electrode potentials were measured with respect to a commercial gel-filled reference electrode (Beckman Coulter A57193).

The TF pH electrodes showed a change on the settling time depending on the solution it was immersed in with a longer settling time especially in pH=10. The electrode showed dependence on the previous solution they were in (Figure 4-13) has shown that the reference electrode responded almost instantly to chloride concentration changes but fast when immersed in pH buffers.

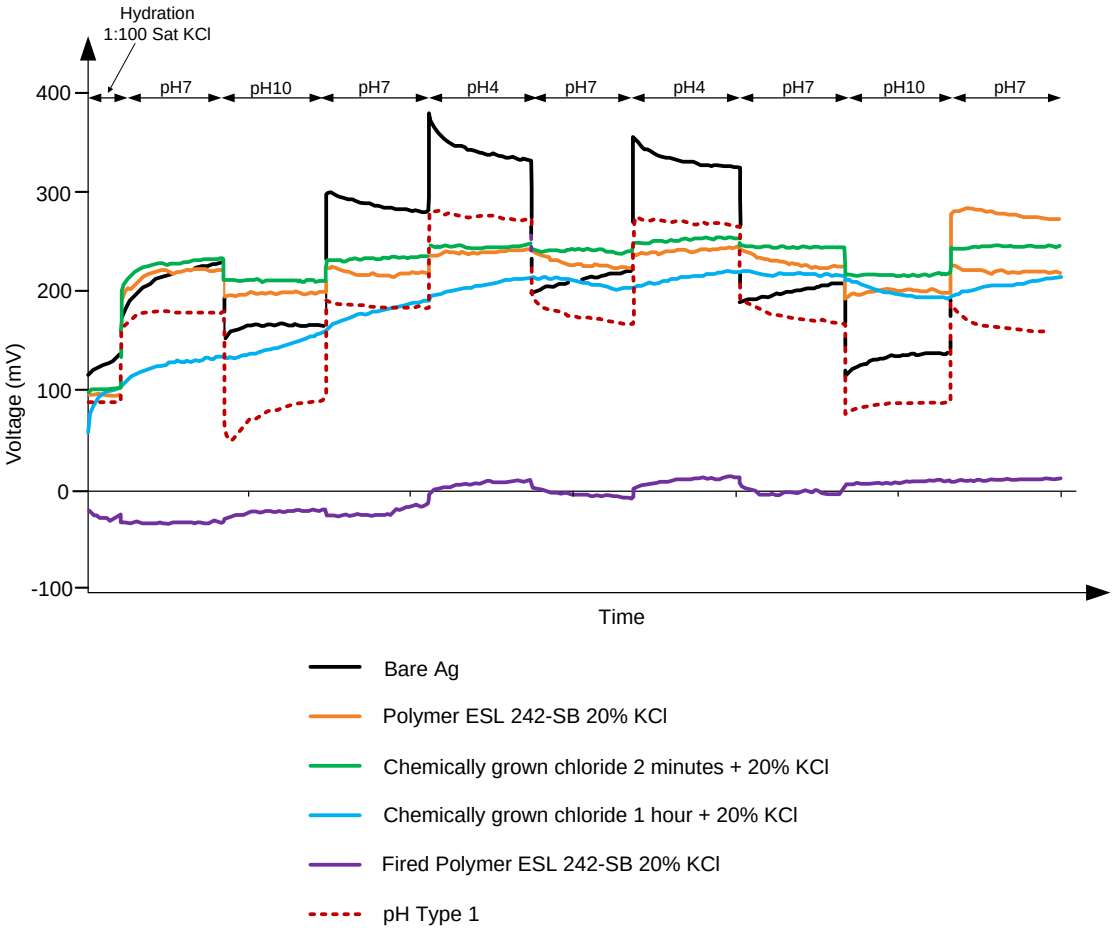

Figure 4-14: TF pH and reference electrodes in pH buffer solutions

Table 44: TF reference electrodes pH sensitivity

No.	TF electrode types	mV/decade $[Cl^-]$
1	Bare Ag	-32
2	Polymer ESL 242-SB 20% KCl	-7
3	Fired Polymer ESL 242-SB 20%KCl	-3
4	Chemically grown chloride (2 minutes) + 20% KCl	-6
5	Chemically grown chloride (1 hour) + 20% KCl	-7
6	Ruthenium oxide ion-selective electrode	-32

The Fired Polymer ESL 242-SB 20% KCl reference electrodes demonstrated a nearly stable potential response in all tested solutions in comparison to Polymer Ag/AgCl 20% KCl and the two chemically grown chloride electrodes (Figure 4-14).

Figure 4-15 has shown the stability of the TF devices as a function of chloride ion concentration.

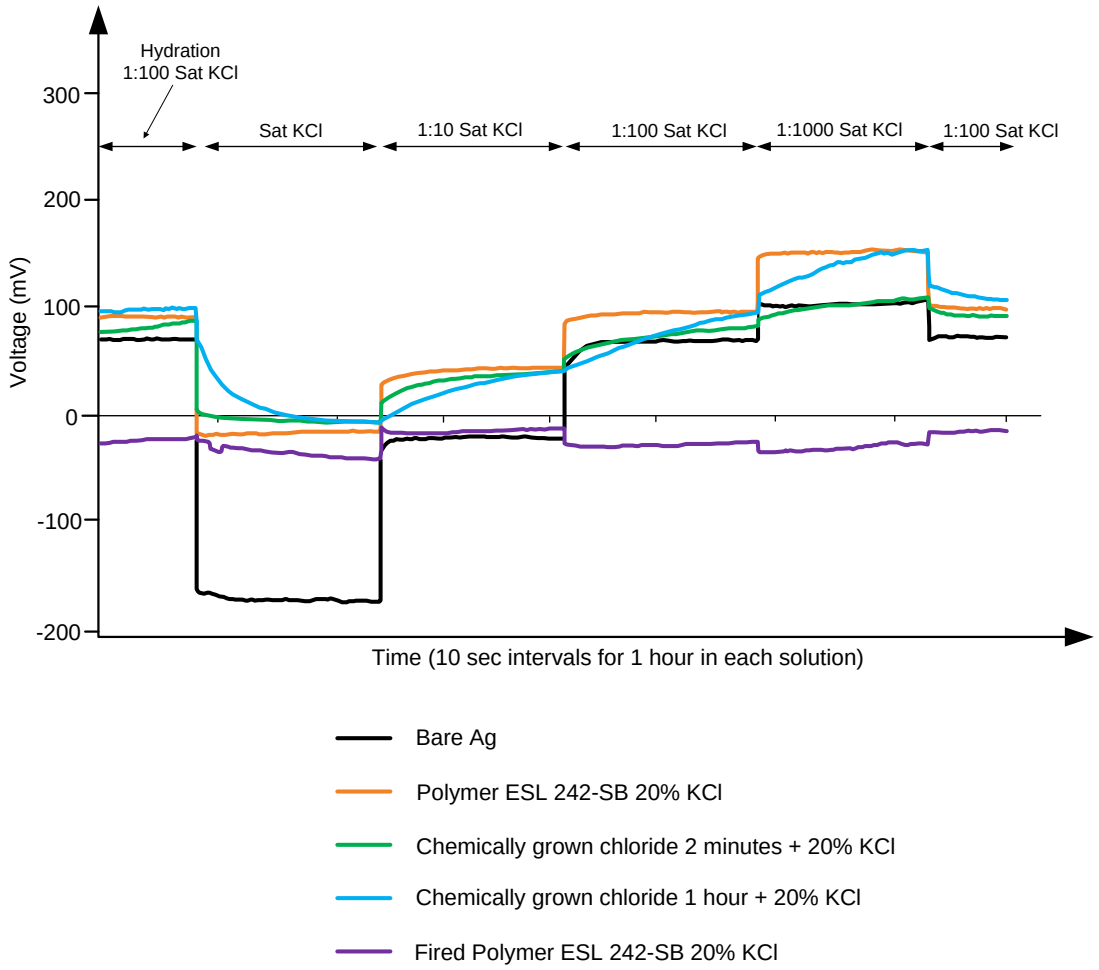

Figure 4-15: TF reference electrodes in KCl solutions

Table 45: TF reference electrodes chloride ion sensitivity

No.	TF electrode types	mV/decade $[Cl^-]$
1	Bare Ag	-59
2	Polymer ESL 242-SB 20% KCl	-30
3	Fired Polymer ESL 242-SB 20%KCl	-2
4	Chemically grown chloride (2 minutes) + 20% KCl	-20
5	Chemically grown chloride (1 hour) + 20% KCl	-30

Overall, the Fired Polymer ESL 242-SB 20% KCl reference electrodes gave the most stable potential response in KCl test solutions and in pH buffer solutions.

Table 45 summarised the sensitivities of the various types of TF reference electrodes. The electrode with chemically grown silver chloride 1 hour has shown an anomaly in the Sat KCl solution by having a higher potential than expected. Presumably, the hydration time for this type of electrode needs to be longer then allowed hydration time for the rest of electrodes. The general potential trend of the chemically grown chloride (1 hour) + 20% KCl electrodes deviates significantly in comparison with other electrodes.

The responses of the TF reference electrodes and TF pH electrode in various pH buffers solutions were shown in Figure 4-15.

The ruthenium oxide pH electrode had showed very repeatable and stable response to the pH buffer changes and also reached a stable potential quite rapidly after immersion in the various pH buffers.

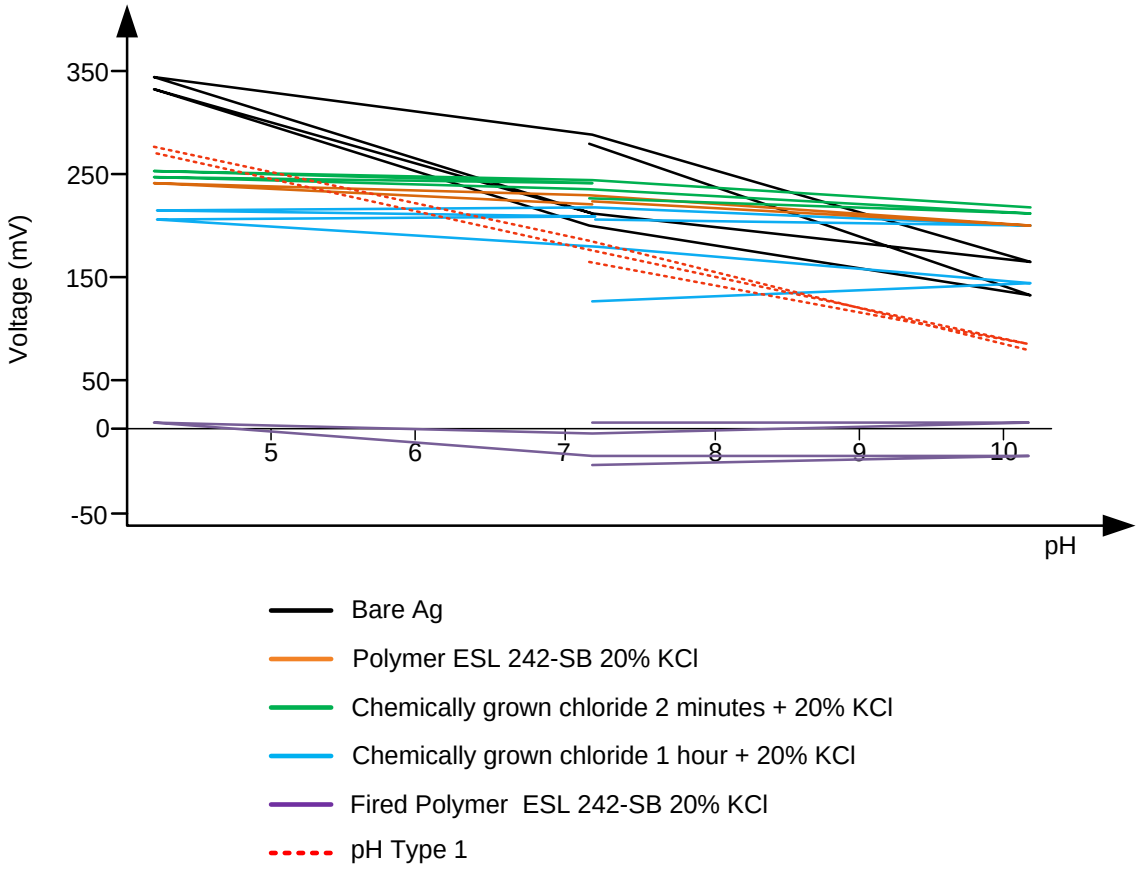

Figure 4-16: TF electrodes potentials as a function of pH

4.2.5.3 Conclusions

The presented results demonstrated the feasibility of the development of low-cost, rugged, miniaturised TF alternatives to the commercially available Ag/AgCl reference electrode and glass pH electrodes but they require further extensive investigation.

Chapter 5 **Discussion and Conclusion**

5.1 Summary of the Thesis Outcomes

The research comprised two investigations where in a laboratory environment different types of miniaturised, solid-state, planar, thick-film Ag/AgCl reference electrodes and thick-film Ruthenium oxide pH ion-sensitive electrodes were tested. The most important, substantial part of this work concentrated on the Ag/AgCl reference electrodes and stems from the previously conducted experimental work that focused on various electrode parameters e.g. window sizes of the waterproofing layer or thickness of the salt reservoir layer. The design of the fabricated TF reference electrodes needed to mimic the kinetics and operation of the conventional electrolyte-filled Ag/AgCl reference electrode. In this study, TF Ag/AgCl reference electrodes with different paste formulations were fabricated and experimentally tested. The characteristics and response of the reference electrodes with respect to variations in the Ag/AgCl layer and KCl salt matrix layer were subsequently investigated. The laboratory tests focuses on the electrodes susceptibility, the length of hydration time and the drift.

All TF reference electrodes were manufactured in the thick-film screen-printed manufacturing process. Generally, the TF reference electrodes of the same type gave very similar responses due to the fabrication process that was controlled with equal printing parameters. In addition, they were significantly repeatable due to the identical electrodes' structure and material composition. TF Ag/AgCl reference electrodes were classified according to the materials used in the manufacturing process. The classification process entailed dividing the reference electrodes into three groups: I. the TF electrodes with a thick active Ag/AgCl layer, II. the TF reference electrodes with a thin active AgCl layer and III. the TF electrodes with a salt matrix layer.

5.1.1 Thick-Film Reference Electrodes with a Thick Active Ag/AgCl layer

The first group of TF devices was composed of the Polymer bound Ag/AgCl paste (GEM C61003P7) and of two Glass based Ag/AgCl pastes (Valencia PPCF2 and Valencia PPCFC3). These electrodes were also known as the TF reference

electrodes with a thick Ag/AgCl active layer. They were manufactured accordingly to the manufacturer paste requirements.

The initial potential for both Polymer bound and Glass bound TF reference electrodes with a thick active Ag/AgCl layer was different when the electrodes hydrated. All the electrodes drifted significantly to a more positive potential and eventually they converged to a roughly common potential at the end of the 3 days drift period. This was believed to be due to the loss of chloride ions from the salt matrix layer to the lower concentrated test solutions and to chloride ions forward diffusion into the salt matrix layer and the thick active Ag/AgCl of chloride ions that caused the chloridisation of exposed Ag.

The TF electrodes with the non-commercial Glass based Ag/AgCl pastes performed slightly better than the Polymer thick active Ag/AgCl reference electrode in terms of stability and susceptibility. The reason for this could lie in the components types used in the Ag/AgCl paste production that gives better results when glass Ag/AgCl paste is used.

5.1.2 Thick-Film Reference Electrodes with a Salt Matrix layer

The second group of TF reference electrodes with salt matrix layer comprises of three types of electrodes. For each electrode, the bottom layer is always silver conductor. For the above layer, the three types of electrodes can be distinguished as: I. a thick Ag/AgCl active layer with KCl salt in ESL 242-SB polymer paste on top; II. a thin Ag/AgCl active layer with KCl salt in ESL 242-SB polymer paste on top and III. only KCL salt in ESL 242-SB polymer paste on top of the silver. For more clarification, refer to Figure 4-8.

The electrode performance has changed when an additional layer of ESL 242-SB with KCl was added on top. Electrodes with low percentage of KCl in the polymer paste have low conductivity. They are more susceptible to noise then the electrodes with high percentage of KCl in the KCl salt matrix layer.

The hydration time was faster for the electrodes with salt matrix layer containing grains of salt. When the electrodes cycled from Sat KCl solution to lower chloride

ion concentration the chloride ions diffused out of the salt reservoir into the more dilute test solution. The loss of chloride ions in the salt matrix layer increased the electrode potential or gave positive change to the electrode potential. After that, the test solution could start to penetrate the porous paste through its empty paths and influenced the dissolution of soluble AgCl from the active layer to the lower strength KCl solution. Subsequently, loss of AgCl gave a decrease or negative change in electrode potential. The hydration time was slower in the electrodes with less amount of KCl salt in the salt matrix layer. These electrodes also have longer lifetimes.

The electrode susceptibility has changed due to diffusion of the chlorine ions in the salt matrix layer. The susceptibility decreased with the increase of KCl salt concentration in the top layer, as happened with the electrodes with 20% by weight of KCl powder in the polymer ink. The electrodes with more salt then 20% by weight in the electrode salt reservoir showed increased susceptibility. At that point the polymer paste was not able to hold more salt in the salt matrix layer.

5.1.3 Thick-film Reference Electrodes with a Thin Active AgCl layer

This third group contained the Fired Polymer ESL 242-SB electrodes. These electrodes distinguished from the other two groups of TF reference electrodes by the presence of a thin active AgCl layer. The fabrication process of these electrodes did not follow the data sheet requisites.

The behaviour of TF reference electrodes with a thin AgCl layer was explained fully in Chapter 4, section 4.2.4. These reference electrodes showed lowest susceptibility to chloride ions in test solutions.

5.1.4 Application

The thick-film screen printing process allows a large degree of variation in the electrode characteristics such as numerous choices of materials. It also offers flexibility in the electrode design. All of these suggest that different reference electrode types are suitable for different applications. The reported results indicate that the TF reference electrodes, both the TF reference electrodes with a thin AgCl

layer and TF reference electrodes with a thin Ag/AgCl layer, are suitable for a variety of subterranean and submerged aqueous applications. The TF reference electrodes with a thick Ag/AgCl later can be used for longer-term deployment in soil sensing where chloride ions concentration changes may not be liable to wide variation as in water (e.g. rivers). These devices are more sensitive to chloride ions concentration changes and have a lower and longer potential drift. The TF reference electrodes with a thin active AgCl layer can be employed for short-term deployments in water (e.g. a river, a stream) where chloride ions concentration changes are vulnerable to wide variation. These devices are less sensitive to chloride ions concentration variation but are affected adversely by a higher rate of drift.

5.2 Future Work

Although, this project has not yet delivered a perfect TF reference electrodes but it help to understand their operation process. In addition, many electrode types with variety of materials used in the fabrication process were tested and evaluated.
The next set of tests for the reference electrode should include:

- To specify the electrodes lifetime, hydration time and drift rate;
- To identify the length of time the electrodes can be stored;
- To test the TF reference electrodes in other chloride solutions;
- To identify the best possible membrane for reference electrode and test it;
- To find how to incorporate the membrane into the electrode;
- To test the TF electrodes for susceptibilities in nitrates and phosphates
- To fabricate the TF reference electrodes with a thin active layer in combined processes by using thick-film screen-printing process together with sputtering and test the new devices as previously for comparison.

Appendices

Appendix 1

Within Appendix 1 is the journal paper published in Sensors and Actuators A: Physical in 2013.

The Effect on Performance of Fabrication Parameter Variations of Thick-Film Screen Printed Silver/Silver Chloride Potentiometric Reference Electrodes

M. Glanc[1], M. Sophocleous[1*], J. K. Atkinson[1], E. Garcia-Breijo[2]*

[1]Faculty of Engineering and the Environment, University of Southampton, United Kingdom
[2]Instituto de Reconocimiento Molecular y Desarrollo Tecnológico,
Universidad Politécnica de Valencia, Spain

Abstract

Thick-film screen printed silver-silver chloride (Ag/AgCl) reference electrodes have been fabricated and investigated as an alternative to liquid electrolyte Ag/AgCl reference electrodes. The performance of the electrodes was examined with variations of the potassium chloride (KCl) concentration in the final (top) layer of the electrode. Also, different types of binder (glass and polymer) were tested for the underlying Ag/AgCl layer. The addition of another layer on top of the KCl containing salt matrix layer has been found to provide a better stability in varying concentrations of KCl test solutions. The electrodes were found to give a satisfactory performance when tested for stability in different pH solutions.

1. Introduction

There has been a growing interest in the development of new, miniaturised and low cost electrochemical sensors suitable for industrial, biomedical and environmental applications [1]. Thick film technologies together with electrochemical methods embrace the requirements for these devices by giving cost competitive solutions for the fabrication of compact, rugged and robust systems [1]. Thick film chemical sensors offer alternative solutions and allow flexible design with a wide range of materials, low cost infrastructure and mass production capability [2-4].

The silver/silver chloride (Ag/AgCl) reference electrode is a reference electrode of the 'second kind' [5] and is the simplest and most practical type of reference electrode used in industry and research. The response of any electrochemical potentiometric electrode is meaningless without a reference electrode against which comparisons can be made [6]. Most commercially available Ag/AgCl reference electrodes are of the fragile and expensive conventional type of electrolyte-filled devices. The thick-film devices reported here are implemented on the same principle as the conventional electrolyte-filled Ag/AgCl reference electrode in that they attempt to mimic its operation through the immobilizing of salt reservoirs in the form of salt matrix layers fabricated as upper layers of a planar design that are in contact with the analyte [7]. The conventional commercial silver/silver chloride reference electrode has a relatively simple construction. It consists of a silver metal electrode coated with silver chloride which is immersed in a saturated filling solution and enclosed in a glass or plastic tube separated from the test solution via a porous plug [8]. The typical planar structure of the thick film equivalent consists of a silver back contact, a waterproofing layer, a silver/silver chloride interfacial

layer and one or more overlapping salt matrix layers containing typically potassium chloride (KCl) powder in a lower layer and potassium nitrate (KNO_3) powder in an upper layer. This double layer approach mimics the double junction type of liquid electrolyte reference electrode that typically contains two liquid electrolytes separated by a porous plug. The research reported here investigates variation of the fabrication parameters of screen-printed thick-film Ag/AgCl reference electrodes, such as salt concentration, layer thickness and interfacial layer material types, and their effect on sensor characteristics. The monitoring of electrode potentials in different test solutions over time has been used as a method to determine hydration times, drift rates, stability and useful lifetime of the devices. A major aspect of the investigation has been the focus on the electrode stability and response time across different ionic concentration solutions arising from the addition of different types of salt containing outer layers. The results contribute towards optimisation of the fabrication parameters of low cost miniaturised screen-printed Ag/AgCl reference electrodes and demonstrate the feasibility of the development of a miniaturised alternative to the commercially available liquid electrolyte filled Ag/AgCl reference electrode through the use of thick-film technology.

The classic commercially available silver/silver chloride reference electrode typically consists of a silver wire coated with silver chloride and surrounded by a saturated solution of KCl (approximately 3.5M) [5]. The silver/silver chloride layer forms the interaction between the ion movement in the KCl solution and the electron movement in the silver wire. In the idealised system the internal element is at equilibrium:

$$AgCl_{(s)} + e^{-} \leftrightarrow Ag_{(s)} + Cl^{-}_{(aq)} \quad \textbf{(1)}$$

The equilibrium potential (E) of the electrode is defined by the Nernst equation:

$$E = E^{\theta} + \left(\frac{RT}{nF}\right) \ln \frac{(a_{Oxi})}{(a_{Red})} \quad \textbf{(2)}$$

Where E^{θ} is the standard potential (V); R is the universal gas constant (8.314 $JK^{-1}mol^{-1}$); T is the absolute temperature (K); n is the number of moles of electrons transferred in the reaction; F is the Faraday constant (96485 C mol^{-1}); a is the activity; Oxi is the oxidant and Red is the reductant. In the case of the Ag/AgCl electrode (2) can be re-written as:

$$E = E^{\theta} + \left(\frac{RT}{nF}\right) \ln \frac{(a_{AgCl})}{(a_{Ag})(a_{Cl^-})} \quad \textbf{(3)}$$

The activity of a species a, is defined as the product of the activity coefficient of the specific substance and its concentration. When the species is at its standard state the activity coefficient can be approximated to 1. In the case of $AgCl$ and Ag, since they are in the solid state, their activity can be equated to their concentrations therefore Eqn. (3) can be expressed as:

$$E = E^{\theta} - \left(\frac{RT}{nF}\right) \ln[a_{Cl^-}] + \left(\frac{RT}{nF}\right) \ln \frac{[AgCl]}{[Ag]} \quad \textbf{(4)}$$

The Nernst equation for a cell at a nominal room temperature of 25°C is frequently expressed in terms of base 10 logarithms, with numerical values replacing the constant coefficients and hence re-writing Eqn. (4) gives:

$$E = E^{\theta} - 0.0592 \log(a_{Cl^-}) + 0.0592(k) \quad \textbf{(5)}$$

Where *k* is the concentration ratio of Ag to AgCl. *The* measured electrode is said to display Nernstian behaviour when its potential (E) decreases by approximately 59mV for every decade change in chloride ion concentration at 25°C and provided that the activity coefficient of chloride ion in the solution is approximately equal to unity.

AgCl is a sparingly soluble salt therefore the solution will become saturated very quickly, which will keep the activity of AgCl constant regardless of the immersed solution. The activity of Ag is controlled by the activity solubility product which is invariant at a certain temperature whilst the activity solubility product is the product of the silver ion activity and the chloride ion activity and hence the potential of the electrode depends on the chloride ion activity of the solution surrounding the electrode.

2. Fabrication process

The electrodes were screen printed onto 50 mm x 50 mm, 0.625 mm thick, 96% alumina substrates (Coorstech). Each substrate was divided into six equal sized electrodes and prescribed with laser lines so that individual electrodes could be easily snapped off along those lines. Therefore, a simultaneous six electrode fabrication was possible as shown in Figure 1.

The electrodes were constructed by successive screen printing of each individual layer. The screen designs for each layer were produced using AUTOCAD to give precise dimensions of the mesh openings and each screen was designed to print a single layer of the electrode. The first layer was the silver conductor so the screen mesh opening was a rectangle with dimensions of 4.61 mm x 44.56 mm. On top of that, a waterproofing layer with a rectangular shape of 6.5 mm x 43.8 mm was deposited, leaving a small window exposing the underlying silver. The window size was a square of 3.4 mm x 3.4 mm while a part of the silver, approximately 4.17 mm x 4.61 mm, was also left exposed at one end for soldering connecting wires, as can be seen in Figure 1. The screen for the Ag/AgCl layer was a square window of 4 mm x 4 mm, slightly bigger than the exposed silver to ensure all the silver was covered. The last two screens (for KCl and for KNO_3) had simple square mesh openings, like the Ag/AgCl window, but with increasing dimensions of 4.5 mm x 4.5 mm and 5 mm x 5 mm respectively, to ensure complete coverage of the previous layer.

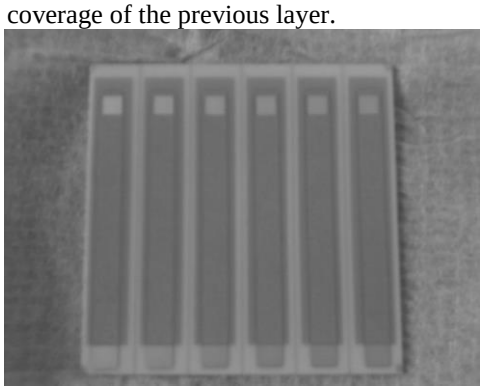

Figure 17: Six simultaneously fabricated reference electrode test strips on a 50mm x 50mm alumina substrate, only the first two layers are present in this case

The screens for first three layers were made from stainless steel with 250 lines per inch, 15 micron emulsion and 45º mesh while the last two were polymer 70W PW 123-70W:133µm with photopolymer emulsion POLYCOL UNO: 113µm thickness. All the screens were manufactured for the Aurel C880 Printer by MCI Cambridge. The silver conductor layer was printed using ESL-9912 ink, on top of which a glass dielectric insulator (ESL 4905-C) was deposited to isolate the conductor from the electrolyte. Different types of Ag/AgCl inks were tested, both polymer and glass based binders, as well as different weight ratios of polymer to KCl as the top layer. The polymer KCl layer was printed using a silicone based ink (ESL 242-SB). The reason different screen types were used was for ease of printing the polymer ESL 242-SB with added KCl, and in order to ensure that the KCl grains would pass through the mesh opening. KCl (Analytical Reagent, Fisher Scientific UK Ltd) was milled into powder of grains smaller than 100 µm and was directly added to the ESL 242-SB paste, adding ESL 402 solvent when required to keep the paste in printable condition.

The construction procedure described above is designed to mimic the construction of a single junction gel-filled commercial reference electrode. Double junction gel-filled reference electrodes are generally found to be more stable and more reliable in time, so in an attempt to improve the stability of the thick-film electrodes, some double junction thick-film reference electrodes were fabricated. The only difference of these electrodes to those described previously is that another layer of ESL 242-SB containing KNO_3 with 1:4 weight ratio was printed on top of the polymer/KCl layer.

Three different types of Ag/AgCl layer were used. One was a polymer based paste provided by Gwent Electronic Materials (GEM C61003P7), the other two types where glass based inks provided by Universidad de

Politécnica de Valencia, Spain. The glass bound Ag/AgCl layers were fabricated from two screen printable pastes that were prepared as follows. Type 1 (Valencia PPCFC3): AgCl (Aldrich 227927) milled to 400 rpm/30min with ethanol (Pulverisette Fritsch), sieve/100μm, Ag (Aldrich 32708-5) sieve/100μm, powder frit (Ferro CF7567FC) sieve/100μm, vehicle (Heraeus V-006), mixed in the ratios 3gr Ag + 3gr AgCl + 2gr frit + 3.84gr vehicle and triple roll milled for 5 minutes. Type 2 (Valencia PPCFB2) is exactly the same as Type 1 with the exception of a different powder frit (Ferro EG2020VEG).

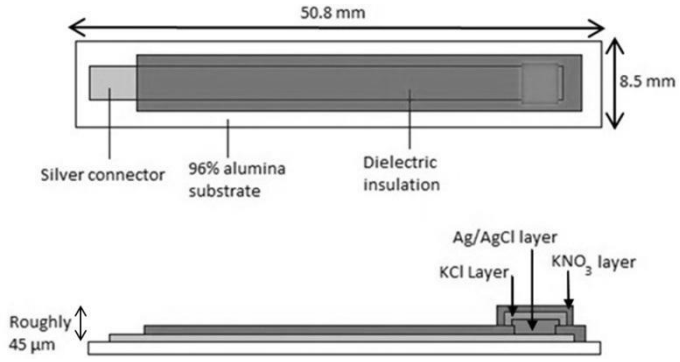

Figure 18: The construction of a Screen-Printed Ag/AgCl reference electrode

The first two layers were held at room temperature for 10 minutes after printing to allow relaxation of surface stresses and then dried in a DEK 1209 infrared mini dryer at 125º C for 15 minutes. They were then cured in a 6 zone belt furnace (BTU VQ41) at a peak temperature of 850º C with an ascent and descent of 50ºC/min and held at peak temperature for 10 minutes. Drying and curing temperatures for each of the pastes comprising the subsequent layers are as detailed in Table 1 below.

Table 46: Curing temperatures and times for each layer

Layer	Paste	Drying temperature (º C)	Drying time (min)	Curing temperature (º C)	Curing time (min)
Silver conductor	ESL-9912-A	125	10 – 15	850	~45
Dielectric insulator	ESL-4905-C	125	10 – 15	850	~45
Glass Ag/AgCl	PPCFB2	150	10	420	~30
Glass Ag/AgCl	PPCFC3	150	10	390	~30
Polymer Ag/AgCl	GEM C61003P7	60	30	-	-
Polymer KCl & KNO3	ESL-242-SB	125	10	150	30

3. Experimental Setup

The performance and stability of the electrodes was tested by measuring their electro potential difference with respect to a commercial gel-filled single junction reference electrode (Beckman Coulter A57193). Three electrodes of each type were tested by soldering wires onto their exposed silver conductor layers and connecting them to the voltmeter. Measurements were carried out using an own design portable data logger. The output signals of the multi-electrodes were acquired using a 36:1 multiplexer architecture, which was formed by two 18:1 channel MOS analogue multiplexers (MAX306, MAXIM) and one 2:1 channel analogue multiplexer (MAX308, MAXIM) thus up to 36 channels could be measured simultaneously. The selection of each channel in the multiplexer was controlled by the microcontroller (PIC18F4550). The sampling rate for the 36 channels was one electrode every 100ms in periods of 10s. A precision CMOS quad micro power operational amplifier

(LMC646, NATIONAL SMC), was connected to the output multiplexer. This operational amplifier has very high input impedance and an ultra-low input bias current of less than 16fA and hence is suited to the signal impedance generated by the potentiometric multi-electrodes. An analogue to digital converter (ADC) (MAX128, MAXIM) with a resolution of 12-bits that can work with either unipolar or bipolar input signals was used. It uses an external or internal reference voltage in order to obtain different full scale ranges. In this case a 2.5V external reference and a bipolar input signal were used. With this configuration the resolution (equivalent to 1 Least Significant Bit) was 1.22mV. The PIC18F4550 microcontroller gathered the data from the ADC using the I^2C bus. The PIC18F4550 was selected for its low power consumption (sleep mode currents down to 0.1 μA typical), 32K of memory program and 2K of RAM and USB port. The software for the PIC18F4550 microcontroller has been designed to scan the voltage for each channel. In the process of measurement, the data were sent to the PC via an RS232 serial communications. The acquisition software was developed using Visual Basic® 6.0 and Microsoft Excel® 2003 software.

A block diagram of the measurement system is shown in Figure 3 together with photographs in Figures 4 and 5.

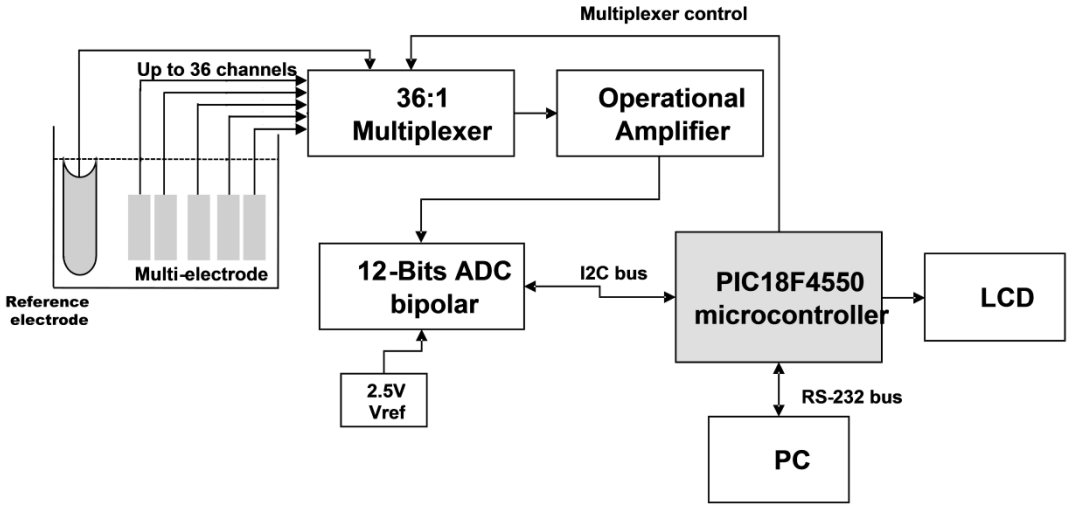

Figure 19: Block diagram of the measurement system

Figure 20: Data Logger on the left and the connection card on the right

The electrodes were attached to a transparent plastic mounting plate that was designed to support the electrodes and immerse only their working part in a test solution, this configuration is shown in Figure 5.

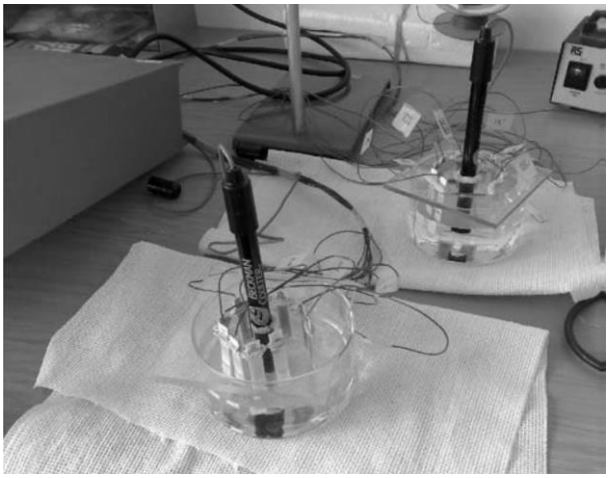

Figure 21: Experimental Setup

The solutions were stirred constantly during testing by a magnetic stirrer to minimise the effect of mass transport from the solution to the electrodes, which is more important at lower concentrations. The experiments were all performed at room temperature of 20 ± 3° C and it is believed that these small variations in temperature can be considered insignificant since the electrode potential sensitivity to temperature is known to be very low. The electrodes were tested in different KCl solutions made by dissolving KCl salt (Analytical Reagent, Fisher Scientific UK Ltd) in de-ionised water. Each set of electrodes was firstly hydrated into a 0.134 M (mol/L) KCl solution overnight and the time sampling interval used for the hydration period was 300 seconds. The hydration period is always required to establish equilibrium of the reversible reaction occurring at the electrode, as shown in Figure 22. After hydration, the electrodes were successively immersed in different concentrations of KCl solutions that were prepared by adding a weighed amount of KCl into 0.4 L of distilled water. For every amount of KCl dissolved the concentration was calculated in terms of molarity based on (6)

$$Molarity = \frac{actual\ mass\ dissolved/molar\ mass}{volume\ of\ solvent} \quad \textbf{(6)}$$

where the units of molarity are moles per litre or Molar (M). The sequence of solutions was 2 M, 1.34 M, 0.134 M and 0.0134 M respectively, and in some cases the sequence was followed twice in succession.

For the last set of experiments the same concentrations were used apart from the strongest concentration of 2 M, when saturated KCl solution (~4M) was introduced, where saturation was determined by the inability of the solution to dissolve any more salt. This saturated solution was then successively diluted with distilled water in ratio steps of 1:10 to yield lower concentration ratios to the saturated KCl solution of 1:10 (~0.4M), 1:100 (~0.04M) and 1:1000 (~0.004M) respectively. Each time the test solution was changed, the electrodes were rinsed in a beaker of distilled water to ensure any salt deposits would dissolve thereby eliminating past solution memory from the electrode surfaces. The electrodes were immersed in each solution for about 40 minutes for step response testing but in cases where the drift of the electrodes was examined the immersion time was in the range of several days.

4. Results & Discussion

Raw data were recorded for each electrode and an average graph of voltage versus time was plotted as shown in Figure 22. Data for each solution were recorded in standard intervals of 5 seconds for a total of an hour and a half. For the hydration period the intervals were 5 minutes for a total of about 13-14 hours. Three electrodes of each type where tested and their ensemble average for every simultaneous reading was calculated. For every solution, an average value for the electrode voltage in that solution was calculated from the ensemble average values of the three electrodes. Using these results, a graph of average electrode voltage versus chloride ion concentration was plotted for each type of electrode to enable better comparison with the theoretical responses as shown in Figure 23. From the graphs of voltage versus chloride ion concentration the gradient of the line

was obtained, hence defining the susceptibility of the electrode to chloride ions, as subsequently tabulated below.

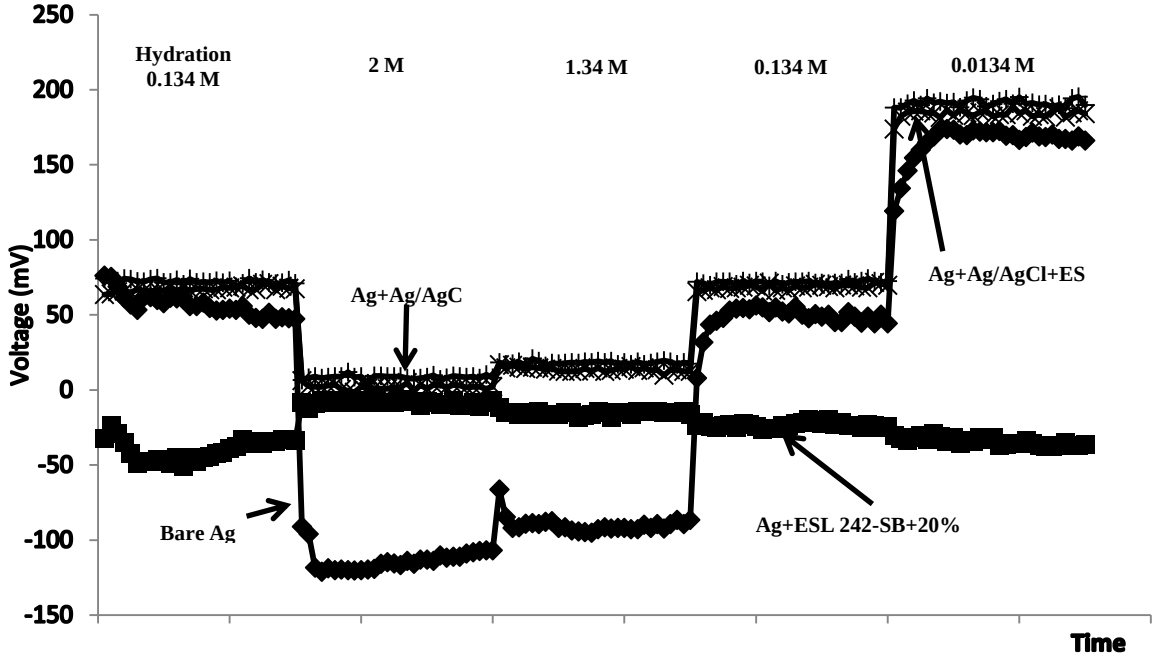

Figure 22: Voltage vs Time in different KCl concentrations

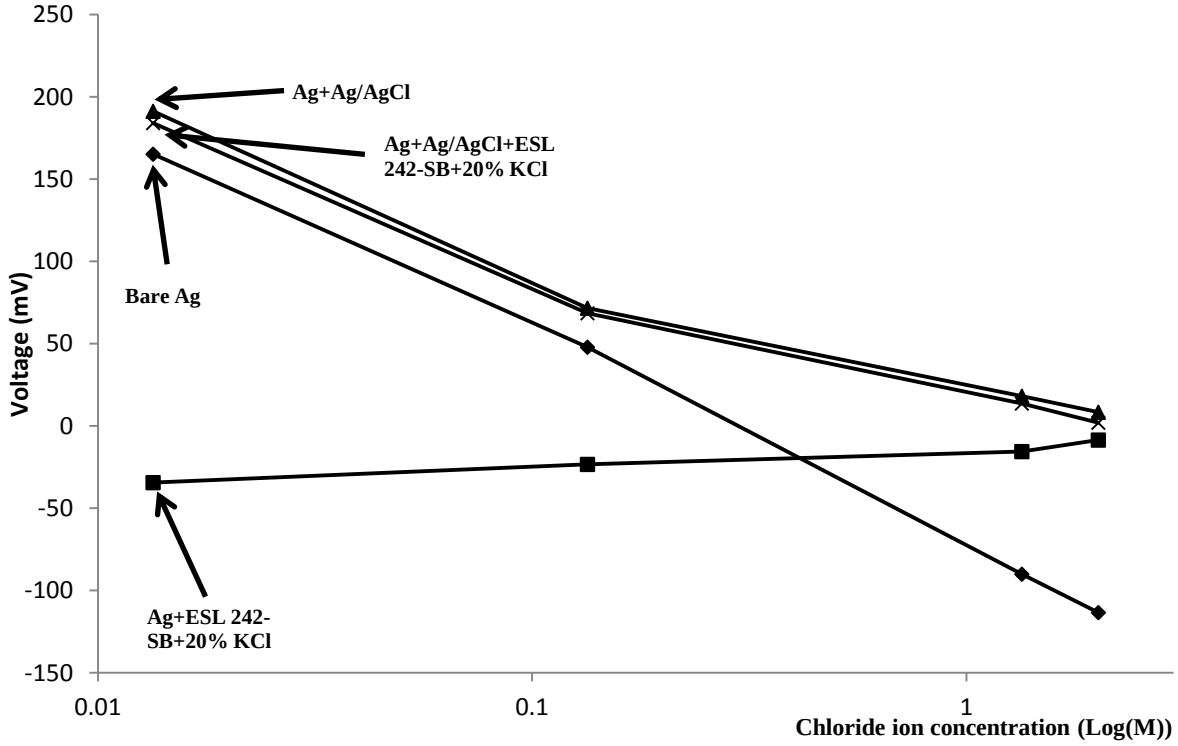

Figure 23: Voltage versus chloride ion concentration on logarithmic scale

Several experiments with different structural types of electrodes were tested by following the same procedure. The results are tabulated and shown in terms of the electrode sensitivity to chloride ions (mV/decade change in chloride concentration), the difference in sensitivity between the three electrodes of each type tested, the correlation (R^2) [9] of their sensitivity with a best fit linear function, and the range of solution concentrations over which the tabulated sensitivity is calculated.

Electrode types were tabulated in separate tables depending on their Ag/AgCl layer type. Table 47 shows the results for the electrodes employing only a bare silver layer. The materials used, as listed in the table, are for the layer deposited on top of the bare Ag layer.

Table 47: Bare Ag electrodes

No	Materials Used	Sensitivity (mV/decade)	Sensitivity difference between electrodes (mV)	R^2	Workable range (M)
1	Bare	-129	+2 -2	0.998	all
2	ESL 242-SB	-	- -	-	-
3	ESL 242-SB + 20% KCl	+11	+7 -7	0.9652	all
4	ESL 242-SB + 20% KNO_3	-	- -	-	-
5	ESL 242-SB + 66% KCl	-84	+8 -4	0.9454	all
6	ESL 242-SB + 71% KCl	-90	+6 -6	0.9611	all
7	ESL 242-SB + 20% KCl + ESL 242-SB	+2	+1 -1	0.8762	all
8	ESL 242-SB + 20% KCl + ESL 242-SB + 20% KCl	+2	+4 -5	0.6214	all
9	ESL 242-SB + 50% KCl + ESL 242-SB	+2	+2 -1	0.9276	all
10	ESL 242-SB + 50% KCl + ESL 242-SB + 20% KCl	+4	- -	0.8701	all
11	ESL 242-SB + 66% KCl + ESL 242-SB	-0.3	+1 -1	0.32	0.0044-0.436
12	ESL 242-SB + 66% KCl + ESL 242-SB + 20% KCl	-3	+3 -3	0.0876	0.0044-0.436

All electrodes were hydrated in 0.134 M KCl solution
Tested range of electrodes 1- 4 was 2M - 0.0134M KCl, electrodes 4-12 in the range 4.35M - 0.004M KCl
Workable range: all = whole range tested

Bare Ag electrodes showed a sensitivity of ~130mV/decade which is approximately double the theoretical Nernstian response. When a layer of pure ESL 242-SB was printed on top of the Ag the response was random and very noisy, which is believed to be because the solution could not easily penetrate the ESL 242-SB layer and therefore the voltage recorded was mainly due to noise from the surroundings. When KCl was introduced into the polymeric layer of ESL 242-SB the response was completely different. Three different percentages by weight of KCl were tested with 20%, 66% and 71% respectively. The sensitivity of this type of electrode decreases with the percentage addition of KCl in the top layer although it appears that there is an optimum weight percentage. If the KCl percentage is too low the electrode has a very low conductivity giving noisy responses, while as the percentage increases the conductivity increases. However, above a certain percentage KCl the ability of the binder to hold the salt on the substrate decreases, which then leads to an increase in the chloride sensitivity of the electrodes.

Adding another layer on top of the KCl layer significantly decreases the susceptibility of the electrodes. All the electrodes with the added layer have a susceptibility of approximately +2 to +4 mV/decade in all chloride concentrations, except the types with 66% KCl, which behave in a stable manner in lower chloride concentrations until the voltage decreases dramatically in saturated chloride solution. As postulated previously, above a certain percentage of added KCl the paste is unable to hold the KCl on the electrode sufficiently and this is most probably the reason the voltage decreases so dramatically in saturated solution, as the saturated solution then directly modifies the surface of the electrode. Although it could be said that these electrodes are not Ag/AgCl reference electrodes because the Ag/AgCl layer is missing, however a SEM scan showed that a AgCl layer is still present. Figure 24 shows a SEM scan of the cross section of the lower silver layer with the ESL 242-SB + 50% KCl layer on top, where the two layers can clearly be seen. As shown in the figure, chlorine atoms were found at the point on the silver layer where the readings were taken (Spectrum 1), where the percentages of each species are as shown in Table 46, which tends to suggest that a thin layer of AgCl has formed. The scanned sample shown in Figure 24 is a new non-tested sample which means that the AgCl is not formed during testing. This was further confirmed when an identical electrode was scanned and the species percentages were found to be approximately the same. Based on this evidence, the AgCl layer is formed during fabrication of the electrode and it is likely that the amount of AgCl formed is determined by the KCl concentration that is used in the layer printed on top of the Ag.

Table 48:SEM scan results

Element	Weight %	Atomic %
Al K	1.18	4.45
Si K	0.24	0.87
Cl K	0.88	2.54
Ag L	97.69	92.14
Totals	100.00	

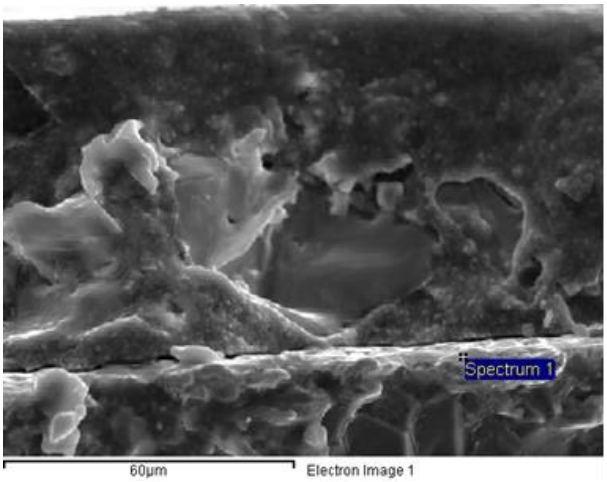

Figure 24: SEM scan of the cross section of a Bare Ag electrode with ESL 242-SB + 50% KCl layer deposited on top

Other types of Ag/AgCl pastes were used to investigate the parameters affecting the performance of the electrodes. One of the pastes was the polymeric C61003P7 from Gwent Electronic Materials containing a ratio of Ag to AgCl of 3:2. The only difference in this type of electrode is the additional Ag/AgCl layer deposited above the Ag layer.

Table 49: Polymer Ag/AgCl GEM C61003P7

No	Materials Used	Sensitivity (mV/decade)	Sensitivity difference between electrodes (mV)	R^2	Workable range (M)
1	Bare	-82	- -	0.9586	all
2	Bare Fired	-122	+20 -13	0.9985	all
3	ESL 242-SB	-82	+1 -1	0.9625	all
4	ESL 242-SB Fired	-26	+1 -1	0.9405	0.134-2
5	ESL 242-SB 6% KCl	-54	- -	1	all
6	ESL 242-SB 20% KCl	-81	- -1	0.966	all
7	ESL 242-SB+20% KCl Fired	-1	+3 -2	0.9469	0.134-2
8	ESL 242-SB 33% KCl	-48	+1 -1	0.9976	all
9	ESL 242-SB 50% KCl	-51	+1 -1	0.9986	all
10	ESL 242-SB 66% KCl	-58	- -	0.995	all
11	ESL 242-SB 71% KCl	-58	- -	0.9951	all

*****All electrodes were hydrated in 0.134 M of KCl solution
******1-9 Tested in range 2M - 0.0134M KCl, 10-11 in the range 4.35M - 0.004M
******* Workable range: all = whole range tested

The bare polymer Ag/AgCl electrodes exhibited a super-Nernstian sensitivity of approx. -82mV/decade. When the ESL 242-SB layer with no KCl salt was printed on top the response became very noisy but showed a similar sensitivity. As shown in Table 49, the variation of the sensitivity is relatively small between the different levels of KCl contained in the top layer and close to the Nernstian value, except in the case of 20%, KCl, which shows an apparently anomalous susceptibility of -81mV/decade. This may have been the result of a fabrication error when this particular batch of electrodes was fabricated.

In Table 4 there are two types of electrodes designated as 'fired', which indicates that the paste was fired at 850ºC instead of the recommended curing temperature of 80ºC (accidentally at first but then later on purpose). In that situation, due to the high temperature involved, the AgCl very likely decomposes or reacts with some other species (e.g. oxygen), with the result that chlorine is evolved. To investigate this, SEM scans were performed of a properly cured polymer Ag/AgCl paste and the 'fired' one. In the case of the 'fired' Ag/AgCl electrode the amount of chloride present was so low that it was approximately the same as the percentage found on the bare Ag electrode. In fact, the performances of the bare Ag and fired polymer Ag/AgCl electrodes were very similar, which reinforces the concept that the performance is critically influenced by the Ag to AgCl ratio.

Table 50 and 6 show another two types of Ag/AgCl pastes that were tested, in which a low temperature glass binder was used with Ag/AgCl ratio of 1:1. These two types of Ag/AgCl pastes perform similarly and are affected by the same amount for each varying parameter with the same trend being observed for the percentage of KCl in the ESL 242-SB layer. At low levels of contained KCl the sensitivity is high compared to the bare Ag/AgCl electrode while as the KCl level increases the electrode chloride sensitivity decreases up to a point (approx. 20%) where it starts increasing again. Above a certain percentage the polymer paste is less able to hold the KCl on the electrode and therefore the sensitivity increases reaching a value close to the Nernstian response. These two glass bound electrode types were also fired at higher temperatures to check if the same response is observed and another SEM scan showed approximately the same results as for the GEM C61003P7 paste, while the performance was found to be similar to that of the 'fired' polymer (row 5, Tables 5 and 6).

The two glass bound electrode types were also tested with an extra layer of ESL 242-SB with 20% KNO_3 deposited as a top layer. This extra layer results in a better stability in different concentrations of KCl but that is believed to be most probably because of the extra ESL 242-SB layer acting as a membrane holding the KCl on the electrode at the same time as allowing water soluble ions to pass through and close the circuit. This theory appears to be substantiated by the similar performance of the bare Ag electrodes with the extra KCl containing ESL 242-SB layer on top (Table 3).

Table 50: Glassy Ag/AgCl PPCFB2

No	Materials Used	Sensitivity (mV/decade)	Sensitivity difference between electrodes (mV)	R^2	Workable range (M)
1	Bare	-50	+4 -4	0.999	all
2	Bare Fired	-35	+7 -8	0.583	all
3	ESL 242-SB 6% KCl	-45	+1 -1	0.998	all
4	ESL 242-SB 20% KCl	-43	+1 -1	0.994	all
5	ESL 242-SB+20% KCl Fired	-8	+4 -4	0.174	all
6	ESL 242-SB 66% KCl	-62	- -1	0.98	all
7	ESL 242-SB 71% KCl	-66	+1 -1	0.99	all
8	ESL 242-SB 20% KCl + ESL 242-SB 20% KNO_3	-15	- -	0.907	all

*****All electrodes were hydrated in 0.134M KCl solution
******1,3,4 Tested in the range 2M-0.0134M KCl; 2,5-8 in the range 4.35M-0.004M KCl
******* Workable range: all = whole range tested in

Table 51: Glassy Ag/AgCl PPCFC3

No	Materials Used	Sensitivity (mV/decade)	Sensitivity difference between electrodes (mV)	R^2	Workable range (M)
1	Bare	-44	+17 -17	0.9996	all
2	Bare Fired	-80	+21 -35	0.9331	all
3	ESL 242-SB 6% KCl	-33	+5 -5	0.9984	all
4	ESL 242-SB 20% KCl	-29	+10 -4	0.9927	all
5	ESL 242-SB 20% KCl Fired	-5	+1 -1	0.4754	0.0044-2
6	ESL 242-SB 66% KCl	-59	+1 -1	0.9837	all
7	ESL 242-SB 71% KCl	-61	- -	0.9903	all
8	ESL 242-SB 20% KCl + ESL 242-SB 20% KNO_3	+4	+1 -1	0.8819	0.0044-2

*****All electrodes were hydrated in 0.134M KCl solution
******1,3,4 Tested in the range 2M-0.0134M KCl; 2,5-8 in the range 4.35M-0.004M KCl
******* Workable range: all = whole range tested in

Selected electrode types were sequentially immersed into three different pH buffers, chosen as pH4, pH7 and pH10, in a test solution sequence of pH 7-4-7-10-7-4-7-10. The averaged results from 3 electrodes of each type are presented in Figure 25. The graph of voltage against pH (Figure 26) shows that the reference electrode potentials are affected by the pH, but only up to a point that is relatively insignificant for most electrochemical applications. The variation of the potential for some of the electrodes was in the range of ±5 mV, which is equivalent to ±0.1 of a pH unit for a near Nernstian thick film pH sensor, such as those reported previously by this research group [10].

From Figure 9 it can be seen that electrodes containing a higher percentage of KCl in their upper layers drift more than those with lower KCl concentrations. The electrodes were tested in a cyclic manner in the different pH solutions and it can be observed that the potential of the higher KCl containing electrodes in the same pH buffer increases slightly each time.

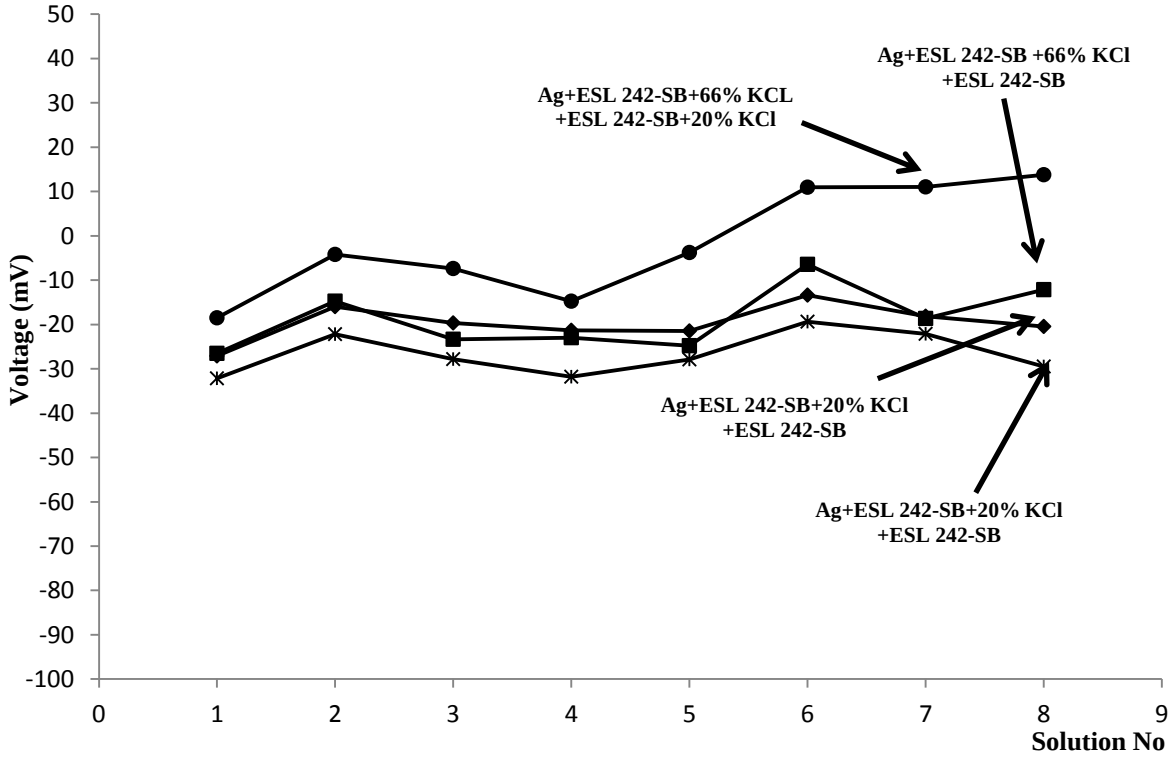

Figure 25: reference electrode potential versus commercial liquid filled Ag/AgCl reference electrode

(tested in solution sequence pH 7-4-7-10-7-4-7-10)

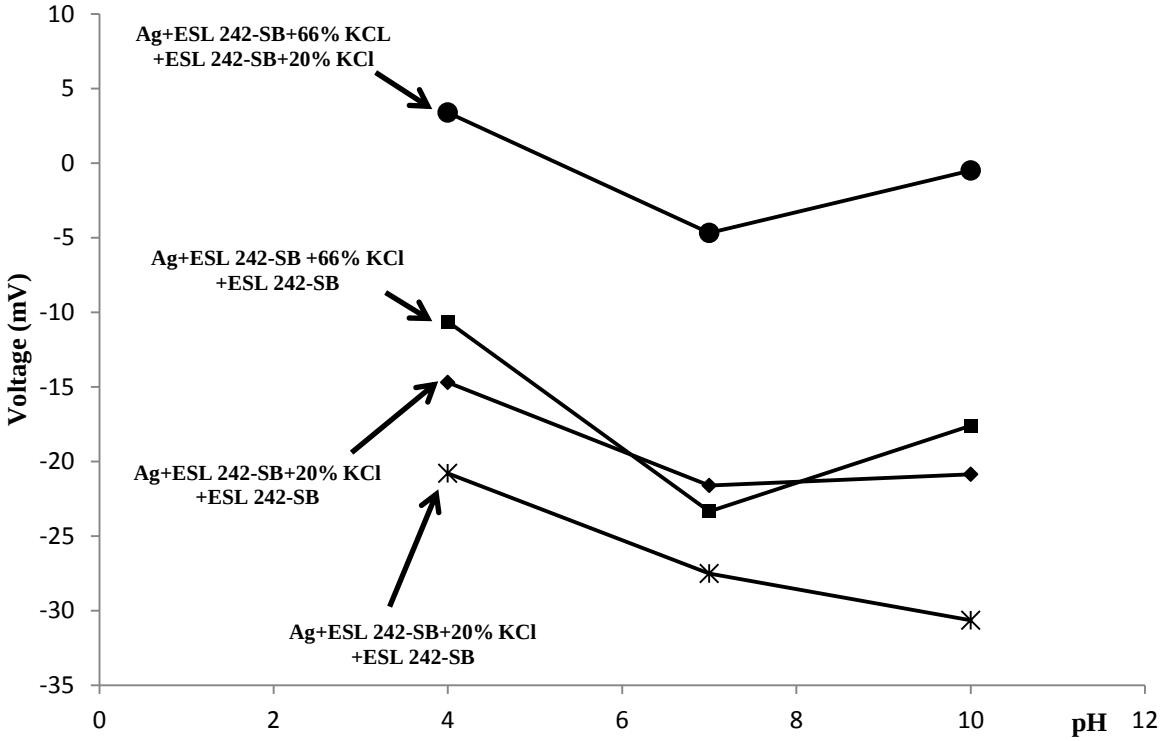

Figure 26: reference electrode potential measured versus commercial liquid-filled Ag/AgCl reference electrode as a function of pH

5. Conclusions

Adding another layer of ESL 242-SB with KCl on top can also affect the performance of the electrodes. At low percentages of KCl in the paste the electrodes have low conductivity, making them more susceptible to noise, as the percentage KCl increases so the noise decreases. Above a certain percentage point the paste has insufficient mechanical stability to hold the KCl on the electrode and the KCl dissolves more easily into the solution increasing the chloride sensitivity of the electrodes.

Firing the Ag/AgCl layer at 850^{o}C has proven to leave the electrode without any AgCl, making it into effectively a bare Ag electrode. From the SEM scans, the chlorine levels in these electrodes were similar to those of the bare Ag electrodes, where some AgCl is formed during fabrication of the electrodes. Most probably some of the surface of the underlying Ag reacts with the KCl forming a small amount of AgCl when the ESL 242-SB layer containing KCl is cured at 150^{o}C.

When another layer of ESL 242-SB is printed on top of the already printed ESL 242-SB with KCl, the performance of the electrodes improves dramatically. The chloride sensitivity of the electrodes decreases to ~+2mV/decade (equivalent to 0.04pH units/decade) which makes the electrodes stable enough to be used at any chloride ion concentration. In this case it is believed that the top layer acts as a membrane holding the KCl on the electrode but at the same time allowing a sufficient level of water soluble ions to pass through and complete the circuit. If higher levels of KCl are added to the top layer the electrode sensitivity increases because more pathways are now present for the water to pass through and "wash out" the KCl of the underlying layer.

The electrodes with best stabilities were also tested in different pH buffers giving satisfactory results with variations in electrode potentials of less than ±5mV in the range from pH4 to pH10. These variations can be considered relatively acceptable, since for most conventional types of pH sensor every unit change in pH produces a change of 59mV, hence resulting in an equivalent error due to the reference electrode of less than ±0.1pH. The electrodes were immersed in the pH buffers in various sequences to check for any modifications the pH buffers might have on the electrodes (e.g. hysteresis) and the results were also found to be satisfactory

since the difference in voltage between each response curve was found to be in the range of one or two millivolts which can also be considered well within the instrumental uncertainty.

Acknowledgements

The authors wish to thank the UK Environment Agency and the National Environmental Research Council for partially supporting this work.

References

[1] A.Gac, J.K. Atkinson, Z. Zhang, R.P. Sion, A comparison of thick-film chemical sensor characteristics in laboratory and on-line industrial process applications, *Measurement Science and Technology*, 13 (2002) 2062-2073.

[2] D. Desmond, B. Lane, J. Alderman, J.D. Glennon, D. Diamond, D.W.M. Arrigan, Evaluation of miniaturised solid state reference electrodes on a silicon based component, *Sensors and Actuators B: Chemical*, 44 (1997) 389-396.

[3] J.K. Atkinson, M. Glanc, M. Prakorbjanya, R.P. Sion, E. Garcia-Breijo, Screen Printed Thick Film Subterranean and Subaqueous Environmental Chemical Sensor Arrays, in: *13th Electronics Packaging Technology Conference*, Singapore (2011).

[4] Ł. Tymeckia, E. Zwierkowskab, R. Konckia, Screen-printed reference electrodes for potentiometric measurements, *Analytica Chimica Acta*, 526 (2004) 3-11.

[5] D.J.G. Ives, G.J. Janz, Reference Electrodes: Theory and practise, Academic Press, Berkeley Square House, London W1, (1961).

[6] A.W.J. Cranny and J.K. Atkinson, Thick film silver-silver chloride reference electrodes, *Measurement Science and Technology*, 9 (1998) 1557-1565.

[7] J.K. Atkinson, M. Glanc, P. Boltryk, M. Sophocleous, E. Garcia-Breijo, An investigation into the effect of fabrication parameter variation on the characteristics of screen-printed thick-film silver/silver chloride reference electrodes, *Microelectronics International*, 28 (2011) 49-52.

[8] U. Guth, F. Gerlach, M. Decker, W. Oelßner, W. Vonau, Solid-state reference electrodes for potentiometric sensors, *Journal of Solid State Electrochemistry*, 13 (2009) 27-39.

[9] R.G.D. Steel and J.H. Torrie, Principles and Procedures of Statistics, New York, (1960).

[10] J.A. Mihell, and J.K. Atkinson, Planar thick-film pH electrodes based on ruthenium dioxide hydrate, *Sensors and Actuators B: Chemical*, 48, (1-3), (1998) 505-511.

Appendix 2

Within Appendix 2 is the journal paper published in Sensors and Actuators A: Physical in 2013.

Performance of miniaturised thick-film solid state pH sensors

M. Glanc-Gostkiewicz[a], M. Sophocleous[b], J.K. Atkinson[b], E. Garcia-Breijo[c]

[a,b]*Faculty of Engineering and the Environment, University of Southampton,Southampton, SO17 1BJ, United Kingdom*
[c]*Instituto de Reconocimiento Molecular y Desarrollo Tecnológico,Universidad Politécnica de Valencia, Valencia, 46022 Spain*

Abstract

The performance of novel solid state Thick-Film pH sensors for water quality sampling that are designed for deployment in remote catchment areas is described. These miniaturised screen printed planar pH sensors are an alternative to conventional glass pH electrodes that have many disadvantages such as high-cost, large size, mechanical fragility and limited shape. The approach adopted here for improvement of the ruggedness of the pH electrode is through its implementation as a screen printed metal oxide (RuO_2) ion selective electrode used in combination with a screen printed silver/silver chloride (Ag/AgCl) reference electrode. Various choices of materials have been evaluated for the fabrication of the Thick-Film pH sensors resulting in a device with a sensitivity of approximately 30mV/pH at ambient temperature.

Keywords: pH sensor; silver/silver chloride; Thick-Film sensors; water quality

Introduction

Rivers are the habitats for living organisms and any changes in the alkalinity or acidity of the water can be critical to the survival of aquatic life. Rivers have some capacity to prevent changes in pH by the structure and composition of the river bed; however drastic changes in pH can have very detrimental effects on river health.

Agricultural industry is a major user of water resources. It also contributes intensively to water pollution through processes such as the use of pesticides and fertilisers, and the spreading of slurries or manure. To detect the contamination of water courses, a network of upstream early warning systems consisting of in situ miniaturised electrochemical sensors is required as a simple alternative to the current methods of downstream detection of pollution in rivers [1]. This approach enables the localization of pollution sources and better control of the environment but requires large numbers of rugged devices suitable for wide scale field deployment. The cost implications of this approach render it unfeasible using conventional electrochemical devices.

Currently the most widely used technique for determination of pH in the laboratory is the glass bulb type pH electrode. This electrode is well-established because of its excellent performances with respect to slope, long-term stability, selectivity, detection limit, and insensitivity versus redox systems [2]. However this traditional glass electrode with an internal liquid reference system exhibits several drawbacks such as mechanical fragility, large size and high cost. Thick-Film technology can resolve these limitations through the fabrication of small, rugged and inexpensive devices which can mimic the commercially available pH electrode and reference electrode systems [3, 4]. Moreover it can implement a competitive solution to the current expensive

environmental monitoring with pH devices by manufacturing sensors with Thick-Film processes where metal oxides can be used to implement the pH sensor active layer [2, 6].

In this paper an investigation, formulation and production process of these alternative thick film pH sensors are described. The devices described here were fabricated specifically for water catchment area monitoring using routine sample collection deployment alongside passive samplers, to provide better estimations of environmental concentrations and uptake rates of pollutants in water courses. The results described here arise from laboratory investigations prior to further investigations in field trials in order to validate their use for environmental sampling.

1.1 pH sensor theory

The pH of a solution can be determined by a potentiometric pH sensor where the potential difference between two electrodes, i.e. a pH sensitive electrode and a reference electrode, is measured. The reference electrode provides a stable constant reference potential regardless of the solution in which is immersed while the ion selective electrode responds to the change of the H^+ concentration in the solution.

The Thick Film pH sensors presented in this study consist of a Thick-Film Ruthenium Oxide ($RuO_2.xH_2O$) pH electrode (one type) and a Thick –Film Ag/AgCl reference electrodes (four types). They are implemented on the same principle as the conventional glass pH electrode and the single junction electrolyte-filled Ag/AgCl reference electrode by attempting to mimic their construction [7].

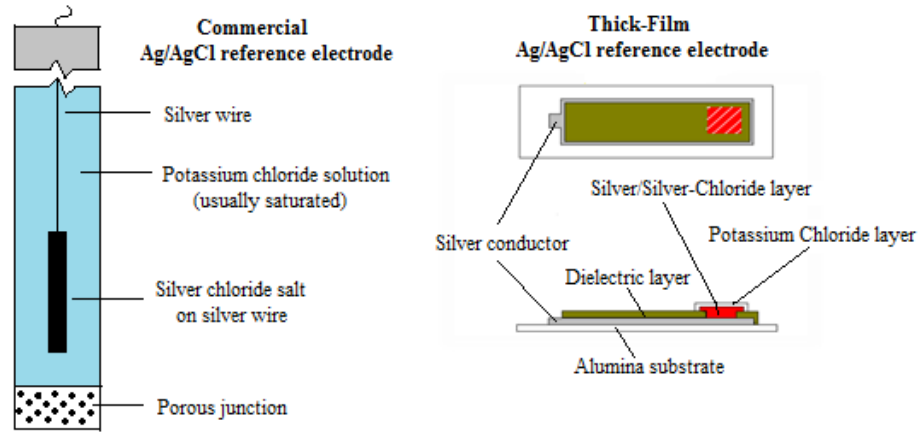

Fig 1. Commercial Ag/AgCl reference electrode (left) and Thick-Film Ag/AgCl reference electrode (right)

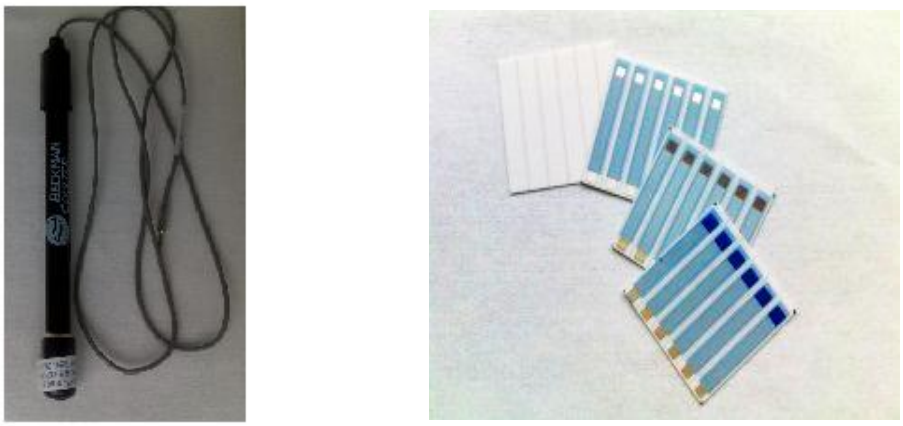

Fig 2. Commercial gel-filled reference electrode (Beckman Coulter A57193) (left) and Thick-film Ag/AgCl reference electrodes (right)

The common reference electrode used in pH measurements consists of a silver wire coated with silver chloride in a fill solution of potassium chloride (KCl). The Ag/AgCl electrode potential response is controlled by the following equilibrium reaction:

$$AgCl_{(s)} + e^- \leftrightarrow Ag_{(s)} + Cl^-_{(aq)} \quad (1)$$

Hence the equilibrium potential of the electrode can be expressed by the Nernst equation:

$$E = E^\theta + \left(\frac{RT}{nF}\right) ln \frac{(a_{AgCl})}{(a_{Ag} a_{Cl^-})} \quad (2)$$

where E^θ is the electrode's standard potential (V), T is the absolute temperature (K), R is the molar gas constant (8.31 J K^{-1} mol^{-1}), F is the Faraday constant (96485 C mol^{-1}), n is the number of electrons involved in the reaction, a_x is the activity of species x (where x is either AgCl, Ag or Cl^-).

The Nernst equation for a cell at a nominal room temperature of 25°C is frequently expressed in terms of base 10 logarithms:

$$E = E^\theta - 0.0592\ log|Cl^-| + 0.0592 \log(k) \quad (3)$$

where k is the ratio of the concentrations of silver chloride to silver. The electrode demonstrates Nernstian behaviour when the measured electrode potential decreases by 59 mV for every decade change in chloride ion concentration at a room temperature of 25˚C. The measured electrode potential can also yield alterations due to changes in the ratio of silver chloride to silver (k).

Fog and Buck proposed and discussed five different possible explanations of the pH response mechanisms of metal oxides and suggested that the most probable theory was that of oxygen intercalation [5, 8, 9]. This mechanism is represented by the equilibrium reaction:

$$MO_x + 2\delta H^+ + 2\delta e^- \leftrightarrow MO_{x-\delta} + \delta H_2O \quad (4)$$

where MO_x is a higher metal oxide and $MO_{x-\delta}$ is a lower metal oxide. The electrode potential for this reaction is given by:

$$E = \frac{RT}{F} ln\ a^1_{H^+} + \frac{RT}{2F} \ln a^s_O + constant \quad (5)$$

where $a^1_{H^+}$ is the proton activity in the liquid phase and a^s_O is the oxygen activity in the solid phase.

McMurray et al. [9], used The Pourbaix Atlas to present another mechanism of only one redox equilibrium between two insoluble ruthenium oxides:

$$RuO_2 + 2H_2O + H^+ + e^- \leftrightarrow H_2O + Ru(OH)_3 \quad (6)$$

The reaction potential being expressed by:

$$E = E_0 - 0.0591\ pH \quad (7)$$

Assuming a near constant activity of the metal oxide, both of these mechanisms predict a Nernstian response of approximately -59mV per pH at ambient temperature (25°C).

Experimental details

2.1 Electrode fabrication

The studied electrodes were screen printed onto 96% alumina substrates (Coorstech) through successive layer deposition. An economical design of each sensor type permitted the simultaneous fabrication of six electrodes on a single, laser prescribed substrate, as shown in Fig. 2. The details of the component materials have been

documented previously [5, 7]. The electrode types used in the experimental setup and their basic structures are shown in Fig. 3.

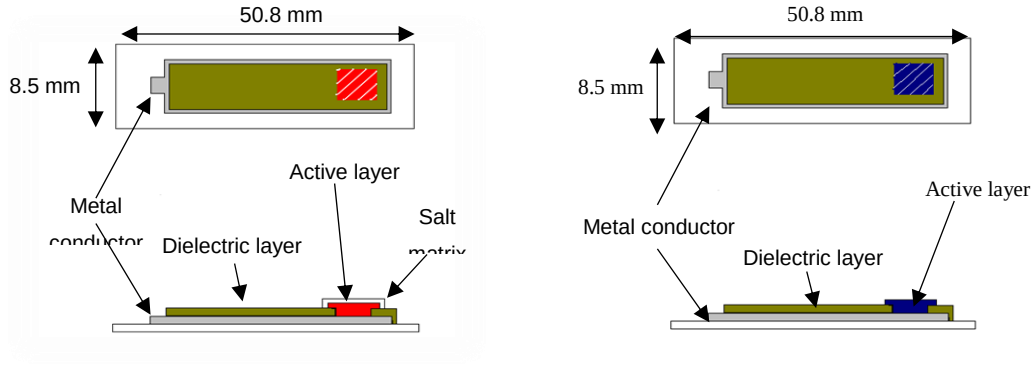

(a) (b)

Fig. 3. (a) Thick-Film reference electrode cross-section; (b) Thick-Film pH ion selective electrode cross-section

The tested devices varied in terms of their electrode active layer construction (Table 1). The same polymer bound Ag/AgCl layer (GEM C61003P7) was use for two types of reference electrodes. However, the 'Fired' Polymer Ag/AgCl electrodes were passed through a furnace at 850°C and, as suggested by the results of an SEM scan, a thin layer of Ag/AgCl was subsequently formed on top of the underlying Ag conductor. Two further types of Thick-Film reference electrodes were tested that do not possess a printed Ag/AgCl layer but instead have a thin layer of AgCl that was chemically grown on the Ag conductor.

Table 1. Types of electrodes with details of the component materials

Electrode type	Conductor layer	Waterproofing layer	Active Layer	Salt matrix layer
Bare Ag	Silver ESL 9912 A	Glass Dielectric ESL 4905 CH	-	-
Reference electrodes				
Polymer Ag/AgCl	Silver ESL 9912 A	Glass Dielectric ESL 4905 CH	Silver/Silver Chloride Paste GEM C61003P7	Polymer ESL 242 SB + 20% KCl powder
Fired Polymer Ag/AgCl	Silver ESL 9912 A	Glass Dielectric ESL 4905 CH	Fired Silver/Silver Chloride Paste GEM C61003P7	Polymer ESL 242 SB + 20% KCl powder
Chemically grown Cl layer 2min	Silver ESL 9912 A	Glass Dielectric ESL 4905 CH	*	Polymer ESL 242 SB + 20% KCl powder
Chemically grown Cl layer 1hr	Silver ESL 9912 A	Glass Dielectric ESL 4905 CH	*	Polymer ESL 242 SB + 20% KCl powder
pH ion selective electrode				
pH electrode	Platinum Gold ESL 5837	Polymer Dielectric GEM 2020823D2	Ruthenium Polymer Paste C50502D7	-

* An exposed silver window was chemically coated with a thin layer of silver chloride by electroplating in 1M HCl.

2.2 Experimental setup

The whole experiment was divided in two parts. Firstly the performance of the Thick-Film reference electrodes was ascertained through sequential testing in different strength KCl solutions. Subsequently a group of the same type of reference electrodes was simultaneously examined with Thick-Film pH electrode in pH buffer solutions in a solution sequence of pH7, 10, 7, 4, 7, 4, 7, 10 and 7.

The KCl test solutions were made by dissolving KCl salt in de-ionised water until the solution reached saturation (Sat KCl solution). All the other solutions were made by diluting the saturated solution in the ratios of one tenth (1:10 Sat KCl), one hundredth (1:100 Sat KCl) and one thousandth (1:1000 Sat KCl). The Thick-

Film sensors were initially hydrated overnight in 1:100 Sat KCl solution and subsequently cycled through the test solutions. The electrode potentials were measured with respect to a commercial gel-filled reference electrode (Beckman Coulter A57193) located centrally within a beaker containing the test solution and surrounded by the Thick-Film electrodes under test. All solutions were stirred using a magnetic stirrer. The test set-up is shown in Fig. 4. The electrodes were connected to a custom designed voltmeter and the experimental data were recorded in 5 seconds intervals with a portable data logger designed and constructed at Universidad Politécnica de Valencia and shown in Fig.5.

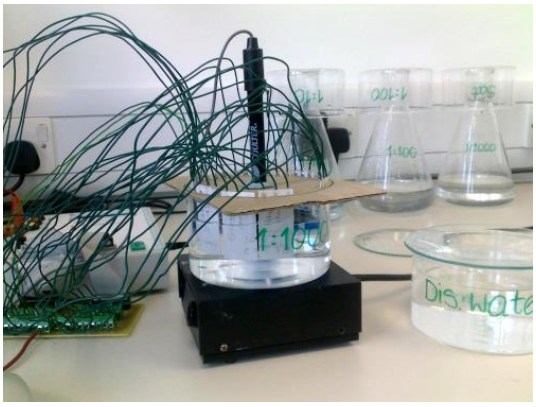

Fig. 4 The experimental setup of the electrodes in KCl test solutions

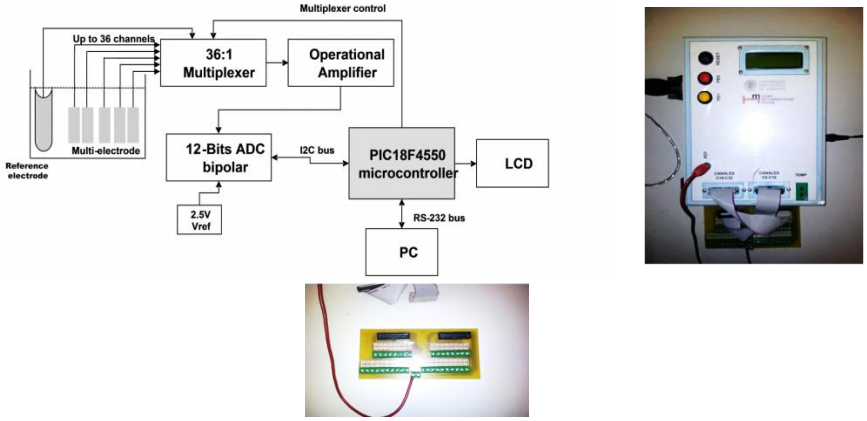

Fig. 5. The block diagram of the measurement system (left) for the data logger (right).

The potentials of the multi-electrodes were acquired using a 36:1 multiplexer architecture, which was formed from two 18:1 channel MOS analogue multiplexers (MAX306, Maxim) and one 2:1 channel analogue multiplexer (MAX308, Maxim). The selection of each channel in the multiplexer was controlled by the microcontroller (PIC18F4550, Microchip Technology). A precision CMOS quad micro power operational amplifier (LMC646, National SMC), was connected to the output multiplexer. This operational amplifier has very high input impedance and an ultra-low input bias current of less than 16fA and hence is suited to the signal impedance generated by the potentiometric multi-electrodes. An analogue to digital converter (MAX128, Maxim) with a resolution of 12-bits was used, with selectable variable external or internal reference voltage in order to obtain different full scale ranges. The software for the PIC18F4550 microcontroller has been designed to scan the voltage for each channel and send the data to a PC via an RS232 serial communications channel. The PC acquisition software was developed using Visual Basic® 6.0 and Microsoft Excel® 2003 software.

Results and Discussions

The Thick-Film electrodes were immersed sequentially in different solutions of higher to lower chloride concentration of Sat KCl (A), 1:10 Sat KCl (B), 1:100 Sat KCl (C) and 1:1000 Sat KCl (D) as well as in various pH buffer solutions as shown in Fig. 6 and 7. Their average responses were calculated and plotted. The bare Ag electrode trace most clearly shows the changes in potential between the testing solutions and the duration of the electrodes immersion in each test solution.

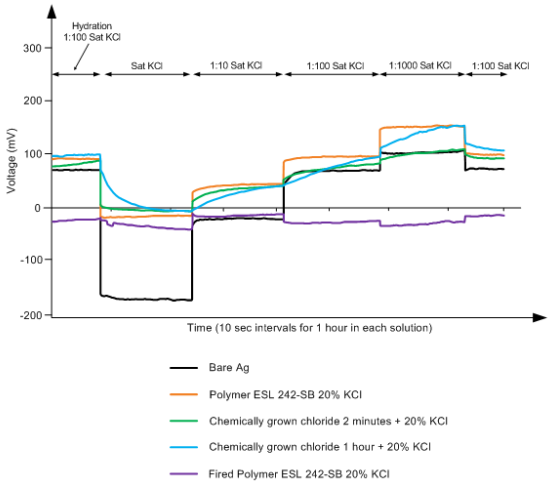

Fig. 6. Thick-Film reference electrodes in KCl solutions.

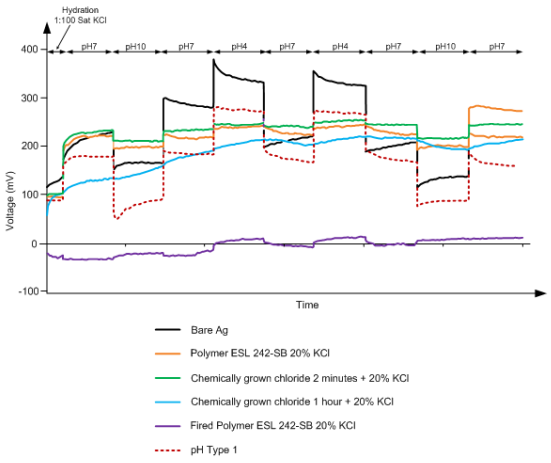

Fig. 7. Thick-Film pH sensors in pH buffer solutions.

To produce a stable voltage from the reference electrode across different ionic concentrations the outer active layers of the electrode consisted of KCl powder in polymer binder to function as a salt matrix layer, which was applied to mimic the commercial gel-filled Ag/AgCl reference electrode design. The grains of the potassium chloride powder form paths in the electrode top layer through which the salt leaches out from the electrode into the electrolyte. Several different concentrations of KCl to polymer binder were tested: 0.6, 3, 6, 20, 66 and 71% by weight respectively. The reference electrodes with the higher concentration of potassium chloride in the salt matrix layer tend to loose salt faster and in consequence their useful lifetime is also more limited. The optimum weight percentage needs to be ratified more precisely, but presently the electrodes with 20% KCl in the outer active layer gave the best results. The Fired Polymer Ag/AgCl + 20% KCl reference electrodes demonstrated nearly stable potential response in all tested solutions in comparison to the Polymer Ag/AgCl + 20% KCl and the two chemically grown chloride electrodes. In all probability, based on the electrode theory, the drift rate of the reference electrodes is also influenced by changes in the AgCl/Ag ratio in the Ag/AgCl paste. It is believed that the optimum ratio of Ag/AgCl still needs to be defined as in all the experiments described here only one type of Ag/AgCl paste was used: Gwent C61003P7, which had an Ag/AgCl ratio of 60:40.

Fig. 8 illustrates the stability of the Thick-Film reference electrodes as a function of chlorine ion concentration. Overall, the performance of the Fired Polymer Ag/AgCl + 20% KCl reference electrode is the most notable in that it gives the flattest and most stable response of all the tested reference electrodes. Table 2 summarises the sensitivities of the various types of Thick-Film reference electrodes. It should be pointed out that the sensitivity of the chemically grown chloride 1 hour electrode was calculated by omitting its apparently anomalous reading in saturated chloride solution.

As previously mentioned and evidenced by Eqn. 3, the potential of the Thick-Film reference electrodes is thought to be influenced by a combination of the chloride ion concentration at the electrode surface and also the ratio of AgCl to Ag forming the electrode surface. Consequently this mechanism may explain the apparently stable behaviour of the Fired Polymer Ag/AgCl + 20% KCl reference electrode. A thin film of sparsely soluble AgCl is believed to form on the surface of the Ag electrode back contact during the process of firing and this has been confirmed through SEM studies of the surface composition of the just fabricated electrode. As the Chloride concentration of the immersion solution decrease the electrode potential will change more positive in line with the Nernst equation. However at the same time the thin layer of sparsely soluble AgCl will be

encouraged to dissolve in the lower concentration solution at a higher rate bringing about a reduction in the AgCl/Ag ratio *k* and hence shifting the electrode potential more negative. Since the AgCl is thin the small changes in its concentration have a pronounced effect on the ratio *k* at the electrode surface and hence these two mechanisms cancel resulting in the flat re:

Table 2 Chloride ion sensitivity.

Electrode type	Sensitivity (mV/log Cl^-)
Bare Ag	-59
Polymer Ag/AgCl + 20%KCl	-30
Fired Polymer Ag/AgCl + 20%KCl	-2
Chemically grown chloride 2min	-20
Chemically grown chloride 1 hour	-30

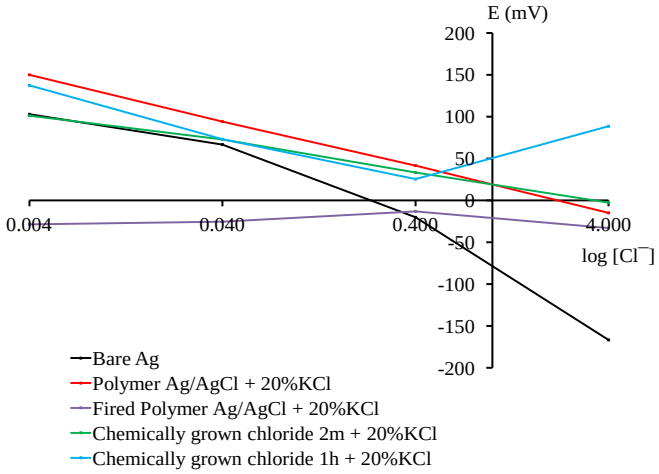

Fig. 8. Thick-Film reference electrode potentials as a function of chloride ion concentration.

The responses of the different Thick-Film reference electrodes and the Ruthenium Oxide pH electrodes in various pH buffers solutions are shown in Fig. 9. The Ruthenium Oxide pH electrodes show very repeatable and stable response to the pH buffer changes and also reach a stable potential quite rapidly after immersion in the various pH buffers, as can be seen in Fig. 7. Most of the reference electrode potentials exhibited some degree of hysteresis effect when cycled through the pH buffer solutions, possibly through conditioning of the electrodes. However the Fired Polymer Ag/AgCl + 20% KCl reference electrode exhibited a remarkably flat response with very little hysteresis. Table 3 summarises the response in mV/pH of all the Thick-Film electrodes over the range of tested pH solutions.

Table 3 pH sensitivity.

Electrode type	Sensitivity (mV/pH)
Bare Ag	-4
Polymer Ag/AgCl + 20%KCl	-32
Fired Polymer Ag/AgCl + 20%KCl	-2
Chemically grown chloride 2min	-6
Chemically grown chloride 1 hour	-11
pH	-32

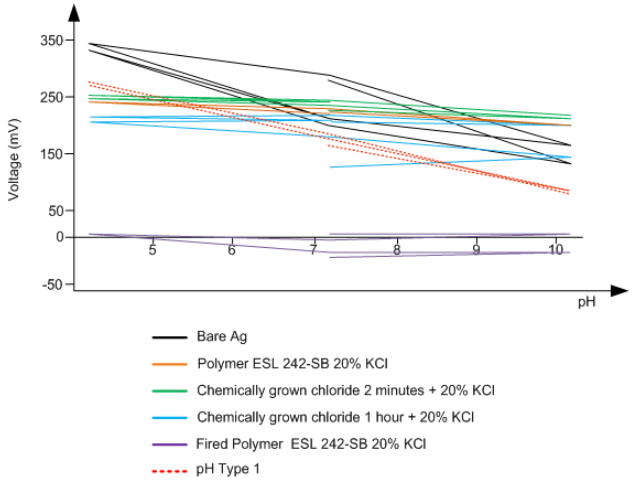

Fig. 9. Thick-Film electrode potentials as a function of pH.

The presented results demonstrate the feasibility of the development of low-cost, rugged, miniaturised Thick-Film alternatives to the commercially available liquid electrolyte filled Ag/AgCl reference electrode and glass pH electrode. The results further contribute towards optimisation of the fabrication parameters for screen-printed Ag/AgCl reference electrodes suitable for use in Thick-Film pH sensors.

Acknowledgements

The authors gratefully acknowledge the support of the UK Environmental Agency for partially funding the corresponding author's PhD research project.

References

[1] Gut U, Vonau W, Zosel J. Recent developments in electrochemical sensor application and technology – a review. *Meas. Sci. Technol.* 2009;**20**:042002

[2] Vonau W, Guth U. pH Monitoring: a review. *J Solid State ELectrochem* 2006;**10**:746-752.

[3] Gac A, Atkinson JK, Zhang Z, Sion RP. A comparison of thick-film chemical sensor characteristics in laboratory and on-line industrial process aplications. *Meas. Sci. Technol* 2002;**13**:2062-2073.

[4] Haskard M, Pitt K. *Thick-Film Technology and Applications*. Port Erin: Electrochemical Publications Ltd; 1997.

[5] Mihell J.A, Atkinson J.K. Planar thick-film pH electrodes based on ruthenium dioxide hydrate. Sensors and Actuators B: Chemical 1998;**48**,1-3: 505-511.

[6] Atkinson J.K, Cranny A.W.J, Glasspool W.V, Mihell J.A. An investigation of the performance characteristics and operational lifetimes of multi-element thick film sensor array used in the determination of water quality parameters. *Sensors and Actuators B: Chemicals* 1999;**54**:215-231.

[7] Atkinson JK, Glanc M, Boltryk P, Sophocleous M, Garcia-Breijo E. An investigation into the effect of fabrication parameter variation on the characteristics of screen-printed thick-film silver/silver chloride reference electrodes. *Microelectronics International* 2011;**28/2**:49-52.

[8] Fog A., Buck R. P. Electronic semiconducting oxides as pH sensors, *Sensors and Actiators* 1984;**5**:137-146.

[9] McMurray H. N., Douglas P., Abbott D. Novel thick-film pH sensors based on ruthenium dioxide-glass composites, *Sensors and Actuators B* 1995;**28**:9-15.

Appendix 3

Within Appendix 3 is the journal paper published in Microelectronics International in 2013.

Thick Film Screen Printed Environmental and Chemical Sensor Array Reference Electrodes Suitable for Subterranean and Subaqueous Deployments

J. K. Atkinson[1], M. Glanc[1], M. Prakorbjanya[1], M. Sophocleous[1], R. P. Sion[2], E. Garcia-Breijo[3]

[1]Faculty of Engineering and the Environment, University of Southampton, United Kingdom
Email: jka@soton.ac.uk
[2]C-Cubed Limited, Whitchurch, United Kingdom
[3]Instituto de Reconocimiento Molecular y Desarrollo Tecnológico,
Universidad Politécnica de Valencia, Spain

Abstract

Purpose - Thick film environmental and chemical sensor arrays designed for deployment in both subterranean and submerged aqueous applications are reported.

Design/methodology/approach - Various choices of materials for reference electrodes employed in these different applications have been evaluated and the responses of the different sensor types are compared and discussed.

Findings - Results indicate that the choice of binder materials is critical to the production of sensors capable of medium term deployment (e.g. several days) as the binders not only affect the tradeoff between hydration time and drift but also have a significant bearing on device sensitivity and stability. Sensor calibration is shown to remain an issue with long term deployments (e.g. several weeks) but this can be ameliorated in the medium term with the use of novel device fabrication and packaging techniques.

Originality/value – The reported results indicates that is possible through careful choice of materials and fabrication methods to achieve near stable thick film reference electrodes that are suitable for use in solid state chemical sensors in variety of different application areas.

Keywords Reference electrodes, Thick-film sensors, Silver/Silver Chloride, Environmental sensors

Paper type Research paper

Introduction

Screen printed (thick-film) fabrication methods are increasingly being used for the fabrication of chemical and environmental sensors. Arrays of these devices are easily co-located onto ceramic and other substrates for application in a variety of areas [Gac et al. 2002; 2004; Glasspool and Atkinson, 2003]. A photograph of a typical example of this type of device, a water quality sensor designed to be used for the simultaneous measurement of pH, temperature, dissolved oxygen concentration, redox potential and conductivity is shown in Figure 1 below.

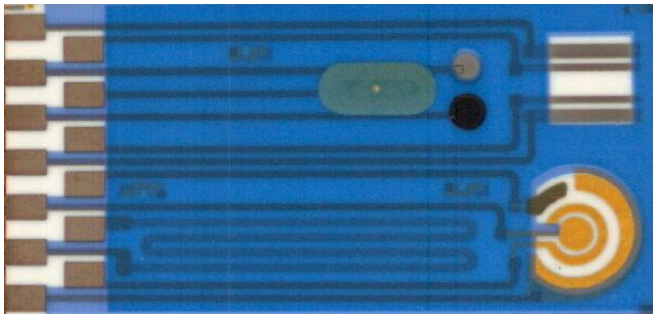

Fig. 1. Multi-element environmental sensor array comprising screen printed pH, temperature, oxygen concentration, redox potential and conductivity sensors printed on a 25mm x 50mm alumina ceramic substrate

Deployment durations of these devices vary with their application and can be broadly classified as being short term, where calibration can be performed between samples (such as a hand held probe for example), medium term (several days) and long term (several weeks of undisturbed operation). As will be discussed here, due to their very nature, thick film chemical sensors are not generally well suited for unlimited operation. They, like most chemical sensors, suffer from electrode drift and require at best recalibration and sometimes complete replacement, depending on the type of sensor and the deployment environment. For example, leaching of functional materials (e.g. immobilized salts) will be faster into low ionic strength solutions than it will be in higher strength solutions. The work reported here concerns itself in particular with drift rates due to salt loss from electrodes and does not take account of other factors that limit deployment durations, such as bio-fouling, although this has been studied previously [Gac et al. 2002] and is currently the subject of a parallel programme of work.

Many of the physical sensors realised in thick film technology are well characterised and simply mimic their macro scale equivalents. Examples include platinum resistance thermometers and conductivity electrodes. Thick film chemical sensors however, often mimic electrochemical equivalents and inevitably require a stable electro-potential (reference electrode) in order to function. Examples include both potentiometric devices such as pH, redox potential and other ion selective electrodes, and amperometric devices such as oxygen sensors and other fuel cells. Although the use of a conventional liquid electrolyte filled commercially obtained reference electrode is often employed in the characterisation of these devices, in order that they may be deployed in field applications they generally require a true solid state version. Various examples of these devices have employed a screen printed reference electrode, generally based on a silver/silver halide electrode. Sometimes the thick-film reference electrode takes the form of a pseudo-reference [Andreescu et al., 2002; Boujita et al., 2000; Matsumoto et al., 2002] whereby the silver/silver halide electrode surface is in direct contact with the analyte. As such the reference electrode function is based on knowledge of the environmental matrix into which it is deployed such that the stability of the electro-potential of the reference electrode is unimportant. In other instances the construction of the reference electrode attempts to mimic the operation of a conventional electrolyte-filled reference electrode usually through the immobilising of a halide salt reservoir on top of the reference electrode material [Mroz et al., 1998; Simonis et al., 2004; Tymeckia et al., 2004; Maminska et al., 2006]. These devices are designed to give absolute as opposed to relative electro-potential stability and are better suited to applications where halide ion concentrations can vary widely, such as where brackish water is usually encountered in estuarine waters, tidal rivers etc.

The reference electrodes reported here are fabricated as screen-printed planar electrodes with a halide salt containing polymer layer deposited as the top layer of the electrode to give some measure of electro-potential stability in a similar manner to that of a conventional electrolyte filled reference electrode. Early attempts at

fabricating electro-potentially stable devices concentrated on the use of a polymer bound potassium chloride filled layer that was screen printed onto a silver/silver chloride layer [Cranny and Atkinson, 1998].

The types of devices described here have previously been employed successfully on chemical and environmental sensor arrays for use in a range of industrial application areas including pH control of power station water feed lines and aqueous printing inks [Gac et al., 2002]. In these cases the analyte matrix was relatively well understood and allowance could be made for electrode potential drift. However recent interest in the use of thick film chemical sensor arrays in longer term environmental monitoring applications in relatively unknown matrices requires that they have much better electro-potential stability than that previously attained.

Typical electrode construction

A typical thick-film electrode (in this case a reference electrode) is shown in Figure 2 below. Details of the component materials and fabrication procedure employed for this particular device have been documented previously [Atkinson et al. 2011]. Fabrication of individual array elements is typically achieved by the successive printing of layers of functional materials (e.g. metal oxide powder suspended in a polymer binder for a pH sensitive layer), metal conductors and waterproofing. An array of such sensors can be economically designed such that many of the individual layers of the sensors are fabricated simultaneously with those of their neighbours. For example many of the underlying conductor materials and overlying waterproofing materials are common to more than one of the sensing elements in the array.

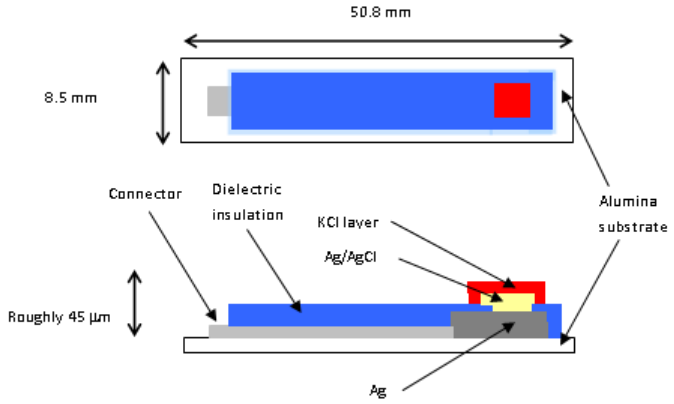

Fig. 2. Cross-sectional view of typical screen printed thick-film electrode suitable for medium term deployment – in this case a silver/silver chloride reference electrode

Electrode fabrication

In order to produce sensor arrays suitable for medium to long term deployment, such as for subterranean applications for example, it is essential to control the electro-potential drift of the reference electrode. This stems from the requirement that calibration is not an available option on deployment, unlike the short term deployment strategies adopted for aqueous and other liquid sampling devices that are discussed in a later section.

Most thick film ion sensitive electrodes (e.g. pH) are found to exhibit reasonably stable potentials over the medium term but the design of a silver/silver chloride reference electrode conflicts with this requirement. This is due to the fact that in order to maintain a constant potential, the electrode requires a chloride salt containment layer of relatively high chloride ion concentration, at least as high as the maximum likely to be encountered in the given application. This high concentration of chloride ions then has a tendency to diffuse out of the salt containment matrix, usually a polymer binder, and into the analyte (e.g. surrounding soil). Attempts at minimising this drift rate are hampered by the need for the electrode to hydrate rapidly and then act as a good ionic conductor to give fast responding sensors when used in combination with an ion selective electrode for example. A reasonable compromise has been found to exist with polymer bound chloride salt concentrations of approximately 20% by weight [Atkinson et al. 2011].

The electrodes reported here were fabricated with an upper layer of ESL242 (modified silicone) containing 20% by weight of potassium chloride (KCl). This upper layer of polymer bound KCl is in contact with an underlying silver/silver chloride layer that is fabricated on top of a silver back contact. In some cases the silver/silver chloride layer employed a commercially obtained polymer bound paste (GEM C61003P7) and in others a glass binder was used. The glass bound silver/silver chloride layers were fabricated from two screen printable pastes that were prepared as follows. Type 1 (Valencia PPCFC3) - AgCl (Aldrich 227927) milled to 400rpm/30min with ethanol (Pulverisette Fritsch), sieve 100µm, Ag (Aldrich 32708-5) sieve 100µm, powder frit (Ferro CF7567FC) sieve 100µm, vehicle (Heraeus V-006), mixed in the ratios 3gr Ag + 3gr AgCl + 2gr frit + 3.84gr vehicle and triple roll milled for 5 minutes. Type 2 (Valencia PPCFB2) is exactly the same as Type 1 with the exception of a different powder frit (Ferro EG2020VEG).

All the reference electrodes had a silver back contact constructed from ESL9912-A. All pastes were screened and fired according to their individual specifications with the exception of one batch of devices employing a polymer bound silver/silver chloride that was accidentally fired at 850 degrees Celsius (as opposed to the specified 150 degrees C) giving some very interesting results as reported below.

The metal oxide pH sensors are constructed in a very similar manner to the electrode shown in Figure 2 but with a polymer bound Ruthenium Oxide top layer (GEM C50502D7). In aqueous media these electrodes work on the principle of an equilibrated electro-potential response as illustrated by Equation 1.

$$2RuO_2 + H_2O + 2e^- \Leftrightarrow Ru_2O_3 + 2OH^- \qquad \text{Eqn. 1}$$

The pH electrodes have previously been found [Mihell and Atkinson, 1998] to exhibit an approximately Nernstian response of 56mV/pH, albeit with small device to device offset potential differences that, depending on the accuracy requirement, may require calibration on deployment, using for example the method described in a following section dealing with the subject of sensor deployment.

Electrode evaluation

Electrode evaluations were undertaken through a series of experiments where the thick film reference electrode potentials were measured against a conventional commercially obtained reference electrode (Beckmann Coulter A57193) whilst being simultaneously immersed into various test solutions. The potential differences between the electrodes were recorded using a purpose constructed computer controlled multi-channel high input impedance analogue to digital converter unit. The test arrangement for the electrodes has been described previously [Atkinson et al., 2011]

The various test solutions included varying concentrations of dissolved KCl that were designed to produce approximately decade step changes of chloride ion concentration, and pH buffer solutions giving step changes of pH4, pH7 and pH10. The drift test solutions of KCl were produced by adding powdered KCl to deionised water to produce a solution concentration of 0.13M. The electrodes were then cycled through the various test fluids in groups in order to ascertain their sensitivity to chloride ion concentration change and their pH response. In the latter case groups of thick film pH electrodes were also tested simultaneously with the thick film reference electrodes.

Experimental results

Testing of thick film reference electrodes in varying chloride ion concentrations

Batches of thick film reference electrodes of varying construction were left to hydrate in a solution of 0.13M potassium chloride for a period of approximately 12 hours and then subjected to cycling through test solutions of varying chloride ion concentration. The tested devices had different types of silver/silver chloride layer binder as described previously in the section detailing electrode construction. After two cycles of testing in varying chloride concentrations the devices were again left the varying chloride concentrations. The entire sequence to soak in a solution of 0.13M potassium chloride, this time for a 3 day “drift period”, after which they were again cycled through of tests is as illustrated in Figure 3.

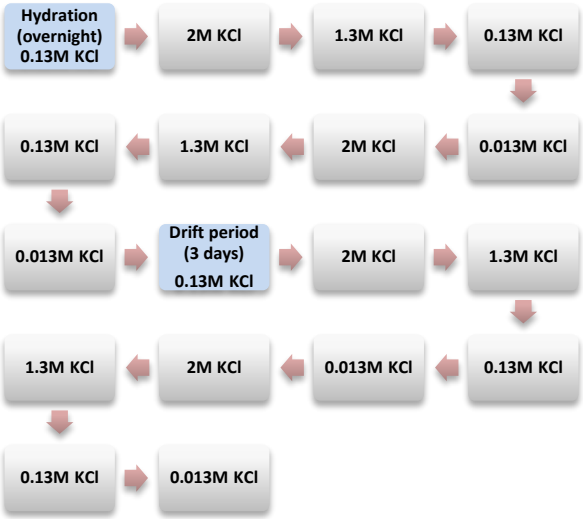

Fig. 3. Sequence for thick-film reference electrode response testing through successive immersion in various solutions.

The time history of the electrode potentials during this extended period of testing is as shown in Figure 5. The traces show the initial hydration period (denoted as A on the graph) and the step response of the electrodes as they are moved between the various test solutions during the testing intervals marked B and D. Figure 4 also shows a distinct drifting of some of the electrode potentials throughout the experiment and in particular during the 3 day interval marked as C. The bottom two traces that exhibit the greatest amount of electrode potential drift correspond to the electrodes that have no silver/silver chloride layer present.

Figure 5 shows the chloride sensitivity of the electrodes as a function of test solution concentration before this 3 day period of electrode potential drift (test interval B), while Figure 6 shows their chloride sensitivity after the 3 days (test interval D).

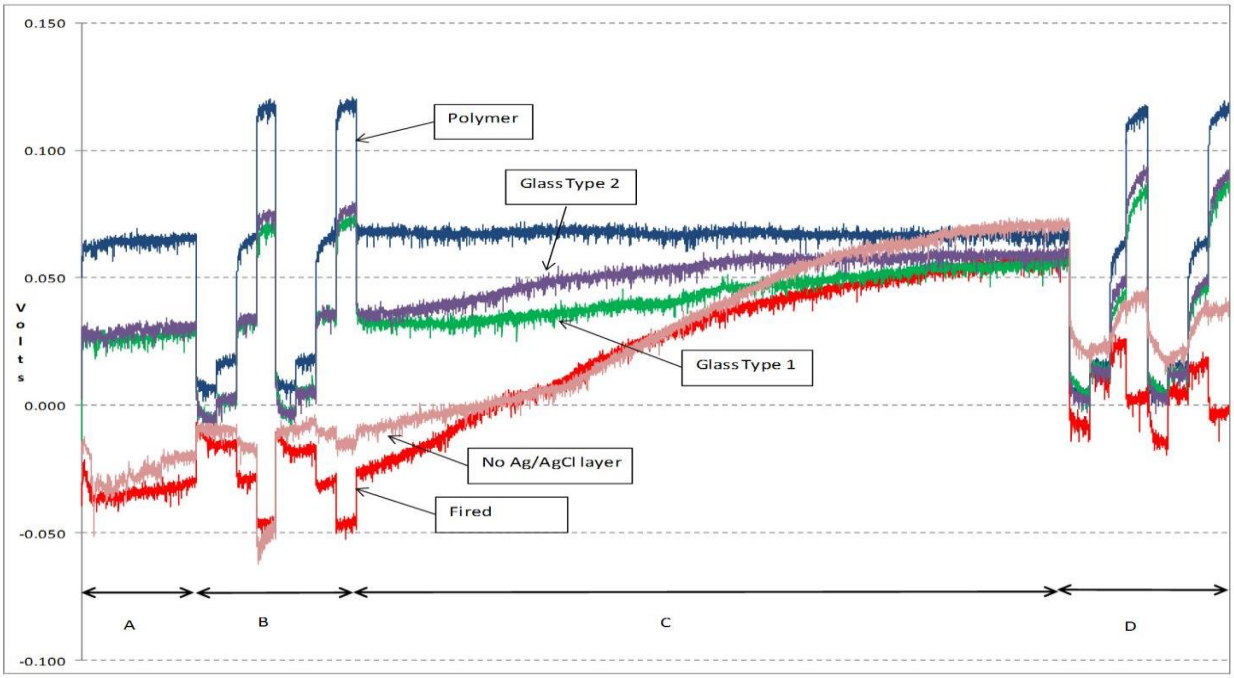

Fig. 4. Time history of reference electrode potentials (voltage relative to commercial reference electrode) during extended period of testing, with interval C corresponding to 3 days.

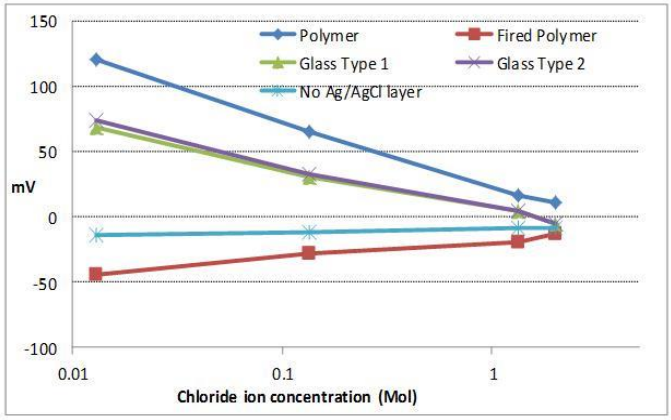

Fig. 5. Sensitivity of thick-film reference electrodes to chloride ion concentration during testing interval B (before 3 day drift period).

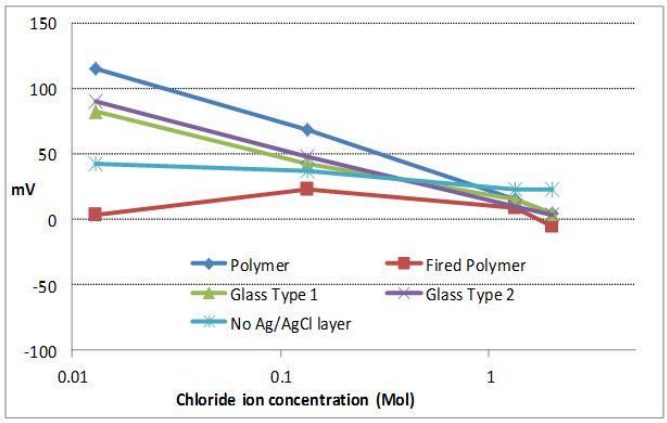

Fig. 6. Sensitivity of thick-film reference electrodes to chloride ion concentration during testing interval D (after 3 day drift period).

Figure 7 shows the response of thick-film pH electrodes (top traces) and thick-film reference electrodes (bottom traces) when the electrodes were cycled between pH buffer solutions in the following sequence: pH 7, 10, 7, 4, 7, 4, 7, 10 and 7.

The silver/silver chloride reference electrodes show some pH sensitivity but this is very repeatable and manifests itself as a slight reduction in the overall sensitivity of the pH electrodes when they are paired with the thick-film reference electrodes.

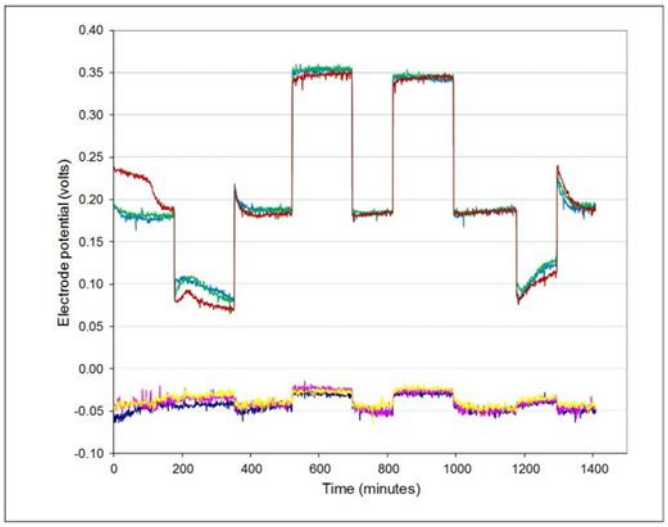

Fig. 7. Typical response of thick-film pH sensors (upper 3 traces) and reference electrodes (lower 3 traces) to successive immersions in pH buffer solutions in the sequence pH 7, 10, 7, 4, 7, 4, 7, 10 and 7.

Discussion

The sensitivities (in mV/decade Cl^-) of all electrode types, both before and after the 3 day drift test, are shown in Table 1.

Table 1: Sensitivity of various different reference electrode types in mV/decade Cl^- before and after 3 day drift testing

Ag/AgCl layer binder type	mV/decade Cl^- before drift test	mV/decade Cl^- after drift test
Polymer bound	-47	-49
Glass - Type 1	-30	-33
Glass - Type 2	-33	-38
Fired polymer	+12.6	-7.6
None (bare Ag)	+2.5	-9.6

It is clear from the results that the reference electrodes with the polymer bound silver/silver chloride layer exhibited the greatest (least desirable) sensitivity to varying chloride concentration (approx. 50mV/decade [Cl^-]), while the devices with no silver/silver chloride layer exhibited the most stable responses (<10mV/decade [Cl^-]). This group included the devices where a polymer bound layer was accidentally fired at high temperature (850 degrees C), thereby effectively removing the silver/silver chloride layer from the surface of the silver back contact, a fact that was later established with the aid of electron microscopy. The sensitivity of both types of devices with glass bound silver/silver chloride layers lay in between these other two types (approx. 30mV/decade [Cl^-]).

The best chloride ion stabilities were obtained with the electrodes that had no silver/silver chloride layer. However, these devices were also the most susceptible to longer term drift. From inspection of Figure 5 it can be seen that the potentials of the electrodes with no silver/silver chloride layer drifted from an initial potential of approximately -25mV w.r.t. the commercially obtained liquid electrolyte reference electrode, to a final potential of approximately +60mV. Likewise the glass bound silver/silver chloride devices drifted from an initial potential difference of approximately +30mV w.r.t. the commercial liquid electrolyte reference electrode to a similar final value of approximately +60mV.

What is also very interesting is the change in the slope of the response of the devices with no silver/silver chloride layer, from positive with respect to increasing chloride ion concentration before the 3 day drift period, to negative with respect to increasing chloride ion concentration after the 3 day drift period. This, coupled with the converging potentials just described, would tend to suggest that the initially bare silver back contact of these electrodes has chloridised during the interim 3 day period. This result also appears to indicate that the initially bare silver electrode, with a covering layer of 20% potassium chloride in polymer binder, has a different response mechanism compared to the silver/silver chloride layer devices.

An apparent anomaly in the results appears with the response of the accidently fired polymer silver/silver chloride sensors. The response to 1:1000 dilution of saturated potassium chloride solution after the 3 day drift period, as shown in Figure 7, does not follow the trend of these electrodes before the 3 day drift period (Figure 6), or indeed any of the other devices, increasing at first positive with increasing chloride concentration and then becoming more negative beyond approx. 0.1M. It is tempting to think this may have been the result of experimental error, however this response was in fact very repeatable over a series of experiments as can be seen in the traces shown in Figure 4, during test interval D. This behaviour of the fired polymer silver electrodes merits further investigation and is believed possibly to be the result of localised changes in the silver/silver chloride ratio within the surface layers of the thick film devices as explained below.

The potential response of the silver/silver chloride electrode is governed by the equilibrium reaction:

$$AgCl_{(s)} + e^- \leftrightarrow Ag_{(s)} + Cl^-_{(aq)} \qquad \text{Eqn. 2.}$$

Hence the equilibrium potential (E) of the electrode is given by the Nernst equation as:

$$E = E^\theta + \left(\frac{RT}{nF}\right) \ln \frac{(Oxi)}{(Red)} \qquad \text{Eqn. 3.}$$

Where E^{θ} is the standard potential (V); R is the universal gas constant (8.314 $JK^{-1}mol^{-1}$); T is the absolute temperature (K); n is the number of moles of electrons transferred in the reaction; F is the Faraday constant (96485 C mol^{-1}); *Oxi* is the activity of the oxidant and *Red* the activity of the reductants.
If the activities of the oxidant and reductants are assumed to be approximately equal to their concentrations the electrode potential is then given by:

$$E = E^{\theta} + \left(\frac{RT}{nF}\right) \ln \frac{[AgCl]}{[Ag][Cl^{-}]} \qquad \text{Eqn. 4.}$$

However, the Nernst equation for a cell is more frequently expressed in terms of base 10 logarithms at approximate room temperature (assumed to be 25°C), in which case Eqn. 4 can be re-written as:

$$E = E^{\theta} + 0.0592 \frac{[AgCl]}{[Ag][Cl^{-}]} \qquad \text{Eqn. 5.}$$

By separating out the dissolved from the solid components Eqn. 5 can then be re-written as:

$$E = E^{\theta} - 0.0592 \log[Cl^{-}] + 0.0592(k) \qquad \text{Eqn. 6.}$$

Where, (k) is the ratio of the concentration of silver chloride to silver, which is generally assumed to be constant in solids. Hence, if at room temperature the measured electrode potential (E) decreases by approximately 59mV for every decade increase in chloride ion concentration, the electrode can be said to display Nernstian behavior.

In most studies of thick-film electrodes, the relative concentrations of silver chloride and silver are generally held to be constant given the quantities of material used in the device fabrication and the fact that they are considered to be in solid form within the porous binder material. However at the surface of a thick film electrode this is not necessarily the case as the partially soluble silver chloride can itself dissolve into solution at the same time as a silver chloride layer can also be grown onto exposed silver particles by chemical reaction, which is particularly the case if the immersion solution contains any significant concentration of chloride ions. This fluctuation in the silver chloride and silver concentrations can result in a forcing of the equilibrium reaction (Eqn.2) within the binder layer, which in turn can affect the potential of the electrode, as explained below. Hence the electrode potential is not simply a function of chloride ion concentration, as assumed by Eqn. 6, but is in fact a more complex equilibrium determined by the solution concentration of chloride ions, the electrode surface concentrations of silver and silver chloride and the ease with which the silver chloride is able to dissolve and re-form, as determined by the binder type for example. It is believed that this mechanism may well account for the behavior of the thick-film electrode types investigated here.

Although the devices were covered by a polymer bound chloride salt layer containing 20% KCl by weight, it is believed from earlier work [Atkinson et al., 2011] that this polymer layer rapidly loses its salt on immersion in solution through dissolution of the KCl, leaving behind a porous layer whose chloride ion concentration approximately corresponds to that of the immersing solution. Consequently, while any exposed silver at the electrode surface is increasingly likely to be chloridised in increasing chloride ion concentration solutions, to give an increasingly positive potential (as per Eqn. 2) there is also the likelihood of increasing dissolution of silver chloride into lower concentration chloride ion solutions to give a subsequently negative change in electrode potential.

In the case of the initially non-silver chloride containing electrode types (bare silver and fired polymer), the overlying polymer bound KCl salt matrix appears to provide a source of chloride ions that enables an initial growth of a thin layer of silver chloride on the electrode surface. The subsequent porosity of the KCl salt matrix layer does not provide an adequate buffer to maintain a relatively stable chloride ion concentration however, as the dissolution and chloridisation of the thin silver chloride layer appear to be controlled to a large extent by the chloride ion concentration of the immersing solution. Hence increased dissolution of silver chloride in increasingly lower chloride ion concentration solutions gives rise to a negative change in electrode potentials, which appears to counterbalance the Nernstian chloride ion response of the thinly formed layer of silver chloride.

In contrast, the silver/silver chloride containing electrodes also experience a negative Nernstian change in potential with increasing chloride ion concentration as per Eqn.6, but do not appear to experience any appreciable change in their equilibrium potential as a result of increased dissolution in low ionic strength solutions. This is believed to be because the concentration ratio *k* within the binder is made up from much larger amounts of silver chloride than in the case of the initially bare silver electrodes. Hence the effect of changes in the surface silver chloride concentration is substantially lower and has less effect on the overall chloride ion response of the electrodes. However, the degree to which these particular electrodes respond, i.e. their sensitivity or slope, is apparently influenced by the binder type.

The polymer bound silver chloride devices exhibited a near Nernstian slope of 50mV per decade chloride ion concentration, compared with the glass bound silver chloride devices which exhibited a slope of approx. 30mV per decade chloride ion concentration. This observation merits further investigation of the device silver/silver chloride layer morphologies, but an initial consideration reveals that the polymer bound devices have a much thicker silver/silver chloride layer of approximately 50-80 microns, compared to their fired glass bound counterparts, which have thicknesses of typically 10-20 microns. It is likely that these differences in layer binder thickness account for the differences in the response due to the increased inhibition of silver chloride ion dissolution in the thick, i.e. less porous polymer devices than their thinner glass bound counterparts. Hence the Nernstian response of the glass bound silver/silver chloride layer devices is counteracted to some extent in lower ionic strength solutions in the higher porosity silver/silver chloride layer devices. Consequently, the higher the porosity of the layer, the more stable was the response of the electrodes, over the range of concentrations tested. These results appear to be commensurate with other work [Cranny et al., 2011] that showed a dependence of chloride response on binder type, whereby weaker binders appeared to exhibit a flatter response at lower chloride concentration levels.

Sensor array deployment

The work reported here derives largely from two projects concerning the application of thick-film chemical and environmental sensor arrays in water and soil sensing. One project (FUSE) part funded by the UK Natural Environment Research Council, involves the deployment of the devices in a floodplain underground sensor network, while the other project, part funded by the UK Environment Agency, seeks to deploy the sensors for water catchment area monitoring. Both these work programs require the use of a combination of remote wireless sensing and hands portable manual testing using a variety of sensing devices.

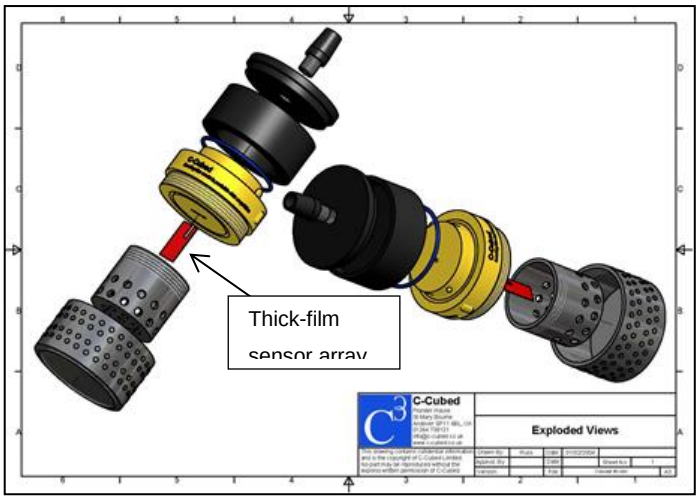

Fig. 8. Typical deployment of thick-film sensor array (red) in immersion probe assembly

A key aspect of all these applications however is the requirement to calibrate the sensors before use and preferably at the point of deployment. This is more easily achieved with hands portable devices and one approach to this is illustrated in Figure 8 whereby a thick film sensor array is mounted in a probe assembly with a waterproofed connector. Behind the waterproof connector are the interface circuits that enable the sensors to be connected, either wired or wirelessly, to a portable personal computer for example, or other suitable form of data acquisition.

The sensor array shown is protected with a cup-like container that screws onto the bottom of the probe assembly and contains holes through which the analyte (e.g. river water) can pass. A further bottom container containing a calibration solution (e.g. with known pH and conductivity values) is then screwed onto and over the protective cup. Deployment then consists of taking an initial reading of sensor values in the known calibration matrix to establish baseline readings (e.g. electrode offset potentials) prior to removal of the bottom container and deployment of the sensor in the analyte.

However, sensors for use in longer term deployments, such as subterranean sensing, do not offer the luxury of this ease of calibration on deployment. Consequently it is important that the reference electrodes used in these applications are able to operate throughout their useful lifetimes without recalibration. Hence in this context, it is generally more important to minimize electrode drift, possibly at the expense of increased chloride ion sensitivity.

Conclusions

It can be concluded from the results reported here that through the careful choice of materials it is possible to fabricate thick film electrochemical sensors that are suitable for a variety of different application areas. For example, for short term deployments in water where chloride ion concentrations are liable to wide variation, it may be preferable to employ a reference electrode with a bare silver back contact (no silver/silver chloride layer) and trade off a higher rate of drift for an increased stability (insensitivity) to chloride ion concentration variation.

However, for longer term deployment, in soil sensing for example, it would appear preferable to employ a device with a thicker silver/silver chloride layer, resulting in an increased sensitivity to chloride ion concentration variation but a lower longer term potential drift. For soil sensing in particular this tradeoff may well prove acceptable given that chloride concentration changes may not be so wide ranging as in a purely aqueous environment. In addition, it has been shown to be possible to utilise a bare silver/silver chloride electrode to track chloride ion concentrations in soil [Cranny et al., 2011] and hence it may be possible to compensate for an unwanted reference electrode chloride ion response in this manner.

Acknowledgements

Two of the authors wish to acknowledge partial support of their studentships by the UK Environment Agency (Monika Glanc) and the UK Natural Environment Research Council (Marios Sophocleous).

References

Andreescu, S., Noguer, T., Magearu, V. and Marty, J-L. (2002) Screen-printed electrode based on AChE for the detection of pesticides in presence of organic solvents, *Talanta* 57 169–176.

Atkinson, J.K., Cranny, A.W.J., Glasspool, W.V. and Mihell, J.A., An investigation of the performance characteristics and operational lifetimes of multi-element thick film sensor arrays used in the determination of water quality parameters, *Sensors and Actuators B: Chemical*, 54, 3, pp 215-231, 1999

Atkinson, J.K., Glanc, M., Boltryk, P., Sophocleous, M. and Garcia-Breijo, E., (2011) An investigation into the effect of fabrication parameter variation on the characteristics of screen-printed thick-film silver/silver chloride reference electrodes, *Microelectronics International*, 28/2, 49–52.

Boujtita, M., Hart, J.P. and Pittson, R. (2000) Development of a disposable ethanol biosensor based on a chemically modified screen-printed electrode coated with alcohol oxidase for the analysis of beer, *Biosensors & Bioelectronics* 15 257–263

Cranny, A.W.J. and Atkinson, J.K. (1998) Thick film silver-silver chloride reference electrodes, M*easurement Science and Technology*, 9, (9), 1557-1565.

Cranny, A.W.J., Harris, N. R., Nie, M., Wharton, J. A., Wood, R. J. K. and Stokes, K. R. (2011) Screen-printed potentiometric Ag/AgCl chloride sensors: Lifetime performance and their use in soil salt measurements. *Sensors and Actuators A: Physical*, 169 (2). pp. 288-294.

Gac, A., Atkinson, J.K., Zhang, Z., Sexton, C.J., Lewis, S.M., Please, C.P. and Sion, R.P., (2004) Investigation of the fabrication parameters of thick film titanium oxide-PVC pH electrodes using experimental designs, *Microelectronics International*, 21/3, 44-53.

Gac, A., Atkinson, J.K., Zhang, Z. and Sion, R.P. (2002) A comparison of thick-film chemical sensor characteristics in laboratory and on-line industrial process applications, *Measurement Science and Technology*, 13, 2062-2073.

Glasspool, W.V. and Atkinson, J.K. (2003) An evaluation of the characteristics of membrane materials suitable for the batch fabrication of dissolved oxygen sensors, *Microelectronics International*, 20, (2), 32-40.

Maminska, R., Dybko, A. and Wroblewski, W. (2006) All-solid-state miniaturised planar reference electrodes based on ionic liquids, *Sensors and Actuators B*, 115 552–557

Matsumoto, T., Ohashi, A. and Ito, N. (2002) Development of a micro-planar Ag/AgCl quasi-reference electrode with long-term stability for an amperometric glucose sensor, *Analytica Chimica Acta* 462 253–259

Mihell, J.A. and Atkinson, J.K. (1998) Planar thick-film pH electrodes based on ruthenium dioxide hydrate, *Sensors and Actuators B: Chemical*, 48, (1-3), 505-511.

Mroz, A., Borchardt, M., Diekmann, C., Cammann, K., Knoll, M. and Dumschat, C. (1998) Disposable reference electrode, *Analyst*, Vol. 123 (1373–1376)

Simonis, A., Lüth, H., Wang J. and Schöning, M.J. (2004) New concepts of miniaturised reference electrodes in silicon technologyfor potentiometric sensor systems, *Sensors and Actuators B* 103 429–435

Tymeckia, Ł., Zwierkowskab, E. and Koncki, R. (2004) Screen-printed reference electrodes for potentiometric measurements, *Analytica Chimica Acta* 526 3–11

Further reading

Floodplain Underground Sensors Network (FUSE) project website is at http://www.fuseproject.org.uk/about

Appendix 4

Within Appendix 4 is the journal paper published in Microelectronics International in 2011.

An investigation into the effect of fabrication parameter variation on the characteristics of screen printed thick film silver/silver chloride reference electrodes

J. K. Atkinson, M. Glanc, P. Boltryk, M. Sophocleous
School of Engineering Sciences, University of Southampton, United Kingdom

E. Garcia-Breijo
Instituto de Reconocimiento Molecular y Desarrollo Tecnológico,
Universidad Politécnica de Valencia, Spain

Abstract

Purpose - Fabrication parameters of screen printed thick film reference electrodes have been experimentally varied and their effect on device characteristics has been investigated.

Design/methodology/approach - The tested devices were fabricated as screen-printed planar structures consisting of a silver back contact, a silver/silver chloride interfacial layer and a final salt reservoir layer containing potassium chloride. The fabrication parameters varied included deposition method and thickness, salt concentration and binder type used for the final salt reservoir layer. Characterisation was achieved by monitoring the electrode potentials as a function of time following initial immersion in test fluids in order to ascertain initial hydration times, subsequent electrode drift rates and useful lifetime of the electrodes. Additionally the effect of fabrication parameter variation on electrode stability and their response time in various test media was also investigated.

Findings - Results indicate that, although a trade-off exists between hydration times and drift rate that is dependent on device thickness, the initial salt concentration levels and binder type also have a significant bearing on the practical useful lifetime. Generally speaking, thicker devices take longer to hydrate but have longer useful lifetimes in a given range of chloride environments. However the electrode stability and response time is also influenced by the type of binder material employed for the final salt reservoir layer.

Originality/value – The reported results help to explain better the behaviour of thick film reference electrodes and contribute towards the optimisation of their design and fabrication for use in solid state chemical sensors.

Keywords Reference electrodes, Thick-film, Silver chloride, Salt reservoir binder

Paper type Research paper

Introduction

The usage of screen printed (thick-film) fabrication methods for chemical and environmental sensor arrays has been growing steadily in recent years with a wide range of devices being reported. Although the use of a conventional electrolyte filled commercially obtained reference electrode is often employed in the characterisation of these devices, some have employed a screen printed reference electrode, generally based on a silver/silver halide electrode. Sometimes the thick-film reference electrode takes the form of a pseudo-reference (e.g. Boujtita et al. 2000, Andreescu et al. 2002 and Matsumoto, et al. 2002) whereby the silver/silver halide electrode surface is in direct contact with the analyte. As such the reference electrode derives its stability from knowledge of the environmental matrix into which it is deployed such that the stability of the electro-potential of the reference electrode is unimportant. In other instances the construction of the reference electrode attempts to mimic the operation of a conventional electrolyte-filled reference electrode usually through the immobilising of a salt reservoir on top of the reference electrode material (e.g. Mroz, et al. 1998, Tymeckia, et al. 2004 and Mami´nska, et al. 2006,).

The devices reported here are fabricated as screen-printed planar electrodes with a salt containing layer deposited on top of the electrode to give some measure of electro-potential stability in a similar manner to that of a conventional electrolyte filled reference electrode. Early attempts at fabricating electro-potentially stable devices (Cranny and Atkinson 1998) concentrated on the use of a polymer bound potassium chloride filled layer that was screen printed onto a silver/silver chloride layer. These devices have previously been employed successfully on chemical and environmental arrays for use in a range of application areas (Mihell and Atkinson, 1998; Atkinson et al. 1999; Gac et al. 2002, 2004; Glasspool and Atkinson, 2003). In all these cases the analyte matrix was relatively well understood and allowance could be made for electrode potential drift. However recent commercial interest in the use of thick film chemical sensor arrays in longer term applications in relatively unknown matrices requires that they have much better electro-potential stability than that previously attained.

Electrode Fabrication

The test electrodes employed for testing here were fabricated on 50.8 mm square, 0.625 mm thick 96% alumina substrates (Coorstech). The substrates were prescribed with laser lines to produce substrates that could be used for the simultaneous fabrication of 6 electrodes at a time (see Figure 1). Individual electrodes could then be snapped from the substrate along the laser scribe lines.

Figure 1: strips of thick film reference electrodes fabricated on a common “snapstrate” showing silver electrical connections at bottom and window exposing silver/silver chloride electrode at top

The cross-sectional view of the individual reference electrodes shown in Figure 2 reveals the construction as a succession of screen printed layers commencing with a silver conductor layer (ESL 9912) onto which is deposited an insulating glass layer (ESL 4905) with a 5mm x 5mm window that exposes the underlying silver layer. A layer of glass bound silver/silver chloride paste (GEM C61003P7) is then printed and fired on top of the silver exposed in the window before a second layer of insulating glass with the same 5mm x 5mm window opening as before is deposited on top. Finally a layer containing potassium chloride is deposited onto the silver/silver chloride layer.

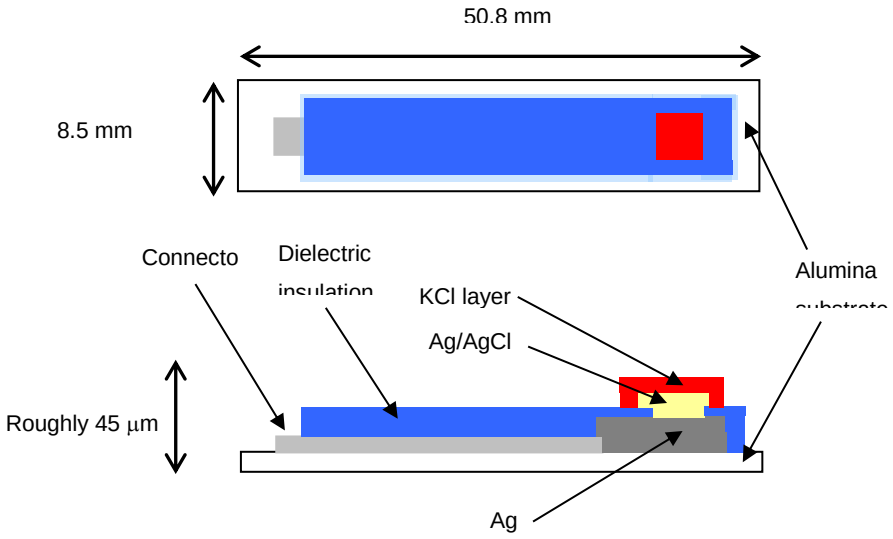

Figure 2:

thick-film reference electrode construction

Two different types of potassium chloride layer were tested with one type consisting of a silicone based polymer paste (ESL 242SB) containing different concentrations of potassium chloride of approx 6%, 3% and 0.6% by weight and the other a solgel made from commercially obtained gelatine dissolved in different concentrations of potassium chloride solution in deionised water (saturated solution, and said saturated solution further diluted with deionised water in ratios of 1:2 and 1:10). The polymer bound salt reservoir was screen printed onto the silver/silver chloride electrodes while the solgel solutions were applied using a dropper to give an approximate droplet volume of 3 ml per electrode.

Electrode Testing

Electrode preparation

The electrodes were initially hydrated in a dibasic sodium phosphate/monobasic potassium phosphate pH7 buffer solution (Oakton) and their electrode potentials were measured with respect to a commercial double junction electrolyte filled reference electrode (Beckman Coulter A57193) using a Keithley 2000 digital multimeter. The electrodes were connected to the multimeter in batches of 10 at a time using a K2000 scan card and held in solution using a mounting plate as illustrated in Figure 3 below.

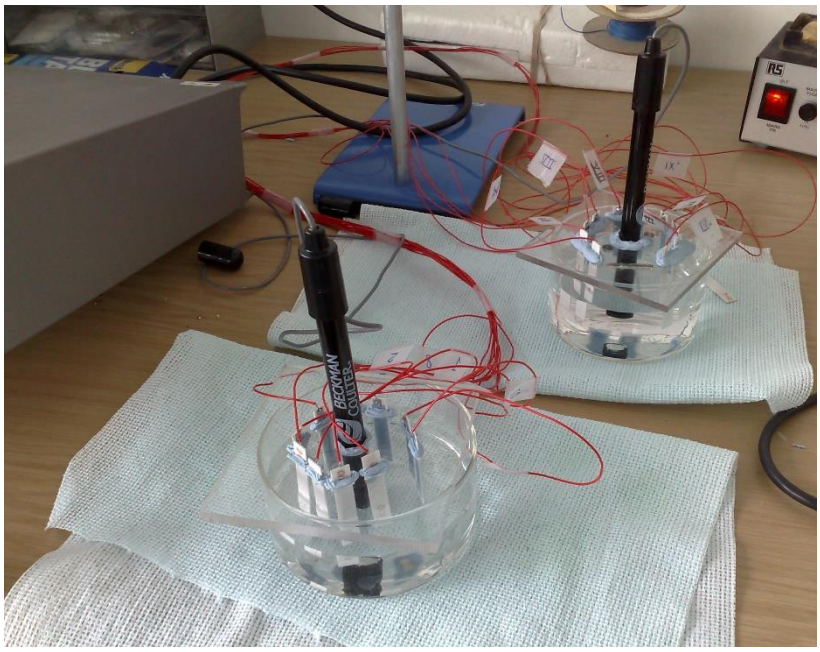

Figure 3: testing of thick-film reference electrodes versus commercial reference electrodes

Test solutions
Different concentrations of potassium chloride test solutions were made by first of all dissolving potassium chloride (BDH 101984L AnalaR) in deionised water until saturation and then diluting this solution in the ratios of 1:10, 1:100 and 1:1000. These solutions were then designated SAT, SAT 1:10, SAT 1:100 and SAT 1:1000 respectively.

The electrodes to be tested were then immersed in each of the test solutions in turn and allowed to stabilise for approx one hour before their individual potentials versus the commercial reference electrode were recorded.

Results

The average electro-potentials of the thick film reference electrodes (plotted versus the commercial reference electrode) hydrating in pH7 buffer as a function of time were as shown in Figure 4.

After an initial period of electro-potential instability lasting approximately one hour the electrodes hydrate and remain relatively stable for a period of approximately 24 hours. After this initially stable period they begin to drift at different rates. It can be seen from Figure 4 that the higher the initial concentration of potassium chloride contained in the electrodes the faster they drift.

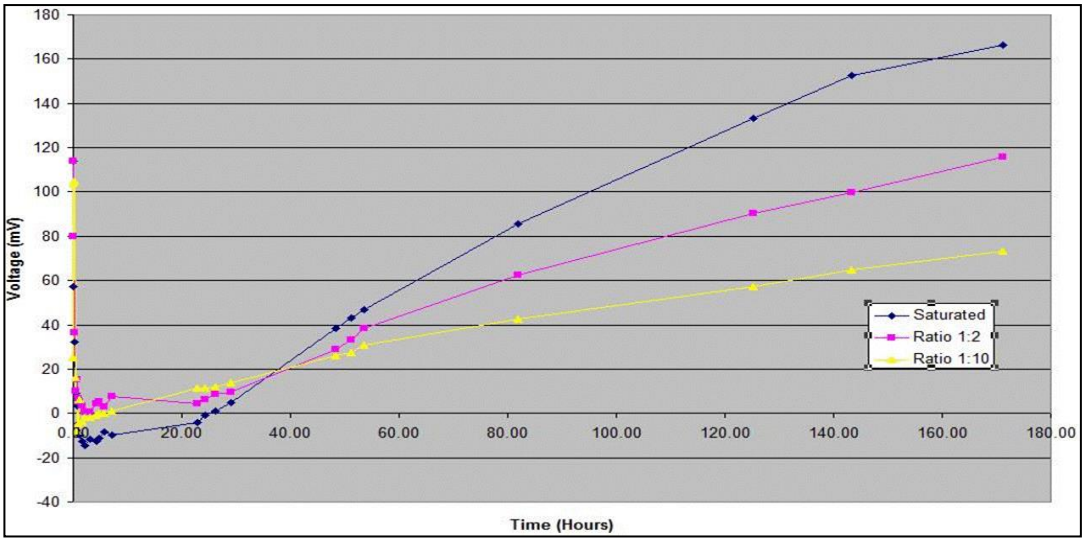

Figure 4: ESL 242-SB/KCl electrodes initially hydrating and then drifting in pH 7 buffer

The average electro-potential response of the electrodes to successive immersions in test solutions of deionised water containing potassium chloride concentrations of A: SAT, B: SAT 1:10, C: SAT 1:100 and D: SAT 1:1000 are as shown in Figure 5.

The electrodes exhibited potential steps of approximately 10mV per decade of test solution potassium chloride concentration with the step sizes being noticeably smaller for the electrodes containing higher initial concentrations of potassium chloride. This should be compared with the step sizes for a bare silver/silver chloride electrode (as shown in Figure 6 for example) of typically between 50 to 100mV per decade of potassium chloride concentration. It should also be noted that the electrode potentials became more NEGATIVE with DECREASING potassium chloride solution concentration.

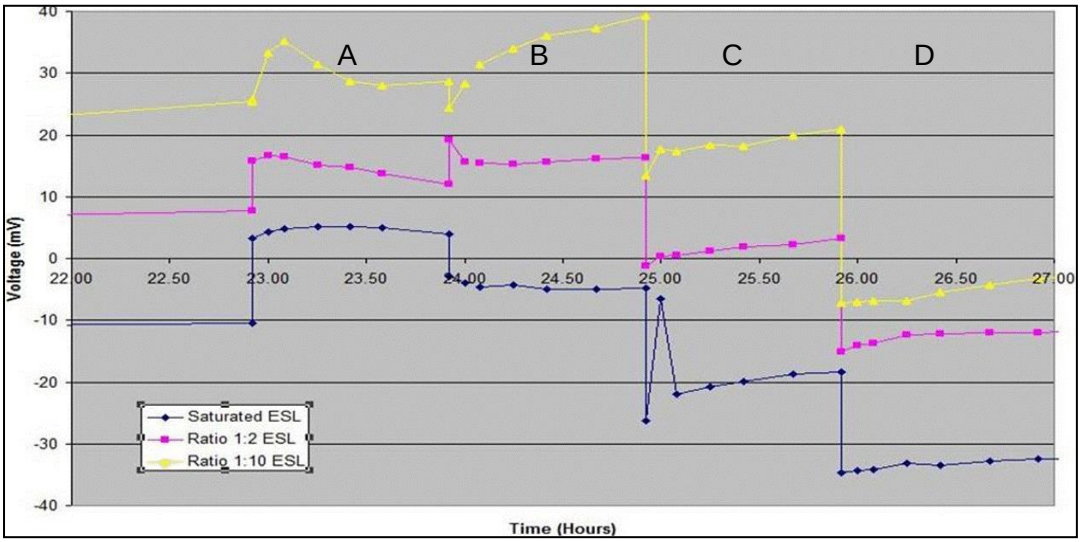

Figure 5: ESL 242-SB/KCl electrode potentials in different concentration KCl solutions

Figure 6 shows the averaged response of the hydrogel electrodes to successive immersions in solutions of deionised water containing the same potassium chloride concentrations as previously described and designated A, B, C and D.

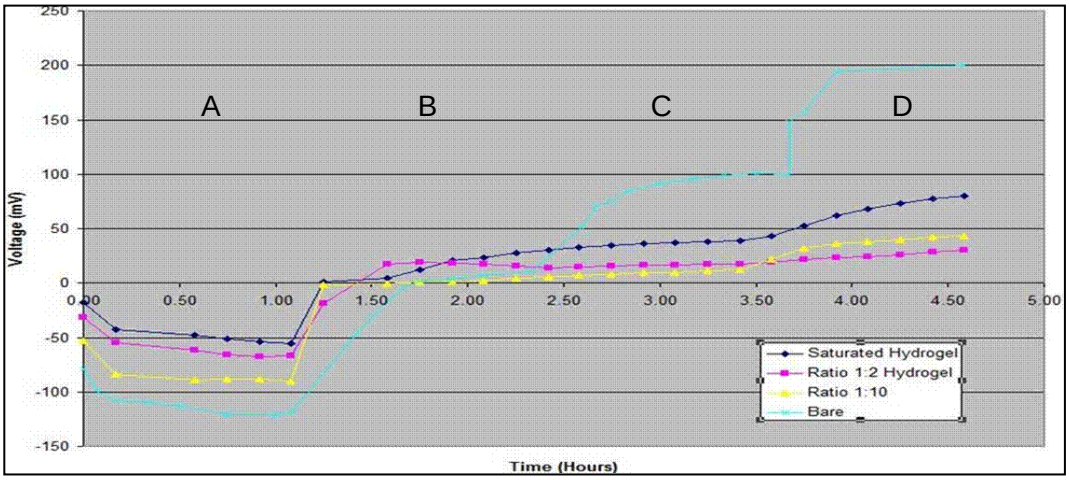

Figure 6: Hydrogel/KCl electrode potentials in different concentration KCl solutions

The responses of the electrodes showed relatively large potential steps (between 50 and 100 mV) for each electrode type when moving from SAT to SAT 1:10 but much lower potential steps thereafter when moving between lower concentration solutions. A bare silver/silver chloride electrode is shown on the same graph for comparison and exhibits step sizes of approx 100mV per decade change in potassium chloride solution concentration. It should also be noted that for the hydrogel electrodes the electrode potentials became more POSITIVE with DECREASING potassium chloride solution concentration.

Conclusions

The reason that the ESL242SB/KCl electrodes gave a potential response to different concentrations of chloride solution that was the opposite of the both the bare Ag/AgCl and the solgel electrodes is thought to be due to a combined response of the silicone polymer itself and the KCl salt concentration in the polymer.

The fact that higher concentrations of KCl gave lower step sizes would tend to suggest that increasing the KCl concentration to an optimum level will result in electrodes that have responses to varying chloride concentration that are almost flat, whereby the KCl response "cancels out" the silicone polymer response.

Conversely, the drift rates of the hydrated ESL242SB/KCl electrodes were heavily influenced by their initial salt concentration, and this is thought to be a function of the number of "pathways" through which the salt can leach out of the polymer binder. This tends to suggest that higher initial KCl levels would result in shorter useful lifetimes as a result of higher drift.
The solgel electrodes appear to offer some promise in that they hydrated far more rapidly (within minutes) and hence gave a useful lifetime sooner than their polymer counterparts. One possibility could be to combine these characteristics in a device whereby the polymer electrode surface is covered with a solgel membrane to reduce salt leach out rates and yet present a rapid hydration time.

References

Andreescu, S., Noguer, T., Magearu, V. and Marty, J-L. (2002) Screen-printed electrode based on AChE for the detection of pesticides in presence of organic solvents**,** *Talanta* 57 169–176.

Boujtita, M., Hart, J.P. and Pittson, R. (2000) Development of a disposable ethanol biosensor based on a chemically modified screen-printed electrode coated with alcohol oxidase for the analysis of beer, *Biosensors & Bioelectronics* 15 257–263

Matsumoto, T., Ohashi, A. and Ito, N. (2002) Development of a micro-planar Ag/AgCl quasi-reference electrode with long-term stability for an amperometric glucose sensor, *Analytica Chimica Acta* 462 253–259

Mroz, A., Borchardt, M., Diekmann, C., Cammann, K., Knoll, M. and Dumschat, C. (1998) Disposable reference electrode, *Analyst,* Vol. 123 (1373–1376)

Simonis, A., Lüth, H., Wang J. and Schöning, M.J. (2004) New concepts of miniaturised reference electrodes in silicon technologyfor potentiometric sensor systems, *Sensors and Actuators B* 103 429–435

Tymeckia, Ł., Zwierkowskab, E. and Koncki, R. (2004) Screen-printed reference electrodes for potentiometric measurements, *Analytica Chimica Acta* 526 3–11

Maminska, R., Dybko, A. and Wroblewski, W. (2006) All-solid-state miniaturised planar reference electrodes based on ionic liquids, *Sensors and Actuators B*, 115 552–557

Cranny, A.W.J. and Atkinson, J.K. (1998) Thick film silver-silver chloride reference electrodes. *Measurement Science and Technology*, 9, (9), 1557-1565.

Mihell, J.A. and Atkinson, J.K. (1998) Planar thick-film pH electrodes based on ruthenium dioxide hydrate. *Sensors and Actuators B: Chemical*, 48, (1-3), 505-511.

Gac, A., Atkinson, J.K., Zhang, Z. and Sion, R.P. (2002) A comparison of thick-film chemical sensor characteristics in laboratory and on-line industrial process applications. *Measurement Science and Technology*, 13, 2062-2073.

Glasspool, W.V. and Atkinson, J.K. (2003) An evaluation of the characteristics of membrane materials suitable for the batch fabrication of dissolved oxygen sensors. *Microelectronics International*, 20, (2), 32-40.

J.K.Atkinson, A.W.J.Cranny, W.V.Glasspool and J.A.Mihell, An investigation of the performance characteristics and operational lifetimes of multi-element thick film sensor arrays used in the determination of water quality parameters, *Sensors and Actuators B: Chemical*, 54, 3, pp 215-231, 1999

A.Gac, J.K.Atkinson, Z Zhang, C.J.Sexton, S.M.Lewis, C.P.Please and R.P.Sion, Investigation of the fabrication parameters of thick film titanium oxide-PVC pH electrodes using experimental designs, *Microelectronics International*, 21/3, 44-53, 2004

K. Tymecki, E. Zwierkowska and R. Koncki, Screen-printed reference electrodes for potentiometric measurements, *Anal. Chim. Acta* **526** (2004), pp. 3–11.

Hassel A.H., Fushimi K., Seo M. (1999) An agar-based silver/silver chloride reference electrode for use in micro-electrochemistry. *Electrochemistry Communications* 1, 180-183.

List of references

1. Guth U., Vonau W. & Zosel J., 2009. Recent developments in electrochemical sensor application and technology - a review. Measurement Science and Technology, 20(4), pp. 1-14.

2. Glasgow H. B. et al., 2004. Real-time remote monitoring of water quality: a review of current applications, and advancements in sensor, telemetry, and computing technologies. Journal of Experimental Marine Biology and Ecology, 300(1-2), pp. 409-448.

3. Gac A. et al., 2002. A comparison of thick-film chemical sensor characteristics in laboratory and on-line industrial process applications. Measurement Science & Technology, 13(12), pp. 2062-2073.

4. Desmond D. et al., 1997. Evaluation of miniaturised solid state reference electrodes on a silicon based component. Sensors and Actuators B: Chemical, 44, pp. 389-396.

5. Atkinson J. K. et al., 2011. Screen Printed Thick Film Subterranean and Subaqueous Environmental Chemical Sensor Arrays. IEEE Electronics Packaging Technology Conference (EPTC), pp. 245-250.

6. Tymecki Ł., Zwierkowska E. & Koncki R., 2004. Screen-printed reference electrodes for potentiometric measurements. Analytica Chimica Acta, 526(1), pp. 3-11.
7. Atkinson J. K. et al., 2013. Thick film screen printed environmental and chemical sensor array reference electrodes suitable for subterranean and subaqueous deployments. Microelectronics International, 30(2), pp. 92-98.

8. Martínez-Máñez R. et al., 2005. A multisensor in thick-film technology for water quality control. Sensors and Actuators A: Physical, 120(2), pp. 580-595.
9. Cranny A. W. J. & Atkinson J. K., 1998. Thick film silver-silver chloride reference electrodes. Meas. Sci. Technol., 9, pp. 1557-1565.

10. Atkinson J. K. et al., 2011. An investigation into the effect of fabrication parameter variation on the characteristics of screen-printed thick-film silver/silver chloride reference electrodes. Microelectronics International, 28(2), pp. 49-52.

11. Glanc-Gostkiewicz M. et al., 2012. Performance of miniaturised thick-film solid state pH sensors. Sensors and Actuators A: Physical, 202, pp. 2-7.

12. Janata J., 2001. Centennial retrospective on chemical sensors. Analyt Chem, 73(5), pp. 150A-153A.

13. Buck R. P. & Lindner E., 2001. Tracing the History of Selective Ion Sensors. Analytical Chemistry, 73, pp. 88A-97A.

14. Haskard M. & Pitt K., 1997. Thick-Film technology and applications. Electrochemical Publications.

15. Hulanicki A., Glab S. & Ingman F., 1991. Chemical sensors definitions and classification. Pure & Appl. Chem. , 63(9), pp. 1247-1250.
16. Grundler P., 2007. An introduction for Scientists and Engineers. Springer: Berlin, Germany.

17. Hanrahan G., Patil D. G. & Wang J., 2004. Electrochemical sensors for environmental monitoring: design, development and applications. J. Environ. Monit., 6, pp. 657-664.

18. Galán-Vidal C. A. et al., 1995. Chemical sensors, biosensors and thick-film technology. Trends in Analytical Chemistry, 4(5).

19. White R. M., 1987. A Sensor Classification Scheme. IEEE Transaction on Ultrasonics, Ferroelectronics and Frequency Control UFFC, 34(2), pp. 124-126.

20. Smith L. R., 2006. Sensors. The Electrical Engineering Handbook. Third Edition. Sensors, Nanoscience, Biomedical Engineering, and Instruments. ed. R.C. Dorf. 2006, RCR Press Taylor & Francis Group: New York, USA.

21. Göpel W., Jones T. A. & Kleitz M., 1991. Chemical and Biochemical Sensors, Part I., Sensors. a Comprehensive Survey. Vol 2.
22. Wang J. & Rogers K., 1995. Electrochemical sensors for environmental monitoring: A review of recent technology. US Environmental Protection Agency, Office of Research and Development, Environmental Monitoring and Support Laboratory.

23. Brett C. M. A., 2001. Electrochemical sensors for environmental monitoring. Strategy and examples. Pure appl. Chem., 73(12), pp. 1969-1977.
24. Harvey D., 1999. Modern Analytical Chemistry. San Francisco, USA: The McGraw-Hill Companies.

25. Alvarez-Icaza M. & Bilewski U., 1993. Mass Production of Biosensors. Analytical Chemistry, 65(11).

26. Koryta J., Dvořák J. & Kavan L., 1993. Principles of Electrochemistry. Chichester, England: John Wiley & Sons Ltd.

27. Smith T. J. & Stevenson K. J., 2006. Handbook of Electrochemistry. Elsevier.

28. Brzozka Z., 2005. Chemical Sensors Research Group -CSRG. [Online] Available at: http://csrg.ch.pw.edu.pl/
[Accessed 22.02.2013]

29. Pletcher D., 2009. A First Course in Electrode Processes. Cambridge, UK: RSC Publishing.

30. Bard A. J. & Faulkner L. R., 2001. Electrochemical methods: Fundamentals and Applications. USA: John Wiley & Sons, Inc.
31. Hahn R., Claude-Luis Berthollet, in Encyclopaedia Britannica.

32. Laidler K. J., Law of mass action., in Encyclopeadia Britannica.

33. Plambeck J. A., 1982. Electrochemical Chemistry: Basic Principles and Applications. USA: John Wiley & Sons.

34. Camoes M. F., 2010. A Century of pH Measurements. Chemistry International, 2010. 32(2): p. 3-7.

35. Carlsberg Group Company. Sørensen Invents the pH Scale.
Available at:
http://www.carlsberggroup.com/Company/heritage/Research/Pages/pHValue.aspx.
[Accessed 15.03.2012]
36. Crawford E., Svante August Arrhenius, in Encyclopeadia Britannica.
37. Bates R. G., 1981. The modern meaning of pH. C R C Critical Reviews in Analytical Chemistry, 10(3): p. 247-278.
38. Ives D. J. G. & Janz G.J., 1961. Reference Electrodes. Theory and Practice. London, UK: Academic Press, Inc.
39. Smith T. J. & Stevenson K.J., 2007. Reference electrodes., in Hanbook of Electrochemistry., C.G. Zoski, Editor., Elsevier: Amsterdam, The Netherlands.
40. Shinwari M.W. et al., 2010. Microfabricated Reference Electrodes and their Biosensing Applications. Sensors. 10: p. 1679-1715.

41. Koryta J., Dvořák J. & Bohackova V., 1966. Electrochemistry. London, UK: Methuen & Co Ltd.

42. Glanc M. et al., 2013. The Effect on Performance of Fabrication Parameter Variations of Thick-Film Screen Printed Silver/Silver Chloride Potentiometric Reference Electrodes. Sensors and Actuators A: Physical, 197: p. 1-8.

43. Guth U. et al., 2009. Solid-state reference electrodes for potentiometric sensors. J Solid State Electrochem, 13: p. 27-39.
44. Ito S. et al., 1995. Improvement of the silver/silver chloride reference electrode and its application to pH measurement. Talanta, 42: p. 1685-1690.

45. Atkinson J.K. et al., 1999. An investigation of the performance characteristics and operational lifetimes of multi-element thick film sensor arrays used in the determination of water quality parameters. Sensors and Actuators B: Chemical, 54: p. 215-231.

46. Vonau W. et al., 2010. An all-solid-state reference electrode. Sensors and Actuators B: Chemical, 144(2): p. 368-373.

47. Prasek J. et al., 2008. Reference electrodes for thick-film sensors. Electronics Technology, 31st International Spring Seminar p. 514 - 517

48. Mroz A. et al., 1998. Disposable reference electrode. Analyst, 123(6): p. 1373-1376.
49. Cranny A. et al., 2011. Screen-printed potentiometric Ag/AgCl chloride sensors: Lifetime performance and their use in soil salt measurements. Sensors and Actuators A: Physical, 169(2): p. 288-294.

50. Harris N. et al., 2016. Application of distributed wireless chloride sensors to environmental monitoring: initial results. IEEE Transactions on Instrumentation and Measurement, 65(4): p. 736-743.

51. Simonis A. et al., 2004. New concepts of miniaturised reference electrodes in silicon technology for potentiometric sensor systems. Sensors and Actuators B: Chemical, 103(1–2): p. 429-435.

52. Mamińska R., Dybko A. & Wróblewski W., 2006. All-solid-state miniaturised planar reference electrodes based on ionic liquids. Sensors and Actuators B: Chemical, 115(1): p. 552-557.

53. Smith R. P., 1933. The activity coefficient of Potassium chloride in aqueous solutions at 0º from electromotive force and freezing point data. Journal of the American Chemical Society, 55(8): p. 3279-3282.

54. Marques A., Ferra M. I. A. & Bandeira M.H., 2006. Activity Coefficients of Potassium Chloride in Aqueous Solutions of Potassium Chloride and Potassium Phthalate. Portugaliae Electrochimica Acta, 24: p. 295-303.

55. O'M Bockris J. & Reddy A.K.N., 1973. Modern Electrochemistry. New York, USA: Plenum Publishing Corporation.

56. Fog A. & Buck R.P., 1984. Electronic semiconducting oxides as pH sensors. Sensors and Actuators. 5(2): p. 137-146.

57. Koncki R. & Mascini M., 1997. Screen-printed ruthenium dioxide electrodes for pH measurements. Analytica Chimica Acta, 351(1-3): p. 143-149.

58. Mihell J. A. & Atkinson J.K., 1998. Planar thick-film pH electrodes based on ruthenium dioxide hydrate. Sensors and Actuators B: Chemical, 1998. 48(1-3): p. 505-511.
59. Wang M., Yao S. & Madou M., 2002. A long-term stable iridium oxide pH electrode. Sensors and Actuators B: Chemical, 81(2-3): p. 313-315.
60. Liu J. H. et al., 1993. Study of thick-film pH sensors. Sensors and Actuators B: Chemical, 13-14: p. 566-567.

61. McMurray H. N., Douglas P. & Abbot D., 1995. Novel thick-film pH sensors based on ruthenium dioxide-glass composites. Sensors and Actuators B: Chemical, 28(1): p. 9-15.

62. Stromquist A., 2004. Simple Screenprinting: Basic Techniques & Creative Projects. Lark Books: New York, USA.

63. Sheng A., 1999. Why Ancient Silk Is Still Gold: Issues in Chinese Textile History. Ars Orientalis, 29: p. 147-168.

64. Bellis M. The History of Printing and Printing Processes.
Available at:
http://inventors.about.com/od/pstartinventions/a/printing.htm?utm_term=history%20of%20screen%20printing&utm_content=p1-main-1-title&utm_medium=sem&utm_source=msn&utm_campaign=adid-024643ed-7208-45a4-8dfe-d42ee687690e-0-ab_msb_ocode-12627&ad=semD&an=msn_s&am=broad&q=history%20of%20screen%20printing&dqi=&o=12627&l=sem&qsrc=999&askid=024643ed-7208-45a4-8dfe-d42ee687690e-0-ab_msb.
[Accessed 06.12.2012]

65. Hobby A., 1997. Screen printing for the industrial user. The history of screen printing.

Available at: http://www.gwent.org/gem_screen_printing.html.
[Accessed 05.10.2010]

66. Holmes P. J. & Loasby R.G., 1976. Handbook of Thick Film Technology. Ayr, Scotland: Electrochemical Publications Limited.

67. Tarr M., Thick film technology.
Available at: http://docslide.us/documents/thick-film-technology.html.
[Accessed 06.14.2012.]

68. Jones R. D., 1982. Hybrid circuit design and manufacture. New York, USA: Basel: M. Dekker.

69. Brighell J. E., White N. M. & Cranny A.W.J., 1988. Sensor applications of thick-film technology. IEE Proceedings I (Solid-State and Electron Devices), 135(4): p. 77-84.

70. Wang J. et al., 1999. Stripping analysis into the 21st century: faster, smaller, cheaper, simpler and better. Analytica Chimica Acta, 385(1-3): p. 429-435.

71. White N. M. & Turner J.D., 1997. Thick-film sensors: past, present and future. Meas. Sci. Technol., 8: p. 1-20.

72. Prudenziati M. & Morten B., 1992. The state of the art in thick-film sensors. Microelectronics Journal, 23(2): p. 133-141.

73. Cranny A. W. J. et al., 1991. A comparison of thick- and thin-film gas-sensitive organic semiconductor compounds. Sensors and Actuators B: Chemical, 4(1-2): p. 169-174.

74. Prudenziati M., 1994. Thick Film Sensors.Handbook of Sensors and Actuators Volume 1. Amsterdam, Holland: Elsevier.

75. Rikoski R. A., 1973. Hybrid Microelectronic Circuits: The Thick Film. New York, USA: John Wiley & Sons Inc.

76. Dorey R.A. & Whatmore R.W., 2004. Electroceramic Thick Film Fabrication for MEMS. Journal of Electroceramics, 12: p. 19-32.

77. Miller O. F., 1974. Screenability and Rheology. Solid State Technology, 17: p. 54-60.

78. Goldberg H. D. et al., 1994. Screen printing: a technology for the batch fabrication of integrated chemical-sensor arrays. Sensors and Actuators B: Chemical, 21: p. 171-183.